Innovative strategies to improve or replace renal proximal convoluted tubule function

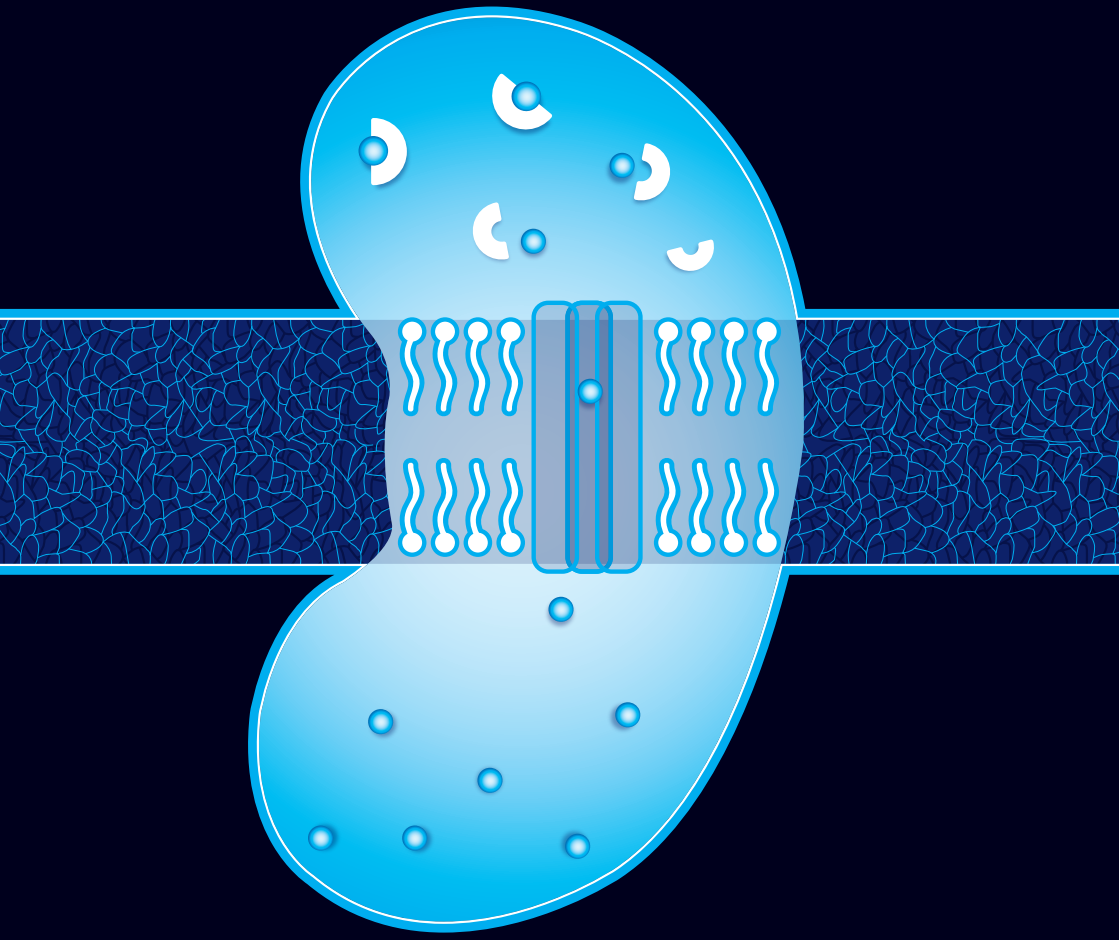

Jitske Jansen

INNOVATIVE STRATEGIES TO IMPROVE OR REPLACE RENAL PROXIMAL CONVOLUTED TUBULE FUNCTION

Jitske Jansen

Colofon

ISBN: 978-90-393-6634-9
Cover design: Dieke Geurtsen & Guus Gijben/proefschrift-aio.nl
Proefschrift layout: proefschrift-aio.nl

The research presented in this thesis formed part of the Netherlands Institute of Regenerative Medicine, co-funded by the Dutch Ministry of Economic Affairs and supported by the Dutch Kidney Foundation.

Publication of this thesis was financially supported by the Radboud University Nijmegen, the Netherlands.

INNOVATIVE STRATEGIES TO IMPROVE OR REPLACE RENAL PROXIMAL CONVOLUTED TUBULE FUNCTION

Proefschrift
ter verkrijging van de graad van doctor
aan de Radboud Universiteit Nijmegen
op gezag van de rector magnificus prof. dr. J.H.J.M. van Krieken,
volgens besluit van het college van decanen
in het openbaar te verdedigen op donderdag 6 oktober 2016
om 10.30 uur precies

door
Jitske Jansen
geboren op 14 maart 1984
te Beek

Promotoren	Prof. dr. R. Masereeuw (Universiteit Utrecht) Prof. dr. J.G.J. Hoenderop Prof. dr. L.P.W.J. van den Heuvel (KU Leuven)
Copromotor	Dr. M.J. Wilmer
Manuscriptcommissie	Prof. dr. D.W. Swinkels Dr. ir. W.F. Daamen Prof. dr. M.C. Verhaar (Universitair Medisch Centrum Utrecht)

TABLE OF CONTENTS

Chapter 1

INTRODUCTION AND OUTLINE OF THE THESIS

INTRODUCTION

Kidney function in health and disease

The kidneys are complex organs and consist of approximately 1 million filtration units per organ, termed nephrons. Each nephron contains over twenty different cell types that, together, play a role in the homeostasis of the organism by taking care of the removal of waste products and the retention of vital components such as electrolytes, peptides and H_2O (1-4). To this end, blood enters the first segment of the nephron, the glomerulus, where filtration will occur under hydrodynamic pressure. The ultrafiltrate containing H_2O and small solutes will enter the proximal tubule epithelial cells where a fraction of the electrolytes, H_2O and other molecules such as amino acids and glucose will be reabsorbed. In addition, active secretion of waste products and drugs from the efferent arteriole and the interstitium into the pro-urine takes place, mediated by transporters present in proximal tubule epithelial cells (PTEC). Downstream the proximal segment, the Loop of Henle, the distal convoluted tubule and collecting tubule and -duct cells are equipped with water- and ion channels and play key roles in the fine tuning of fluid and ion homeostasis. Moreover, the kidneys fulfill an endocrine and metabolic function, which contributes further to the maintenance of the physiological balance in the human body and in preventing the development of acute or chronic renal failure (5).

The incidence of acute kidney injury (AKI) is an increasing global concern and is characterized by a high mortality rate of over 50% in critically ill patients. AKI is defined as an abrupt loss of kidney function and renal replacement therapy such as hemodialysis is urgently required (6-8). The onset of acute kidney injury (AKI) is often complex, but cardiac failure, renal thrombosis, obstruction of the urinary tract and sepsis-induced acute tubular necrosis are known causal factors (7). Although less severe AKI is partially reversible, still the disease is associated with adverse irreversible outcomes and predisposes to chronic kidney disease (CKD) (6). CKD is classified in five stages based on measured or estimated glomerular filtration rate (m/eGFR). Stage 1 reflects normal kidney function (mGFR >90 ml/min/1.73m2) though evidence for reduced kidney function is present, whereas stage 5 represents end-stage renal disease (ESRD) with a severe decline in kidney function of over 80% and renal replacement therapy is required. In addition to unresolved AKI, the development of chronic kidney disease (CKD) can be caused by a wide variety of underlying diseases (e.g. cardiovascular disease, diabetes mellitus,

auto-immune disease, sepsis), aging or nephrotoxic agents (7, 9-12). But also conditions in which the kidneys are primarily affected are known, often due to genetic disorders, like polycystic kidney disease, Alport syndrome, nephropathic cystinosis, nephrotic syndrome and electrolyte and acid-base balance disorders (2, 13-16). As the kidneys have an important role in many physiological processes, it has been shown that renal dysfunction in turn also contributes to the onset or progression of other diseases such as cardiovascular disease, mineral and bone disorders, anemia and neurological disorders (10, 17-19). Over the past years, more knowledge is gained to unravel the molecular mechanisms of kidney (-related) diseases, using state-of-the-art platforms such as whole exome sequencing, metabolomics and proteomics. Nevertheless, many causes have, as of yet, not been elucidated and appropriate therapeutic modalities are often absent or only diminish the progression of renal disease.

Pitfalls of CKD treatment

The preferred treatment option for ESRD is organ transplantation. Unfortunately, a profound shortage in donor organs results in a waiting list for a patient of about 3 - 5 years, depending on blood type (20). Alternatively, patients are treated with peritoneal or hemodialysis, if possible at home to affect the patients' lifestyle as minimal as possible (figure 1.1). In more advanced stages, i.e. severe clinical complications associated with ESRD, patients have to be treated at a medical center to have better monitored and more successful dialysis sessions. A major drawback of in-center dialysis is the frequency and the duration; 3 times a week for approximately 4 hours per dialysis session, which has an enormous impact on the independency and the socioeconomic status of the patient. In addition, hemodialysis treatment has its restrictions as this method removes only a minor fraction of the waste products, predominantly the small uremic solutes (Molecular Weight (MW) <500 Da), from the patients' blood (10). Next to the hampered clearance capacity, the endocrine and metabolic functions cannot be replaced by hemodialysis. In a retrospective cohort study performed by Bradbury et al., it was shown that hemodialysis has a high yearly mortality risk of approximately 5-27%. The mortality rate was highest during the first three months after treatment initiation predominantly due to cardiac arrest (21). In patients chronically treated with hemodialysis the most frequent cause of death is cardiovascular disease. Together, the mortality rate in hemodialysis treated patients is 10-20 times higher than in the general population (22).

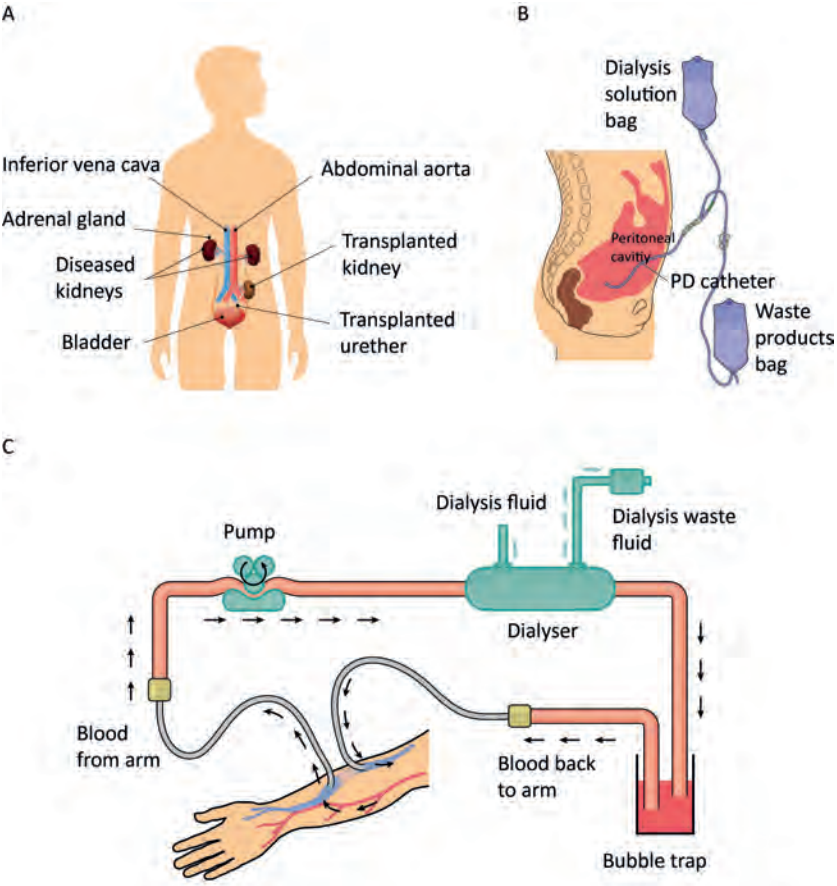
A
Inferior vena cava
Abdominal aorta
Adrenal gland
Diseased kidneys
Transplanted kidney
Bladder
Transplanted urether
B
Dialysis solution bag
Peritoneal cavity
PD catheter
Waste products bag
C
Pump
Dialysis fluid
Dialysis waste fluid
Dialyser
Blood from arm
Blood back to arm
Bubble trap

Figure 1.1 Schematic presentation of three available renal replacement therapies. (a) The transplanted donor organ is implemented in the patient, while both affected kidneys will remain in the body. A donor organ is the preferred treatment option for patients suffering from ESRD. (b) During peritoneal dialysis, a permanent tube will be connected to the patients' abdomen and the peritoneum will be used as a membrane which allow for the removal of small waste products from the blood into the dialysis waste fluid. Peritoneal home-dialysis is possible as long as infections are suppressed and the quality of the peritoneum is maintained. (c) For hemodialysis, vascular access can be accomplished via three ways i) a central venous catheter ii) an arteriovenous fistula which is a surgical connection between an artery and a vein to achieve a suitable access point or iii) an arteriovenous graft which is a biocompatible tube surgically connected between an artery and a vein. The patients' blood will pass the dialyser, which consists of numerous hollow fiber membranes, and ultrafiltration processes occur. During dialysis, small waste products will be removed from the blood into the dialysis waste fluid and the filtered blood will return to the patient. In general, hemodialysis is performed three times a week and four hours per session, often in a dialysis center or hospital.

The clinical impact of uremic toxins

Over the last years, knowledge on the role of accumulated waste products in the pathophysiology of kidney (-related) disease has greatly expanded. Retention solutes that interact negatively with biological systems are called uremic toxins. Dietary protein breakdown is a classical source of uremic toxin generation, as well as more alternative sources such as environmental factors. In addition, elevated levels of native molecules such as β2-microglobulin or parathyroid hormone are classified as uremic toxins as they modify physiological processes (10). Uremic toxins can be divided in three classes, based on their chemical properties that affect the clearance capacity during dialysis. Class 1 consists of small water-soluble solutes (MW <500 Da) such as urea, which can be easily removed using dialysis. Class 2 contains the middle molecules (MW >500 Da) such as β2-microglobulin, which can only be cleared using large-pore dialyzer membranes. Class 3 is composed of the protein-bound uremic toxins such as the tryptophan end-metabolites indoxyl sulfate (figure 1.2) or kynurenic acid. In general, the latter solutes have a MW <500 Da but are difficult to remove by dialysis as they are bound to plasma proteins which greatly extents their MW (23). The European Uremic Toxin Work Group (http://www.uremic-toxins.org/) is one of the leading international workgroups performing uremic toxin-related research. The EUTox workgroup identified over 100 uremic toxins and developed a web-based database to provide and collect knowledge on the pathologies associated with many of these solutes in CKD (www.uremic-toxins.org/DataBase, 9, 23, 24). For example, elevated plasma levels of cationic metabolites, such as guanidines derived from the arginine metabolism, were found to exert pro-inflammatory effects on the expression of leukocyte surface molecules and showed the possible interference of leukocytes with endothelial cells resulting in cardiovascular events (18, 25). In addition, anionic tryptophan and tyrosine end-metabolites, indoxyl sulfate, p-cresyl sulfate and p-cresyl glucuronide, associated also with cardiovascular disease via leucocyte activation and endothelial damage (19, 26). Moreover, elevated tryptophan-derived kynurenic acid levels might initiate neurological disorders, lipid metabolism disorder and anemia (17). Moreover, these anionic as well as cationic uremic toxins showed to interfere with renal drug handling. For example the renal clearance of the histamine H2-receptor antagonist, cimetidine, was found to be compromised (27-29). It was suggested that in uremia, various toxins directly or competitively inhibit in- and efflux transporters and drug-metabolism enzymes present in PTEC (30, 31), hence, contributing to CKD progression.

The current status of bioartificial kidney engineering

During the last decades hemodialysis treatment, pioneered by Dr. Kolff in the 1940's (32), has not been successfully modified to significantly improve waste product removal. To date, dialysis remains the only treatment option to partially replace kidney function. The development of an extracorporeal bioarticial kidney (BAK) device containing human PTEC to aid uremic toxin removal could be a promising new platform. PTEC are equipped with drug transporters to facilitate transepithelial transport of protein-bound endo- and xeno-biotics from the blood compartment into the lumen. At the basolateral membrane, organic anion transporter 1 and -3 (OAT1/3) mediate the uptake of anionic solutes, like indoxyl sulfate and multi drug resistance protein 2 and -4 (MRP2; MRP4) and Breast Cancer Resistance Protein (BCRP) facilitate their efflux (4, 33). For organic cations, organic cation transporter 2 (OCT2) mediates their uptake, and the Multidrug and Toxin Extrusion proteins MATE1 and MATE2K as well as P-glycoprotein (P-gp) and BCRP may be responsible for their luminal excretion (4, 33). In principle, implementing PTEC in an extracorporeal dialysis device containing numerous hollow fiber membranes could enhance uremic toxin removal and consequently reduce uremia and its associated complications in CKD patients (33). In the late 80's of last century, the first BAK device was initiated by Aebischer *et al.*, in which PTECs derived from animal sources where cultured on hollow fiber membranes (34). Several years later, Humes *et al.* developed a multifiber bioreactor containing porcine cells that showed transport of electrolytes, glucose, para-amminohippurate and, moreover, where metabolically active (35). Nowadays, it is known that animal-derived cell models, such as the frequently used dog- and porcine-derived, MDCK and LLC-PK1, respectively, lack many of the required proteins to support uremic toxins secretion via a BAK device (33). In addition, the application of non-human cell sources to treat human subjects is not preferable; therefore, many BAK studies using primary human PTEC were performed (36-39). Nowadays, the differentiation of stem cells into renal lineages is a promising platform to aid autologous BAK engineering. Hence, in depth research is required to unravel differentiation processes towards kidney-like cells and its associated cellular function prior to BAK implementation (40-42). The main focus in the majority of recently published BAK studies was to investigate the immunomodulatory effects in patients suffering from AKI (36, 38). Initially, promising results were obtained in phase I and II clinical trials, in which critically ill patients showed reduced cytokine levels and long-term survival improvement compared to the non-treated group. Unfortunately, a clinical phase IIb trial failed due to difficulties

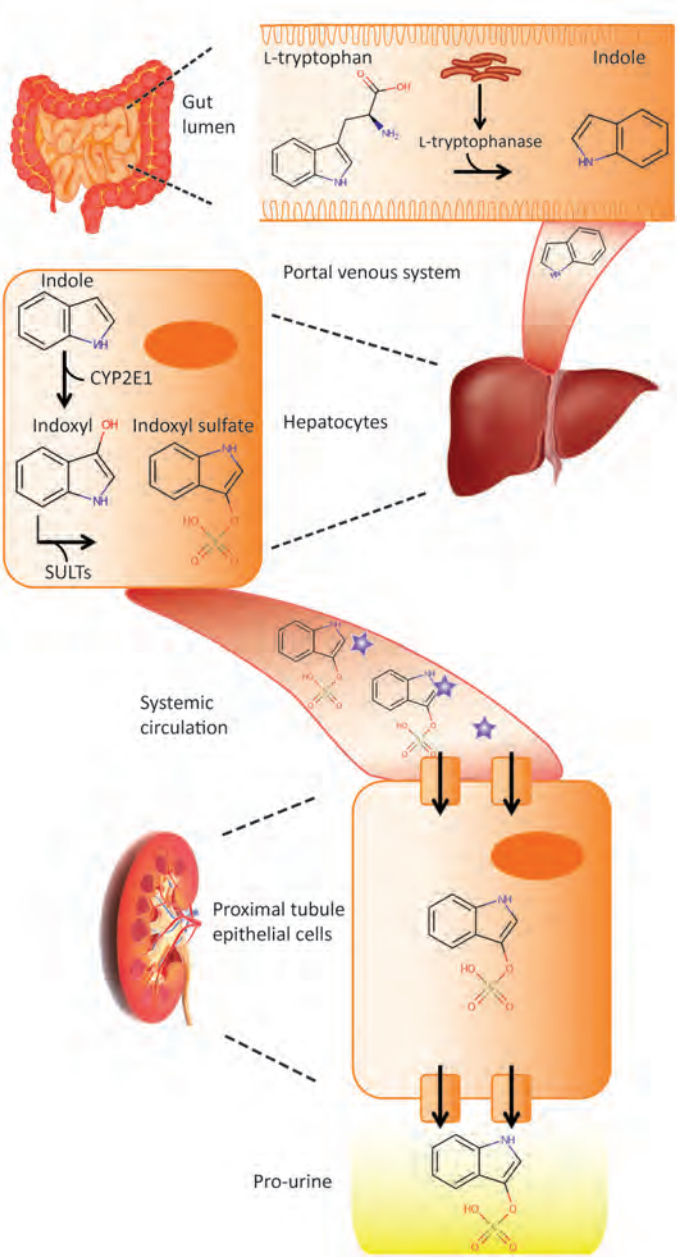
Gut
lumen
L-tryptophan
Indole
L-tryptophanase
Portal venous system
Indole
CYP2E1
Indoxyl
Indoxyl sulfate
Hepatocytes
SULTs
Systemic
circulation
Proximal tubule
epithelial cells
Pro-urine

Figure 1.2 Biosynthesis of indoxyl sulfate.

The dietery amino acid L-tryptophan is converted into indole in the gut lumen by the bacterial enzyme L-tryptophanase. Next, indole will enter the liver via the portal venous system and will be oxidized by cytochrome P450 2E1 (CYP2E1) into indoxyl. Subsequently, indoxyl will be sulfanized (SULTs: sulfotransferases) into indoxyl sulfate and the protein-bound end-metabolite will be removed from the systemic circulation into the pro-urine via active transport in the proximal segment of the kidneys.

* = human serum albumin

in the manufacturing process of the BAK and the study design (43). Therefore, alternative platforms should be investigated which require well characterized cell models in combination with appropriate biomaterials to support cellular maintenance.

OUTLINE OF THE THESIS

The aim of this thesis was to develop new therapeutic interventions for patients suffering from renal insufficiency, as current treatment modalities lack the ability to replace or ameliorate kidney function. Acute and chronic kidney diseases have major adverse effects on many biological systems in the human body and contribute to high morbidity and mortality rates. Appropriate therapeutic platforms to aid renal function could finally result in improved quality of life for patients and reduced mortality. In **Chapter 2** we describe the successful development of conditionally immortalized PTEC (ciPTEC) models isolated from human kidney tissue. The newly established models were thoroughly characterized and compared with the ciPTEC model isolated from urine, as cells exfoliated in urine are often thought to be partly dedifferentiated. Using genetic, protein and functional approaches, physiological characteristics of these models were investigated in detail and their potency to aid BAK engineering was evaluated. In **Chapter 3** we show the molecular mechanism of dexamethasone treatment as a possible new therapeutic intervention to reduce AKI-mediated PTEC injury. We unravelled the effects of dexamethasone on mitochondrial metabolism in an experimental inflammatory condition by analyzing various mitochondrial markers like reactive oxygen species (ROS), mitochondrial membrane potential, oxygen consumption, oxidative phosphorylation system (OXPHOS) complex activity but also mitochondrial mass, protein expression of OXPHOS complexes and cellular pH levels. In **Chapter 4** the current knowledge of bioengineering in the field of regenerative nephrology is described. In this review, a historical overview of bioartificial kidney development and the current state-of-the-art, including implementation of bioengineered membranes and the relevance of extracellular matrices was described. Next, the use of relevant renal epithelial cell lines versus the use of stem cells that need to be implemented in a suitable device are discussed. Moreover, the future of regenerative nephrology is being discussed including synthetic biotechnology approaches to improve the BAK. In **Chapter 5**, the development of a living membrane by culturing ciPTEC on polyethersulfone (PES)-based biofunctionalized 2D membranes is shown. In

this study, the coating was optimized to preserve high membrane permeance and to obtain optimal culture conditions on PES biomaterials. The properties of creatinine transport in tight epithelial cell monolayers on biofunctionalized PES membranes were studied and compared to a commercially available culture insert system. **Chapter 6** describes the next step towards BAK engineering. The coating, as applied in 2D biofunctionalized PES membranes, was optimized for 3D hollow fiber membrane (HFM) approaches and membrane properties were studied. Again, the coating appeared to be crucial to develop a successful bioartificial renal tubule containing a tight cell monolayer. As a first step in uremic solute transport, the active uptake of a known fluorescent OCT2 substrate in bioartificial renal tubules was investigated in real-time using a tailor made flow system. In the final experimental part of this thesis, **Chapter 7**, the transepithelial clearance of protein-bound anionic uremic toxins in bioartifical renal tubules was studied. First, the handling of anionic uremic toxins was investigated in flat monolayers and the pivotal role of in- and efflux transporters was demonstrated. Next, the properties of ciPTEC monolayers on biofunctionalized polyethersulfone hollow fiber membranes with respect to epithelial barrier function was studied. Finally, the transepithelial transport of protein-bound indoxyl sulfate and kynurenic acid in bioartifical renal tubules was investigated in real-time using a similar flow system as described in chapter 6. A general discussion in the context of the current knowledge regarding bioartificial kidney engineering accompanied by future perspectives is presented in **Chapter 8**, followed by a summary of this thesis in **Chapter 9**.

REFERENCES

1. Bogum J, Faust D, Zuhlke K, Eichhorst J, Moutty MC, Furkert J, et al. Small-molecule screening identifies modulators of aquaporin-2 trafficking. J Am Soc Nephrol. 2013;24:744-58.
2. Lainez S, Schlingmann KP, van der Wijst J, Dworniczak B, van Zeeland F, Konrad M, et al. New TRPM6 missense mutations linked to hypomagnesemia with secondary hypocalcemia. Eur J Hum Gen. 2014;22:497-504.
3. van der Hagen EA, Lavrijsen M, van Zeeland F, Praetorius J, Bonny O, Bindels RJ, et al. Coordinated regulation of TRPV5-mediated Ca(2)(+) transport in primary distal convolution cultures. Pflugers Arch. 2014;466:2077-87.
4. Masereeuw R, Mutsaers HA, Toyohara T, Abe T, Jhawar S, Sweet DH, et al. The kidney and uremic toxin removal: glomerulus or tubule? Sem Nephrol. 2014;34:191-208.
5. Boron WF, Boulpaep EL. Medical Physiology. 2003. p. 743-4.
6. Hoste EA, Bagshaw SM, Bellomo R, Cely CM, Colman R, Cruz DN, et al. Epidemiology of acute kidney injury in critically ill patients: the multinational AKI-EPI study. Intensive Care Med. 2015;41:1411-23.
7. Lameire NH, Bagga A, Cruz D, De Maeseneer J, Endre Z, Kellum JA, et al. Acute kidney injury: an increasing global concern. Lancet. 2013;382:170-9.
8. Siew ED, Davenport A. The growth of acute kidney injury: a rising tide or just closer attention to detail? Kidney Int. 2015;87:46-61.
9. Neirynck N, Vanholder R, Schepers E, Eloot S, Pletinck A, Glorieux G. An update on uremic toxins. Int Urol Nephrol. 2013;45:139-50.
10. Vanholder R, De Smet R. Pathophysiologic effects of uremic retention solutes. J Am Soc Nephrol. 1999;10:1815-23.
11. Fox CS, Matsushita K, Woodward M, Bilo HJ, Chalmers J, Heerspink HJ, et al. Associations of kidney disease measures with mortality and end-stage renal disease in individuals with and without diabetes: a meta-analysis. Lancet. 2012;380:1662-73.
12. Artz MA, Boots JM, Ligtenberg G, Roodnat JI, Christiaans MH, Vos PF, et al. Conversion from cyclosporine to tacrolimus improves quality-of-life indices, renal graft function and cardiovascular risk profile. Am J Transplant. 2004;4:937-45.
13. Savige J, Gregory M, Gross O, Kashtan C, Ding J, Flinter F. Expert guidelines for the management of Alport syndrome and thin basement membrane nephropathy. J Am Soc Nephrol. 2013;24:364-75.
14. van Gulick JJ, Gevers TJ, van Keimpema L, Drenth JP. Hepatic and renal manifestations in autosomal dominant polycystic kidney disease: a dichotomy of two ends of a spectrum. Neth J Med. 2011;69:367-71.
15. Wilmer MJ, Schoeber JP, van den Heuvel LP, Levtchenko EN. Cystinosis: practical tools for diagnosis and treatment. Pediatr Nephrol. 2011;26:205-15.

16. Ronco P, Debiec H. Pathophysiological advances in membranous nephropathy: time for a shift in patient's care. Lancet. 2015;385:1983-92.
17. Uwai Y, Honjo H, Iwamoto K. Interaction and transport of kynurenic acid via human organic anion transporters hOAT1 and hOAT3. Pharmacol Res. 2012;65:254-60.
18. Glorieux GL, Dhondt AW, Jacobs P, Van Langeraert J, Lameire NH, De Deyn PP, et al. In vitro study of the potential role of guanidines in leukocyte functions related to atherogenesis and infection. Kidney Int. 2004;65:2184-92.
19. Pletinck A, Glorieux G, Schepers E, Cohen G, Gondouin B, Van Landschoot M, et al. Protein-bound uremic toxins stimulate crosstalk between leukocytes and vessel wall. J Am Soc Nephrol. 2013;24:1981-94.
20. Kidney Link. http://www.kidneylink.org. 2014.
21. Bradbury BD, Fissell RB, Albert JM, Anthony MS, Critchlow CW, Pisoni RL, et al. Predictors of early mortality among incident US hemodialysis patients in the Dialysis Outcomes and Practice Patterns Study (DOPPS). Clin J Am Soc Nephrol. 2007;2:89-99.
22. de Jager DJ, Grootendorst DC, Jager KJ, van Dijk PC, Tomas LM, Ansell D, et al. Cardiovascular and noncardiovascular mortality among patients starting dialysis. Jama. 2009;302:1782-9.
23. Vanholder R, De Smet R, Glorieux G, Argiles A, Baurmeister U, Brunet P, et al. Review on uremic toxins: classification, concentration, and interindividual variability. Kidney Int. 2003;63:1934-43.
24. Duranton F, Cohen G, De Smet R, Rodriguez M, Jankowski J, Vanholder R, et al. Normal and pathologic concentrations of uremic toxins. J Am Soc Nephrol. 2012;23:1258-70.
25. Schepers E, Glorieux G, Dou L, Cerini C, Gayrard N, Louvet L, et al. Guanidino compounds as cause of cardiovascular damage in chronic kidney disease: an in vitro evaluation. Blood Purifn. 2010;30:277-87.
26. Barreto FC, Barreto DV, Liabeuf S, Meert N, Glorieux G, Temmar M, et al. Serum indoxyl sulfate is associated with vascular disease and mortality in chronic kidney disease patients. Clin J Am Soc Nephrol. 2009;4:1551-8.
27. Jansen J, De Napoli IE, Fedecostante M, Schophuizen CM, Chevtchik NV, Wilmer MJ, et al. Human proximal tubule epithelial cells cultured on hollow fibers: living membranes that actively transport organic cations. Sci Rep. 2015;5:16702.
28. Schophuizen CM, De Napoli IE, Jansen J, Teixeira S, Wilmer MJ, Hoenderop JG, et al. Development of a living membrane comprising a functional human renal proximal tubule cell monolayer on polyethersulfone polymeric membrane. Acta Biomater. 2015;14:22-32.
29. Schophuizen CM, Wilmer MJ, Jansen J, Gustavsson L, Hilgendorf C, Hoenderop JG, et al. Cationic uremic toxins affect human renal proximal tubule cell functioning through interaction with the organic cation transporter. Pflugers Archiv. 2013;465:1701-14.

30. Mutsaers HA, van den Heuvel LP, Ringens LH, Dankers AC, Russel FG, Wetzels JF, et al. Uremic toxins inhibit transport by breast cancer resistance protein and multidrug resistance protein 4 at clinically relevant concentrations. PloS One. 2011;6:e18438.
31. Mutsaers HA, Wilmer MJ, Reijnders D, Jansen J, van den Broek PH, Forkink M, et al. Uremic toxins inhibit renal metabolic capacity through interference with glucuronidation and mitochondrial respiration. Biochim Biophys Acta. 2013;1832: 142-50.
32. Kroop IG. America's initial application of the Kolff artificial kidney. Hemodialysis international International Symposium on Home Hemodialysis. 2010;14:346-7.
33. Jansen J, Fedecostante M, Wilmer MJ, van den Heuvel LP, Hoenderop JG, Masereeuw R. Biotechnological challenges of bioartificial kidney engineering. Biotechnol Adv. 2014;32:1317-27.
34. Aebischer P, Ip TK, Panol G, Galletti PM. The bioartificial kidney: progress towards an ultrafiltration device with renal epithelial cells processing. J Eur Soc Artif Organs. 1987;5:159-68.
35. Humes HD, MacKay SM, Funke AJ, Buffington DA. Tissue engineering of a bioartificial renal tubule assist device: in vitro transport and metabolic characteristics. Kidney Int. 1999;55:2502-14.
36. Humes HD, Weitzel WF, Bartlett RH, Swaniker FC, Paganini EP, Luderer JR, et al. Initial clinical results of the bioartificial kidney containing human cells in ICU patients with acute renal failure. Kidney Int. 2004;66:1578-88.
37. Tasnim F, Deng R, Hu M, Liour S, Li Y, Ni M, et al. Achievements and challenges in bioartificial kidney development. Fibrogenesis Tissue repair. 2010;3:14.
38. Tumlin J, Wali R, Williams W, Murray P, Tolwani AJ, Vinnikova AK, et al. Efficacy and safety of renal tubule cell therapy for acute renal failure. J Am Soc Nephrol. 2008;19:1034-40.
39. Dankers PY, Boomker JM, Huizinga-van der Vlag A, Wisse E, Appel WP, Smedts FM, et al. Bioengineering of living renal membranes consisting of hierarchical, bioactive supramolecular meshes and human tubular cells. Biomaterials. 2011;32:723-33.
40. Buffington DA, Pino CJ, Chen L, Westover AJ, Hageman G, Humes HD. Bioartificial Renal Epithelial Cell System (BRECS): A Compact, Cryopreservable Extracorporeal Renal Replacement Device. Cell Med. 2012;4:33-43.
41. Lam AQ, Freedman BS, Morizane R, Lerou PH, Valerius MT, Bonventre JV. Rapid and efficient differentiation of human pluripotent stem cells into intermediate mesoderm that forms tubules expressing kidney proximal tubular markers. J Am Soc Nephrol. 2014;25:1211-25.
42. Takasato M, Er PX, Chiu HS, Maier B, Baillie GJ, Ferguson C, et al. Kidney organoids from human iPS cells contain multiple lineages and model human nephrogenesis. Nature. 2015;526:564-8.

43. Humes HD, Buffington D, Westover AJ, Roy S, Fissell WH. The bioartificial kidney: current status and future promise. Pediatr Nephrol. 2014;29:343-51.

Section 1

PERFORMANCE OF HUMAN PROXIMAL TUBULE EPITHELIAL CELL MODELS TO AID RENAL BIOENGINEERING AND KIDNEY DISEASE MODELING

Chapter 2

A MORPHOLOGICAL AND FUNCTIONAL COMPARISON OF PROXIMAL TUBULE CELL LINES ESTABLISHED FROM HUMAN URINE AND KIDNEY TISSUE

ABSTRACT

Promising renal replacement therapies include the development of a bioartificial kidney using functional human kidney cell models. In this study, human conditionally immortalized proximal tubular epithelial cell (ciPTEC) lines originating from kidney tissue (ciPTEC-T1 and ciPTEC-T2) were compared to ciPTEC previously isolated from urine (ciPTEC-U).

Subclones of all ciPTEC isolates formed tight cell layers on Transwell inserts as determined by transepithelial resistance, inulin diffusion, E-cadherin expression and immunocytochemistry. Extracellular matrix genes collagen I and -IV α1 were highly present in both kidney tissue derived matured cell lines ($p<0.001$) compared to matured ciPTEC-U, whereas matured ciPTEC-U showed a more pronounced fibronectin I and laminin 5 gene expression ($p<0.01$ and $p<0.05$, respectively). Expression of the influx carrier Organic Cation Transporter 2 (OCT2), and the efflux pumps P-glycoprotein (P-gp), Multidrug Resistance Protein 4 (MRP4) and Breast Cancer Resistance Protein (BCRP) were confirmed in the three cell lines using real-time PCR and Western blotting. The activities of OCT2 and P-gp were sensitive to specific inhibition in all models ($p<0.001$). The highest activity of MRP4 and BCRP was demonstrated in ciPTEC-U ($p<0.05$). Finally, active albumin reabsorption was highest in ciPTEC-T2 ($p<0.001$), while Na^+-dependent phosphate reabsorption was most abundant in ciPTEC-U ($p<0.01$).

In conclusion, ciPTEC established from human urine or kidney tissue display comparable functional PTEC specific transporters and physiological characteristics, providing ideal human tools for bioartificial kidney development.

INTRODUCTION

Worldwide, about 2 million people suffering from renal disorders are treated with hemo- or peritoneal dialysis and this number still increases. Main factors contributing to this increase are aging, an increased incidence of diabetes mellitus and hypertension (1-3). Known limitations of the current dialysis methods as treatment modalities are related to the relatively poor clearance of protein-bound uremic retention solutes (4). Up to now, a large number of compounds have been classified as uremic retention solutes (5) and their accumulation may have severe clinical implications, such as renal fibrosis, bone disorders, cardiovascular disease and mental disorders (6). The preferred treatment of patients with end-stage renal disease (ESRD) is transplantation (7), which improves their quality of life and substantially reduces costs associated with extended dialysis (8). However, tremendous shortages of donor organs as well as complications arising from immunosuppressive treatment and organ rejection after transplantation are profound problems worldwide (9-11).

To replace kidney function, tissue engineering is a promising avenue of research to overcome the limitations of currently available renal replacement therapies (12). The development of functional and stable human renal epithelial cell models that are able to actively excrete uremic retention solutes, is a promising step towards a bioartificial kidney device. In the kidney, a heterogeneous cell system is present of which the proximal tubular epithelial cells (PTEC) play an important role in the excretion of endo- and xenobiotics, including uremic retention solutes. The excretory pathway is mediated via a complex interplay involving solute carriers, like OCT2 (SLC22A2), OAT3 (SLC22A6) and OAT3 (SLC22A8) (13), and ATP-binding cassette efflux pumps, such as p-glycoprotein; P-gp (ABCB1), MRP4 (ABCC4) and BCRP (ABCG2) (14). Besides waste product excretion, reabsorption of filtered solutes, such as phosphate, glucose, urate and albumin, occurs in PTEC (15-18).

In our group, a stable PTEC cell line isolated from human urine was developed (ciPTEC-U) (19). This cell line demonstrated functional characteristics of important in- and efflux transporters as well as active albumin and sodium-dependent phosphate transport (19), has proven to be valuable in elucidating renal pathological mechanisms (20-23) and in studying renal physiological transport pathways (24,25). However, as this cell line originates from urine, it could be argued that ciPTEC-U might not reflect the physiological situation

as close as cells directly derived from kidney tissue. Cells originating from urine are often thought to be exfoliated from tissue due to apoptosis-induced loss of function (26). Recently it was shown that overcrowding of epithelial cells due to proliferation and migration, induces the extrusion of living cells to maintain homeostasis in epithelial cell numbers (27). The aim of this study was to compare ciPTEC-U (19) with newly established human proximal tubular epithelial cell lines from human kidney tissue with respect to important functional properties. Human PTEC were isolated from nephrectomized kidneys followed by subcloning and immortalization techniques. Characterizing the newly established human proximal tubular epithelial cell lines will allow us to determine whether the sample source influences renal functional properties of cell lines in culture. Insights in these characteristics allows to identify the most suitable cell line for further development of a bioartificial kidney device.

MATERIALS AND METHODS

Chemicals and cell culture materials

All chemicals were purchased from Sigma-Aldrich (Zwijndrecht, The Netherlands) unless stated otherwise. Cell culture plates were purchased from Greiner Bio-One (Monroe, NC) and Transwell inserts were obtained from Corning Costar (cat. no 3460, New York, NY).

Ethics statement

The kidney tissue used for cell line development in this study was obtained from non-transplanted donors, after given informed consent. These organs could not be transplanted due to quality loss of the veins during surgery. No clinical history of renal disorders or any other chronic disease was identified.

Isolation and culture of ciPTEC from kidney tissue

Purification and isolation of renal epithelial cells from kidney tissue was performed as described previously (28). In short, epithelial cells were isolated by a gradient sieving procedure and subjected to collagenase digestion (29). The collected primary fraction was transferred to supplemented PTEC culture media: phenol-red free DMEM-HAM's F12 medium (catalogue number 11039, Lonza, Basel, Switzerland) containing 10% (v/v) FCS (Greiner Bio-One, Monroe, NC), 5 mg/ml insulin, 5 mg/ml transferrin, 5 ng/ml selenium, 36 ng/ml hydrocortisone, 10 ng/ml EGF and 40 pg/ml tri-iodothyronine. Primary

cells were immortalized within the first two passages. Immortalization was performed using a combination of hTERT and SV40t as described previously (19,30). To obtain a homogeneous culture, cells were subcloned using irradiated NIH 3T3 fibroblast as non-dividing feeder cells (30). After culturing for 2 weeks at 33°C, 5% (v/v) CO_2, single cell clones were visible and picked using cloning discs drained in trypsin-EDTA (MP Biomedicals, Solon, OH). Single cell clones were transferred to a well plate and grown until confluent at 33°C, 5% (v/v) CO_2. Optimal seeding conditions were determined for each obtained ciPTEC line in well plates and Transwell inserts (50 µg/ml collagen IV coating for ciPTEC-U (C6745-1ml) by testing morphological characteristics and monolayer integrity properties using a cell density range (data not shown). According to the conditions described previously (19), ciPTEC were cultured for 24 h at 33°C 5% (v/v) CO_2 to proliferate and subsequently transferred to 37°C, 5% (v/v) CO2 for 7 days to mature. Up to at least 40 cell passage numbers were used to investigate proliferation and functional properties following prolonged culturing. Phase contrast images were captured using a Leica DM IL phase contrast microscope.

Immunocytochemistry

To investigate morphology and polarization characteristics of the ciPTEC monolayers, immunocytochemistry was performed using cells cultured on polyester Transwell inserts. Matured ciPTEC were fixed using 2% (w/v) paraformaldehyde in HBSS supplemented with 2% (w/v) sucrose for 5 min and permeabilized in 0.3% (v/v) triton X-100 in HBSS for 10 min. To prevent non-specific binding of antibodies, cells were exposed to block solution containing 2% (w/v) bovine serum albumin fraction V (Roche, Woerden, The Netherlands) and 0.1% (v/v) tween-20 in HBSS for 30 min. Cells were incubated with antibodies diluted in block solution against the tight junction protein zonula occludens 1 (ZO-1, 1:50 dilution, Invitrogen, Carlsbad, CA) for 1 h, followed by incubation with goat-anti-rabbit-Alexa488 conjugate (1:200, Life Technologies Europe BV, Bleiswijk, The Netherlands) for 30 min. Finally, DAPI nuclei staining (300 nM, Life Technologies Europe BV) was performed for 5 min. Protein expression and localization were examined using the Olympus FV1000 Confocal Laser Scanning Microscope (Olympus, Tokyo, Japan) and images were captured using the Olympus software FV10-ASW version 1.7. Next, cell size measurements were performed using Image J software (version 1.40g).

Transepithelial barrier functions

Transepithelial resistance of matured ciPTEC monolayers on Transwell inserts was measured using the Millicell electrical resistance volt-ohm system (Millipore, Billerca, MA). Measurements were performed as described in the manufacturer's protocol. To determine the tightness of the ciPTEC monolayers, inulin-FITC (Sigma-Aldrich) diffusion was measured of matured ciPTEC cultured on Transwell inserts. Both apical and basolateral compartments were washed once with HBSS buffer (Life Technologies Europe BV), prior to 0.1 mg/ml inulin-FITC in HBSS basolateral exposure for 1h at 37°C, 5% (v/v) CO_2. Fluorescence was detected by measuring samples (200 µl) at excitation wavelength 485 nm and emission wavelength 535 nm, using a CytoFluor II Microplate reader (MTX Lab Systems, Vienna, VA).

To investigate monolayer development further, the presence of E-cadherin, a calcium-dependent cell-cell adhesion protein abundantly expressed in PTEC cells (31), was investigated in proliferating and matured cells. After harvesting, cells were fixed and permeabilized using 4% (w/v) PFA and 0.1 % (v/v) saponin in HBSS on ice for 10 min. After centrifuging, cell pellets were resuspended in rat anti-E-cadherin antibody (1:100 in HBSS) and incubated at RT for 30 min. Next, cells were centrifuged again, pellets resuspended in goat anti-rat Alexa 488 conjugate (1:200, Life Technologies Europe BV, Bleiswijk, The Netherlands) and incubated at RT for 30 min. After a final centrifuge step, cells were resuspended in HBSS buffer and measured using a flowcytometer (FACSCalibur BD, software BD CellQuest Pro version 6.0, Becton Dickinson, Franklin Lakes, NJ) gating on live cells (a total of 15,000 cells counted). Separate cell fractions were incubated solely with goat anti-rat Alexa 488 conjugate and signal measured was set as a negative control. Next to the extracted geometric mean data, representative flowcytometer histograms are shown to illustrate signal intensities (Alexa 488/FL1 signal).

Gene expression of relevant transporters and extracellular matrix proteins in ciPTEC

Total RNA was isolated from proliferating and matured cells using TRIzol (Life Technologies Europe BV) and chloroform extraction according to the manufacturer's protocol. The Omniscript RT kit (Qiagen, Venlo, The Netherlands) was used to synthesize cDNA. The mRNA expression levels of PTEC transporter genes were detected using gene specific primer-probe sets (Table S2.1, Applied Biosystems, CA, USA) and TaqMan Universal PCR Master Mix (Applied Biosystems). The quantitative PCR reactions were performed

using the CFX96 Real Time PCR system (Bio-Rad Laboratories, Veenendaal, The Netherlands) and data were analyzed using the CFX Manager software (Bio-Rad Laboratories). The mRNA expression levels of extracellular matrix (ECM) genes were investigated using primer sets (Table S2.2) and SybrGreen PCR Master Mix (Qiagen). The quantitative PCR reactions were performed using the ABI 7900HT sequence detection system (Applied Biosystems, Nieuwekerk a/d IJssel, The Netherlands). Data of matured cells were normalized to expression levels of the reference gene GAPDH, and were expressed as fold increase compared to matured ciPTEC-U (19). To compare expression levels from the proliferating towards matured stage per cell line, data of matured cells were expressed as fold increase compared to the corresponding proliferating cells (supplemental figures S2.1 and S2.2).

Determination of proximal tubular specific transporter proteins

To detect proteins of interest in proliferating and matured cells, membrane fractions were obtained by ultracentrifugation. Confluent cell layers cultured in T175 flasks were harvested and homogenized in 30 ml buffer containing 18 mM Tris-HCL (pH 7.4), 6 mM EGTA, 0.3 M mannitol and protease inhibitors (100 mM phenylmethane sulphonylfluoride, 5 mg/ml aprotinin, 5 mg/ml leupeptin, and 5 mg/ml pepstatin). The suspension was homogenized using a tight fitting Dounce homogenizer (Kimble Chase LLC, Vineland, NJ) followed by ultracentrifugation (Sorval WX80, Thermo Fisher Scientific, Walhtam, MA) at 100,000 x *g* for 45 min at 4°C. Finally, the membrane pellets were resuspended in 100 µl RIPA buffer containing 1% (w/v) Igepal CA630, 0.5% (w/v) Na-deoxycholate, 0.1% (v/v) SDS (Amersham Biosciences, NJ, USA) and protease inhibitors (0.01% (v/v) phenylmethane sulphonylfluoride, 3% (v/v) aprotinin and 1 mM sodium orthovanadate). The amount of total protein was measured using the Bio-Rad protein detection reagent system (Bio-Rad Laboratories). Protein expression of Organic Cation Transporter 2 (OCT2), P-glycoprotein (P-gp), Multidrug Resistance Protein 4 (MRP4) and Breast Cancer Resistance Protein (BCRP) was investigated by Western blotting using 12%, 6%, 6% and 10% (w/v) sodium dodecyl sulphate polyacrylamide gel electrophoresis (SDS-PAGE), respectively. The iBlot Dry Blotting System (Life Technologies Europe BV) was used for transferring proteins from the gels onto a nitrocellulose membrane. To prevent non-specific binding of antibodies, membranes were blocked in PBS supplemented with 0.1% (v/v) tween-20 (PBS-T) and 5% (w/v) milk powder (Campina, Woerden, The Netherlands) for 30 min. Subsequently, membranes were washed three times in PBS-T. Next, membranes were

incubated for 1.5 h with rabbit anti-OCT2 antibody (1:500, Alpha Diagnostic International, San Antonio, TX), mouse anti-P-gp antibody (1:200, Abcam, Cambridge, UK), rabbit anti-MRP4 antibody (1:100, M49, (32)) or mouse anti-BCRP (1:200, Abcam®, Cambridge, UK). As a loading control mouse anti-β-actin (1:100,000) or rabbit anti-Na, K-ATPase antibody (α-subunit, 1:2,000, C356-M09 (33)) was used. Subsequently, after three washing steps in PBS-T, membranes were exposed to secondary antibodies Alexa fluor® 680 goat anti-rabbit IgG (1:10,000, Life Technologies Europe BV), IRDye 800 goat anti-mouse IgG (1:10,000, Rockland, PA) or IRDye 800 goat anti-rabbit IgG (1:10,000, Rockland, PA) for 1.5 h. Fluorescence was quantified using the Odyssey Infrared Imaging System (version 2.1, LICOR® Biosciences, Lincoln, NE). Data of proliferating and matured cells were normalized to protein expression levels of the loading control and plotted in absolute pixel intensities.

Transport assays of renal in- and efflux proteins

The activity of the renal OCT influx proteins was measured as previously described by Schophuizen *et al.* (25). In short, harvested matured cell suspensions were exposed to the fluorescent OCT substrate 4-(4-(dimethylamino)styryl)-N-methylpyridinium iodide (ASP^+) in the presence or absence of 5 mM OCT inhibitor tetrapentylammonium chloride (TPA). Data plotted were corrected for cell numbers.

The activity of the renal efflux protein P-gp in ciPTEC was examined by measuring the amount of calcein accumulation (34). In short, matured cells were exposed to 1 μM calcein-AM (Life Technologies Europe BV) in the presence or absence of 5 μM P-gp inhibitor PSC833 (Tocris Biosciences, Bristol, UK) for 1 h at 37°C, 5% (v/v) CO_2. Fluorescence in lysed cells was measured and data plotted were corrected for protein concentrations.

To evaluate transport characteristics of the renal efflux transporters BCRP and MRP4 (32,35), ciPTEC were exposed to kynurenic acid, the end product of tryptophan metabolism. Kynurenic acid is a known uremic retention solute and a substrate for both renal efflux transporters (24,36). To investigate the transport properties of these proteins, cells were cultured in 24 well plates and matured monolayers were gently washed three times using krebs-henseleit buffer supplemented with 10 mM Hepes (pH 7.4, adjusted with Tris-HCl). Subsequently, cells were pre-incubated with supplemented krebs-henseleit buffer in the presence or absence of 5 μM KO143, a known BCRP inhibitor (37), and 5 μM MK 571 a known MRP inhibitor (38) (Alexis Biochemicals, Leiden,

The Netherlands) at 37°C, 5% (v/v) CO_2 for 2 h. After pre-incubation, cells were exposed to 10 µM ^{3}H-kynurenic acid (Scopus Research BV, Wageningen, The Netherlands) at 37°C for 2 h. The uptake was terminated by washing the cells 3 times with ice-cold supplemented krebs-henseleit buffer. Cells were lysed using 0.1% (v/v) triton X-100. To each sample 2 ml of scintillation liquid was added and radioactivity was detected using liquid scintillation counting. Counts measured in supplemented krebs-henseleit buffer (blank) were subtracted and data plotted were corrected for protein concentrations.

Albumin and phosphate uptake assays

To investigate albumin uptake mediated by endocytosis, matured ciPTEC were exposed to serum free medium for 4 h at 37°C, 5% (v/v) CO_2. Subsequently, cells were exposed to 50 µg/ml BSA-FITC and incubated at 37°C, 5% (v/v) CO_2 for 30 min. In addition, experiments were performed at 4°C to inhibit endocytosis. After the incubation period, cells were harvested and centrifuged at 1,500 x g for 5 min. The cell pellet was resuspended in 4% (w/v) paraformaldehyde in PBS. Finally, intracellular albumin was measured using a flowcytometer (FACSCalibur BD, software BD CellQuest Pro version 6.0, Becton Dickinson, Franklin Lakes, NJ) gating on live cells (15,000 cells counted). Data was analyzed using FlowJo software (version 9.2) and relative net uptake data was plotted next to the actual flowcytometer histograms.

Phosphate uptake was performed in confluent monolayers cultured at 33°C and 37°C, 5% (v/v) CO_2 with $^{32}PO_4$ (Perkin Elmer, Waltham, MA) as described earlier by Malmstrom *et al.* (19,39). Cells were cultured in 24 well plates and gently washed three times using wash buffer (20 mM Hepes, 5.6 mM $CaCl_2$, 10.8 mM KCl, 2.4 mM $MgCl_2$, 274 mM NaCl) at 37°C. To determine the sodium-dependent uptake of phosphate, experiments were performed in the absence of sodium by replacing NaCl with 274 mM N-methyl-D-glucamine. The uptake buffer was added for 5 min at 37°C consisting of wash buffer, supplemented with 0.22 mM phosphate with 1.0 µCi/mL $^{32}PO_4$ added as tracer. The uptake was terminated by washing the cells five times with ice-cold wash buffer. Cells were lysed using 0.5 ml 0.05 M Na^+-deoxycholate in 0.1 M NaOH. To each sample 2 ml of scintillation liquid was added and radioactivity was detected using liquid scintillation counting. Counts measured in wash buffer (blank) were subtracted and data plotted were corrected for protein concentrations.

Data analysis

All data are expressed as mean ± SEM Statistical analysis was performed using one-way ANOVA analysis followed by Dunnett's Multiple Comparison test or, where appropriate, an unpaired *t* test with GraphPad Prism version 5.02 (La Jolla, CA). A p-value of <0.05 was considered significant.

RESULTS

Successful development of ciPTEC lines from human kidney tissue isolates

To appreciate the functional capacity of ciPTEC-U (19), new PTEC cell lines were generated from human kidney tissue and characterized to compare with ciPTEC-U. PTEC isolates were obtained from three different kidney donors and primary cells were grown successfully. All cell cultures that were immortalized using SV40t and hTERT, were found resistant to both hygromycin B and geneticin (G418) thereby confirming successful transduction. Next, cells were subcloned to obtain homogenous cell lines after which cell proliferation could be maintained for up to at least cell passage 42 without morphological changes. From the original three kidney isolates, different subclones were obtained. Based on mRNA expression levels of PTEC transporters, morphology and monolayer tightness, two out of twenty six kidney subclones were selected (ciPTEC-T1 and -T2) for detailed characterization. The ciPTEC-T1 and -T2 originated from the same donor and were compared in great detail with ciPTEC-U (19). Figure 2.1a represents a flow chart of the isolation and selection procedure performed in this study. Representative phase contrast images of the selected clones ciPTEC-T1 and -T2 are shown in Figure 2.1b. Transduction of kidney tissue derived cultures with hTERT solely did not result in suitable cell lines as determined by morphology and cell proliferation (data not shown).

Morphological characteristics and extracellular matrix investigation

Optimal seeding conditions to obtain confluent layers of ciPTEC in well plates and Transwell inserts were determined as indicated in table 2.1. A collagen IV coating of 50 µg/ml stimulated the development of a homogeneous tight layer of ciPTEC-U on Transwell inserts. Interestingly, no coating was necessary for ciPTEC-T1 and -T2 to develop a homogeneous cell monolayer on the inserts (Figure 2.2a - c). In well plates, confluent ciPTEC monolayers were obtained without any additional coatings.

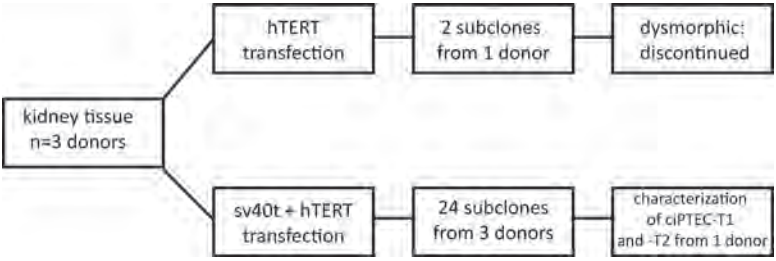

Figure 2.1a Flow chart of clone selection.
Schematic overview of the cell isolation process from kidney tissue upon establishment of clonal cell lines. Cells were isolated from three donors and 26 subclones were selected in a first round. These subclones were characterized morphologically, but also gene expression levels of PTEC specific transporters were investigated. Transduction of kidney tissue derived cultures with hTERT solely did not result in suitable cell lines as determined by morphology and cell proliferation. Finally, two clones from the same donor obtained after combined SV40 and hTERT transductions were chosen for detailed characterization (ciPTEC-T1 and -T2), based on PTEC specific morphological characteristics and highest gene expression levels of PTEC transporters.

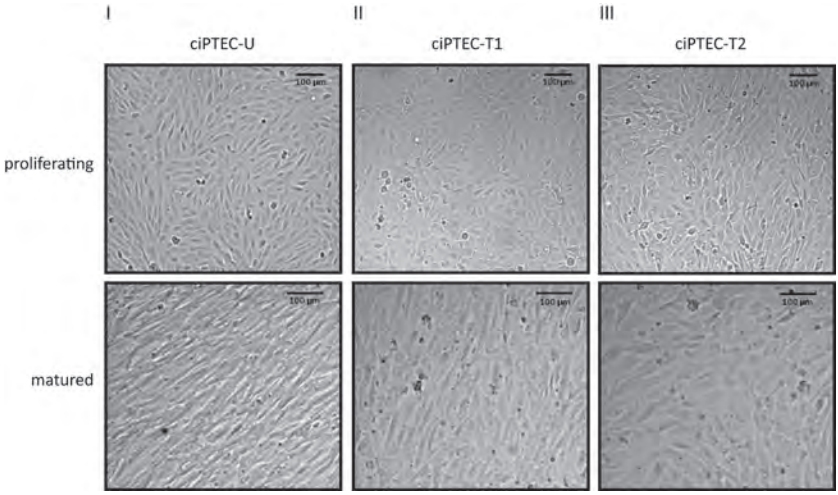

Figure 2.1b Representative phase contrast images of ciPTEC.
Proliferating (33°C, 5% (v/v) CO_2) and fully matured (7 days at 37°C, 5% (v/v) CO_2) ciPTEC-U passage 40 (I), -T1 passage 38 (II), and -T2 passage 42 (III) are shown.

The tight junction protein zonula occludens-1 (ZO-1) in PTEC is a marker for the integrity and polarity of the cell layer. Furthermore, tight junctions contain interacting proteins that regulate differentiation, proliferation and gene expression, indicating an important role in PTEC functionality (40). Cells cultured on Transwell inserts, were stained against ZO-1 and the protein expression was examined using confocal microscopy. A clear ZO-1 expression was visible for all three cell lines (Figure 2.2a - c). A z-scan depicts the fluorescent signal of tight junction expression at the cell boundaries in each ciPTEC model, but most abundantly in ciPTEC-U, and confirms polarization of the cells. Next to this, we determined cell diameter and observed a larger span for matured ciPTEC-T1 (19.4 µm ± 0.8, $p<0.001$; Figure 2.2b) and -T2 (21.7 µm ± 0.6, $p<0.001$; Figure 2.2c) as compared to matured ciPTEC-U (10.9 µm ± 0.6; Figure 2.2a). Both ciPTEC cell lines isolated from kidney tissue showed a larger span compared to ciPTEC-U when cultured in similar uncoated cell culture flasks, at both temperatures (Figure 2.1b). This indicates that cell size differences were not influenced by a collagen IV coating but may possibly source related.

Cell monolayer tightness was examined further by determination of the paracellular permeability of the cell monolayers using the diffusion marker inulin (41). CiPTEC cultured on Transwell inserts were basolaterally exposed to FITC-inulin. No differences were observed in inulin flux between the ciPTEC-U versus kidney tissue derived cell lines, as shown in table 2.2. Furthermore, the epithelial barrier integrity was investigated by measuring the transepithelial electric resistance (TEER). Cell lines were cultured on Transwell inserts and the TEER was measured in matured cells (Table 2.2). CiPTEC-T1 demonstrated a higher resistance (140 ± 4 Ω/cm^2, $p<0.05$) as compared to ciPTEC-U (124 ± 3 Ω/cm^2), whereas no significant differences were observed between ciPTEC-T2 (126 ± 4 Ω/cm^2) and ciPTEC-U.

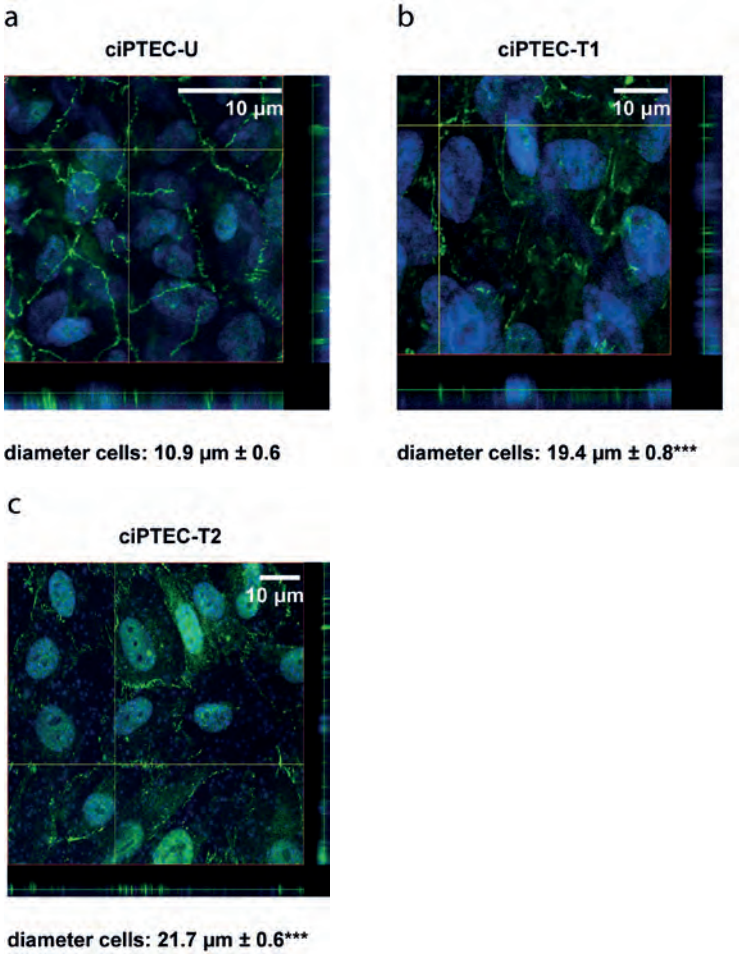

Figure 2.2 Expression of ZO-1 protein in ciPTEC.
Representative confocal images of ZO-1 (green) in x-y and y-z planes are shown (nuclei are stained with DAPI (blue)) in matured (37°C) ciPTEC cultured on Transwell inserts. (a-c) The expression of ZO-1 (green fluorescent) was determined at the cell boundaries and was most abundantly present in ciPTEC-U (a). Furthermore, the average cell diameter was measured, demonstrating a significantly larger cell size of ciPTEC-T1 and -T2 as compared to ciPTEC-U. Note: ciPTEC-U were cultured on collagen IV coated surfaces, whereas ciPTEC-T1 and -T2 were cultured on uncoated Transwell inserts. *** = $p<0.001$, using one-way ANOVA analysis followed by Dunnett's multiple comparison test.

Table 2.1 Optimal ciPTEC seeding density in well plates and Transwell inserts

Cell line	Well plates seeding density (cells. cm^{-2})	Transwell inserts seeding density (cells. cm^{-2})
ciPTEC-U	4.8×10^4	1.3×10^5
ciPTEC-T1	1.9×10^4	0.60×10^5
ciPTEC-T2	1.9×10^4	0.60×10^5

ciPTEC cultured at indicated densities resulted in tight monolayer formation upon 7 days maturation.

Table 2.2 Transepithelial barrier functions of ciPTEC

Cell line	Inulin diffusion (pmol. min^{-1}. cm^{-2})	TEER (Ω/cm^2)
ciPTEC-U	9.3 ± 0.4	124 ± 3
ciPTEC-T1	8.0 ± 0.7	140 ± 4*
ciPTEC-T2	9.2 ± 0.5	126 ± 4

Monolayer integrity was measured using inulin flux and transepithelial electric resistance determination. * = $p<0.05$, using one-way ANOVA analysis followed by Dunnett's multiple comparison test. Data presented are means of three independent experiments and expressed as mean ± SEM.

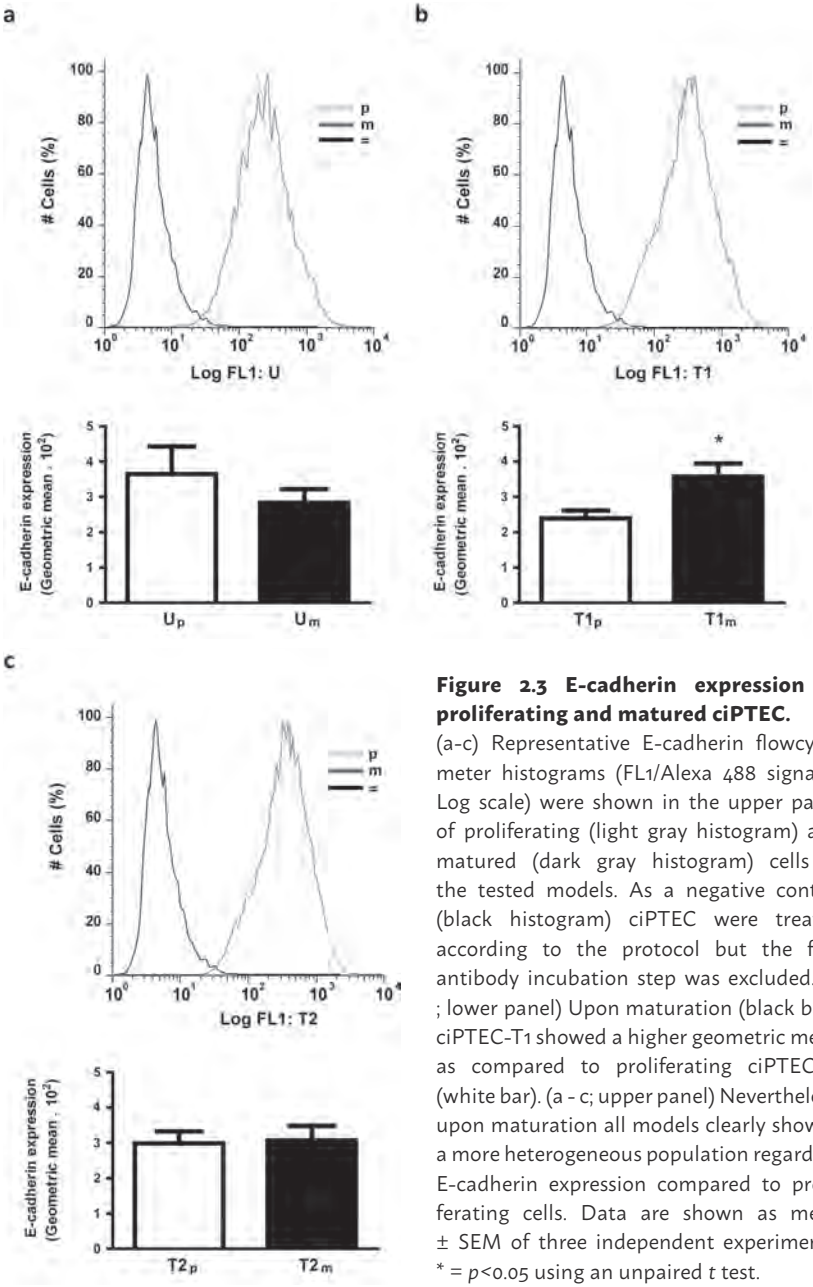

Figure 2.3 E-cadherin expression in proliferating and matured ciPTEC.
(a-c) Representative E-cadherin flowcytometer histograms (FL1/Alexa 488 signal – Log scale) were shown in the upper panel of proliferating (light gray histogram) and matured (dark gray histogram) cells in the tested models. As a negative control (black histogram) ciPTEC were treated according to the protocol but the first antibody incubation step was excluded. (b ; lower panel) Upon maturation (black bar), ciPTEC-T1 showed a higher geometric mean as compared to proliferating ciPTEC-T1 (white bar). (a - c; upper panel) Nevertheless, upon maturation all models clearly showed a more heterogeneous population regarding E-cadherin expression compared to proliferating cells. Data are shown as mean ± SEM of three independent experiments. * = $p<0.05$ using an unpaired *t* test.

The cell-cell adhesion protein E-cadherin was clearly present in the models tested (Figure 2.3) in proliferating (light gray histogram) as well as in matured (dark gray histogram) ciPTEC compared to the negative control (black histogram), emphasizing the abundant epithelial characteristics of these models. Interestingly, matured ciPTEC showed a more heterogeneous population compared to proliferating ciPTEC. Based on geometric mean data extracted from these histograms, matured ciPTEC-T1 only showed a more abundant prevalence of E-cadherin when compared to proliferating ciPTEC-T1.

To gain more insight in complexes involved in cell development (42,43), the presence of ECM genes was investigated. The mRNA expression levels of collagen I and –IV αI, fibronectin I and laminin 5 (LAMA5; alpha-5 subunit of laminin-10, -11 and -15) were detected in matured ciPTEC-U, -T1 and -T2. Interestingly, significant differences were observed between the cell lines. In matured ciPTEC-T1 and -T2 a higher expression of collagen I - and IV αI (Figure 2.4a and b, $p<0.001$) was observed compared to matured ciPTEC-U. Whereas fibronectin I and laminin 5 expression was lower in matured kidney tissue derived cell lines (fibronectin I ciPTEC-T1 and -T2: $p<0.01$, laminin 5 ciPTEC-T2: $p<0.05$, ciPTEC-T1: not significant) compared to ciPTEC-U. In supplemental figure S2.1, mRNA expression levels of these genes in proliferating versus matured cells are shown. Matured tissue derived cell lines showed an increased collagen I αI (supplemental figure S2.1a; $p<0.001$), fibronectin I (supplemental figure S2.1c; $p<0.001$) and laminin 5 (supplemental figure S2.1d; $p<0.05$) gene expression, whereas matured ciPTEC-U showed a less pronounced genetic ECM profile. Interestingly, collagen IV αI (supplemental figure S2.1b) gene expression upon maturation was lower ($p<0.001$) in each cell line compared to proliferating cells.

Gene and protein expression levels of PTEC specific transporters

The excretion of endo- and xenobiotics in the proximal tubular system is mediated via various important in- and efflux transporters like OCT2, P-gp, MRP4 and BCRP (13,14). The presence of these PTEC specific transporters was investigated on gene and protein level in matured ciPTEC-U, -T1 and -T2. The mRNA expression levels of most transporters (Figure 2.5) were comparable between the three matured cell lines, except for OCT2 in ciPTEC-T1 ($p<0.05$) and BCRP in ciPTEC-T2 ($p<0.05$) which showed a higher expression as compared to matured ciPTEC-U. In supplemental figure S2.2,

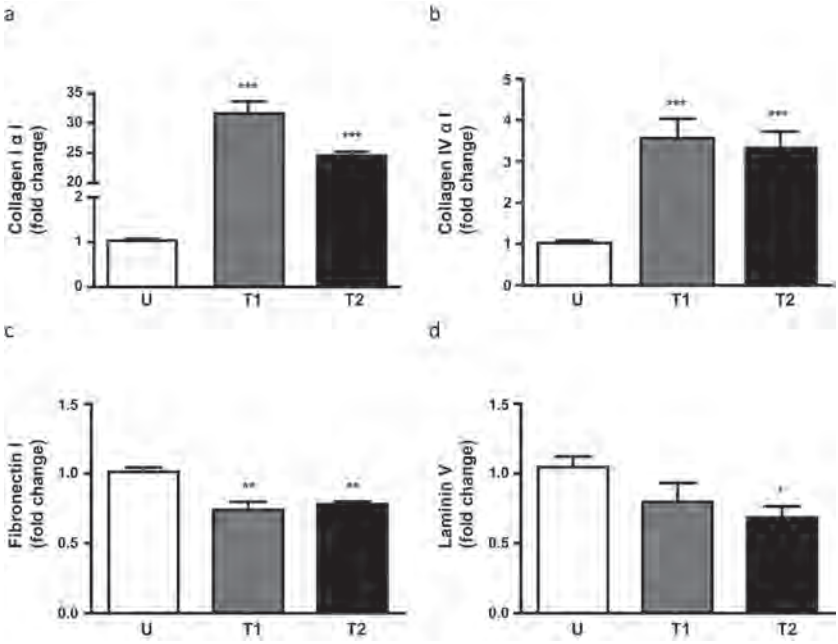

Figure 2.4 Expression of extracellular matrix genes in matured ciPTEC models.
(a and b) Both cell lines derived from kidney tissue showed a higher gene expression of collagen I α1 (a) and –IV α1 (b) compared to ciPTEC-U. (c) In ciPTEC-T1 and -T2, a lower gene expression of fibronectin I was observed compared to ciPTEC-U. (d) In ciPTEC-T2, a lower gene expression of laminin 5 was observed compared to ciPTEC-U. Expression levels were corrected for corresponding GAPDH mRNA levels and data are expressed as fold change and compared to ciPTEC-U. Data are presented as means of three independent experiments ± SEM * = $p<0.05$, ** = $p<0.01$, ***= $p<0.001$, using an ANOVA analysis followed by Dunnett's multiple comparison test.

mRNA expression levels of these genes in proliferating versus matured cells are shown. Each matured cell line showed an increased OCT2 gene expression (supplemental figure S2.2a; ciPTEC-U and -T1 $p<0.05$, ciPTEC-T2 $p<0.001$), whereas P-gp (supplemental figure S2.2b) and MRP4 (supplemental figure S2.2c) gene expressions were more abundantly only in matured tissue-derived cell lines (P-gp ciPTEC-T1 $p<0.01$, ciPTEC-T2 $p<0.05$; MRP4 ciPTEC-T2 $p<0.01$). Although not significant, the gene expression of BCRP (supplemental figure S2.2d) showed less expression upon maturation in each cell line.

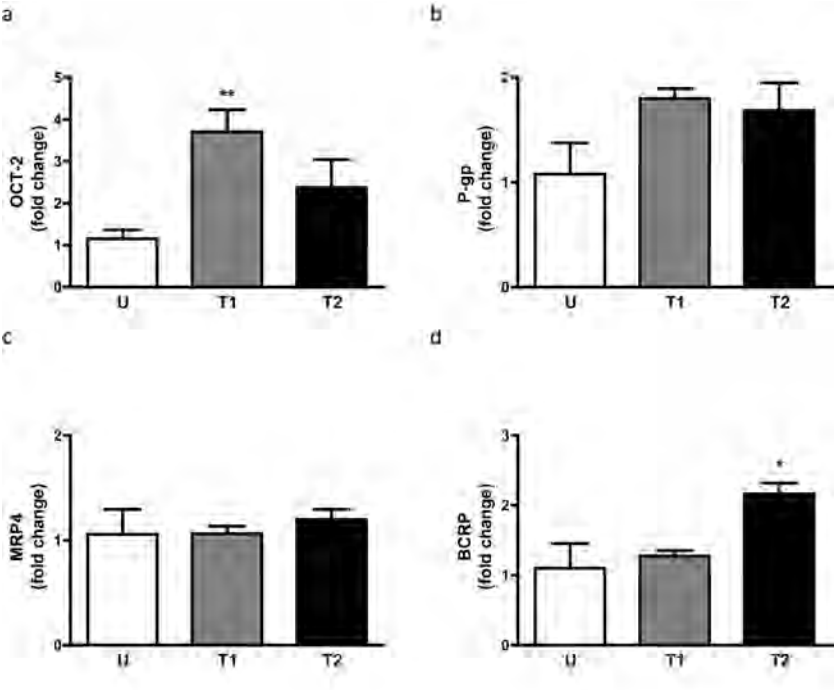

Figure 2.5 Expression of proximal tubular specific transporters in matured ciPTEC models.

(a) In ciPTEC-T1 a higher observed compared to ciPTEC-U. Expression levels were corrected for corresponding GAPDH mRNA levels and data were expressed as fold change and compared to ciPTEC-U. Data are presented as means of three independent experiments ± SEM * = $p<0.05$, ** = $p<0.01$, using an ANOVA analysis followed by Dunnett's multiple comparison test.OCT2 gene expression was observed compared to ciPTEC-U. (b and c) No significant differences in P-gp (b) and MRP4 (c) gene expressions were observed between the three cell lines. (d) In ciPTEC-T2 a higher BCRP gene expression was.

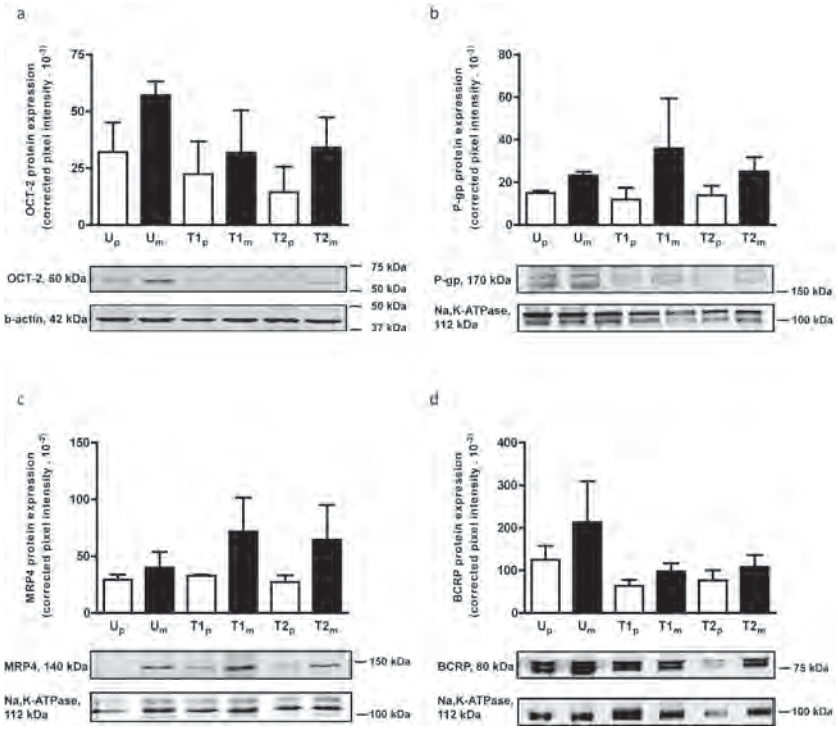

Figure 2.6 Protein expression of OCT2, P-gp, MRP4 and BCRP in membrane fractions of ciPTEC-U, -T1 and -T2.

(a - d) Although not significant, all matured (black bars) ciPTEC showed a slight increased OCT2 (a), P-gp (b), MRP4 (c) and BCRP (d) expression compared to proliferating (white bars) ciPTEC. Signal intensities were corrected for the corresponding reference protein, which was used as a loading control and expression was analyzed semi-quantitative by measuring pixel intensity. Note that due to Western blot conditions Na,K-ATPase appears in multiple bands (b and c). Hence, for semi-quantification the intensity between 100 - 120 kDa was used as a reference. To semi-quantify the OCT2 expression, β-actin was used as a reference protein since the molecular mass of β-actin (42 kDa) is more within the mass range of OCT2 (60kDa) than Na, K-ATPase (112 kDa). The blots presented are representative for protein expression in the ciPTEC models. Data are presented as means of three independent experiments ± S.E.M and statistical analysis was performed using an ANOVA analysis followed by Dunnett's multiple comparison test.

In fully differentiated cells, a non-significant but recurrent trend in abundance of transport protein expression was observed, which points towards a somewhat higher expression of the investigated transporters as compared to the corresponding proliferating cells (Figure 2.6). The expression levels between the different cell lines in their proliferating or matured state was not significantly different.

Functional transport in ciPTEC

To functionally characterize OCTs, we used a recently established assay based on the uptake of the fluorescent marker substrate ASP^+ in ciPTEC suspensions (25) . All three cell lines showed a clear ASP+ uptake, which was sensitive to inhibition by TPA ($p<0.001$), indicating active OCTs present in each ciPTEC model (Figure 2.7a). To compare the activity between the cell lines, the net ASP+ uptake was calculated, which was higher in ciPTEC-U (80 ± 8 RFU/1,000 cells) compared to ciPTEC-T1 (53 ± 2 RFU/1,000 cells; $p<0.05$), whereas no difference was observed between ciPTEC-U and -T2 (net transport 71 ± 5 RFU/1,000 cells).

The functional expression of P-gp was examined by measuring intracellular accumulation of calcein in matured cells, as described earlier (34). The inhibitor PSC833 was used to obtain accumulated intracellular fluorescent signals due to P-gp inhibition (Figure 2.7b). An increased accumulation was determined in all ciPTEC cell lines ($p<0.001$), indicating functional P-gp present in each ciPTEC model. To compare the activity between the cell lines, the net calcein fluorescence was determined and a clearly higher calcein accumulation was observed in both cell lines established from kidney tissue (ciPTEC-T1 7.3 ± 0.6 RFU x 10^3.mg $protein^{-1}.cm^{-2}$; $p<0.01$ and ciPTEC-T2 7.2 ± 0.4 RFU x 10^3.mg $protein^{-1}.cm^{-2}$; $p<0.05$) compared to ciPTEC-U (5.3 ± 0.4 RFU x 10^3.mg $protein^{-1}.cm^{-2}$).

The functional properties of BCRP and MRP4 were investigated by exposing matured ciPTEC models to kynurenic acid (Figure 2.7c). The compounds MK571 in combination with KO143 were used as MRP4 and BCRP inhibitors, respectively (37,38). A higher accumulation was observed in ciPTEC-U in the presence of inhibitors ($p<0.05$). In both tissue derived cell lines, kynurenic acid accumulation was slightly increased in presence of the inhibitors but this effect was not significant. To investigate and compare the BCRP and MRP4 properties between matured ciPTEC models, the net accumulation of kynurenic acid was calculated and compared to ciPTEC-U (1.1 ± 0.4 pmol.mg $protein^{-1}.cm^{-2}$), but no differences were observed (ciPTEC-T1 0.7 ± 0.6 pmol.mg $protein^{-1}.cm^{-2}$, ciPTEC-T2 0.9 ± 0.3 pmol.mg $protein^{-1}.cm^{-2}$).

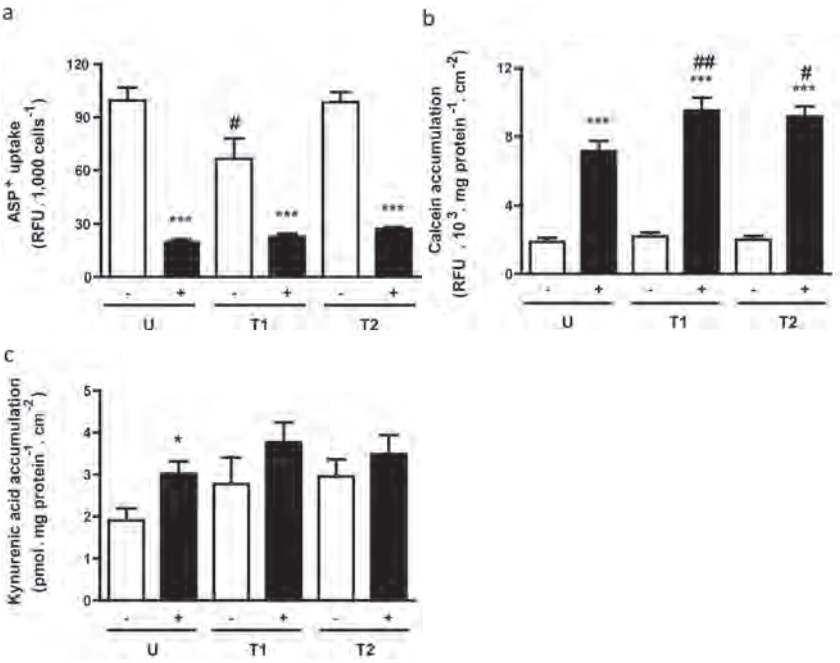

Figure 2.7 Functional in- and efflux proteins in matured ciPTEC.
(a) OCT2 mediated ASP+ uptake was measured in matured ciPTEC in the presence (black bars) or absence (white bars) of an inhibitor, TPA (5 mM). All ciPTEC models showed ASP+ uptake which was sensitive to inhibition by TPA, confirming specific OCT activity. In ciPTEC-T1 the net ASP+ uptake (values without inhibitor subtracted from values in presence of TPA) was lower compared to ciPTEC-U. (b) The P-gp activity in matured ciPTEC was measured in the presence (black bars) or absence (white bars) of a P-gp inhibitor, PSC833. An increased accumulation of calcein was observed in all cell lines in the presence of the P-gp inhibitor. Moreover, in ciPTEC-T1 and –T2 the net calcein accumulation (values without inhibitor subtracted from values in presence of PSC833) was higher as compared to ciPTEC-U. (c) The activity of MRP4 and BCRP in matured ciPTEC was detected in the presence (black bars) or absence (white bars) of the inhibitors, MK571 and KO143. A significant increased accumulation of kynurenic acid was observed in ciPTEC-U in the presence of the inhibitors. Although not significant, a slight increase in accumulation of kynurenic acid was detected in ciPTEC-T1 and -T2. The net kynurenic acid accumulation (values without subtracted from values in presence of both inhibitors) showed no differences between the cell lines. Data are presented as means of three independent experiments ± SEM * = $p<0.05$, *** = $p<0.001$ compared to data in the absence of inhibitors per cell line, using an unpaired t test. # = $p<0.05$, ## = $p<0.01$ compared to net activity in ciPTEC-U, using an ANOVA analysis followed by Dunnett's multiple comparison test.

a

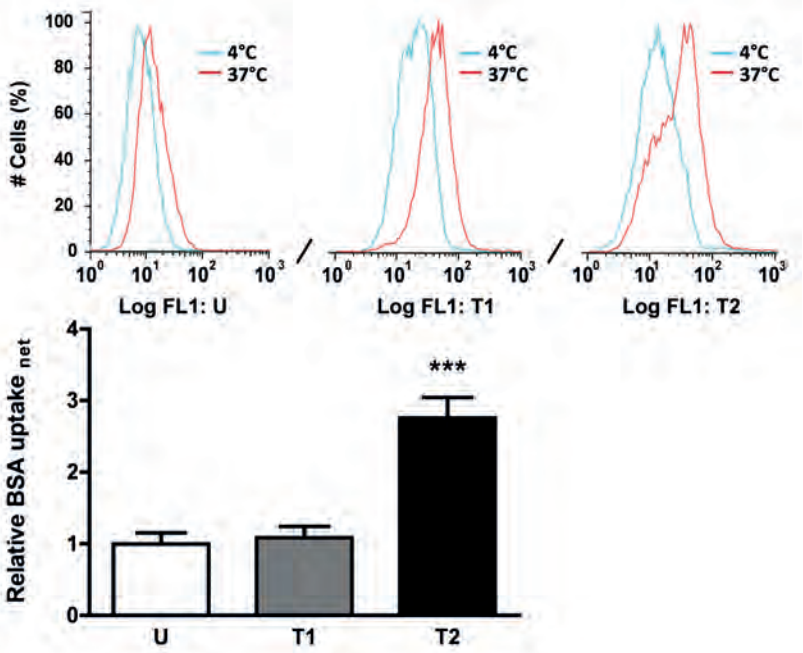
4°C
37°C
Cells (%)
Log FL1: U
Log FL1: T1
Log FL1: T2
Relative BSA uptake net
***
U
T1
T2

b

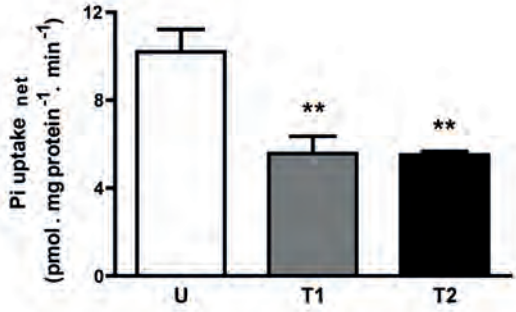
Pi uptake net
(pmol . mg protein-1 . min-1)
**
**
U
T1
T2

Figure 2.8 Essential reabsorption of albumin and phosphate in PTEC.
(a; upper panel) The albumin reabsorption was detected in matured cells incubated at 4°C (blue histogram) and 37°C (red histogram) during experimental processing (15,000 cells counted). The signal intensities obtained at 37°C clearly showed specific reabsorption in each model. (a; lower panel) The net albumin reabsorption was determined in matured ciPTEC and calculated by subtracting a-specific reabsorption data detected at 4°C from values determined at 37°C. Significantly increased albumin reabsorption was observed in ciPTEC-T2 as compared to ciPTEC-U. (b) The net sodium-dependent phosphate uptake was investigated in matured ciPTEC and calculated by subtracting sodium-independent uptake data from the uptake determined in presence of sodium. A significantly increased sodium-dependent phosphate uptake was detected in ciPTEC-U compared to ciPTEC-T1 and T2. Data are shown as mean ± SEM of three independent experiments.
** = $p < 0.01$, *** = $p < 0.001$, using one-way ANOVA analysis followed by Dunnett's multiple comparison test.

In addition to uremic toxin (UT) excretion, proximal tubule cells also play an important role in renal reabsorption processes. Wilmer et al. (19) and Gorvin et al. (20) previously reported on the presence of megalin in ciPTEC-U and specific megalin mediated albumin endocytosis was confirmed with the megalin-blocker recombinant receptor-associated protein (RAP). The temperature-sensitive reabsorption of albumin was investigated in the three cell lines (Figure 2.8a; upper panel). The reabsorption was similar in ciPTEC-T1 as compared to ciPTEC-U, whereas ciPTEC-T2 demonstrated a higher uptake of albumin (Figure 2.8a; lower panel; $p<0.001$).

Another PTEC feature concerns sodium-dependent phosphate re-absorption, mediated via NaPi-IIa and NaPi-IIc and driven by the free energy provided by the electrochemical gradient for Na^+. The transporters are located at the luminal side of proximal tubular cells (16). The mRNA expression of both phosphate transporters was confirmed in proliferating and matured cells (supplemental figure S2.3) and uptake in matured ciPTEC-U, -T1 and -T2 was studied (Figure 2.8b). Sodium-dependent phosphate uptake was found to be lower in ciPTEC-T1 and –T2 ($p<0.01$) as compared to ciPTEC-U. In proliferating cells sodium-dependent phosphate uptake was determined as well (supplemental figure S2.4), however, the uptake was clearly higher in matured cells as compared to proliferating cells.

DISCUSSION

In this study, human conditionally immortalized proximal tubular epithelial cell lines were successfully developed from kidney tissue. Characterization of the newly established human cell lines and comparison with a cell line isolated from urine revealed that cells from both sources comparably maintain renal physiological properties. A broad range of parameters was endogenously present in the three cell lines, including the ability to form tight monolayers, ECM deposition and diverse transport activities. On a functional level, the cells isolated from kidney tissue were able to compete with the previously characterized cell line isolated from urine (ciPTEC-U), while collagen I and -IV α1 gene expression was more pronounced in cells derived from renal tissue samples.

To maintain homeostatic cell numbers in the epithelium, live cell extrusion can take place in epithelial cells into the tubular lumen (27). Although viable

cells can be exfoliated in urine, their release might be the result of reduced capability to excrete ECM proteins as demonstrated in this study. The cell lines derived from kidney tissue showed a more pronounced endogenous expression of collagen I and -IV α1 as compared to ciPTEC-U, and monolayer formation of the urine derived cell line was clearly improved by collagen IV coating of culture material. These findings suggest that despite the more abundant gene expression of both fibronectin I and laminin 5 in matured ciPTEC-U, lower levels of essential collagen I and IV α1 expression prevents these cells from developing tight monolayers. In the kidney, the ECM proteins play an important role in intracellular signaling including cell proliferation, survival and migration as well in repair (42,43). Therefore, it could be argued, that ciPTEC-U has limited properties with respect to ECM and related signaling functions. However, based on the functional data and E-cadherin expression obtained in this study, ciPTEC-U nicely competes with the cells originally derived from kidney tissue. Functionally active OCT2, P-gp, MRP4 and BCRP mediated transport was detected in all models tested, and no superior cell line with respect to the activity of the investigated transport proteins was identified. Furthermore, active albumin reabsorption and sodium-dependent phosphate uptake were measured in ciPTEC-U, ciPTEC-T1 and -T2, with only small variations between the cell lines.

Gene and protein expressions of OCT2, P-gp, MRP4 and BCRP transporters confirmed the endogenous presence of these proteins in ciPTEC-U, -T1 and -T2. The small differences between the three cell models most likely reflect the biovariability. Importantly, the ciPTEC models showed an extensive endogenous expression profile upon maturation, emphasizing the differentiation capacity of these human PTEC lines by immortalization using the temperature sensitive SV40 tsA58 antigen. In the panel of transporters tested, only BCRP was less abundantly present in matured cells as compared to proliferating cells (supplemental figure S2.2d). This observation can be explained by the role of this efflux pump in kidney regeneration where it has a distinct function during cell development and a less prominent expression upon maturation (45).

Interestingly, although the gene expression levels of the four transporters investigated were lower in matured ciPTEC-U as compared to matured ciPTEC-T1 and -T2, their protein expressions and activities were almost equal in the three models. These observations might reflect differences in post-transcriptional or -translational regulation of the transport proteins. The first

step from mRNA to protein can be influenced by epigenetic alterations in signaling molecules, such as Wnt proteins and DNA-binding factors which play a key role in proximal tubular cell development (46). The differences in the next step from inactive to a functional and active transport protein can possibly be influenced by an altered activity of kinases and/or phosphatases responsible for phosphorylation and dephosphorylation, respectively (47). Future research directed towards these pathways should reveal how the four transporters can be modulated in the cell lines.

Robust transport activity was undoubtedly proven for OCTs and P-gp, while the activity of MRP4 and BCRP was less pronounced with the assay used. For the latter transporters the combined substrate kynurenic acid (36) was used in combination with inhibitors for MRP4 and BCRP. A plausible explanation for the limited effect of both inhibitors on kynurenic acid accumulation may be the absence of a specific uptake transporter for kynurenic acid. The uremic metabolite was proven to be an equally potent substrate for the basolaterally expressed organic anion transporters 1 (OAT3) and -3 (OAT3) (48). OAT3 and OAT3 form important influx transporters in proximal tubular cells and determinants in the excretion of a variety of organic anions, including waste products from normal metabolism and drugs (49,50). Unfortunately, these transporters are absent on gene, protein and functional levels in the immortalized cell lines isolated from both urine and kidney tissue (data not shown). Although the expression of OATs has been observed in primary proximal tubular cells (51), the levels decrease dramatically during the first days of culturing and are lost after cell passaging (unpublished observations). This phenomenon has already been described in 1990 by J.H. Miller (52) and has, as of yet, not been solved. Stable expression of these OATs in renal cell lines may not only be of importance for studying regenerative nephrology, but may also be of great value for drug development in pharmaceutical industry. Next to the OAT transporters, OATP4C1 is another known anion uptake transporter expressed at the basal membrane of proximal tubule cells (53). The gene expression was studied in these cell lines and the expression of OATP4C1 was confirmed in matured cells (an average C(t) value of 27.2 ± 0.1 was detected). Assays to demonstrate the functionality of this transporter are in progress. To study the role of transporters in disposition of new pharmaceutical entities and to identify potential drug-drug interactions, a need exists for human models predictive for renal drug handling (44,54,55). Future research will be directed to further develop and optimize such models. Next to the functional basolateral uptake and apical efflux transport, active

albumin reabsorption and sodium-dependent phosphate uptake are essential processes occurring in human PTEC. Both mechanisms were detected in our ciPTEC models, although differences were observed between the cell lines. These findings underline the heterogeneity with respect to their endocytosis-mediated albumin uptake via megalin, and NaPi-IIa and -IIc mediated sodium-dependent phosphate uptake. As described before, post-transcriptional and -translational differences in these cell lines might explain the observed variability.

Isolating functional renal epithelial cells from human urine and applying conditional immortalization strategies could be a valuable tool in tissue engineering for personalized medicine in patients suffering from renal disorders, e.g. in development of a bioartificial kidney, or so called renal assist device (RAD)(12). Indications exist that residual renal function in CKD represents urine produced by tubular secretion rather than glomerular filtration (56). Residual renal function is a predictor of survival in patients treated with dialysis (57). Retaining or improving active tubular secretion processes may have profound effects on clinical outcome of CKD patients and the use bioartificial devices may be a good treatment alternative for this patient population (12). However, the amount and the quality of functional cells in urine originating from these patients might be questionable. In this study, cells from healthy volunteers were transduced using hTERT in combination with the temperature sensitive SV40t gene (19,30). Although Wieser et al. (58) previously used a single transduction of hTERT only to immortalize primary renal cells, in our laboratory this method did not lead to successful immortalization and hTERT only transductions resulted in dysmorphic cells. A great advantage of using the combined immortalization strategy is that cells can remain in their proliferating state at 33°C, thereby providing an unlimited cell source. Maturation can be initiated by transferring cells to 37°C, upon which the expression of SV40t in ciPTEC decreases (19) and expression levels of PTEC specific proteins adequately increases (supplemental figure S2.1 – S2.3). These findings support their suitability for studying regenerative nephrology. However, the oncogene transductions used require stringent biological safety regulation (e.g. filters absorbing eventually disrupted cells) before implementing in any clinical application, which is the focus of ongoing research and obviously a thorough risk assessment is needed. The use of serum-free culture conditions might be favorable to reduce a possible host immune response. However, culturing the ciPTEC models using serum-free medium for more than 24h induces epithelial-to-mesenchymal transition

(EMT) and results in a loss of PTEC-specific characteristics (data not shown). Serum-replacement compounds might be an appropriate alternative, but to this end comprehensive research is required to study the possible effect in these PTEC models prior to implementation.

In conclusion, the human renal lines established from urine and kidney tissue display a comparable variety of functional PTEC specific transporters with maintained reabsorption mechanisms. Interestingly, a different ECM profile was observed in the cell lines isolated from kidney tissue as compared to the cell line isolated from cells exfoliated in urine. The cell models presented here could serve as valuable tools to study proximal tubule physiology and pharmacology. Furthermore, the availability of inexhaustible sources of functional human proximal tubule epithelial cells could allow for further development and up scaling of bioartificial kidney devices.

Acknowledgment

This research forms part of the Project P3.01 BioKid of the research program of the BioMedical Materials institute, co-funded by the Dutch Ministry of Economic Affairs. The financial contribution of the Dutch Kidney Foundation is gratefully acknowledged (IK08.03 and KJPB 11.0023) and the Netherlands Institute for Regenerative Medicine (NIRM, grant no. FES0908) and the Netherlands Organization for Scientific Research (016.130.668).

REFERENCES

1. Fox CS, Matsushita K, Woodward M, Bilo HJ, Chalmers J, Heerspink HJ, Lee BJ, Perkins RM, Rossing P, Sairenchi T, et al. Associations of kidney disease measures with mortality and end-stage renal disease in individuals with and without diabetes: a meta-analysis. Lancet 380: 1662-1673, 2012.
2. Mahmoodi BK, Matsushita K, Woodward M, Blankestijn PJ, Cirillo M, Ohkubo T, Rossing P, Sarnak MJ, Stengel B, Yamagishi K, et al. Associations of kidney disease measures with mortality and end-stage renal disease in individuals with and without hypertension: a meta-analysis. Lancet 380: 1649-1661, 2012.
3. Winearls CG, Glassock RJ. Classification of chronic kidney disease in the elderly: pitfalls and errors. Nephron Clin Pract. 119 Suppl 1: c2-4, 2011.
4. Krieter DH, Hackl A, Rodriguez A, Chenine L, Moragues HL, Lemke HD, Wanner C, Canaud B. Protein-bound uraemic toxin removal in haemodialysis and post-dilution haemodiafiltration. Nephrol Dial Transplant. 25: 212-218, 2010.
5. Vanholder R, Van Laecke S, Glorieux G. What is new in uremic toxicity? Pediatr Nephrol 23: 1211-1221, 2008.
6. Vanholder R, De Smet R. Pathophysiologic effects of uremic retention solutes. J Am Soc Nephrol. 10: 1815-1823, 1999.
7. Morgan BR, Ibrahim HN. Long-term outcomes of kidney donors. Curr Opin Nephrol Hypertens. 20: 605-609, 2011.
8. Wolfe RA, Ashby VB, Milford EL, Ojo AO, Ettenger RE, Agodoa LY, Held PJ, Port FK. Comparison of mortality in all patients on dialysis, patients on dialysis awaiting transplantation, and recipients of a first cadaveric transplant. N Engl J Med. 341: 1725-1730, 1999.
9. Artz MA, Boots JM, Ligtenberg G, Roodnat JI, Christiaans MH, Vos PF, Moons P, Borm G, Hilbrands LB. Conversion from cyclosporine to tacrolimus improves quality-of-life indices, renal graft function and cardiovascular risk profile. Am J Transplant. 4: 937-945, 2004.
10. Hoorn EJ, Walsh SB, McCormick JA, Furstenberg A, Yang CL, Roeschel T, Paliege A, Howie AJ, Conley J, Bachmann S, et al. The calcineurin inhibitor tacrolimus activates the renal sodium chloride cotransporter to cause hypertension. Nat Med. 17: 1304-1309, 2011.
11. Segev DL. Innovative strategies in living donor kidney transplantation. Nature Rev Nephrol 8: 332-338, 2012.
12. Humes HD, Buffington D, Westover AJ, Roy S, Fissell WH. The bioartificial kidney: current status and future promise. Pediatr Nephrol. 29: 343-351, 2014.
13. Koepsell H, Endou H. The SLC22 drug transporter family. Pflugers Arch. 447: 666-676, 2004.

14. Masereeuw R, Russel FG. Regulatory pathways for ATP-binding cassette transport proteins in kidney proximal tubules. AAPS J. 14: 883-894, 2012.
15. Anzai N, Ichida K, Jutabha P, Kimura T, Babu E, Jin CJ, Srivastava S, Kitamura K, Hisatome I, Endou H, et al. Plasma urate level is directly regulated by a voltage-driven urate efflux transporter URATv1 (SLC2A9) in humans. J Biol Chem. 283: 26834-26838, 2008.
16. Forster IC, Hernando N, Biber J, Murer H. Proximal tubular handling of phosphate: A molecular perspective. Kidney Int. 70: 1548-1559, 2006.
17. Gekle M. Renal tubule albumin transport. Annu Rev Physiol. 67: 573-594, 2005.
18. Triplitt CL. Understanding the kidneys' role in blood glucose regulation. Am J Manag Care 18: S11-16, 2012.
19. Wilmer MJ, Saleem MA, Masereeuw R, Ni L, Van Der Velden TJ, Russel FG, Mathieson PW, Monnens LA, Van Den Heuvel LP, Levtchenko EN. Novel conditionally immortalized human proximal tubule cell line expressing functional influx and efflux transporters. Cell Tissue Res. 339: 449-457, 2010.
20. Gorvin CM, Wilmer MJ, Piret SE, Harding B, van den Heuvel LP, Wrong O, Jat PS, Lippiat JD, Levtchenko EN, Thakker RV. Receptor-mediated endocytosis and endosomal acidification is impaired in proximal tubule epithelial cells of Dent disease patients. Proc Natl Acad Sci. U. S. A. 110: 7014-7019, 2013.
21. Mekahli D, Sammels E, Luyten T, Welkenhuyzen K, van den Heuvel LP, Levtchenko EN, Gijsbers R, Bultynck G, Parys JB, De Smedt H, et al. Polycystin-1 and polycystin-2 are both required to amplify inositol-trisphosphate-induced Ca2+ release. Cell Calcium 51: 452-458, 2012.
22. Wilmer MJ, Kluijtmans LA, van der Velden TJ, Willems PH, Scheffer PG, Masereeuw R, Monnens LA, van den Heuvel LP, Levtchenko EN. Cysteamine restores glutathione redox status in cultured cystinotic proximal tubular epithelial cells. Biochim Biophys Acta. 1812: 643-651, 2011.
23. Mutsaers HA, Wilmer MJ, Reijnders D, Jansen J, van den Broek PH, Forkink M, Schepers E, Glorieux G, Vanholder R, van den Heuvel LP, et al. Uremic toxins inhibit renal metabolic capacity through interference with glucuronidation and mitochondrial respiration. Biochim Biophys Acta. 1832: 142-150, 2013.
24. Mutsaers HA, van den Heuvel LP, Ringens LH, Dankers AC, Russel FG, Wetzels JF, Hoenderop JG, Masereeuw R. Uremic toxins inhibit transport by breast cancer resistance protein and multidrug resistance protein 4 at clinically relevant concentrations. PLoS ONE 6: e18438, 2011.
25. Schophuizen CM, Wilmer MJ, Jansen J, Gustavsson L, Hilgendorf C, Hoenderop JG, van den Heuvel LP, Masereeuw R. Cationic uremic toxins affect human renal proximal tubule cell functioning through interaction with the organic cation transporter. Pflugers Arch. 465: 1701-1714, 2013.

26. Rosenblatt J, Raff MC, Cramer LP. An epithelial cell destined for apoptosis signals its neighbors to extrude it by an actin- and myosin-dependent mechanism. Curr Biol. 11: 1847-1857, 2001.
27. Eisenhoffer GT, Loftus PD, Yoshigi M, Otsuna H, Chien CB, Morcos PA, Rosenblatt J. Crowding induces live cell extrusion to maintain homeostatic cell numbers in epithelia. Nature 484: 546-549, 2012.
28. van Setten PA, van Hinsbergh VW, van der Velden TJ, van de Kar NC, Vermeer M, Mahan JD, Assmann KJ, van den Heuvel LP, Monnens LA. Effects of TNF alpha on verocytotoxin cytotoxicity in purified human glomerular microvascular endothelial cells. Kidney Int. 51: 1245-1256, 1997.
29. Reubsaet FA, Veerkamp JH, Monnens LA. Sulfated glycosaminoglycan content of glomerular and tubular basement membranes of individuals of different ages. Nephron 41: 344-347, 1985.
30. Saleem MA, O'Hare MJ, Reiser J, Coward RJ, Inward CD, Farren T, Xing CY, Ni L, Mathieson PW, Mundel P. A conditionally immortalized human podocyte cell line demonstrating nephrin and podocin expression. J Am Soc Nephrol. 13: 630-638, 2002.
31. Hills CE, Jin T, Siamantouras E, Liu IK, Jefferson KP, Squires PE. 'Special k' and a loss of cell-to-cell adhesion in proximal tubule-derived epithelial cells: modulation of the adherens junction complex by ketamine. PLoS ONE 8: e71819, 2013.
32. van Aubel RA, Smeets PH, Peters JG, Bindels RJ, Russel FG. The MRP4/ABCC4 gene encodes a novel apical organic anion transporter in human kidney proximal tubules: putative efflux pump for urinary cAMP and cGMP. J Am Soc Nephrol. 13: 595-603, 2002.
33. Koenderink JB, Geibel S, Grabsch E, De Pont JJ, Bamberg E, Friedrich T. Electrophysiological analysis of the mutated Na,K-ATPase cation binding pocket. J Biol Chem. 278: 51213-51222, 2003.
34. van de Water FM, Boleij JM, Peters JG, Russel FG, Masereeuw R. Characterization of P-glycoprotein and multidrug resistance proteins in rat kidney and intestinal cell lines. Eur J Pharm Sci. 30: 36-44, 2007.
35. Huls M, Brown CD, Windass AS, Sayer R, van den Heuvel JJ, Heemskerk S, Russel FG, Masereeuw R. The breast cancer resistance protein transporter ABCG2 is expressed in the human kidney proximal tubule apical membrane. Kidney Int. 73: 220-225, 2008.
36. Dankers AC, Mutsaers HA, Dijkman HB, van den Heuvel LP, Hoenderop JG, Sweep FC, Russel FG, Masereeuw R. Hyperuricemia influences tryptophan metabolism via inhibition of multidrug resistance protein 4 (MRP4) and breast cancer resistance protein (BCRP). Biochim Biophys Acta. 1832: 1715-1722, 2013.
37. Allen JD, van Loevezijn A, Lakhai JM, van der Valk M, van Tellingen O, Reid G, Schellens JH, Koomen GJ, Schinkel AH. Potent and specific inhibition of the breast cancer resistance protein multidrug transporter in vitro and in mouse intestine by a novel analogue of fumitremorgin C. Mol Cancer Ther. 1: 417-425, 2002.

38. Luders AK, Saborowski R, Bickmeyer U. Inhibition of multidrug/xenobiotic resistance transporter by MK571 improves dye (Fura 2) accumulation in crustacean tissues from lobster, shrimp, and isopod. Comp Biochem Physiol C Toxicol Pharmacol. 150: 368-371, 2009.
39. Malmstrom K, Stange G, Murer H. Intracellular cascades in the parathyroid-hormone-dependent regulation of Na+/phosphate cotransport in OK cells. Biochem J. 251: 207-213, 1988.
40. Kirk A, Campbell S, Bass P, Mason J, Collins J. Differential expression of claudin tight junction proteins in the human cortical nephron. Nephrol Dial Transplant. 25: 2107-2119, 2010.
41. Kwon O, Nelson WJ, Sibley R, Huie P, Scandling JD, Dafoe D, Alfrey E, Myers BD. Backleak, tight junctions, and cell- cell adhesion in postischemic injury to the renal allograft. J Clin Invest. 101: 2054-2064, 1998.
42. Nony PA, Schnellmann RG. Interactions between collagen IV and collagen-binding integrins in renal cell repair after sublethal injury. Mol Pharmacol. 60: 1226-1234, 2001.
43. Pozzi A, Zent R. Integrins in kidney disease. J Am Soc Nephrol. 24: 1034-1039, 2013.
44. Giacomini KM, Huang SM. Transporters in drug development and clinical pharmacology. Clin Pharmacol. Ther. 94: 3-9, 2013.
45. Huls M, Schoeber JP, Verfaillie CM, Luttun A, Ulloa-Montoya F, Menke AL, van Bolderen LR, Woestenenk RM, Merkx GF, Wetzels JF, et al. Deficiency of either P-glycoprotein or breast cancer resistance protein protect against acute kidney injury. Cell Transplant. 19: 1195-1208, 2010.
46. Woroniecki R, Gaikwad AB, Susztak K. Fetal environment, epigenetics, and pediatric renal disease. Pediatr Nephrol. 26: 705-711, 2011.
47. Terabayashi T, Sakaguchi M, Shinmyozu K, Ohshima T, Johjima A, Ogura T, Miki H, Nishinakamura R. Phosphorylation of Kif26b promotes its polyubiquitination and subsequent proteasomal degradation during kidney development. PLoS ONE 7: e39714, 2012.
48. Uwai Y, Honjo H, Iwamoto K. Interaction and transport of kynurenic acid via human organic anion transporters hOAT1 and hOAT3. Pharmacol Res. 65: 254-260, 2012.
49. Hagos Y, Burckhardt G, Burckhardt BC. Human organic anion transporter OAT1 is not responsible for glutathione transport but mediates transport of glutamate derivatives. Am J Physiol Renal Physiol. 304: F403-409, 2013.
50. Wang L, Sweet DH. Interaction of Natural Dietary and Herbal Anionic Compounds and Flavonoids with Human Organic Anion Transporters 1 (SLC22A6), 3 (SLC22A8), and 4 (SLC22A11). Evid Based Complement Alternat Med. 2013: 612-527, 2013.
51. Brown CD, Sayer R, Windass AS, Haslam IS, De Broe ME, D'Haese PC, Verhulst A. Characterisation of human tubular cell monolayers as a model of proximal tubular xenobiotic handling. Toxicol Appl Pharmacol. 233: 428-438, 2008.

52. Miller JH. Sodium-sensitive, probenecid-insensitive p-aminohippuric acid uptake in cultured renal proximal tubule cells of the rabbit. Proc Soc Exp Biol Med. 199: 298-304, 1992.
53. Yamaguchi H, Sugie M, Okada M, Mikkaichi T, Toyohara T, Abe T, Goto J, Hishinuma T, Shimada M, Mano N. Transport of estrone 3-sulfate mediated by organic anion transporter OATP4C1: estrone 3-sulfate binds to the different recognition site for digoxin in OATP4C1. Drug Metab. Pharmacokinet. 25: 314-317, 2010.
54. Ahlin G, Hilgendorf C, Karlsson J, Szigyarto CA, Uhlen M, Artursson P. Endogenous gene and protein expression of drug-transporting proteins in cell lines routinely used in drug discovery programs. Drug Metab Dispos. 37: 2275-2283, 2009.
55. Jenkinson SE, Chung GW, van Loon E, Bakar NS, Dalzell AM, Brown CD. The limitations of renal epithelial cell line HK-2 as a model of drug transporter expression and function in the proximal tubule. Pflugers Arch. 464: 601-611, 2012.
56. Lowenstein J. The anglerfish and uremic toxins. FASEB J. 25: 1781-1785, 2011.
57. Marquez IO, Tambra S, Luo FY, Li Y, Plummer NS, Hostetter TH, Meyer TW. Contribution of residual function to removal of protein-bound solutes in hemodialysis. Clin J Am Soc Nephrol. 6: 290-296, 2011.
58. Wieser M, Stadler G, Jennings P, Streubel B, Pfaller W, Ambros P, Riedl C, Katinger H, Grillari J, Grillari-Voglauer R. hTERT alone immortalizes epithelial cells of renal proximal tubules without changing their functional characteristics. Am J Physiol Renal Physiol. 295: F1365-1375, 2008.

SUPPLEMENTARY DATA

Table S2.1 Taqman primer-probe sets – PTEC transporter genes.

PTEC transporter gene	Catalogue number
OCT-2 (*SLC22A2*)	hs01010723_m1
P-glycoprotein (*ABCB1*, P-gp)	hs01067802_m1
MRP4 (*ABCC4*)	hs00195260_m1
BCRP (*ABCG2*)	hs00184979_m1
NaPi-IIa (*SLC34A1*)	hs00161828_m1
NaPi-IIc (*SLC34A3*)	hs02341448_m1
OATP4C1 (*SLCO4C1*)	hs00698884_m1
GAPDH	hs99999905_m1

Table S2.2 Primer sequences – Extracellular matrix genes (ECM)

ECM gene	Forward sequence	Reverse sequence
collagen I α1	GCCTCAAGGTATTGCTGGAC	ACCTTGTTTGCCAGGTTCAC
collagen IV α1	TGGTGACAAAGGACAAGCAG	GGTTCACCCTTTGGACCTG
fibronectin I	CTGGCCGAAAATACATTGTAAA	CCACAGTCGGGTCAGGAG
laminin V	GAGGCCCAGGAGCTCAAC	GACAGCTCCTGCTTCCTTTG
GAPDH	CTGCCGTCTAGAAAAACCTG	GTCCAGGGGTCTTACTCCTT

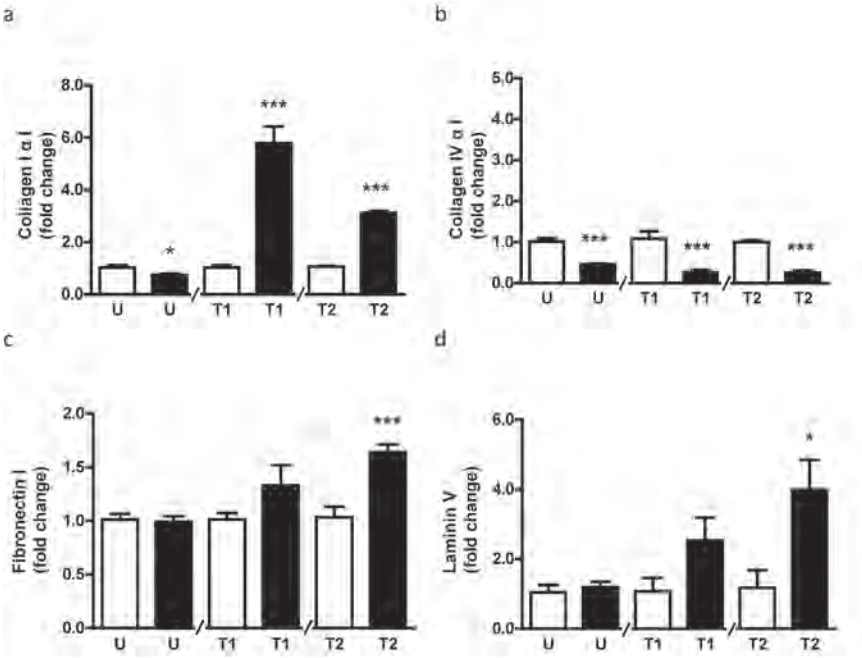

Figure S2.1, related to figure 2.4.
(a) In mature (black bars) ciPTEC-U, a significantly decreased gene expression of collagen I α1 was observed compared to proliferating ciPTEC-U. Both matured cell lines derived from kidney tissue showed a significantly increased gene expression of collagen I α1. (b) All tested matured cell lines showed a significantly decreased gene expression of collagen IV α1 compared to the corresponding proliferating cells. (c and d) In matured ciPTEC-T2, a significantly increased gene expression of fibronectin I (c) and laminin 5 (d) was observed compared to proliferating ciPTEC-T2. Expression levels were corrected for corresponding GAPDH mRNA levels and data were expressed as fold change and compared to proliferating ciPTEC per cell line. Data are means of three independent experiments and presented as mean ± S.E.M. * = $p<0.05$, ***= $p<0.001$, using an unpaired *t* test.

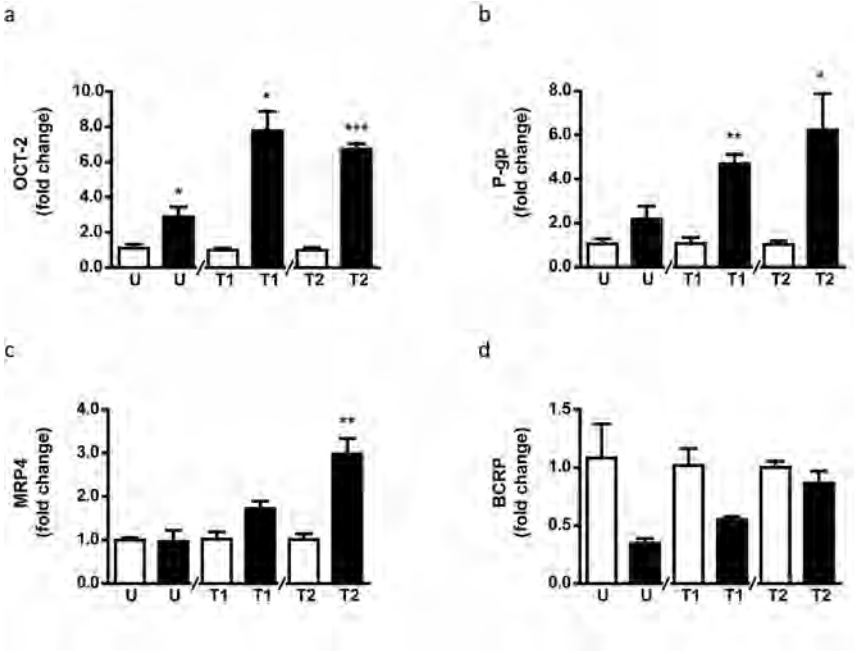

Figure S2.2, related to figure 2.5.
(a) In all matured (black bars) ciPTEC a significantly increased OCT-2 gene expression was observed compared to the corresponding proliferating (white bars) ciPTEC. (b) In matured ciPTEC-T1 and -T2, a significantly increased gene expression of P-gp was observed. (c) In matured ciPTEC-T2 a significantly increased MRP4 gene expression was detected. (d) No significant differences in gene expression levels of BCRP were observed between matured and proliferating ciPTEC. Expression levels were corrected for corresponding GAPDH mRNA levels and data were expressed as fold change and compared to proliferating ciPTEC per cell line. Data are means of three independent experiments and presented as mean ± S.E.M. * = $p<0.05$, ** = $p<0.01$, ***= $p<0.001$, using an unpaired *t* test.

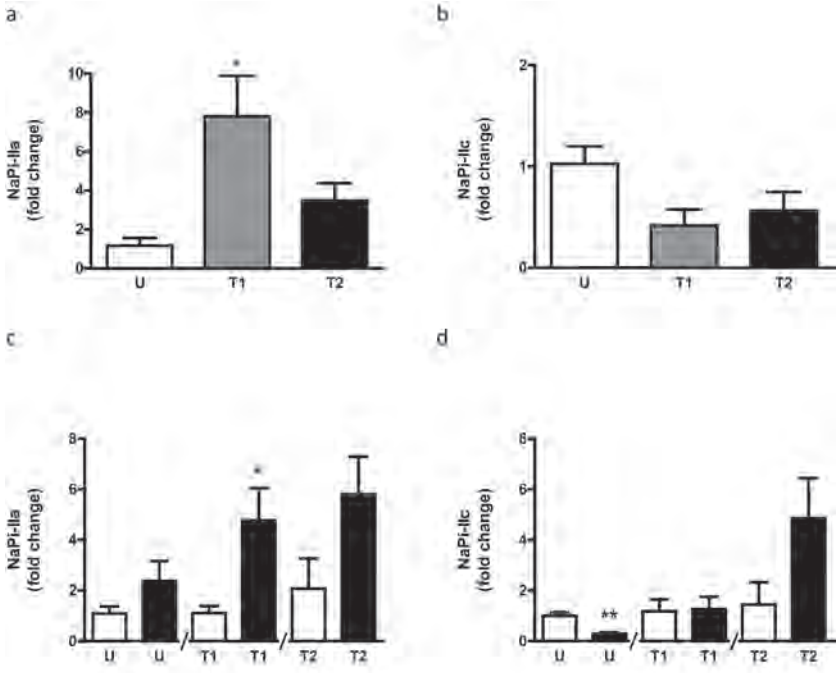

Figure S2.3, related to figure 2.8b.
(a) In ciPTEC-T1 a higher NaPi-IIa gene expression was observed compared to ciPTEC-U. (b) No significant differences in NaPi-IIc gene expression were observed between the three cell lines. (c) In matured ciPTEC-T1 (black bar) a significantly increased gene expression of NaPi-IIa was observed compared to the corresponding proliferating ciPTEC (white bar). Although not significant, ciPTEC-U and -T2 showed a trend of increased NaPi-IIa gene expression upon maturation. (d) In matured ciPTEC-U significantly less NaPi-IIc gene expression was observed compared to proliferating ciPTEC-U. No significant differences in gene expression levels of NaPi-IIc were observed between matured and proliferating ciPTEC-T1 and -T2. Expression levels were corrected for corresponding GAPDH mRNA levels. Data were expressed as fold change and compared to ciPTEC-U (a - b) or compared to the corresponding proliferating ciPTEC model (c - d). Data are presented as means of three independent experiments ± S.E.M. * = $p<0.05$ using an ANOVA analysis followed by Dunnett's multiple comparison test (a - b). * = $p<0.05$, ** = $p<0.01$ using an unpaired *t* test (c - d).

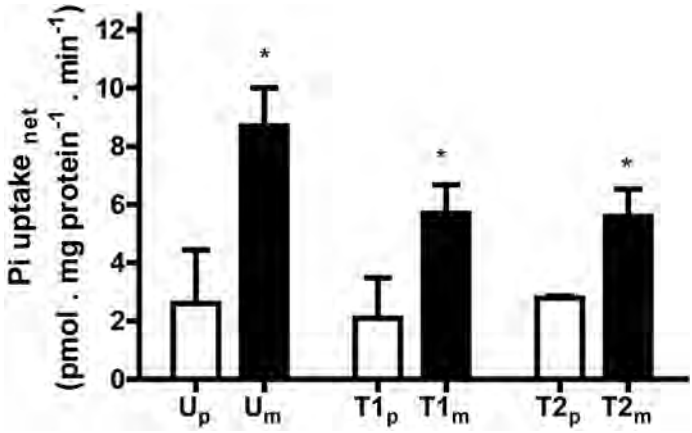

Figure S2.4, related to figure 2.8b.
The net sodium-dependent phosphate uptake was investigated in proliferating (white bars) and matured (black bars) ciPTEC and calculated by subtracting sodium-independent uptake data from the uptake determined in presence of sodium. A significantly increased sodium-dependent phosphate uptake was detected upon maturation in each ciPTEC model compared to proliferating cells. Data are shown as mean ± S.E.M. of three independent experiments. * = $p<0.05$ using an unpaired *t* test.

Chapter 3

MILD INTRACELLULAR ACIDIFICATION BY DEXAMETHASONE ATTENUATES MITOCHONDRIAL DYSFUNCTION IN A HUMAN INFLAMMATORY PROXIMAL TUBULE EPITHELIAL CELL MODEL

Schirris T.J.J.[1,2*], Jansen J.[1,3,4,5*], Mihajlović M.[5], van den Heuvel L.P.[4,6], Masereeuw R.[5,†], Russel F.G.M.[1,2,†]

Manuscript submitted, 2016

[1] *Department of Pharmacology and Toxicology, Radboud University Medical Center, Radboud Institute for Molecular Life Sciences, Nijmegen, The Netherlands*
[2] *Center for Systems Biology and Bioenergetics, Nijmegen Center for Mitochondrial Disorders, Radboud University Medical Center, Nijmegen, 6500HB, The Netherlands*
[3] *Department of Physiology, Radboud University Medical Center, Radboud Institute for Molecular Life Sciences, Nijmegen, The Netherlands.*
[4] *Department of Pediatrics, Radboud University Medical Center, Nijmegen, The Netherlands.*
[5] *Division of Pharmacology, Utrecht Institute for Pharmaceutical Sciences, Utrecht, The Netherlands.*
[6] *Department of Pediatric Nephrology & Growth and Regeneration, Catholic University Leuven, Leuven, Belgium.*

*,† Authors contributed equally

ABSTRACT

Patients suffering from septic acute kidney injury (AKI) demonstrate poor survival rates and often require renal replacement therapy. Glucocorticoids may protect the kidneys during sepsis by stimulating mitochondrial function. Here, we studied the beneficial mitochondrial effects of dexamethasone in an experimental inflammatory proximal tubule epithelial cell model. Lipopolysaccharide (LPS) treatment of cells led to increased cytokine excretion rates, higher cellular ROS levels, and a reduced mitochondrial membrane potential and respiratory capacity, which were all attenuated by dexamethasone. OXPHOS complex V (CV) activity was enhanced upon dexamethasone treatment, whereas the other complex activities remained unchanged. This could not be explained by an increase in mitochondrial mass or the expression of its major regulator PPARγ coactivator-1α (PGC-1α). However, dexamethasone specifically induced CV and not CIV expression. Finally, we demonstrated that dexamethasone acidified the intracellular milieu and consequently reversed the LPS-induced alkalisation. Dexamethasone restores mitochondrial function under inflammatory conditions by decreasing the cellular pH and increasing CV expression to correct for the inhibitory effect of the acidified environment on this complex. Besides the mechanistic insights into the beneficial effects of dexamethasone during renal cellular inflammation, our work also supports a key role for mitochondria in this process and, hence, provides novel therapeutic avenues for the treatment of patients suffering from septic AKI.

INTRODUCTION

The prevalence of acute kidney injury (AKI) in critically ill patients has rapidly increased over the past two decades and puts a high burden on healthcare worldwide (1). AKI occurs in approximately 30 - 40% of patients admitted to the intensive care unit (ICU) (2), and is associated with 20% of all hospitalised adults worldwide (3). Though depending on AKI severity, the average mortality rate in these patients is over 50% and even less severe manifestations are associated with profound short- and long-term adverse effects, such as chronic kidney disease (4). The pathogenesis of AKI is highly complex and often multi-causal, but the septic form provoked by endotoxins originating from gram-negative bacteria is the most common cause of disease onset. Research spanning several decades illustrated beneficial effects of many different agents (*e.g.* approved drugs, natural compounds, hormones and peptides), which are also based on a wide variety of renal protective mechanisms (*e.g.* antioxidant, anti-inflammatory, or anti-apoptotic effects, or the activation of autophagy) (5). Still, most of these strategies have not yet reached clinical studies, and none are applied in a clinical setting (5). Treatment with alkaline phosphatase (AP) might, however, pave ways towards successful AKI treatment, as two phase-II trials demonstrated improved renal function in critically ill patients with sepsis-associated acute kidney injury treated with the enzyme alkaline phosphatase (AP) (6). Moreover, the molecular mechanism of AP was partially unravelled and showed that dephosphorylation of LPS-induced extracellular ADP and ATP might be key in the renal protective effect (7). Likewise, further clinical validation should demonstrate the efficacy and efficiency of AP prior to clinical implementation. As future renal replacement therapy, bioartificial kidneys containing renal proximal tubule epithelial cells have been suggested to exert immunomodulatory effects in animals models and patients with AKI, though controlled randomised multi-centre human studies have not yet shown conclusive beneficial evidence (8-10). As effective treatment modalities are not available yet, renal function can only partially be replaced using haemodialysis (1).

Recently, treatment of cardiac surgery patients with the glucocorticoid dexamethasone has been proposed as a new strategy to attenuate AKI (11, 12). The potency of dexamethasone to reduce septic AKI was also demonstrated in rodent *in vivo* studies and renal epithelial cells exposed to the *E.coli* endotoxin lipopolysaccharide (LPS) (13-15). Encouraging results were obtained with respect to attenuated cytokine levels, improved glomerular

filtration rate (GFR), suppressed pro-apoptotic proteins and reduced renal mitochondrial injury. Furthermore, Johannes and Tsao *et al.*, demonstrated that dexamethasone inhibited inducible NO synthase (iNOS) activity, prevented hypoxic injury and improved fluid balance in rat kidneys (16,17). In addition, it has been shown that dexamethasone exerts nephroprotective effects via stimulation of multi drug resistance protein-2 (MRP2) via non-genomic stimulation involving multiple kinases. This renal efflux transporter is expressed in the apical membrane of proximal tubule epithelial cells and has an important detoxification function through the excretion of endo- and xenobiotics into the pro-urine (18).

The postulated beneficial effects of dexamethasone in septic-induced AKI are promising, however, the exact molecular mechanism of action has not been unravelled. Increasing evidence points towards the role of mitochondria in the pathophysiology of AKI (3, 15, 19). Mitochondria are responsible for ATP production via the oxidative phosphorylation system (OXPHOS) and are highly dense in the proximal as well as in the distal segment of the nephron (20). During septic conditions, mitochondrial injury was observed in human proximal tubule epithelial cells (PTECs), HK-2. The suppression of cytochrome *c* oxidase (COX; complex IV in OXPHOS) expression, most likely under the regulation of increased expression of Bcl-2 pro-apoptotic proteins, may contribute to mitochondrial dysfunction (15). Consequently, elevated reactive oxygen species (ROS) will affect renal tubular function, thereby initiating the development of AKI. COX and Bcl-2 protein expression were partially restored upon dexamethasone treatment, suggesting a possible mitochondrial target (15). Peroxisome proliferator-activated receptor gamma (PPARγ) coactivator - 1α (PGC-1α), a known key regulator of mitochondrial biogenesis and predominantly expressed in proximal tubules, was also suppressed (19, 21). Upon recovery, PGC-1α was restored indicating another possible mitochondrial target for therapeutic intervention to treat or prevent AKI. Such a protective role of PGC-1α was recently associated with the regulation of nicotinamide adenine dinucleotide (NAD) biosynthesis and subsequent alteration of the cellular oxidative status (22). However, further elucidation of the targets by which dexamethasone influences mitochondrial homeostasis pathways during AKI is required.

In this study, human conditionally immortalised proximal tubule epithelial cells (ciPTEC, (23)) were used to unravel the molecular mechanism of action of dexamethasone to attenuate septic AKI. This model was extensively

characterised in our laboratory and demonstrated a broad range of PTEC-specific transport and metabolic functions (23). Cells were challenged with LPS to mimic septic AKI and were co-incubated with dexamethasone to induce metabolic recovery. We demonstrate improved mitochondrial respiration, OXPHOS complex activity, membrane potential, attenuated ROS production. These effects of dexamethasone were not mediated via PGC-1α induced mitochondrial biogenesis, but could be associated with a restoration of cellular pH.

MATERIALS AND METHODS

Chemicals and cell culture materials

Chemicals were purchased from Sigma-Aldrich (Zwijndrecht, The Netherlands) unless stated otherwise. Cell culture plates were purchased from Greiner Bio-One (Monroe, NC, United States of America).

Cell culture and experimental design

Human conditionally immortalised PTEC isolated from kidney tissue (ciPTEC-T1 (24)) were cultured in phenol-red free DMEM-HAM's F12 medium (Lonza, Basel, Switzerland) containing 10% (v/v) FCS (Greiner Bio-One, Monroe, NC, United States of America), 5 µg/ml insulin, 5 µg/ml transferrin, 5 ng/ml selenium, 36 ng/ml hydrocortisone, 10 ng/ml EGF and 40 pg/ml tri-iodothyronine (complete PTEC medium (23)). In all experiments, cells were seeded using a density of 25,000 cells/cm^2 on uncoated surfaces, unless stated otherwise. Cells were cultured for 24 hours at 33°C, 5% (v/v) CO_2, to proliferate and subsequently transferred to 37°C, 5% (v/v) CO_2 for 7 days to mature. On day 6, cells were exposed to control medium (complete PTEC medium) or medium supplemented with LPS (10 µg/ml, (39)) for 24 hours at 37°C, 5% (v/v) CO_2 to induce endotoxemia (see also Figure 3.2A). After 20 hours incubation, control or LPS-treated cells were co-incubated in the presence or absence of dexamethasone (10 µM). Subsequently, various parameters were investigated following the experimental protocols described below.

Enzyme-linked Immuno Sorbent Assay

The cytokine production of Interleukin-6 (IL-6; #DY206, R&D systems, Abingdon, UK) and -8 (IL-8; #DY208, R&D systems) in ciPTEC under control or inflammatory conditions in the presence or absence of dexamethasone was quantified using Enzyme-linked Immuno Sorbent Assays (ELISAs) as

previously described by Schophuizen *et al.* (40). The optical density of each well was measured using the iMark Microplate reader (BioRad, Veenendaal, The Netherlands) set to 460 nm and were background corrected using readings obtained at 540 nm.

High-resolution respirometry

Cellular and mitochondrial respiration was measured at 37°C using a two-chamber Oxygraph equipped with Datlab 5 recording and analysis software (Oroboros Instruments, Innsbruck, Austria), as previously described previously (41-43). Briefly, exposed cells were harvested and approximately 1.5×10^6 cells were resuspended in mitochondrial respiration medium MiR05 (Oroboros Instruments, Innsbruck, Austria). To determine the P:O ratio we slightly modified the previously described approach (43, 44). Routine respiration was recorded followed by digitonin permeabilisation (10 µg/ $1\cdot10^6$ cells) of the cell membrane. Next, malate (2 mM) and glutamate (10 mM) were added to determine the STATE 4 respiration. STATE 3 respiration was obtained by the addition of ADP (220 nM), after which the oxygen consumption rate was allowed to decrease to the level of STATE 4 respiration, indicating a complete conversion of ADP in ATP. The P:O ratio was calculated dividing the amount of ADP used by the amount of oxygen used by the mitochondria to use all the ADP. Next, the mitochondrial complex-specific respiration was determined using complex-specific substrates and ADP (4 mM). Glutamate (10 mM) and malate (2 mM) were used as CI substrates, succinate (10 mM) for CII and ascorbate (2 mM) plus TMPD (0.5 mM) as CIV substrates. The glycerol-3-phosphate dyhydrogenase (G3PDH) respiration was measured in the presence of glycerophosphate (20 mM) and flavine adenine dinucleotide (10 µM) and was terminated by antimycin A (2.5 µM). To inhibit CI and CII, rotenone (0.5 µM) and atpenin A5 (50 nM, Enzo Life Sciences, Raamdonksveer, The Netherlands) were added, respectively. Finally, the integrity of the mitochondrial outer membrane was tested using 10 µM cytochrome c (respiratory rate increase should be less than 10%) (45).

Mitochondrial membrane potential analysis

Cells were seeded in 35 mm Fluorodishes (World Precision Instruments GmbH, Berlin, Germany) and cultured accordingly. Exposed cells were loaded with tetramethylrhodamine methyl ester (100nM) (TMRM, Thermo Fisher Scientific, Bleiswijk, The Netherlands) for 25 minutes at 37°C, 5% (v/v) CO_2. Next, cells were washed once using krebs-henseleit buffer supplemented with Hepes (10 mM, KHH) (pH 7.4), and images were captured using a temperature-

controlled chamber connected to an inverted microscope (Axiovert 200M, Carl Zeiss, Sliedrecht, The Netherlands) using a x63, 1.25 NA Plan NeoFluor oil immersion objective. As a positive control, the known uncoupling agent carbonyl cyanide-4-(trifluoromethoxy)phenylhydrazone (FCCP) was used at the end of each measurement. Images were corrected for background and uneven illumination followed by analysis where images were masked with a binarised image for mitochondrial morphology using Image Pro Plus software (version 6.3, Media Cybernetics, Silver Spring, MD, United States of America) as previously described (46).

Reactive oxygen species generation analysis

To measure cellular reactive oxygen species (ROS), ciPTEC-T1 were seeded in flat bottom 96-well black/clear plates (Corning, Badhoevedorp, The Netherlands). Exposed cells were loaded with 5-(and-6)-chloromethyl-2′,7′-dichlorodihydrofluorescein diacetate, acetyl ester (CM-H_2DCFDA, 10 µM, Thermo Fisher Scientific, Bleiswijk, The Netherlands) in KHH buffer for 20 minutes at 37°C, 5% (v/v) CO_2 to measure cellular reactive oxygen species. Mitochondrial ROS production was detected using the redox-sensitive and cell-permeant probe hydroethidium (10 µM, Thermo Fisher Scientific, Bleiswijk, The Netherlands) in exposed ciPTEC. Subsequently, cells were washed twice using KHH buffer and imaging was performed using a BD Pathway 855 high-throughput microscope (Becton Dickinson, Drachten, The Netherlands). Images were background corrected and average CM-DCF or hydroethidium intensity per cellular pixel was determined Image Pro Plus software (version 6.3, Media Cybernetics, Silver Spring, MD, United States of America).

OXPHOS complex and citrate synthase activities

Approximately 6×10^6 exposed ciPTEC-T1 cells were harvested and resuspended in Tris-HCl buffer (10 mM). Next, samples were pottered in the presence of sucrose (215 mM) to obtain a homogenous fraction. Samples were centrifuged for 10 minutes at 600 g to remove cellular debris. The supernatant containing mitochondria was centrifuged for 10 minutes at 14,000 g. The pellet was resuspended in Tris-HCl buffer (pH 7.6), snap frozen in liquid N_2 and stored at -80°C until usage. The catalytic capacity of the OXPHOS complexes was measured using a spectrophotometric method, as previously described (47). Citrate synthase activity was determined simultaneously as described previously (48). The catalytic activity of CI - IV and citrate synthase were corrected for mg cellular protein.

Cytosolic pH measurements

ciPTEC-T1 were seeded in 35 mm Fluorodishes (World Precision Instruments GmbH, Berlin, Germany) and cultured accordingly. Exposed cells were loaded with the cytosolic pH-sensitive reporter molecule BCECF-AM (5 µM, 2',7'-Bis-(2-Carboxyethyl)-5-(and-6)-Carboxyfluorescein acetoxy methyl ester form) (Thermo Fisher Scientific, Bleiswijk, The Netherlands) in KHH buffer and incubated for 15 minutes at 37°C. Cells were washed three times using KHH buffer and imaging was performed using an inverted microscope (Axiovert 200M, Carl Zeiss, Sliedrecht, The Netherlands). BCECF fluorescence was sequentially excited at the isosbestic point (440 nm) (100 ms) and at the H^+-sensitive wavelength (490 nm) (100 ms). Fluorescent images were captured at 530 nm emission wavelength. Images were analysed using Image Pro Plus software (version 6.3, Media Cybernetics, Silver Spring, MD, United States of America). After background correction the 490/440 emission ratio was used to quantify cellular pH (43, 49).

Immunocytochemistry

ciPTEC were cultured on human collagen IV coated (50 µg/ml in Hank's Balanced Salt Solution (HBSS), Thermo Fisher Scientific, Bleiswijk, The Netherlands) µ-slide 8 well chambers (Ibidi GmbH, Martinsried, Germany). As controls, cells were exposed to resveratrol (10 µM) for 48 hours at 37°C, 5% (v/v) CO_2 to induce the expression of PCG-1α, COX and complex V, whereas rapamycin (500 nM) was used for 48 hours to attenuate the expression of the proteins of interest as it is a known mTOR-dependent mitophagy inducer. First, exposed ciPTEC were incubated using mitotracker red (400nM, Thermo Fisher Scientific, Bleiswijk, The Netherlands) for 30 minutes at 37°C, 5% (v/v) CO_2. Next, cells were fixed using 2% (w/v) paraformaldehyde in HBSS supplemented with 2% (w/v) sucrose for 5 minutes and permeabilised using 0.3% (v/v) Triton X-100 in HBSS for 10 minutes, all at room temperature (rT). To prevent a-specific binding of antibodies, cells were blocked using 2% FCS (v/v), 2% (w/v) BSA fraction V (Roche, Woerden, The Netherlands) and 0.1% (v/v) Tween-20 in HBSS for 30 minutes. Next, cells were incubated against PCG-1α (1:50 dilution in block solution; clone 3G6; Cell Signaling Technology, Leiden, The Netherlands), COX (1:100 dilution in block solution; ab14705, Abcam, Cambridge, United Kingdom) and CV (1:100 dilution in block solution; clone 7H10BD4F9, Mitosciences, Abcam, Cambridge, United Kingdom) for 1 hour at rT. Subsequently, cells were incubated with goat-anti-rabbit- or goat-anti-mouse-Alexa488 conjugate (1:200, Abcam, Cambridge, United Kingdom) and finally nuclei were stained using DAPI (300 nM, Thermo

Fisher Scientific, Bleiswijk, The Netherlands) for 5 minutes at rT. Images were captured using the Olympus FV1000 Confocal Laser Scanning Microscope (Olympus, Tokyo, Japan) and the Olympus software FV10-ASW version 1.7. Images were analysed using Image Pro Plus software (version 6.3, Media Cybernetics, Silver Spring, MD, United States of America). For both the COX and CV images, background was subtracted and subsequently a mitochondrial binary mask was created using the mitotracker red images. Next, the mitochondrial mask was combined with the COX or CV images and the intensity per mitochondrial pixel was quantified. The PGC-1α images were combined with a nuclear binary mask instead of a mitochondrial mask, which was made using the DAPI images.

Data analysis

All data are expressed as mean ± S.E.M of multiple independent replicates as indicated. Statistical analysis was performed using GraphPad Prism version 5.02 (La Jolla, CA, United States of America). A one-way or two-way ANOVA analysis was performed followed by the appropriate post-hoc analysis as indicated. A p-value of <0.05 was considered significant.

RESULTS

Dexamethasone attenuates LPS-induced endotoxemia associated mitochondrial dysfunction

Production of IL-6 and IL-8 in renal cells was clearly stimulated upon twenty-four hour LPS treatment (42 ± 7 ng×ml^{-1}, $p<0.01$ vs. 37 ± 9 ng×ml^{-1}, $p<0.05$, respectively) (Fig. 3.1A and 1B), thereby mimicking the human responses in our model. In addition, Peters *et al.*, also demonstrated recently that LPS treatment of ciPTEC provides a valid model to study sepsis-induced endotoxemia (7). Upon co-treatment with dexamethasone the IL-6 production tended to be decreased as compared to LPS treatment (Fig. 3.1A), where the significant IL-8 production was vanished (Fig. 3.1B).

Here, we further investigated the cellular responses to LPS by evaluating the generation of reactive oxygen species (ROS). Exposure of ciPTEC to LPS for 24 hours led to increased ROS levels (123 ± 6%, $p< 0.001$), as determined by the general ROS indicator 5-(and-6)-chloromethyl-2′,7′-dichlorofluorescein CM-DCF (Fig. 3.2B). However, increased ROS production was not observed when mitochondrial superoxide anions were measured (Fig. 3.2C). The latter

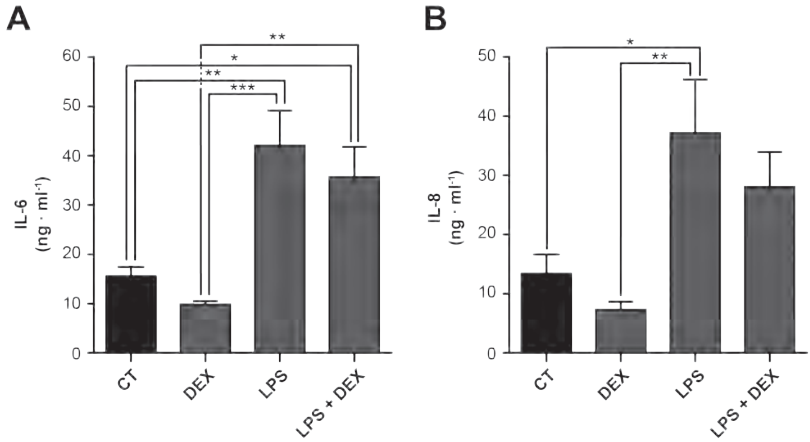

Figure 3.1 Dexamethasone co-treatment reduced IL-6 and IL-8 cytokine production in LPS-induced endotoxemia.

To induce endotoxemia ciPTEC proximal tubule cells were exposed to 10 μg/mL lipopolysacharide (LPS) for 20 hours. Subsequently, the cells were co-treated with dexamethasone (10 μM, DEX) for 4 hours, as indicated in figure 3.2A, and (a) IL-6 and (b) IL-8 cytokine excretion into the culture medium was measured by ELISA. Statistical analysis: one-way ANOVA with Tukey's post-hoc analysis: *p<0.05, **p<0.01, ***p<0.001. Mean ± SEM, n = 5 independent experiments.

could probably be explained by the versatility of superoxide anions, which are rapidly degraded into hydrogen peroxide, which is quickly detoxified either enzymatically by catalase or via the reduction of glutathione (GSH) (Fig. 3.2D). A brief 4 hours co-treatment of the cells with dexamethasone was sufficient to reverse the observed LPS-induced ROS generation (Fig 3.2A and B), and respiratory inhibition by increasing OXPHOS CI- (25 ± 9%, p< 0.05) and CII-driven respiration (38 ± 11%, p< 0.01) compared to control LPS-treated cells (Fig 3.3A-C). Of note, CIV-driven respiration was not reduced after LPS treatment, which could be explained by the auto-oxidative potential of the substrates used (*i.e.* ascorbate and TMPD) leading to a decreased sensitivity (Fig. 3.3C). Importantly, respiratory inhibition by LPS was only apparent upon maximal stimulation of the respiratory chain in permeabilised cells, as observed for the CI- (32 ± 13%, p< 0.001), CII- (27 ± 13%, p< 0.001), and glycerophosphate dehydrogenase (G3PDH; 34 ± 16%, p< 0.01)-driven respiration, but not under basal conditions (Fig. 3.3B and C).

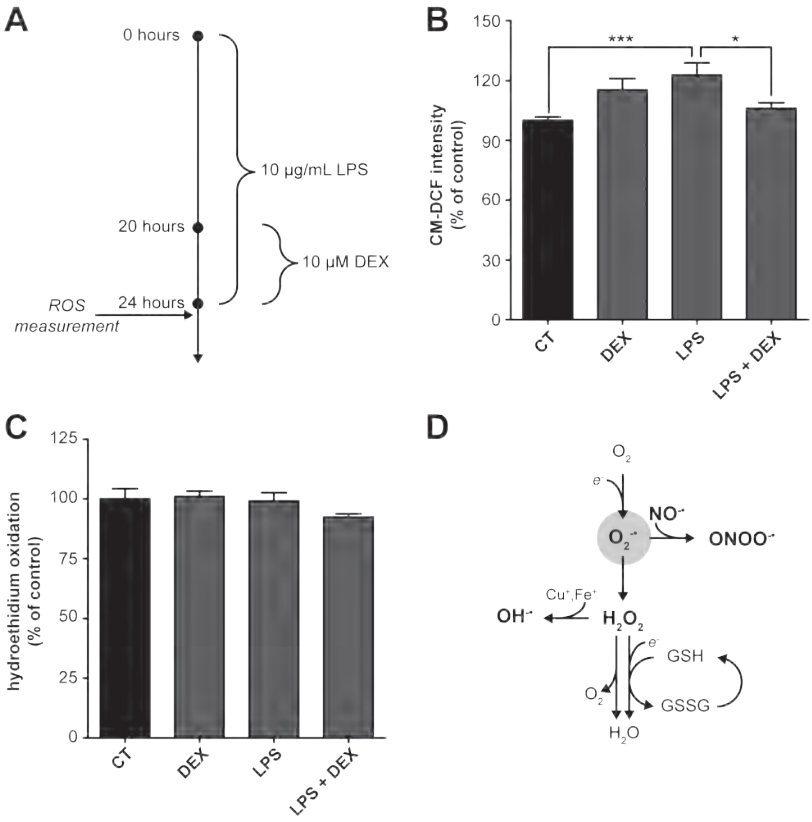

Figure 3.2 LPS-induced endotoxemia is characterised by ROS generation and is attenuated by dexamethasone treatment.

(a) To induce endotoxemia ciPTEC proximal tubule cells were exposed to 10 µg/mL lipopolysacharide (LPS) for 20 hours. Subsequently, the cells were co-treated with dexamethasone (10 µM, DEX) for 4 hours. (b,c) After dexamethasone and/or LPS exposure the generation of reactive oxygen species (ROS) is examined using (B) CM-DCF or (c) hydroethidium for the detection of general cellular ROS species or superoxide anions ($O_2^{\cdot-}$), respectively. Values were normalised to control (CT): CM-DCF (766 ± 64 arbitrary intensity units), hydroethidium (343 ± 64 arbitrary intensity units). (d) Cellular fate of superoxide anions into reactive nitrogen species ($NO^{\cdot}$, $ONOO^{\cdot-}$), hydroxyl radicals ($OH^{\cdot}$) and hydrogen peroxide (H_2O_2). Statistical analysis: one-way ANOVA with Tukey's post-hoc analysis: *p<0.05, ***p<0.001. Mean ± SEM, n = 3 independent experiments.

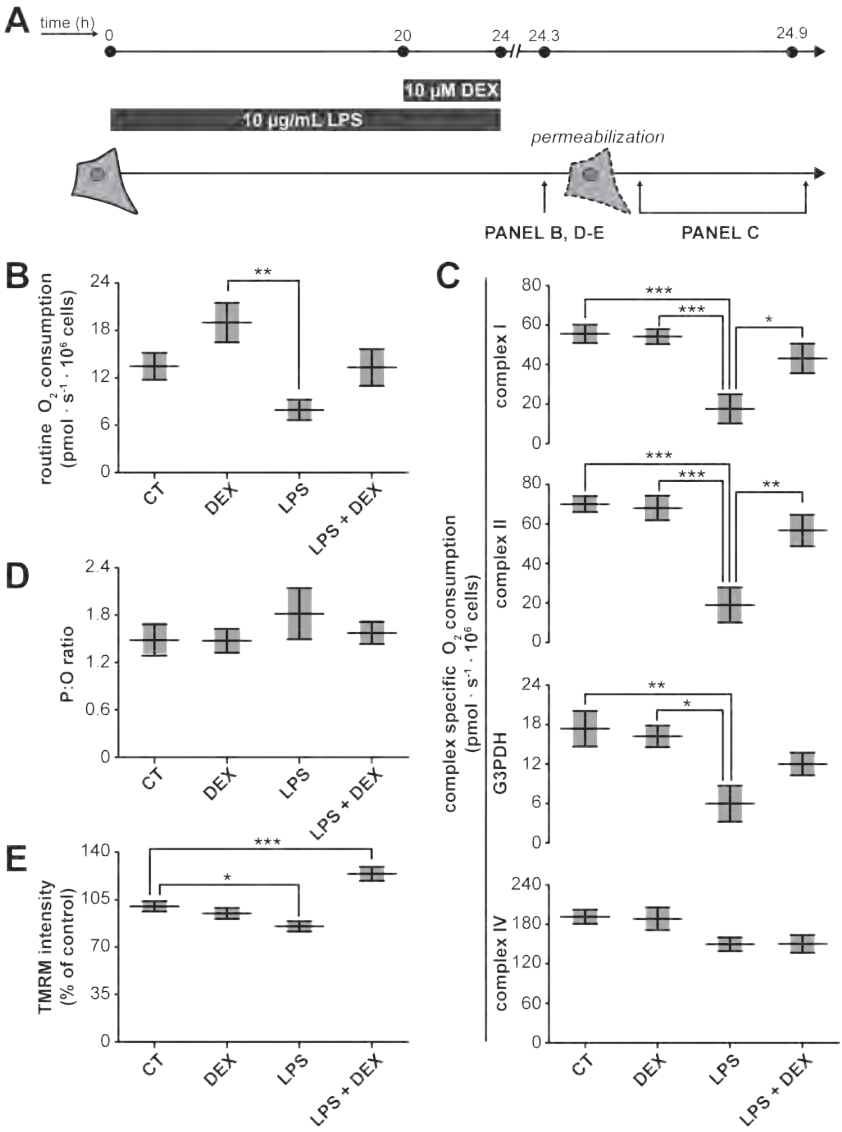
A
time (h)
0
20
24
24.3
24.9
10 µM DEX
10 µg/mL LPS
permeabilization
PANEL B, D-E
PANEL C
B
routine O2 consumption (pmol · s-1 · 10^6 cells)
CT
DEX
LPS
LPS + DEX
C
complex specific O2 consumption (pmol · s-1 · 10^6 cells)
complex I
complex II
G3PDH
complex IV
D
P:O ratio
E
TMRM intensity (% of control)

Figure 3.3 LPS-induced endotoxemia leads to severe mitochondrial dysfunction which is restored by dexamethasone treatment.
(a) Cells were treated with LPS and dexamethasone (DEX) as described in detail in figure 3.2A. (b) Next, cells were harvested and transferred to the chambers of the respirometer to determine routine oxygen consumption. (c) After permeabilisation of the plasma membrane, OXPHOS complex I (CI)-, CII-, glycerol-3-phosphate dehydrogenase (G3PDH)-, and CIV-driven oxygen consumption rates were measured. (d) The mitochondrial coupling was determined using the P:O ratio, before the measurement of the complex-specific respiratory rates, and calculated dividing the amount of ADP used by the amount of oxygen used by the mitochondria to use all the ADP (220 nM). (e) Alternatively, mitochondrial coupling was determined by measuring the mitochondrial membrane potential using the cationic dye tetramethylrhodamine methyl ester (TMRM). Values were normalised to control (CT): 158 ± 22 arbitrary intensity units. Statistical analysis: one-way ANOVA with Tukey's post-hoc analysis: *p<0.05, **p<0.01, ***p<0.001. Mean ± SEM, n = 3 independent experiments.

Such a specific pattern points to a decreased mitochondrial respiratory reserve capacity, which can be explained by a decreased mitochondrial membrane potential or a decreased substrate availability. The ATP produced per oxygen atom reduced by the OXPHOS system (i.e. P:O ratio), provides an indication for the mitochondrial coupling of both processes. The observed tendency of LPS to increase the P:O is in line with the idea that coupling was decreased (Fig. 3.3D), which was confirmed after measuring the mitochondrial membrane potential using TMRM (Fig. 3.3E). Dexamethasone co-exposure corrected the LPS-induced depolarisation of the mitochondrial membrane potential, which corroborates the other beneficial effects on mitochondrial function, and even showed hyperpolarisation (Fig. 3.3E; 124 ± 5%, p< 0.001).

Dexamethasone increases OXPHOS complex V activity and its expression

Respiratory inhibition combined with a decreased mitochondrial membrane potential after LPS exposure could potentially be explained by a direct inhibition of one of the OXPHOS complexes. We could, however, not detect inhibition of LPS on the enzyme activity of the individual CI to CV activities (Fig. 3.4). Surprisingly, CV enzyme activity was enhanced upon dexamethasone treatment (123 ± 10%, p< 0.05), and also, but not significantly, when cells were exposed to LPS (Fig. 3.4). Moreover, increased CV activity could provide an explanation for the increased mitochondrial membrane potential, when the complex runs into reverse mode (e.g. pumps electrons

from the mitochondrial matrix to the inner membrane space at the expense of ATP). Besides an increase in the intrinsic enzyme activity, induction could also be due to an enhanced complex V expression. However, citrate synthase activity, a marker of mitochondrial mass, did not change upon dexamethasone or LPS exposure (Fig. 3.5A). To exclude a role of mitochondrial biogenesis the expression of PGC-1α was investigated, which is a master regulator of mitochondrial biogenesis (Fig. 3.5B) (24). Although the positive regulator of mitochondrial mass, resveratrol, induced nuclear PGC-1α expression, no significant changes were found after 4 hours dexamethasone treatment (Fig. 3.5C). Using immunocytochemistry, we could confirm that CV expression per mitochondrial pixel was increased (Fig. 3.6; 140 ± 6%, p< 0.001), which was reduced by rapamycin, an mTOR-dependent mitophagy inducer. To investigate whether the increased CV expression was specific for this complex, we also determined CIV expression (Fig. 3.7), which was up regulated by resveratrol but not by dexamethasone (Fig. 3.7B).

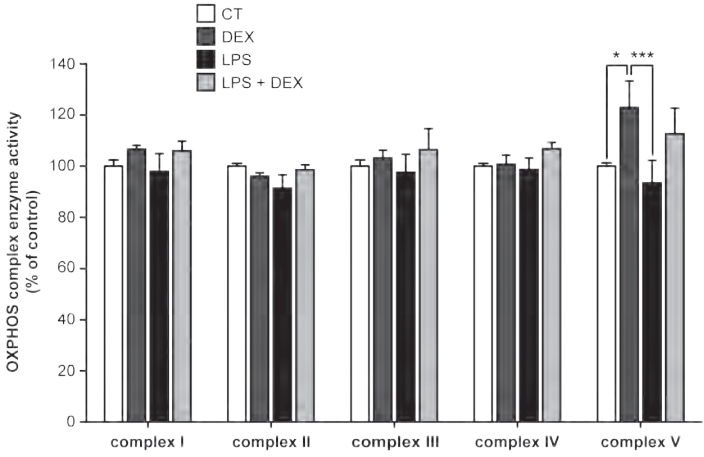

Figure 3.4 Dexamethasone leads to an increased enzyme activity of OXPHOS complex V without affecting the activity of complex I-IV.
Cells were treated with LPS and dexamethasone (DEX) as described in detail in figure 3.2A. Next, cells were harvested and complex I-V enzyme activity was measured spectrophotometrically. Values were corrected for cellular protein and normalised to control (CT): complex I (160 ± 9 U×mg protein^{-1}), complex II (220 ± 7 U×mg protein^{-1}), complex III (202 ± 6 U×mg protein^{-1}), complex IV (183 ± 10 U×mg protein^{-1}), complex V (282 ± 87 U×mg protein^{-1}). Statistical analysis: two-way ANOVA with Bonferroni's post-hoc analysis: *p<0.05, ***p<0.001. Mean ± SEM, n = 3 independent experiments.

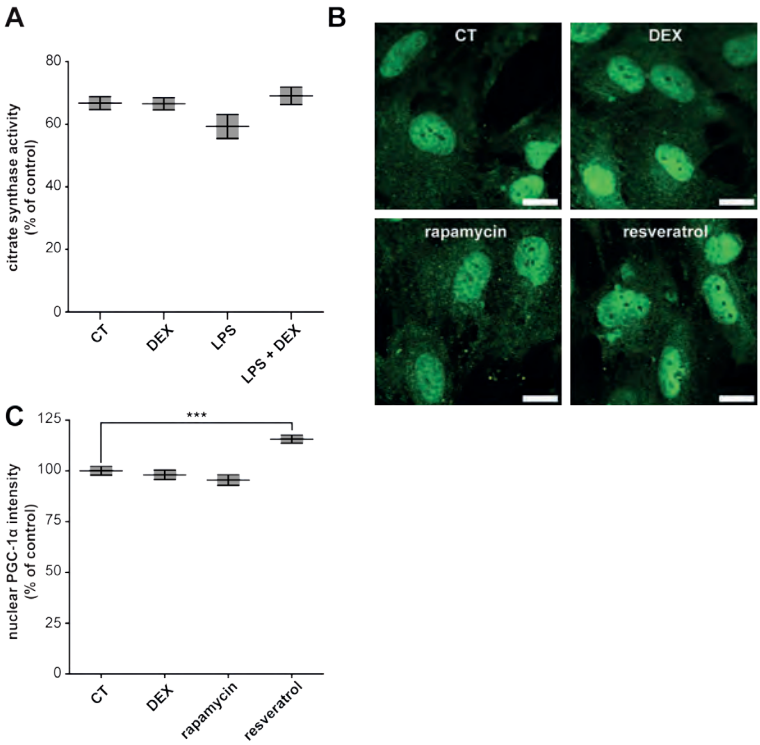

Figure 3.5 Mitochondrial mass and PGC-1a expression are not affected by dexamethasone.

(a) Cells were treated with LPS and dexamethasone (DEX), as described in detail in figure 3.2A. Next, cells were harvested and citrate synthase activity was measured spectrophotometrically as a measure of mitochondrial mass. Values were corrected for cellular protein and normalised to control (CT): 362 ± 28 U×mg protein^{-1}. Statistical analysis: one-way ANOVA with Tukey's post-hoc analysis: no statistical differences were observed. Mean ± SEM, n = 3 independent experiments. (b) The expression of PGC-1α, a master regulator of mitochondrial biogenesis, was measured using immunocytochemistry after 4 hours dexamethasone treatment (10 μM, DEX). In addition, cells were incubated for 48 hours with rapamycin (500 nM) or resveratrol (10 μM) as known negative and positive regulators of PGC-1α and mitochondrial mass (scale: 20 μm) (c) The nuclear PGC-1α expression was quantified using a nuclear mask based on DAPI staining. Values were normalised to control (CT): 15900 ± 370 arbitrary intensity units. Statistical analysis: one-way ANOVA with Dunnett's post-hoc analysis: ***$p<0.001$. Mean ± SEM, n ≥ 253 individual cells analysed in n = 3 independent experiments.

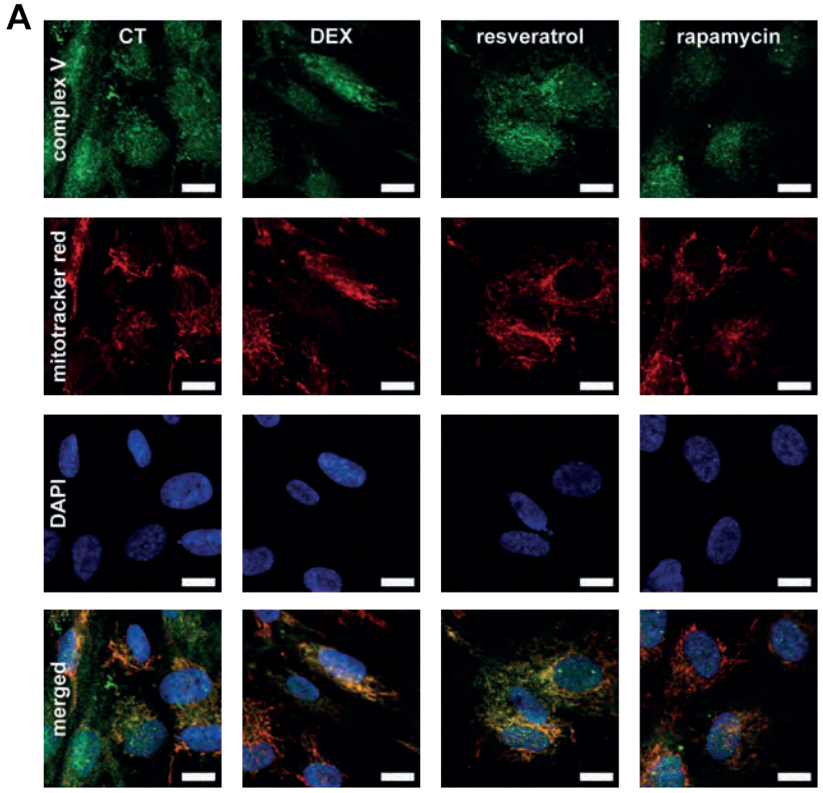
A
CT
DEX
resveratrol
rapamycin
complex V
mitotracker red
DAPI
merged
B
complex V expression
(% of control)
200
150
100
50
0
***
***
CT
DEX
resveratrol
rapamycin

Figure 3.6 Dexamethasone increases OXPHOS complex V expression.
(a) The expression of OXPHOS complex V was measured using immunocytochemistry after 4 hours dexamethasone treatment (10 μM, DEX). In addition, cells were incubated for 48 hours with rapamycin (500 nM) or resveratrol (10 μM) as known negative and positive regulators of mitochondrial mass. Mitochondria were stained with mitotracker red and nuclei with DAPI to determine the cellular localisation (scale: 20 μm). (b) The mitochondrial complex V expression was quantified using a mitochondrial mask based on the mitotracker red staining. Values were normalised to control (CT): 40.4 ± 1.1 arbitrary intensity units/ mitochondrial pixel. Statistical analysis: one-way ANOVA with Dunnett's post-hoc analysis: ***$p<0.001$. Mean ± SEM, $n \geq 89$ individual cells analysed in $n = 3$ independent experiments.

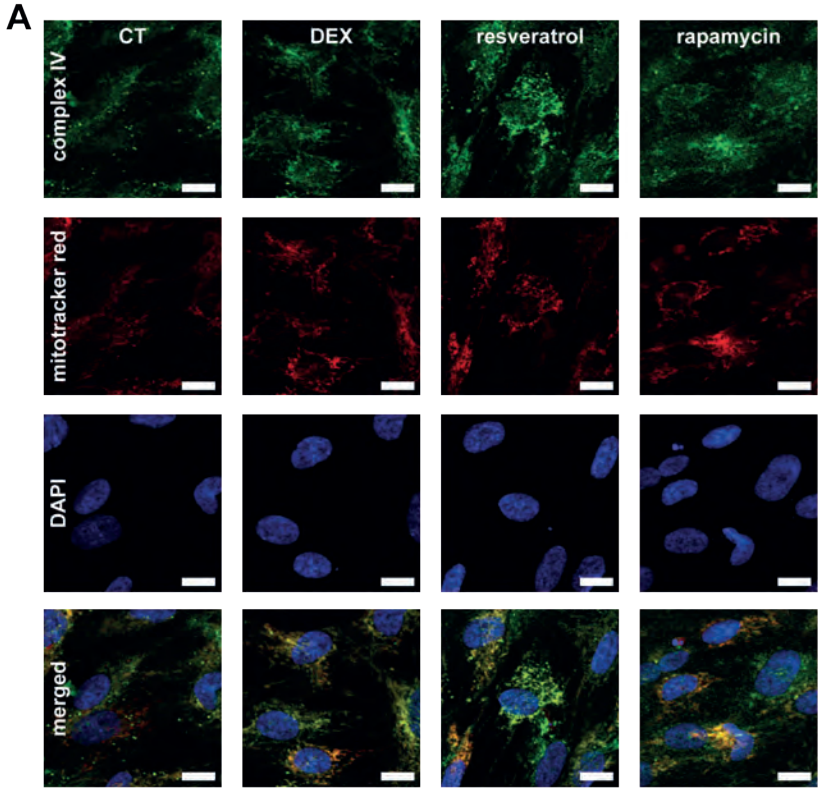
A
CT
DEX
resveratrol
rapamycin
complex IV
mitotracker red
DAPI
merged
B
complex IV expression (% of control)
200
150
100
50
0
***
CT
DEX
resveratrol
rapamycin

Figure 3.7 Dexamethasone does not affect the OXPHOS complex IV expression.
(a) The expression of OXPHOS complex IV was measured using immunocytochemistry after 4 hours dexamethasone treatment (10 μM, DEX). In addition, cells were incubated for 48 hours with rapamycin (500 nM) or resveratrol (10 μM) as known negative and positive regulators of mitochondrial mass. Mitochondria were stained with mitotracker red and nuclei with DAPI to determine the cellular localisation (scale: 20 μm). (b) The mitochondrial complex IV expression was quantified using a mitochondrial mask based on the mitotracker red staining. Values were normalised to control (CT): 33.2 ± 1.5 arbitrary intensity units/ mitochondrial pixel. Statistical analysis: one-way ANOVA with Dunnett's post-hoc analysis: ***p<0.001. Mean ± SEM, n ≥ 89 individual cells analysed in n = 3 independent experiments.

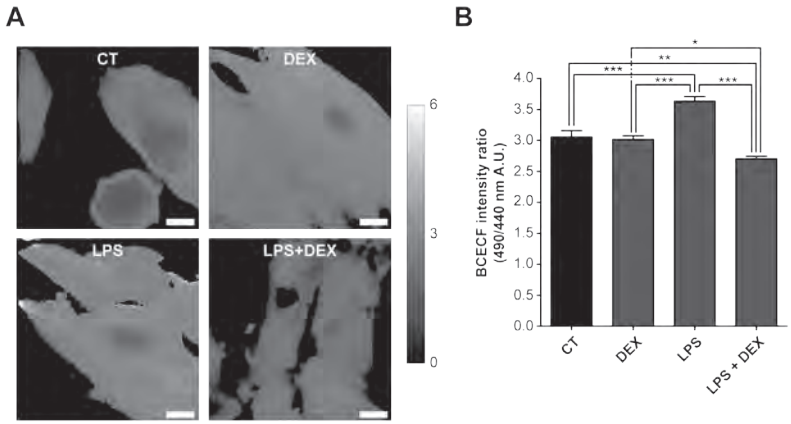

Figure 3.8. LPS-induced endotoxemia alkalisation of the intracellular pH is reversed by dexamethasone co-treatment.
(a) Cells were treated with LPS and dexamethasone (DEX) as described in detail in figure 3.2A. After exposure, intracellular pH was measured using the ratiometric probe BCECF. pH levels were determined using ratio images which were obtained by dividing the 490 nm by the 440 nm image, (b) and quantified on a single cell level. Statistical analysis: one-way ANOVA with Tukey's post-hoc analysis: *p<0.05, **p<0.01, ***p<0.001. Mean ± SEM, n ≥ 77 individual cells analysed in n = 3 independent experiments.

Dexamethasone reverses LPS-induced cellular alkalisation

The increased CV expression could potentially be explained as a compensatory mechanism of the reduced intracellular pH upon dexamethasone treatment, as an acidified milieu is known to inhibit activity of the complex (25, 26). Indeed, we observed that the BCECF ratio, providing a measure of the cellular pH, increased after LPS exposure, indicative of an intracellular alkalisation (Fig. 3.8A and B; 114 ± 2%, $p<0.001$). Such an increased intracellular pH is also in line with the observed decreased mitochondrial membrane potential (Fig. 3.3E), which depends on the ΔpH between the matrix (~ 7.8) and inner membrane space (~7.0). The mitochondrial outer membrane is permeable for protons, thus the pH of the inner membrane space will be equal to the cytosolic pH. A raise in intracellular pH will therefore cause dissipation of the ΔpH and as a consequence the mitochondrial membrane potential. When co-exposed to dexamethasone the BCECF ratio decreased indicative of a slight but significant cellular acidification (Fig. 3.8B; 87 ± 2%, $p< 0.05$). As mentioned, this will result in a minor inhibition of complex V, which could explain its increased expression as a compensatory response, further contributing to the restoration of the LPS-induced decrease in mitochondrial function.

DISCUSSION

AKI is characterised by high mortality rates in patients admitted to the ICU, as efficient treatment modalities are absent. Maintaining renal mitochondrial function is considered to be essential for a better outcome of AKI, therefore, these organelles could be of interest as therapeutic targets (3). In this study, we confirmed the importance of mitochondrial function in human PTEC during experimental inflammatory conditions and we demonstrated mechanistic insights into the beneficial effects of dexamethasone treatment. We showed that dexamethasone attenuates the LPS-induced inflammatory response, illustrated by a reduced cytokine excretion. These findings were corroborated by a small but significant dexamethasone-mediated intracellular acidification and, as a consequence, an attenuation of the LPS-induced mitochondrial dysfunction. LPS-induced endotoxemia resulted in a decreased mitochondrial respiration, decreased mitochondrial membrane potential and increased ROS generation, which is explained by alkalisation of the intracellular milieu. These data are compatible with the postulated central role of mitochondria in sepsis-induced AKI in patients.

In addition, we demonstrated a possible new mechanism contributing to the development of inflammatory conditions. Previously, AKI-associated mitochondrial mechanisms were predominantly attributed to a decreased metabolic capacity, such as an increased ROS generation, decreased mitochondrial biogenesis and mitochondrial permeability pore opening, leading to apoptosis (3, 19).

Although the dexamethasone-induced changes in intracellular pH have not been associated earlier with the beneficial effects in AKI, it has been reported previously that the glucocorticoid leads to intracellular acidification in proximal tubule cells. This acidification was explained by the stimulating effect of dexamethasone on the basolatoral sodium-bicarbonate (Na^+:HCO_3^-) co-transporter (NBC1) and the sodium-proton (Na^+,H^+) exchanger (NHE3) at the luminal side (27, 28), which together with Na^+,K^+-ATPase activity are responsible for the renal bicarbonate reabsorption under physiological conditions (29). Although the activity of both transporters was enhanced by dexamethasone, only the NBC1 expression was found to be increased (27). Combined with an efflux stoichiometry of 1:3 for the Na^+:HCO_3^- efflux, the net effect of dexamethasone causes a drop in the intracellular HCO_3^- concentration and consequently in the pH (27, 28, 30). However, NHE3 expression has been demonstrated to increase upon LPS exposure in monocytes (31) and leads to an extracellular acidification in proximal tubule cells (32). The latter also being characteristic for inflammatory conditions, which has been associated with decreased cytokine production rates in epithelial cells (33), indicating the complex interplay of the different pathways affected by LPS and dexamethasone.

The drop in intracellular pH after co-treatment with dexamethasone does, however, provides an explanation for the observed up-regulation of mitochondrial complex V expression, as the slightly acidified environment is known to inhibit the mitochondrial F_1F_o ATP synthase (CV)(25, 26). Such an induction of the complex V expression can also be observed in iron- and ethanol-induced mitochondrial dysfunction, and could be considered as a more general response to mitochondrial damage (34, 35). In addition, our results provide an explanation for the previously observed increased expression of the mitochondrial F_1F_o ATP synthase and the adenine nucleotide translocator (36), as both are inhibited by a low intracellular pH (25, 26). The latter also emphasizes the important role of the cellular pH in the observed mitochondrial responses after LPS and dexamethasone treatment.

Besides restoration of the intracellular pH and mitochondrial function, dexamethasone is also expected to have other beneficial effects on the progression of AKI. Dexamethasone has been demonstrated to increase the renal microvascular oxygenation, which is also expected to improve the respiratory capacity resulting from a decreased oxygen availability (17). In addition, dexamethasone is known to inhibit iNOS and thereby to decrease the formation of NO, which has a vasodilatory action and can form nitrogen radicals. Previous studies did illustrate that iNOS expression is indeed decreased upon dexamethasone treatment, however, the NO levels were not fully reversed or were even unchanged (16, 17). This gives rise to the idea that not all NO-mediated oxidative stress originates from iNOS, which is in line with a central role of mitochondrial dysfunction in the AKI pathogenesis. Although our work confirms such a role and supports previous results showing mitochondrial CIII as a major ROS generation site (37), we cannot exclude other effects of dexamethasone. For example, dexamethasone appeared to be an inhibitor of NADPH oxidase (NOX)-2-dependent ROS generation as well (38).

Until now almost all *in vivo* and patient studies showed beneficial effects of dexamethasone in a prophylactic setting (11, 14, 16, 19). This warrants further investigation of the potential beneficial effects of dexamethasone treatment at the manifestation of AKI in animal models and patients. However, dexamethasone intervention, in general, is limited by its narrow therapeutic window. This is probably also the main reason for the equivocal effects observed in clinical trials, whereas low-dose treatments show beneficial effects opposed to no or detrimental effects of high-dose regimens (11, 12, 16, 17). Future research should provide better insight into the balance between efficacy and safety of dexamethasone treatment. Alternatively, novel pharmaceutical interventions could be investigated, which also target the cellular pH without impacting the adverse mechanisms activated upon high-dose dexamethasone treatment.

In conclusion, we provide mechanistic insights into the observed beneficial effects of dexamethasone in AKI and emphasize a key role of mitochondria in the disease. The striking effects on intracellular pH, hence, provide novel therapeutic avenues for effective treatment of patients suffering from septic AKI.

Innovation

AKI is associated with more than 20% of all adult hospitalisations worldwide, has a poor prognosis, and the underlying mechanism remains poorly understood. Although a key role for mitochondrial damage has been recognised, its aetiology remains elusive. Our results demonstrate that cellular alkalisation could be the initiating event underlying LPS-induced mitochondrial dysfunction in a human proximal tubule epithelial cell model. Moreover, we provide a rationale for the beneficial effects of the glucocorticoid dexamethasone in AKI, as it corrects cellular pH and, consequently, mitochondrial function. Eventually this will provide novel therapeutic avenues for the treatment of septic AKI.

Acknowledgments

This research was supported as part of the Netherlands Organization for Scientific Research (NWO) Centers for Systems Biology Research initiative (CSBR09/013V) and the Netherlands Institute for Regenerative Medicine (NIRM, Grant no. FES0908). We thank G.H. Renkema for the OXPHOS complex enzyme activity measurements.

REFERENCES

1. Lameire NH, Bagga A, Cruz D, De Maeseneer J, Endre Z, Kellum JA, et al. Acute kidney injury: an increasing global concern. Lancet. 2013;382(9887):170-9.
2. Siew ED, Davenport A. The growth of acute kidney injury: a rising tide or just closer attention to detail? Kidney international. 2015;87(1):46-61.
3. Ishimoto Y, Inagi R. Mitochondria: a therapeutic target in acute kidney injury. Nephrology, dialysis, transplantation : official publication of the European Dialysis and Transplant Association - European Renal Association. 2015.
4. Hoste EA, Bagshaw SM, Bellomo R, Cely CM, Colman R, Cruz DN, et al. Epidemiology of acute kidney injury in critically ill patients: the multinational AKI-EPI study. Intensive care medicine. 2015;41(8):1411-23.
5. Yang Y, Song M, Liu Y, Liu H, Sun L, Peng Y, et al. Renoprotective approaches and strategies in acute kidney injury. Pharmacology & therapeutics. 2016;163:58-73.
6. Kaushal GP, Shah SV. Challenges and advances in the treatment of AKI. Journal of the American Society of Nephrology : JASN. 2014;25(5):877-83.
7. Peters E, Geraci S, Heemskerk S, Wilmer MJ, Bilos A, Kraenzlin B, et al. Alkaline phosphatase protects against renal inflammation through dephosphorylation of lipopolysaccharide and adenosine triphosphate. British journal of pharmacology. 2015;172(20):4932-45.
8. Tumlin J, Wali R, Williams W, Murray P, Tolwani AJ, Vinnikova AK, et al. Efficacy and safety of renal tubule cell therapy for acute renal failure. Journal of the American Society of Nephrology : JASN. 2008;19(5):1034-40.
9. Fissell WH, Dyke DB, Weitzel WF, Buffington DA, Westover AJ, MacKay SM, et al. Bioartificial kidney alters cytokine response and hemodynamics in endotoxin-challenged uremic animals. Blood purification. 2002;20(1):55-60.
10. Humes HD, Weitzel WF, Fissell WH. Renal cell therapy in the treatment of patients with acute and chronic renal failure. Blood purification. 2004;22(1):60-72.
11. Jacob KA, Leaf DE, Dieleman JM, van Dijk D, Nierich AP, Rosseel PM, et al. Intraoperative High-Dose Dexamethasone and Severe AKI after Cardiac Surgery. Journal of the American Society of Nephrology : JASN. 2015.
12. Scrascia G, Guida P, Rotunno C, de Luca Tupputi Schinosa L, Paparella D. Anti-inflammatory strategies to reduce acute kidney injury in cardiac surgery patients: a meta-analysis of randomized controlled trials. Artificial organs. 2014;38(2):101-12.
13. Kadova Z, Dolezelova E, Cermanova J, Hroch M, Laho T, Muchova L, et al. IL-1 receptor blockade alleviates endotoxin-mediated impairment of renal drug excretory functions in rats. American journal of physiology Renal physiology. 2015;308(5): F388-99.

14. Chen Y, Du Y, Li Y, Wang X, Gao P, Yang G, et al. Panaxadiol Saponin and Dexamethasone Improve Renal Function in Lipopolysaccharide-Induced Mouse Model of Acute Kidney Injury. PloS one. 2015;10(7):e0134653.
15. Choi HM, Jo SK, Kim SH, Lee JW, Cho E, Hyun YY, et al. Glucocorticoids attenuate septic acute kidney injury. Biochemical and biophysical research communications. 2013;435(4):678-84.
16. Tsao CM, Ho ST, Chen A, Wang JJ, Li CY, Tsai SK, et al. Low-dose dexamethasone ameliorates circulatory failure and renal dysfunction in conscious rats with endotoxemia. Shock. 2004;21(5):484-91.
17. Johannes T, Mik EG, Klingel K, Dieterich HJ, Unertl KE, Ince C. Low-dose dexamethasone-supplemented fluid resuscitation reverses endotoxin-induced acute renal failure and prevents cortical microvascular hypoxia. Shock. 2009;31(5):521-8.
18. Prevoo B, Miller DS, van de Water FM, Wever KE, Russel FG, Flik G, et al. Rapid, nongenomic stimulation of multidrug resistance protein 2 (Mrp2) activity by glucocorticoids in renal proximal tubule. The Journal of pharmacology and experimental therapeutics. 2011;338(1):362-71.
19. Tabara LC, Poveda J, Martin-Cleary C, Selgas R, Ortiz A, Sanchez-Nino MD. Mitochondria-targeted therapies for acute kidney injury. Expert reviews in molecular medicine. 2014;16:e13.
20. Boron WF, Boulpaep EL. Medical Physiology: A Cellular and Molecular Approach: W.B. Saunders; 2003.
21. Tran M, Tam D, Bardia A, Bhasin M, Rowe GC, Kher A, et al. PGC-1alpha promotes recovery after acute kidney injury during systemic inflammation in mice. The Journal of clinical investigation. 2011;121(10):4003-14.
22. Tran MT, Zsengeller ZK, Berg AH, Khankin EV, Bhasin MK, Kim W, et al. PGC1alpha drives NAD biosynthesis linking oxidative metabolism to renal protection. Nature. 2016.
23. Jansen J, Schophuizen CM, Wilmer MJ, Lahham SH, Mutsaers HA, Wetzels JF, et al. A morphological and functional comparison of proximal tubule cell lines established from human urine and kidney tissue. Experimental cell research. 2014;323(1):87-99.
24. Fernandez-Marcos PJ, Auwerx J. Regulation of PGC-1α, a nodal regulator of mitochondrial biogenesis. The American Journal of Clinical Nutrition. 2011;93(4):884S-90S.
25. Forkink M, Manjeri GR, Liemburg-Apers DC, Nibbeling E, Blanchard M, Wojtala A, et al. Mitochondrial hyperpolarization during chronic complex I inhibition is sustained by low activity of complex II, III, IV and V. Biochimica et biophysica acta. 2014;1837(8):1247-56.
26. Chinopoulos C. Mitochondrial consumption of cytosolic ATP: not so fast. FEBS letters. 2011;585(9):1255-9.

27. Ali R, Amlal H, Burnham CE, Soleimani M. Glucocorticoids enhance the expression of the basolateral Na+:HCO3- cotransporter in renal proximal tubules. Kidney international. 2000;57(3):1063-71.
28. Ruiz OS, Wang LJ, Pahlavan P, Arruda JA. Regulation of renal Na-HCO3 cotransporter: III. Presence and modulation by glucocorticoids in primary cultures of the proximal tubule. Kidney international. 1995;47(6):1669-76.
29. Soleimani M, Burnham CE. Physiologic and molecular aspects of the Na+:HCO3- cotransporter in health and disease processes. Kidney international. 2000;57(2):371-84.
30. Peng J, He X, Wang K, Tan W, Wang Y, Liu Y. Noninvasive monitoring of intracellular pH change induced by drug stimulation using silica nanoparticle sensors. Analytical and bioanalytical chemistry. 2007;388(3):645-54.
31. Gaidano G, Ghigo D, Schena M, Bergui L, Treves S, Turrini F, et al. Na+/H+ exchange activation mediates the lipopolysaccharide-induced proliferation of human B lymphocytes and is impaired in malignant B-chronic lymphocytic leukemia lymphocytes. Journal of immunology. 1989;142(3):913-8.
32. Silva PHI, Girardi ACC, Rebouças NA. Differential responses of proximal tubule Na+/H+ exchanger NHE3 to low pH: comparison between metabolic and respiratory acidosis. The FASEB Journal. 2012;26(1 Supplement):689.5.
33. Hackett AP, Trinick RE, Rose K, Flanagan BF, McNamara PS. Weakly acidic pH reduces inflammatory cytokine expression in airway epithelial cells. Respiratory research. 2016;17(1):82.
34. Kim M-S, Kim J-S, Cheon C-I, Cho D-H, Park J-H, Kim K-I, et al. Increased expression of the F 1 F o ATP synthase in response to iron in heart mitochondria. BMB reports. 2008;41(2):153-7.
35. Mashimo K, Arthur PG, Ohno Y. Ethanol Dose- and Time-dependently Increases alpha and beta Subunits of Mitochondrial ATP Synthase of Cultured Neonatal Rat Cardiomyocytes. Journal of Nippon Medical School = Nippon Ika Daigaku zasshi. 2015;82(5):237-45.
36. Arvier M, Lagoutte L, Johnson G, Dumas JF, Sion B, Grizard G, et al. Adenine nucleotide translocator promotes oxidative phosphorylation and mild uncoupling in mitochondria after dexamethasone treatment. American journal of physiology Endocrinology and metabolism. 2007;293(5):E1320-4.
37. Kruzel ML, Actor JK, Radak Z, Bacsi A, Saavedra-Molina A, Boldogh I. Lactoferrin decreases LPS-induced mitochondrial dysfunction in cultured cells and in animal endotoxemia model. Innate immunity. 2010;16(2):67-79.
38. Huo Y, Rangarajan P, Ling EA, Dheen ST. Dexamethasone inhibits the Nox-dependent ROS production via suppression of MKP-1-dependent MAPK pathways in activated microglia. BMC neuroscience. 2011;12:49.

39. Heemskerk S, Peters JG, Louisse J, Sagar S, Russel FG, Masereeuw R. Regulation of P-glycoprotein in renal proximal tubule epithelial cells by LPS and TNF-alpha. Journal of biomedicine & biotechnology. 2010;2010:525180.
40. Schophuizen CM, Hoenderop JG, Masereeuw R, Heuvel LP. Uremic Toxins Induce ET-1 Release by Human Proximal Tubule Cells, which Regulates Organic Cation Uptake Time-Dependently. Cells. 2015;4(3):234-52.
41. Schirris TJ, Renkema GH, Ritschel T, Voermans NC, Bilos A, van Engelen BG, et al. Statin-Induced Myopathy Is Associated with Mitochondrial Complex III Inhibition. Cell metabolism. 2015;22(3):399-407.
42. Schirris TJJ, Ritschel T, Herma Renkema G, Willems PHGM, Smeitink JAM, Russel FGM. Mitochondrial ADP/ATP exchange inhibition: a novel off-target mechanism underlying ibipinabant-induced myotoxicity. Scientific Reports. 2015;5:14533.
43. Liemburg-Apers DC, Schirris TJ, Russel FG, Willems PH, Koopman WJ. Mitoenergetic Dysfunction Triggers a Rapid Compensatory Increase in Steady-State Glucose Flux. Biophysical journal. 2015;109(7):1372-86.
44. De Rasmo D, Gattoni G, Papa F, Santeramo A, Pacelli C, Cocco T, et al. The beta-adrenoceptor agonist isoproterenol promotes the activity of respiratory chain complex I and lowers cellular reactive oxygen species in fibroblasts and heart myoblasts. European journal of pharmacology. 2011;652(1-3):15-22.
45. Kuznetsov AV, Veksler V, Gellerich FN, Saks V, Margreiter R, Kunz WS. Analysis of mitochondrial function in situ in permeabilized muscle fibers, tissues and cells. Nature protocols. 2008;3(6):965-76.
46. Koopman WJ, Verkaart S, Visch HJ, van der Westhuizen FH, Murphy MP, van den Heuvel LW, et al. Inhibition of complex I of the electron transport chain causes O2-. -mediated mitochondrial outgrowth. American journal of physiology Cell physiology. 2005;288(6):C1440-50.
47. Janssen AJ, Trijbels FJ, Sengers RC, Smeitink JA, van den Heuvel LP, Wintjes LT, et al. Spectrophotometric assay for complex I of the respiratory chain in tissue samples and cultured fibroblasts. Clinical chemistry. 2007;53(4):729-34.
48. Janssen AJ, Trijbels FJ, Sengers RC, Wintjes LT, Ruitenbeek W, Smeitink JA, et al. Measurement of the energy-generating capacity of human muscle mitochondria: diagnostic procedure and application to human pathology. Clinical chemistry. 2006;52(5):860-71.
49. Ozkan P, Mutharasan R. A rapid method for measuring intracellular pH using BCECF-AM. Biochimica et biophysica acta. 2002;1572(1):143-8.

Section 2

BIOARTIFICIAL KIDNEY ENGINEERING FROM 2D TOWARDS 3D FUNCTIONAL BIOENGINEERED RENAL TUBULES

Chapter 4

BIOTECHNOLOGICAL CHALLENGES OF BIOARTIFICIAL KIDNEY ENGINEERING

Jansen J[123*], Fedecostante M[123*], Wilmer MJ[1], van den Heuvel LP[3,4], Hoenderop JGJ[2], Masereeuw R[1†]

Biotechnology Advances, 32, 1317-27, 2014.

Departments of [1]Pharmacology and Toxicology, [2]Physiology, [3]Pediatric Nephrology, Radboudumc, Nijmegen, The Netherlands.
Department of [4]Pediatrics, Catholic University Leuven, Leuven, Belgium.

* Authors contributed equally

ABSTRACT

With the world-wide increase of patients with renal failure, the development of functional renal replacement therapies have gained significant interest and novel technologies are rapidly evolving. Currently used renal replacement therapies insufficiently remove accumulating waste products, resulting in the uremic syndrome. A more preferred treatment option is kidney transplantation, but the shortage of donor organs and the increasing number of patients waiting for a transplant warrant the development of novel technologies. The bioartificial kidney (BAK) is such promising biotechnological approach to replace essential renal functions together with the active secretion of waste products. The development of the BAK requires a multidisciplinary approach and evolves at the intersection of regenerative medicine and renal replacement therapy. Here we provide a concise review embracing a compact historical overview of bioartificial kidney development and highlighting the current state-of-the-art, including implementation of living-membranes and the relevance of extracellular matrices. We focus further on the choice of relevant renal epithelial cell lines versus the use of stem cells and co-cultures that need to be implemented in a suitable device. Moreover, the future of the BAK in regenerative nephrology is discussed.

INTRODUCTION

The need for novel renal replacement therapies

The kidneys play a crucial role in the health balance of organisms by the excretion of waste products, the reabsorption of essential compounds and its endocrine and metabolic activities (1-5). The complex organ contains functional components, the nephrons, consisting of numerous cell types to fulfill its vital tasks (figure 4.1). Onset of acute kidney injury (AKI) or chronic kidney disease (CKD), can be multifactorial and caused by eg. hypertension, aging, obesity, diabetes mellitus, auto-immune disease or drug-induced nephrotoxicity (6-11). In CKD the retention and accumulation of a variety of endogenous metabolites is a hallmark, associated with a broad range of pathologies constituting the uremic syndrome. Patients undergoing chronic hemodialysis (3-4 times weekly) or peritioneal dialysis have a markedly reduced survival attributable to cardiovascular disease, hypertension, bone disorders and reduced cognitive function. Progression of renal disease through fibrosis can eventually lead to anuria (12-16).

Current dialysis therapies only partly replace renal excretion, suggesting that the waste products (putative uremic toxins) are actively being secreted by the kidneys rather than filtered. Vanholder and colleagues pioneered in establishing the European Uremic Toxin Workgroup Database (EUTox; http://www.uremic-toxins.org), and defined a list of over 150 compounds divided in three classes: 1) small water-soluble compounds (< 500 Da) that readily pass dialysis membranes, 2) middle molecules (>500 Da) for which filtration is limited due to size and charge, and 3) the protein-bound solutes which are a class of compounds difficult to clear by current dialysis modalities. The removal of the latter group depends on active tubular secretion shifting protein binding to the free fraction. For this, the renal proximal tubule cells of the kidneys are equipped with multiple transporters with overlapping substrate specificities that vigorously cooperate in basolateral uptake and luminal (urinary) excretion (17). In addition to the limited clearance capacity of the current renal replacement therapies, the lack of metabolic and endocrine functions contribute further to disease progression, morbidity and mortality (18). Best treatment option is organ transplantation but a major shortage of donor organs (in Europe and the United States, the waiting list for a new patient nowadays is 4 years (19)), as well as complications related to immunosuppressive therapy after transplantation warrant novel approaches such as BAK development (7, 8, 20).

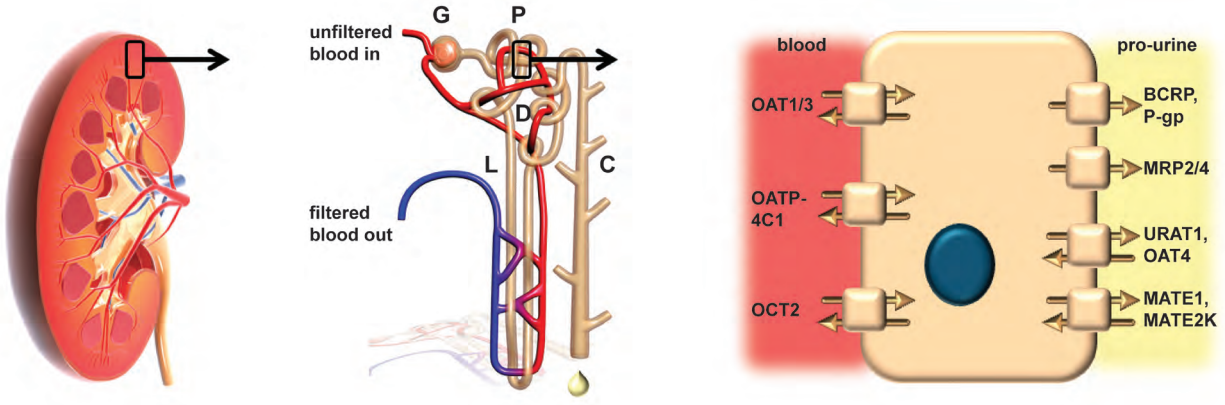

Figure 4.1 Renal physiology from organ to cell.
(left and middle) A cross-section of the human kidney which approximately consists of 1 million nephrons, the functional components of this organ. (middle) Unfiltered blood will enter the glomerulus (G) and small solutes and H_2O will be excreted via ultrafiltration into Bowman's space which is contiguous with the lumen of the proximal tubule. Subsequently, the proximal tubule epithelial cells (P) will reabsorb H_2O and compounds such as amino acids, glucose and albumin from the filtered fraction, next to the active excretion of endo- and xenobiotics into the pro-urine mediated by in- and efflux transporters. In addition, 65% of the total amount of electrolytes will be reabsorbed via paracellular pathways. Downstream the proximal tubule segment the Loop of Henle (L), the distal convoluted tubule (D) and collecting tubule and - duct cells (C) are localized. In brief, these cell types are equipped with specific water and ion channels involved in the homeostasis of water and electrolyte balance, finally contributing to a healthy multi-organ microenvironment. (right) Endogenous and exogenous solutes will be excreted into the lumen mediated via proximal tubule specific ATP-binding cassette - and solute carrier transporter proteins (e.g. basolateral influx organic anion transporter-1 and -3 (*SLC22A6*/OAT1, *SLC22A8*/OAT3), solute carrier organic anion transporter 4C1 (*SLCO4C1*/OATP4C1), organic cation transporter-2 (*SLC22A2*/OCT-2) and apical efflux breast cancer resistance protein (*ABCG2*/BCRP), P-glycoprotein (*ABCB1*/P-gp), multidrug resistance protein-2 and -4 (*ABCC2*/MRP2, *ABCC4*/MRP4), solute carrier 47A1 (*SLC47A1*/MATE1), solute carrier 47A2 (*SLC47A2*/MATE-2K), organic anion transporter-4 (*SLC22A9*/OAT4), organic urate transporter-1 (*SLC22A12*/URAT1)).

Historical overview of the BAK

The BAK is a promising biotechnological approach to replace essential renal functions, including excretory, metabolic and endocrine pathways. Although major developmental progress has been made over the last decades, a clinically applicable system has, as of yet, not been realized. The development of BAKs evolves at the intersection of regenerative medicine and renal replacement therapy. As shown in figure 4.2, BAKs combine a haemofilter used in conventional dialysis with a bioreactor unit containing renal proximal tubule epithelial cells (PTEC), termed a renal assist device (RAD) (21).

An historical overview of pioneering studies in the field of artificial and bioartificial kidney engineering is presented in figure 4.3, and started in June 1947 with the presentation of the rotating drum dialyzer at the Scientific Session of the Annual Meeting of the American Medical Association by Drs. Kolff, Fishman and Kroop (22). Forty years later, Aebischer *et al.* proposed the combination of an ultrafiltration device with an exchanger whose semi permeable hollow fibers are covered with renal epithelial cells as a design for a BAK (23). Aebischer and co-workers demonstrated that continuous ultrafiltration can be maintained for relatively long periods in the absence of anticoagulation, using non-human kidney epithelial cells (dog or porcine derived) (23).

In 1999, Humes *et al.* enriched and adapted the BAK concept, utilizing porcine renal proximal tubule cells (LLC-PK1) cultured on semipermeable polysulfone (PSF) hollow fiber membranes upon which extracellular matrix (pronectin-L) was layered to enhance cells attachment and growth (24). They successfully achieved tissue engineering of a bioartificial tubule as a confluent monolayer in a single hollow fiber bioreactor system. In the same year, Humes *et al.* successfully scaled-up from a single-fiber system to a multifiber bioreactor, which also allowed active vectorial transport of sodium, bicarbonate, glucose and organic anions, enabling functional maintenance. Moreover, it was demonstrated that the cells in the device were metabolically active, and capable of ammoniagenesis, glutathione metabolism and 1,25-dihydroxyvitamin D_3 synthesis (25).

Five years later they started applying renal cell therapy in the treatment of patients with acute and chronic renal failure. For these studies, the BAK comprised of a continuous venovenous haemofiltration circuit connected to a synthetic haemofiltration cartridge and the RAD. Despite demonstrated

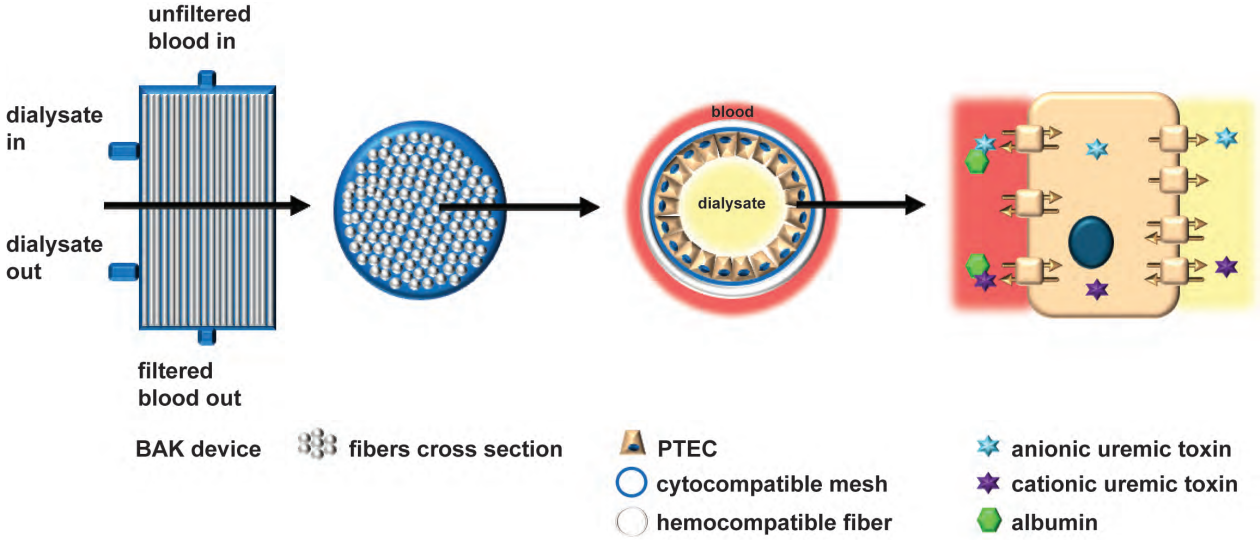

Figure 4.2 BAK composition and mechanism.
Separated in- and outlets for the patient's blood and the dialysate are incorporated in a BAK. The device will consist of numerous hollow fiber polymeric membranes with hemocompatible properties. The inner surface of the hollow fiber membrane will be modified in order to induce cytocompatibility to stimulate monolayer integrity. A homogeneous and polarized cell monolayer will stimulate excretion of endo- and xenobiotics (e.g. protein-bound uremic toxins) and reabsorption of solutes (e.g. phosphate). Importantly, host albumin and IgG components will be retained due to appropriate molecular cut-off values of the membrane. Furthermore, potential metabolic and endocrine functions of the cells can contribute to an improved homeostatis of the patient.

1947

Kroop, I.G. et al. : America's initial application of the Kolff artificial kidney

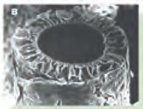

1987

Aebischer, P. et al. : The bioartificial kidney: progress towards an ultrafiltration device with renal epithelial cells processing.

Aebisher P et al. : Renal epithelial cells grown on semipermeable hollow fibers as a potential ultrafiltrate processor

1999-2004

Humes, H.D. et al. : Replacement of renal function in uremic animals with a tissue-engineered kidney (1999)

Humes, H.D. et al. : Tissue engineering of a bioartificial renal tubule assist device: in vitro transport and metabolic characteristics (1999)

Humes, H.D., W.F. Weitzel, and W.H. Fissell: Renal cell therapy in the treatment of patients with acute and chronic renal failure (2004)

2011-2013

Ni, M. et al. : Characterization of membrane materials and membrane coatings for bioreactor units of bioartificial kidneys (2011)

Buffington, D.A. et al. :Bioartificial Renal Epithelial Cell System (BRECS): A Compact, Cryopreservable Extracorporeal Renal Replacement Device (2012)

Oo, Z.Y., et al. : A novel design of bioartificial kidneys with improved cell performance and haemocompatibility (2013)

2014

Figure 4.3 Bioartificial kidney development timeline. Pioneers in the field of artificial and bioartificial kidney engineering are represented. In June 1945, Willem Johan Kolff performed the first successful treatment of acute kidney injury in a female suffering from acute kidney injury using an artificial kidney. In the next decades, devices improved and became more sophisticated by implementing renal epithelial cells cultured on hollow fiber membranes in order to replace transport, metabolic and endocrine functions.

metabolic activity and systemic effects, the RAD treatment was discontinued for safety reasons because platelet count levels reached a lower limit of 35,000 per mm^3 (26, 27).

In 2011, Ni *et al.* extended the BAK concept with the characterization of the membrane materials and coatings adapted in bioreactor units (28). The BAK bioreactor unit consisted of different porous membranes (Polyethersulfone/polyvinylpyrrolidone (PES/PVP), polysulfone/polyvinylpyrrolidone (PSF/PVP) and PSF only)) seeded with human primary PTEC. For clinical applications, it is mandatory that PTEC remain a tight differentiated epithelium on membranes. *In vitro* results demonstrated that human derived PTEC showed unsatisfactory adhesion and proliferation on a variety of polymeric membranes or a combination of PSF/PVP materials, which was used in the bioreactor unit after coating with an extracellular matrix (ECM). In concert, single ECM molecule coating showed insufficient improvement of cell performance on non-PTEC-compatible membrane materials either. On the other hand, a double coating with 3,4-dihydroxy-L-phenylalanine (L-DOPA) and an ECM molecule (collagen IV) markedly improved PTEC performance and resulted in the formation of differentiated epithelia on PSF/PVP membranes (28).

In 2012, Buffington *et al.* introduced the Bioartificial Renal Epithelial Cell System (BRECS). This is a regular cell bioreactor designed to be fully cryopreservable at -80°C or -140°C. This unique design allowed for long-term storage and on-demand use for acute clinical applications. The BRECS was designed to maintain a dense population of adult human renal epithelial cells grown on porous, niobium-coated carbon disks within the system. After the cells reach an optimal density, the BRECS can be cryopreserved, transported, and stored, thereby alleviating many practical limitations previously encountered by cell-based therapies (29). This design represented the newest technology in conservation of human renal epithelial cells.

One year later, Oo *et al.* introduced a novel model of BAK with improved cell performance and haemocompatibility for large animal studies (30). It was demonstrated that PTEC performance was improved on the outer non-haemocompatible polyarylethersulfone surfaces. Moreover, under these conditions membrane coatings were not required (30). This new BAK design greatly improved haemocompatibility and safety**,** and allowed the bloodline to discontinue to the bioreactor rapidly in case of problems.

All the devices proposed here have the promise to be combined to produce a wearable or implantable BAK for renal replacement therapy that may significantly diminish morbidity and mortality in patients with acute or chronic kidney disease. However, those systems have, as of yet, not shown to fully embrace the ability to excrete protein-bound uremic retention solutes.

REQUIREMENTS FOR RENAL CELL MODELS

Characteristics of proximal tubular epithelial cells

For optimal urinary excretion of endo- en xenobiotics, the renal tubular epithelium is equipped with an organic anion and an organic cation system. These systems comprise of transporters belonging to the solute carrier family (SLC; e.g. Organic Cation Transporter 2 (OCT2; SLC22A2), Organic Anion Transporter 1 and 3 (OAT1/3; SLC22A6 and SLC22A8), Organic Anion Transporting Polypeptide 4C1 (OATP4C1; SLCO4C1), the Multidrug and Toxin Extrusion proteins (MATEs; SLC47A1/2)) and the ATP-binding cassette transporter family (P-glycoprotein (P-gp also termed MDR1; ABCB1), Multidrug Resistance Proteins 2 and 4 (MRP2/4; ABCC2/4), and Breast Cancer Resistance Protein (BCRP; ABCG2)), as schematically depicted in figure 4.1 (17, 31, 32). Roughly distinguished, basolateral uptake of organic anions is mediated by OAT1 and OAT3 and their urinary efflux by MRP2, MRP4. For organic cations, OCT2 is the predominant carrier for facilitated transport into renal proximal tubule cells and MATE1, MATE2K and P-gp mediate their urinary efflux. BCRP and OATP4C1 might handle both organic anions and cations in renal proximal tubule epithelial cells (17).

Renal cell culture models

Diverse cell lines and primary renal PTEC cultures have been used to study BAK engineering as a potent therapeutic approach (26, 28, 30, 33-38). Various research groups applied the porcine derived LLC-PK1 cell model for BAK engineering (23, 30). The functionality of the cationic influx transporter OCT2 in LLC-PK1 was confirmed by unidirectional transport of creatinine and tetraethylammonium using regular cell culture techniques (39, 40). However, limited expression and function of other transporters, such as the efflux pumps BCRP and P-gp, was demonstrated (41, 42). In addition, its non-human origin limits the suitability of LLC-PK1 for BAK approaches.

For clinical applications, human origin of the cells is highly preferred but very few models are available. Human primary tubular cell cultures (HPTC) reflect most closely the physiological demands and functionally express various organic anion plus cation transporters essential for uremic retention solutes excretion. Moreover, essential reabsorptive mechanisms, such as phosphate and albumin endocytosis, were demonstrated to be present (43-45). Nevertheless, HPTC application is hampered by the large batch-to-batch variability in quality and function. Most transport systems were found to be down-regulated upon cell culturing. Moreover, the isolation and culture of a sufficient number of primary cells required for a BAK with maintained epithelial characteristics, is highly challenging.

To overcome these hurdles, (conditionally) immortalized PTEC of human origin have been developed, including HK-2 (46) and ciPTEC (47, 48). The immortalization strategies allow for sufficient cell numbers, and cells remain stable in expression and function of essential proteins upon prolonged culturing (47). A variety of functional SLC and ABC-transporters, known to be involved in protein-bound uremic toxin excretion, have proven to be present. In 1994, HK-2 was successfully established by Ryan *et al.* by transduction of renal epithelial cells using recombinant retrovirus containing the human papillomavirus type 16 E6/E7 genes. This cell line has been widely distributed and applied for studying renal pharmacology and physiology, although the lack of OCTs, OATs and BCRP was demonstrated (49-53). In contrast to HK-2, ciPTEC displays specific functional influx and efflux systems in line with primary HPTC (47, 48, 54). A potential uremic toxin influx transporter is OCT2, which was demonstrated to be present and found predictive for human renal organic cation handling (54). The interaction between several anionic uremic toxins and two important efflux pumps present at the apical membrane of the proximal tubule, MRP4 and BCRP, was demonstrated as well. Moreover, the interaction of the uremic toxins with an important class of metabolism enzymes, namely UDP-glucuronosyltransferases (UGT), and mitochondrial succinate dehydrogenase activity was confirmed (55). The latter results presented a novel pathway via which uremic retention solutes affect the metabolic capacity of the kidney and might affect drug disposition during CKD. This functionality in ciPTEC is a great breakthrough which allows us to have a translational model predictive for studying renal excretory function through the transport machinery. One drawback of all renal cell lines is the lack of OAT1 and OAT3 expression on gene, protein and functional level. Although the expression of OATs has been observed in primary HPTC (43),

the levels decrease dramatically during the first days of culturing and are lost after cell passaging. This phenomenon has already been described in 1992 by Miller *et al.* (56) and has, as of yet, not been solved.

MEMBRANES AND MATRIX BIOLOGY: HOW TO MAINTAIN FUNCTIONALITY

Bioactive membranes

Nowadays, the development of synthetic biomaterials rapidly progresses and their applications depend on their controlled, well-characterized composition, degradation and physical properties (57, 58). PSF describes a family of thermoplastic polymers and are known for their toughness and stability at high temperatures. In addition, PSFs are used in specific applications and often are a superior replacement of polycarbonates. PSF allows easy manufacturing of membranes with reproducible properties and controllable pore size, explaining their current use in hemodialysis (59). PES is derived from PSF with low protein retention and, when combined with PVP, an ideal balance can be realized between hydrophilicity and biocompatibility due to PES' hydrophilic nature. Their asymmetric pore structure offers a perfect balance between highly selective filtration characteristics and high fluxes with minimized flux barriers (60).

Mimicking the basement membrane including a native extracellular matrix (ECM) with its fiber-like morphology and display of bioactive signals is a prerequisite for optimal epithelial cell function in vitro. However Nur, E.K.A., *et al.* and Schindler, M., *et al.* demonstrated the cells did not respond to specific bioactive signals, but were only influenced by the topology provided by the fiber-like structure (61, 62). Moreover, Dankers et al. (38) developed a membrane more suitable for BAK systems. Promising results with respect to cell viability, brush border enzyme activities, tight cell monolayer formation and the expression of various transporters and ECM proteins were observed when cultured in static conditions in HPTC cultures on bioactive supramolecular membranes. These characteristics were improved further in perfusion conditions (38). The benefits of this membrane was contributed to the unique properties of the supramolecular polymer used. The electrospun microfibers resemble the structure of the ECM, composed of nanofibers formed by stacking of ureido-pyrimidinone (UPy) dimers in the lateral direction assisted by additional urea functionalities (38, 57). Furthermore,

Khan *et al.* provided a clear insight on the attachment of bioactive peptides and proteins to self-assembled peptide amphiphile nanofibers via a chemo-selective native chemical ligation reaction. This allowed functional peptides integration in order to design an optimal biomaterial for cell attachment, creating a 'living membrane' (58).

The extracellular matrix

The native ECM is a key factor in inter- and intracellular signaling, regeneration and support, and forms a depot for growth factors. The ECM composition can be divided into two major components: the basement membrane (BM) and the stromal matrix (SM; figure 4.4). The BM is a sheet-like scaffold for tissue's peripheral cells, including the vasculature as a scaffold for endothelial cells. The SM is made up of larger, fibrous structures, which provide much of the structural support of the ECM. Glycosaminoglycans (GAGs) are most representative ECM molecules, and are long unbranched polysaccharides consisting of repeating sugar dimers. GAGs can be divided in heparan sulfates, chondroitin sulfates and hyaluronic acid. Hyaluronic acid is the only GAG that is not bound to core proteins. When a GAG is covalently bound to a core protein, it is named a proteoglycan (PG) (63). The major biological function of proteoglycans is to provide hydration and swelling pressure to the tissue giving the resistance to compression forces (64). Proteoglycans and GAGs, also known as the proteoglycan glycomatrix, play an important role in the modulation of the innate immune system, as well as in tissue remodeling during inflammatory disease processes (65).

Fibers are other important ECM components. Type I collagen is the predominant component of the SM and of the ECM. Native collagen I is porous, adhesive to many cell types, and provides a strong scaffold upon which cells can attach and grow. Collagen IV is a non-fibrillar collagen and exists in small sheets as a predominant component of the BM. Collagen IV is known to be able to augment smooth muscle cell differentiation from various stem cell populations (63). It has been localized also to the dermal-epidermal junction, in capillaries, and beneath endothelial cells in larger vessels. Ultrastructurally it has been shown to be a specific component of the lamina densa (66). ECM also constitutes of other molecules, including fibronectin, which is a high molecular glycoprotein present in blood, connective tissue and at the cell surface. It is believed to be involved in cells attachment to the surrounding ECM, collagen and GAGs (67).

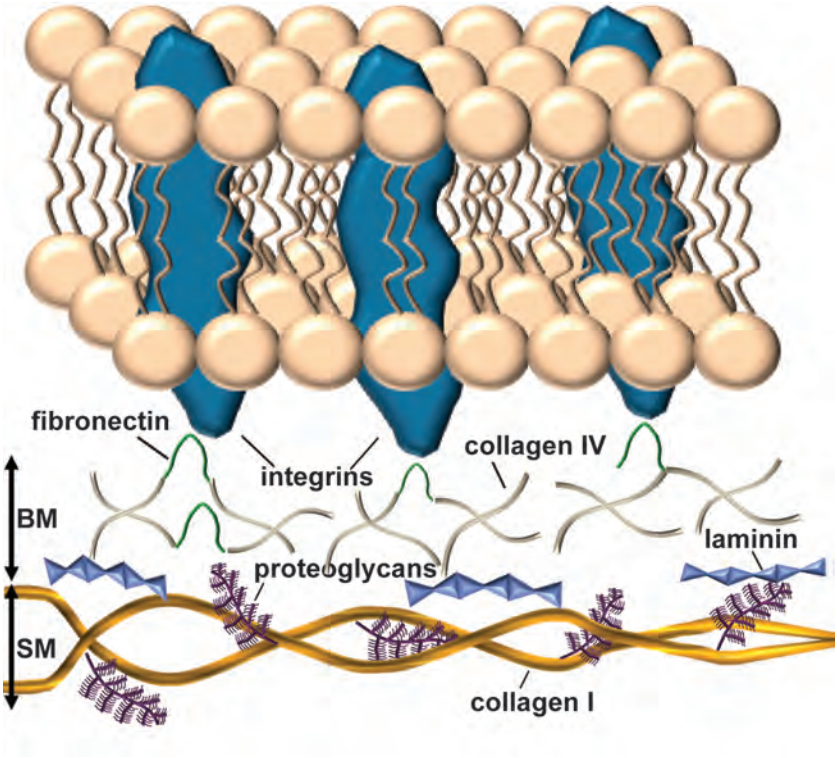

Figure 4.4 Essential extracellular matrix components.
The native ECM is a key factor in inter- and intracellular signaling, regeneration, support and is a depot for growth factors, indicating its high relevance in cell maintenance. The cell-ECM adhesion and signaling is mediated by integrins, which are transmembrane receptors located in the PTEC plasmamembrane. The ECM composition can be divided into two major components: the basement membrane (BM) and the stromal matrix (SM). The BM is a sheet-like scaffold and is mainly characterized by fibronectin, proteoglycans, laminin and collagen IV. The SM is made up of larger, fibrous structures, which provide the major structural support of the ECM. Collagen I, proteoglycans and GAGs belong to this strate.

Most BMs are rich in α1 and α2 chains, suggesting that these chains may be required for embryonic development. The α3-α6 (IV) chains, however, are selectively expressed in small subsets of BMs and are expressed late in development. Thus, their loss might be expected to cause tissue-specific defects. Mutations of the α3-5 (collagen IV) genes in humans have been associated with Alport syndrome, a hereditary glomerulonephritis that leads to end-stage renal disease (68).

Cell adhesion to extracellular components can occur either by focal adhesions, connecting the ECM to actin filaments of the cell, or hemidesmosomes, connecting the ECM to intermediate filaments, such as keratin. This cell-to-ECM adhesion is regulated by specific cell-surface cellular adhesion molecules known as integrins. Integrins bind cells to ECM structures, including fibronectin and laminin, and also to integrin proteins on the surface of other cells (63).

Taken together, the constant interchange between cells and the ECM determines cell fate and triggers the shift from proliferation to structure formation (69). Integrating core ECM components into cyto- and hemo-compatible biomaterials will contribute to maintaining renal epithelial cell functionality upon prolonged appliance.

HK-2 and Human PTEC growth on bioactive membranes

Optimal renal cell performance on biomaterials is dependent on the presence of an appropriate ECM. In vivo, the native ECM is a key factor in inter- and intracellular signaling, support and regeneration. To advance cell attachment, supportive membranes can be coated using ECM components, i.e. bioactivating the membrane. In the past few years some research groups tested different ECM compounds as BAK coating (table 4.1 and 4.2) using a cell line (HK-2) or HPTC. In general, a ECM coating is applied to the BAK membranes for 1-2 hours (34), prior to seeding the renal epithelial cells onto the membranes. The ECM coating stimulates cell adhesion and differentiation; successful cell differentiation causes ECM production by the epithelium (47) eventually increasing their adherence and phenotype on the membrane with prolonged durability. Zhang et al. demonstrated that after 2-3 weeks with a maximum of 4 weeks (34), the cell monolayer is still viable and intact on the BAK membrane. The monolayer integrity is in relation with the ECM coating combination used (collagen IV was always present in those successful combinations).

Table 4.1 – Successful ECM coating used in HK-2 monolayer formation

Coating type and concentration	Source	Surface material	Seeding density (cells/cm²)	Monolayer formation: ZO-1	Ref.
Laminin (100 µg/ml)	Human	24-wells plate polystyrene	$1.4x10^5$	2	(34)
Gelatin (1 mg/ml)	Porcine	24-wells plate polystyrene	$1.4x10^5$	2	(34)
Matrigel (70x diluted)	Mouse	24-wells plate polystyrene	$1.4x10^5$	2	(34)
3,4-Dihydroxy-L-phenylalanine (DOPA)	NM	PES/PVP membranes	$1x10^5$	5	(28)

Optimal monolayer formation and cell attachment can be studied by the ZO-1 staining using a scoring system ranging from 1 to 5, accordance to Zhang *et al.* (28) The ZO-1 pattern scores are reported in relation with different ECM coatings and surface materials used until now. NM= not mentioned

Table 4.2 – Successful ECM coating used in HPTC monolayer formation

Coating type and concentration	Source	Surface material	Seeding density (cells/cm²)	Monolayer formation: ZO-1	Ref.
Collagen IV (150 µg/ml)	Human	24-wells plate polystyrene	$1.4x10^5$	4-5	(34)
Laminin (100 µg/ml)	Human	24-wells plate polystyrene	$1.4x10^5$	4-5	(34)
Gelatin (1mg/ml)	Porcine	24-wells plate polystyrene	$1.4x10^5$	2-3	(34)
collagen IV (150 µg/ml) + 3,4-Dihydroxy-Lphenylalanine (DOPA)	Human	PES/PVP membranes	$5 x10^4$	3	(28)
Collagen IV (150 µg/ml)	Human	PET	$1x10^5$	4	(28)
Collagen IV (150 µg/ml)	human	tissue culture polystyrene (TCPS)	$1x10^5$	4	(28)

Optimal monolayer formation and cell attachment can be studied by the ZO-1 staining using a scoring system ranging from 1 to 5, accordance to Zhang et al. (28) The ZO-1 pattern scores are reported in relation with different ECM coatings and surface materials used until now.

Collagen IV appeared to be one of the best ECM coatings in both PES/PVP and PET membranes. Interestingly, optimal results were obtained when collagen IV was coated after a first layer of L-DOPA (28). L-DOPA is the catecholamine's precursor (dopamine, noradrenaline, and adrenaline) obtained via tyrosinase biosynthesis from the amino acid L-tyrosine and shown to be involved in the formation of mussels adhesive proteins (70). L-DOPA is negatively charged, and the combination with collagen IV, positively charged, create the optimal condition, up to now, for attachment and differentiation (table 4.1 and 4.2) (28). Apart from that combination, other ECM molecules combinations showed no cells attachment superiority. Although collagen IV itself may play an optimal role for HPTC attachment (table 4.2), stressing the fact that a more "biological" ECM coating is needed instead of a synthetic one.

Optimal monolayer formation and cell attachment can be studied by the tight junction protein zonula occludens-1 (ZO-1) staining using a scoring system ranging from 1 to 5, accordance to Zhang *et al.* ((34), table 4.1 and 4.2). Few studies were conducted using different cell models, but in tables 4.1 and 4.2 we show only the studies related to cells from human origin (HPTC and HK-2). In particular, we focused on optimal cells attachment using varying surface materials and ECM coatings. Less favorable ECM coatings data were collected as well and shown in supplementary table S4.1. The application of these coatings, including pronectin F, Poly-D-Lysine, Poly-L-Lysine and collagen I, resulted in poor monolayer formation and no positive ZO-1 staining (28, 34).

RENAL EPITHELIUM IMPROVEMENT USING CO-CULTURE AND STEM CELL APPROACHES

Co-culture applications

BAK engineering could be improved further by applying more than one renal cell type within a device. This requires a more comprehensive approach, but might enable to maintain differentiated epithelium during prolonged application. In vivo, paracellular pathways across the leaky proximal tubular epithelium are mediated along the tight junction proteins of the cells in order to reabsorb solutes and water (71). The combination of proximal tubular cells with endothelial cells or epithelial cells from down-stream nephron segments might be favorable in order to improve monolayer tightness and maintain or even enhance transport and metabolic activity. Finally, this might result in improved resistance against uremic conditions

and enhanced PTEC functionality in BAK. In table 4.3 relevant co-culture studies are summarized for HK-2 or HPTCs combined with various cell lines and growth factors. Aydin et al. (72), showed the co-culture of HK-2 and HPTCs with endothelial cells (HMEC-1; a human dermal microvasculature cell line) and HK-2 cells cultured on HMEC-1 extracellular matrix conditioned filters, which resulted in monolayer integrity improvement as measured by transepithelial resistance and paracellular leakage of inulin. In total, 99 genes were found to be up- or downregulated in co-culture which are involved in various cellular pathways, such as extracellular matrix signal transduction, cell-cell communications (i.e. through release of the cytokines IL-6 and IL-1β). No enhanced effects on monolayer integrity was observed when HK-2 was co-cultured in HMEC-1 conditioned medium (72). In addition, as described by Tasnim et al., an increased mRNA expression level of drug transporters, such as OAT1, OAT3 and OCT, as well as increased activity of the metabolic enzyme, γ-glutamyltransferase (GGT), was found when HPTC were co-cultured with HUVEC (73). In addition, as studied by Bertocchi et al., the co-culture of HK-2 with EA.hy 926 cells (Human Umbilical Vein Endothelial Cells (HUVECs) fused with a bronchial carcinoma cell line) showed a positive effect on cell integrity and viability when nitric oxide (NO) was inhibited, suggesting a cytoprotective effect caused by epithelial and endothelial cross-talk (74). Inducible NO synthase (iNOS) is constitutively expressed in the kidney tubular epithelium and is involved in the maintenance of diverse physiological processes, but upon induction involved in renal pathologies (75). Ameliorated but also attenuated NO levels contribute to various disorders, such as cardiovascular disease and acute or chronic kidney disease. Culturing epithelial cells in more physiological conditions using bilayer formation with endothelial cells resulted in improved monolayer integrity. As shown by Miya *et al.*, next to the co-culture using HUVEC cells, hepathocyte growth factor (HGF), solely or accompanied by HUVEC cells, appeared to play an exclusive and cumulative role in cell proliferation, invasion, migration and tubulogenesis (i.e. the formation of tubules in epithelial or endothelial cells) of primary cells cultured in Matrigel. This gel is a rich ECM culture environment stimulating the development of 3D cellular structures (76). Particularly enhanced proliferation and migration properties detected in these co-culture applications revealed interesting characteristics that could be favorable in BAK approaches. For example, recovery of cells in uremic conditions might be enhanced in the presence of HGF to enable proliferation and, as a consequence, prolong functional BAK platforms. Obviously, the animal-derived Matrigel as a potential HFM coating strategy is not compatible with human treatment

Table 4.3: Monolayer integrity and maintenance effects of HK-2 and human primary tubule epithelial cells in co-culture

Proximal tubule line	Cell Lines/ growth factors	Results	Comments	Ref.
HK-2 cells (ATCC, Rockville, MD)	Human dermal microvascular endothelial cell (HMEC-1)	↑TEER and ↓ inulin leakage 99 altered gene expression levels	Exclusive role for endothelium-derived ECM Altered genes related to cell-cell communication, ECM proteins, transport proteins.	(72)
Human primary proximal tubular cells (HPT)	Primary glomerular microvasular endothelial cells (GMEC)	↑TEER and ↓ Inulin leakage		(72)
HK-2 cells (ATCC, Rockville, MD)	EA.hy 926 (HUVEC fused with bronchial carcinoma cell line)	↑Monolayer integrity and vitality	Injurious effects of nitric oxide synthase inhibited	(74)
Primary human renal PTEC (Lonza, Walkersville, MD)	HUVEC +/- HGF (20 ng/ml)	↑ tubular structure ↑ cell proliferation ↑ cell invasion and migration	Cumulative effect of HUVEC and HGF	(76)
HPTC (ScienCell Research Laboratories, Carlsbad, CA)	HUVEC and HRGEC	↑ mRNA of GGT, CD13, AQP1, OAT1, OAT3, OCT1, GLUT5, NA^+/K^+ ATPase, NBC1 and SGLT2 transporters ↑GGT activity ↑ cell proliferation	Altered mRNA expression levels in co-cultured HUVEC of VEGF, FGF-2, HGF, TGF-β1, PDGF-A, A2M, DCN, FST, FSTL-3 and FGFR-2 HUVECs.	(73)

HK-2: human kidney cell line -2; TEER: transepithelial electric resistance; ECM: extracellular matrix; HUVEC: Human umbilical vein endothelial cells; HGF: hepathocyte growth factor; HRGEC: human renal glomerular endothelial cells; GGT: γ-glutamyltransferase; CD13: aminopeptidase-N; AQP1: aquaporin 1; OAT1: organic anion transporter - 1; OAT3: organic anion transporter - 3; OCT1: organic cation transporter - 1; GLUT5: glucose transport protein - 5; NBC1: Na^+/HCO_3^- cotransporter - 1; SGLT2: sodium/ glucose cotransporter - 2; VEGF: vascular endothelial growth factor; FGF-2: fibroblast growth factor - 2; TGF-β1: transforming growth factor - beta 1; PDGF-A: platelet-derived growth factor alpha chain; A2M: alpha-2-macroglobulin; DCN: decorin: FST: follistatin; FSTL-3: follistatin-like 3; FGFR-2: fibroblast growth factor receptor 2.

approaches and should be replaced by appropriate surface modifications (e.g. L-DOPA in combination with collagen IV (28)). To date, the effect of uremic conditions in co-culture approaches has not been studied. Interestingly, the favorable co-culture effects observed in monolayer integrity, cell metabolism and transport capacity as reviewed here might indicate oppurtunities for BAK applications to maintain or even enhance proximal tubule epithelial characteristics upon prolonged usage when exposed to uremic conditions. Therefore, future research is required to study protein-bound uremic toxins effects on PTEC monoculture versus co-culture of PTEC combined with, for example, cells from up- or down-stream nephron segments or specific growth factors.

Renal regeneration using stem cells

In the past few years, various research groups developed and characterized CD133+ multipotent cells isolated from human kidney able to differentiate into renal epithelial cells (29, 77, 78). These cells are capable of high expansion of at least 10^8 cells in perfusion culture and high viability, glucose transport and glutathione metabolism were established. Moreover, after lipopolysaccharide stimulation of these cells, active 1,25-di-hydroxyvitamin D_3 derivative was found confirming endocrine function (29, 77). Furthermore, its immunologic activity was demonstrated by IL-8 production (29, 37), signifying the relevance of these cells for BAK applications. Moreover, it was shown that extrarenal stem cells, including embryonic stem cells (ESCs), bone marrow-derived stem cells and amniotic fluid-derived stem cells, are capable of differentiating in renal epithelial cells using specific nephrogenic factors (79-83). For BAK purposes, Narayanan et al. demonstrated functional differentiated hESC (i.e. GGT activity and intracellular cAMP response to parathyroid hormone) when cultured in perfusion bioreactors, indicating opportunities for hESC in BAK development (82). Though ESCs and BMDCs showed promising regenerative capacities, ethical concerns, mainly for ESCs, and tumor formation risk hamper a short-term application. In contrast, amniotic fluid-derived stem cells are relatively easy to get to from routine clinical amniocentesis specimens, and phenotypic and genotypic characteristics upon prolonged culturing were shown to be maintained as well as self-renewal properties (84). Renal regeneration and survival in AKI mice was enhanced after amniotic fluid-derived stem cell treatment, indicating a promising avenue in future research (81). In addition, the use of induced pluripotent stem cells (iPSCs) as a source for cells restoring tubule epithelium is a relatively new era. The application of human iPSC is potentially a powerful tool in regenerative medicine and toxicology screening

programs (85-88), but their use in regenerative nephrology has, as of yet, to be demonstrated. iPSC can be generated from cells exfoliated in urine followed by reprogramming cell cultures (89), indicating high suitability for autologous BAK development or for establishment of appropriate disease models.

PRECLINICAL AND CLINICAL BAK APPLICATIONS IN AKI PATIENTS

In a preclinical study, HPTCs were cultured in a RAD and *ex vivo* performance was successfully applied in acutely uremic dogs (37). Next, the FDA approved Phase I/II clinical evaluation was performed, in which the effect of RAD treatment for 24h in ten patients suffering from AKI and multiorgan failure with predicted hospitality mortality rates above 85%, was studied (27). Five out of ten critically ill patients were able to complete 24h RAD treatment and encouraging results were obtained which reflected, for example, ameliorated endocrine functions whereas proinflammatory cytokines (i.e. IL-6, G-CSF) and plasma creatinine levels diminished after treatment. A promising feature should be stated regarding the device itself as well. The cell viability, integrity and metabolic functions were still retained after 24h of use and cell loss during therapy appeared to be less than 0.01%. However, 40% of the patient group passed away in the post-RAD treatment period due to comorbidities within 30 days. To investigate safety and efficacy of RAD treatment in greater detail, more multicenter clinical studies were performed in ICU patients suffering from AKI and multiorgan failure (90-92). In these trials, ameliorated kidney function and reduced cytokine levels were observed resulting in reduced mortality. Interestingly, an altered inflammatory response was also observed in a selective cytopheretic inhibitory device (without cells) indicating possible immunomodulatory effects of this synthetic membrane on circulating leucocytes in patients suffering from sepsis and multiorgan failure (90). A follow-up study has been designed to specifically address the latter phenomenon (93).

CONCLUSION AND FUTURE PERSPECTIVES

Concluding remarks

The development of a BAK requires a complex interaction of functional cells and a fine-tuned ECM coating on cyto- and hemocompatible biomaterials. Here, we concisely described the current status of BAK engineering with

an overview of key factors. In the field of regenerative nephrology, the need for stable cell models that remain functional upon prolonged culturing time is still present. Although primary renal epithelial cells (29) or stem cell applications might embrace the possibility of high cell expansions, stable expression and maintained functionality of waste eliminating transporters is still challenging. The application of primary proximal tubular cells in a BAK system is hampered by their limited availability as human kidney material is sparse. Even when cell proliferation can be stimulated by optimal application of growth factors, a high batch-to-batch variability in expression and function of primary renal epithelial cells is a major drawback for primary cells in BAK development. Future research needs to be directed towards the elucidation of optimal surface modifications using a well defined ECM complex to enhance proliferation and allow stable expression of relevant proteins in primary renal epithelial cells (94). On the other hand, using primary renal epithelial cells permits to isolate autologous cells from kidney biopsies, paving the way to develop a valuable tool in personalized medicine. However, the number of cells isolated from a kidney biopsy will be limited and a direct obstacle to develop a fully functional BAK device. A solution to overcome this hurdle, is to immortalize cells using transduction strategies. Obviously, an application containing immortalized cells cannot longer be classified as an autologous approach. From an autologous point of view, hESC or iPSC applications might offer suitable alternatives in future BAK development (82, 88). To overcome current limitations of renal primary epithelial cells, implementation of human ciPTEC, which showed stable functionality of PTEC specific transporters (47, 48, 54), might be favorable in BAK devices. To date, transcellular transport in ciPTEC of uremic cationic and anionic uremic toxins in 2D and 3D approaches is in progress and interesting data have been obtained ((47) and unpublished data). In addition to BAK applications, such models are potentially predictive for renal drug handling by studying the role of transporters in disposition of new pharmaceutical entities, to identify possible drug-drug interactions and potential (drug-induced) nephrotoxicity (95). Obviously, the application of immortalized cell lines, with a potential risk of provoking oncogenic responses upon disruption, will require extensive research to eventually establish a safe and solid device. Consequently, detailed risk assessments prior to any clinical trial will be crucial.

The improvement of renal replacement therapy using BAK systems seemed to be promising in uremic animals, but also in patients suffering from AKI (27, 36, 37, 90-92, 96). Multicenter randomized clinical trials are currently ongoing

in AKI patient groups and outcomes will be analyzed thoroughly (93), prior to any further assessment in CKD or end-stage renal disease patients BAK treatment. A major difference between AKI and CKD or end-stage renal disease treatment is related to the inflammatory status of the patient. In AKI patients, a BAK device appeared to result in increased survival rate due to immunomodulation (26). In CKD or ESRD patients the inflammatory response will influence disease progression, which is related to the accumulation of protein-bound uremic retention solutes as well (14, 15, 97). Therefore, cells applied in a BAK should actively secrete retention solutes and, in the end, induce clearance of protein-bound uremic retention solutes below a certain threshold to diminish disease progression. Maintenance of the functional capacity of cells upon prolonged BAK application is the ultimate prerequisite.

A more long-term objective is to reduce the BAK size without affecting its functionality. The implantable bio-artificial kidney hypothesis has been drawn up in the last few years (98, 99). Up to now, the bioartificial hemofilter devices implantation has been performed in small animal studies. The main problem encountered in these studies was cells long-term viability in the system. Eventhough it will be a valuable perspective for clinical purposes as this might improve patients physiological condition because current dialysis treatment is not sufficient for that purpose. Moreover, implanting a bio-artificial kidney will ultimately decrease the burden of wearing an extra-corporal renal device improving further patients quality of life (98-100).

An optimal ECM surface is favorable to support and maintain proximal epithelial cell proliferation and differentiation when cultured in 2D and 3D applications. So far, maintaining a tight functional renal epithelium *in vitro* is highly challenging and is a hurdle to overcome prior to enabling a stable functional BAK. For future research, synthetic biomaterials are of high interest to enable prolonged renal epithelial cell functionality in a BAK. This type of ECM mimics a comprehensive and dynamic environment in comparison to more straightforward and commonly used collagen, laminin and gelatin coatings. In the end, decellularized ECM surfaces might result in enhanced differentiation and maintenance of PTEC characteristics and might even be a more dynamic environment compared to synthetic biomaterials. Decellularization of whole organs, is commonly used to facilitate the constructive remodeling of a variety of tissues (101). The procedure is characterized by the perfusion of the whole organ with a detergent, mainly SDS, which completely remove the nuclear material leaving the ECM construct

intact that can be used as a biological scaffold (102-107). In kidney regeneration studies, this approach was recently described and applied in various animal studies (102-105). The main focus was to obtain an ECM construct reflecting the native membrane in order to stimulate cellular adhesion and functional renal properties when recellularized using embryonic stem cells (102, 107). A successful cell attachment and hematopoietic differentiation was demonstrated in these studies. Translating this decellularization technique into a human BAK system would be a major breakthrough and could further enhance cell viability and functionality when cultured on bio-compatible membranes. Yet, such approach is highly elaborative and definitely requires more research.

Moreover, combining endothelial or other epithelial cells from downstream nephron segments with PTECs resulted in improved cell monolayer integrity (72-74, 76) and may possibly enhance resistance against uremic conditions. Obviously, elucidating optimal combinations of cell types is of high interest and further research is required. Based on recent studies reviewed here, this is a promising avenue for BAK platforms as well.

Interestingly, Kusuba *et al.* (108) and Smeets *et al.* (109) demonstrated that almost any proximal tubular cell is able to dedifferentiate upon injury to stimulate tubular repair and this characteristic is not restricted to a fixed CD133+ progenitor stem cell population within the kidney. This finding is a promising aspect to aid BAK engineering and regeneration. For future applications, if renal progenitor cells express a stable and broad range of proximal tubule specific transporters, then the implementation and maintenance of autologous cells in a bioartificial cell system device might be possible. However, invasive techniques are required to extract cells from a patient's kidney, which implies obvious restrictions. Moreover, the feasibility of autologous cell applications depends on the condition of a patient's kidney and may not be applicable in patients suffering from AKI. An appropriate, and favorable, alternative for autologous cell procedures in a BAK to treat CKD patients might be the use of pluripotent stem cells isolated from urine samples (89). Human iPCs isolated from urine samples showed multi-differentiation properties, potentially indicating valuable autologous cell sources for application in regenerative medicine. The immunologic response will probably not be triggered upon regular autologous cell device treatment compared to non-autologous cell approaches, improving health conditions in patients suffering from renal disorders.

Future perspectives

For future applications the translation towards a wearable BAK for CKD patients would be highly favorable and will remarkably increase the quality of life. A sophisticated but efficient and non-invasive treatment might result in a substantial reintegration in professional and social environment. Although the development of appropriate BAK devices is expensive, the rapid development currently seen in up-scaling and automation techniques for cell therapy purposes indicates that current cost estimates may well be outdated in few years' time. Obviously, a thorough evaluation should be applied based on FDA guidelines to investigate the potency of a BAK in public health care (110). Other applications, such as disease modeling, drug discovery and drug development, may also contribute to the final economic value of a BAK.

To date, encouraging BAK results were obtained by various outstanding research groups (29, 30, 96). However, the implementation of BAK in public healthcare on short-term is challenging and not yet foreseen. Limiting aspects of BAK development are related to restricted cell sources and functional transcellular transport properties in 3D approaches, as reviewed here. Insight in current approaches contribute to comprehensive future research in order to stimulate the development of stable and functional BAK devices for prolonged applications in various patients groups.

Acknowledgments

The financial contribution of the Dutch Kidney Foundation is gratefully acknowledged (KJPB 11.0023), the Netherlands Institute for Regenerative Medicine (NIRM, Grant no. FES0908), the FP7-PEOPLE-2012-ITN BioArt (316690) and the Netherlands Organization for Scientific Research (016.130.668).

REFERENCES

1. Layton, A.T., Modeling Transport and Flow Regulatory Mechanisms of the Kidney. ISRN Biomath. 2012. 2012(2012).
2. Deneke, S.M. and B.L. Fanburg, Regulation of cellular glutathione. Am J Physiol. 1989. 257(4 Pt 1): p. L163-73.
3. Tannen, R.L. and S. Sastrasinh, Response of ammonia metabolism to acute acidosis. Kidney Int. 1984. 25(1): p. 1-10.
4. Maack, T., Renal handling of low molecular weight proteins. Am J Med. 1975. 58(1): p. 57-64.
5. Deetjen, P., (The remarkable accomplishments of the kidney--from molecular mechanisms to organ function). Verh Dtsch Ges Pathol. 1989. 73: p. 1-5.
6. Vanholder, R. and R. De Smet, Pathophysiologic effects of uremic retention solutes. J Am Soc Nephrol. 1999. 10(8): p. 1815-23.
7. Artz, M.A., et al., Conversion from cyclosporine to tacrolimus improves quality-of-life indices, renal graft function and cardiovascular risk profile. Am J Transplant. 2004. 4(6): p. 937-45.
8. Hoorn, E.J., et al., The calcineurin inhibitor tacrolimus activates the renal sodium chloride cotransporter to cause hypertension. Nat Med. 2011. 17(10): p. 1304-9.
9. Glaudemans, B., et al., Novel NCC mutants and functional analysis in a new cohort of patients with Gitelman syndrome. Eur J Hum Genet. 2012. 20(3): p. 263-70.
10. Fox, C.S., et al., Associations of kidney disease measures with mortality and end-stage renal disease in individuals with and without diabetes: a meta-analysis. Lancet. 2012. 380(9854): p. 1662-73.
11. Winearls, C.G. and R.J. Glassock, Classification of chronic kidney disease in the elderly: pitfalls and errors. Nephron Clin Pract. 2011. 119 Suppl 1: p. c2-4.
12. Vanholder, R., S. Van Laecke, and G. Glorieux, What is new in uremic toxicity? Pediatr Nephrol. 2008. 23(8): p. 1211-21.
13. Vanholder, R., R. De Smet, and N. Lameire, Protein-bound uremic solutes: the forgotten toxins. Kidney Int Suppl. 2001. 78: p. S266-70.
14. Pletinck, A., et al., Protein-bound uremic toxins stimulate crosstalk between leukocytes and vessel wall. J Am Soc Nephrol. 2013. 24(12): p. 1981-94.
15. Liabeuf, S., et al., Does p-cresylglucuronide have the same impact on mortality as other protein-bound uremic toxins? PLoS One. 2013. 8(6): p. e67168.
16. Boron WF, Boulpaep EL. Medical Physiology. 2003. 737 - 876.
17. Masereeuw, R., et al., The Kidney and Uremic Toxin Removal: Glomerulus or Tubule? Semin Nephrol. 2014. 34(2): p. 191-208.
18. Krieter, D.H., et al., Protein-bound uraemic toxin removal in haemodialysis and post-dilution haemodiafiltration. Nephrol Dial Transplant. 2010. 25(1): p. 212-8.

19. Kidney Link 2014; Available from: http://www.kidneylink.org/TheWaitingList.aspx.
20. Gellermann, J., et al., Mycophenolate mofetil versus cyclosporin A in children with frequently relapsing nephrotic syndrome. J Am Soc Nephrol. 2013. 24(10): p. 1689-97.
21. Tasnim, F., et al., Achievements and challenges in bioartificial kidney development. Fibrogenesis Tissue Repair. 2010. 3: p. 14.
22. Kroop, I.G., America's initial application of the Kolff artificial kidney. Hemodial Int. 2010. 14(4): p. 346-7.
23. Aebischer, P., et al., The bioartificial kidney: progress towards an ultrafiltration device with renal epithelial cells processing. Life Support Syst. 1987. 5(2): p. 159-68.
24. Humes, H.D., et al., Tissue engineering of a bioartificial renal tubule assist device: in vitro transport and metabolic characteristics. Kidney Int. 1999. 55(6): p. 2502-14.
25. Humes, H.D., et al., Replacement of renal function in uremic animals with a tissue-engineered kidney. Nat Biotechnol. 1999. 17(5): p. 451-5.
26. Humes, H.D., W.F. Weitzel, and W.H. Fissell, Renal cell therapy in the treatment of patients with acute and chronic renal failure. Blood Purif. 2004. 22(1): p. 60-72.
27. Humes, H.D., et al., Initial clinical results of the bioartificial kidney containing human cells in ICU patients with acute renal failure. Kidney Int. 2004. 66(4): p. 1578-88.
28. Ni, M., et al., Characterization of membrane materials and membrane coatings for bioreactor units of bioartificial kidneys. Biomaterials. 2011. 32(6): p. 1465-76.
29. Buffington, D.A., et al., Bioartificial Renal Epithelial Cell System (BRECS): A Compact, Cryopreservable Extracorporeal Renal Replacement Device. Cell Med. 2012. 4(1): p. 33-43.
30. Oo, Z.Y., et al., A novel design of bioartificial kidneys with improved cell performance and haemocompatibility. J Cell Mol Med. 2013. 17(4): p. 497-507.
31. Koepsell, H. and H. Endou, The SLC22 drug transporter family. Pflugers Arch. 2004. 447(5): p. 666-76.
32. Masereeuw, R. and F.G. Russel, Regulatory pathways for ATP-binding cassette transport proteins in kidney proximal tubules. AAPS J. 2012. 14(4): p. 883-94.
33. Oo, Z.Y., et al., The performance of primary human renal cells in hollow fiber bioreactors for bioartificial kidneys. Biomaterials. 2011. 32(34): p. 8806-15.
34. Zhang, H., et al., The impact of extracellular matrix coatings on the performance of human renal cells applied in bioartificial kidneys. Biomaterials. 2009. 30(15): p. 2899-911.
35. Sanechika, N., et al., Development of bioartificial renal tubule devices with lifespan-extended human renal proximal tubular epithelial cells. Nephrol Dial Transplant. 2011. 26(9): p. 2761-9.
36. Saito, A., et al., Evaluation of bioartificial renal tubule device prepared with lifespan-extended human renal proximal tubular epithelial cells. Nephrol Dial Transplant. 2012. 27(8): p. 3091-9.

37. Humes, H.D., et al., Metabolic replacement of kidney function in uremic animals with a bioartificial kidney containing human cells. Am J Kidney Dis. 2002. 39(5): p. 1078-87.
38. Dankers, P.Y., et al., The use of fibrous, supramolecular membranes and human tubular cells for renal epithelial tissue engineering: towards a suitable membrane for a bioartificial kidney. Macromol Biosci. 2010. 10(11): p. 1345-54.
39. Saito, H., et al., Transcellular transport of organic cation across monolayers of kidney epithelial cell line LLC-PK. Am J Physiol. 1992. 262(1 Pt 1): p. C59-66.
40. Urakami, Y., et al., Transcellular transport of creatinine in renal tubular epithelial cell line LLC-PK1. Drug Metab Pharmacokinet. 2005. 20(3): p. 200-5.
41. Kuteykin-Teplyakov, K., et al., Differences in the expression of endogenous efflux transporters in MDR1-transfected versus wildtype cell lines affect P-glycoprotein mediated drug transport. Br J Pharmacol. 2010. 160(6): p. 1453-63.
42. Takada, T., H. Suzuki, and Y. Sugiyama, Characterization of polarized expression of point- or deletion-mutated human BCRP/ABCG2 in LLC-PK1 cells. Pharm Res. 2005. 22(3): p. 458-64.
43. Brown, C.D., et al., Characterisation of human tubular cell monolayers as a model of proximal tubular xenobiotic handling. Toxicol Appl Pharmacol. 2008. 233(3): p. 428-38.
44. Jang, K.J., et al., Human kidney proximal tubule-on-a-chip for drug transport and nephrotoxicity assessment. Integr Biol (Camb). 2013. 5(9): p. 1119-29.
45. Lash, L.H., D.A. Putt, and H. Cai, Membrane transport function in primary cultures of human proximal tubular cells. Toxicology. 2006. 228(2-3): p. 200-18.
46. Ryan, M.J., et al., HK-2: an immortalized proximal tubule epithelial cell line from normal adult human kidney. Kidney Int. 1994. 45(1): p. 48-57.
47. Jansen, J., et al., A morphological and functional comparison of proximal tubule cell lines established from human urine and kidney tissue. Exp Cell Res. 2014. 323(1): p. 87-99.
48. Wilmer, M.J., et al., Novel conditionally immortalized human proximal tubule cell line expressing functional influx and efflux transporters. Cell Tissue Res. 2010. 339(2): p. 449-57.
49. Jenkinson, S.E., et al., The limitations of renal epithelial cell line HK-2 as a model of drug transporter expression and function in the proximal tubule. Pflugers Arch. 2012. 464(6): p. 601-11.
50. Ke, J.T., et al., Gliquidone decreases urinary protein by promoting tubular reabsorption in diabetic Goto-Kakizaki rats. J Endocrinol. 2014. 220(2): p. 129-41.
51. Romiti, N., G. Tramonti, and E. Chieli, Influence of different chemicals on MDR-1 P-glycoprotein expression and activity in the HK-2 proximal tubular cell line. Toxicol Appl Pharmacol. 2002. 183(2): p. 83-91.
52. Tramonti, G., et al., P-glycoprotein in HK-2 proximal tubule cell line. Ren Fail. 2001. 23(3-4): p. 331-7.

53. Mutsaers, H.A., et al., Basolateral transport of the uraemic toxin p-cresyl sulfate: role for organic anion transporters? Nephrol Dial Transplant. 2011. 26(12): p. 4149.
54. Schophuizen, C.M., et al., Cationic uremic toxins affect human renal proximal tubule cell functioning through interaction with the organic cation transporter. Pflugers Arch. 2013. 465(12): p. 1701-14.
55. Mutsaers, H.A., et al., Uremic toxins inhibit renal metabolic capacity through interference with glucuronidation and mitochondrial respiration. Biochim Biophys Acta. 2013. 1832(1): p. 142-50.
56. Miller, J.H., Sodium-sensitive, probenecid-insensitive p-aminohippuric acid uptake in cultured renal proximal tubule cells of the rabbit. Proc Soc Exp Biol Med. 1992. 199(3): p. 298-304.
57. Dankers, P.Y., et al., Bioengineering of living renal membranes consisting of hierarchical, bioactive supramolecular meshes and human tubular cells. Biomaterials. 2011. 32(3): p. 723-33.
58. Khan, S., et al., Post-assembly functionalization of supramolecular nanostructures with bioactive peptides and fluorescent proteins by native chemical ligation. Bioconjug Chem. 2014. 25(4): p. 707-17.
59. ULProspector. Available from: http://plastics.ides.com/generics/44/polysulfone-psu.
60. Membrane GmbH. Available from: http://www.membrana.com/index.php/products-for-new-therapies/micropesr.
61. Nur, E.K.A., et al., Three-dimensional nanofibrillar surfaces promote self-renewal in mouse embryonic stem cells. Stem Cells. 2006. 24(2): p. 426-33.
62. Schindler, M., et al., A synthetic nanofibrillar matrix promotes in vivo-like organization and morphogenesis for cells in culture. Biomaterials. 2005. 26(28): p. 5624-31.
63. Kuraitis, D., et al., Exploiting extracellular matrix-stem cell interactions: a review of natural materials for therapeutic muscle regeneration. Biomaterials. 2012. 33(2): p. 428-43.
64. Yanagishita, M., Function of proteoglycans in the extracellular matrix. Acta Pathol Jpn. 1993. 43(6): p. 283-93.
65. Clark, S.J., P.N. Bishop, and A.J. Day, The Proteoglycan Glycomatrix: A Sugar Microenvironment Essential for Complement Regulation. Front Immunol. 2013. 4: p. 412.
66. Sage, H., Collagens of basement membranes. J Invest Dermatol. 1982. 79 Suppl 1: p. 51s-59s.
67. Ruoslahti, E., Fibronectin. J Oral Pathol, 1981. 10(1): p. 3-13.
68. Miner, J.H. and J.R. Sanes, Molecular and functional defects in kidneys of mice lacking collagen alpha 3(IV): implications for Alport syndrome. J Cell Biol. 1996. 135(5): p. 1403-13.

69. Song, J.J. and H.C. Ott, Organ engineering based on decellularized matrix scaffolds. Trends Mol Med. 2011. 17(8): p. 424-32.
70. Waite, J.H., Mussel power. Nat Mater. 2008. 7(1): p. 8-9.
71. Garcia, N.H., C.R. Ramsey, and F.G. Knox, Understanding the Role of Paracellular Transport in the Proximal Tubule. News Physiol Sci. 1998. 13: p. 38-43.
72. Aydin, S., et al., Influence of microvascular endothelial cells on transcriptional regulation of proximal tubular epithelial cells. Am J Physiol Cell Physiol. 2008. 294(2): p. C543-54.
73. Tasnim, F. and D. Zink, Cross talk between primary human renal tubular cells and endothelial cells in cocultures. Am J Physiol Renal Physiol. 2012. 302(8): p. F1055-62.
74. Bertocchi, C., et al., Differential effects of NO inhibition in renal epithelial and endothelial cells in mono-culture vs. co-culture conditions. Cell Physiol Biochem. 2010. 26(4-5): p. 669-78.
75. Heemskerk, S., et al., Selective iNOS inhibition for the treatment of sepsis-induced acute kidney injury. Nat Rev Nephrol. 2009. 5(11): p. 629-40.
76. Miya, M., et al., Enhancement of in vitro human tubulogenesis by endothelial cell-derived factors: implications for in vivo tubular regeneration after injury. Am J Physiol Renal Physiol. 2011. 301(2): p. F387-95.
77. Westover, A.J., D.A. Buffington, and H.D. Humes, Enhanced propagation of adult human renal epithelial progenitor cells to improve cell sourcing for tissue-engineered therapeutic devices for renal diseases. J Tissue Eng Regen Med. 2012. 6(8): p. 589-97.
78. Bussolati, B., et al., Isolation of renal progenitor cells from adult human kidney. Am J Pathol. 2005. 166(2): p. 545-55.
79. Kim, D. and G.R. Dressler, Nephrogenic factors promote differentiation of mouse embryonic stem cells into renal epithelia. J Am Soc Nephrol. 2005. 16(12): p. 3527-34.
80. Qian, H., et al., Bone marrow mesenchymal stem cells ameliorate rat acute renal failure by differentiation into renal tubular epithelial-like cells. Int J Mol Med. 2008. 22(3): p. 325-32.
81. Rota, C., et al., Human amniotic fluid stem cell preconditioning improves their regenerative potential. Stem Cells Dev. 2012. 21(11): p. 1911-23.
82. Narayanan, K., et al., Human embryonic stem cells differentiate into functional renal proximal tubular-like cells. Kidney Int. 2013. 83(4): p. 593-603.
83. Takasato, M., et al., Directing human embryonic stem cell differentiation towards a renal lineage generates a self-organizing kidney. Nat Cell Biol. 2014. 16(1): p. 118-26.
84. De Coppi, P., et al., Isolation of amniotic stem cell lines with potential for therapy. Nat Biotechnol. 2007. 25(1): p. 100-6.
85. Laustriat, D., J. Gide, and M. Peschanski, Human pluripotent stem cells in drug discovery and predictive toxicology. Biochem Soc Trans. 2010. 38(4): p. 1051-7.

86. Yu, J., et al., Induced pluripotent stem cell lines derived from human somatic cells. Science. 2007. 318(5858): p. 1917-20.
87. Kang, M. and Y.M. Han, Differentiation of human pluripotent stem cells into nephron progenitor cells in a serum and feeder free system. PLoS One. 2014. 9(4): p. e94888.
88. Lam, A.Q., et al., Rapid and efficient differentiation of human pluripotent stem cells into intermediate mesoderm that forms tubules expressing kidney proximal tubular markers. J Am Soc Nephrol. 2014. 25(6): p. 1211-25.
89. Zhou, T., et al., Generation of human induced pluripotent stem cells from urine samples. Nat Protoc. 2012. 7(12): p. 2080-9.
90. Humes, H.D., et al., A selective cytopheretic inhibitory device to treat the immunological dysregulation of acute and chronic renal failure. Blood Purif. 2010. 29(2): p. 183-90.
91. Ding, F., et al., The effects of a novel therapeutic device on acute kidney injury outcomes in the intensive care unit: a pilot study. ASAIO J. 2011. 57(5): p. 426-32.
92. Tumlin, J.A., et al., The effect of the selective cytopheretic device on acute kidney injury outcomes in the intensive care unit: a multicenter pilot study. Semin Dial. 2013. 26(5): p. 616-23.
93. Pino, C.J., et al., Cell-based approaches for the treatment of systemic inflammation. Nephrol Dial Transplant. 2013. 28(2): p. 296-302.
94. Uzarski, J.S., et al., New strategies in kidney regeneration and tissue engineering. Curr Opin Nephrol Hypertens. 2014. 23(4): p. 399-405.
95. Giacomini, K.M. and S.M. Huang, Transporters in drug development and clinical pharmacology. Clin Pharmacol Ther. 2013. 94(1): p. 3-9.
96. Takahashi, H., et al., Evaluation of bioartificial renal tubule device prepared with human renal proximal tubular epithelial cells cultured in serum-free medium. J Artif Organs. 2013. 16(3): p. 368-75.
97. Poveda, J., et al., p-Cresyl sulphate has pro-inflammatory and cytotoxic actions on human proximal tubular epithelial cells. Nephrol Dial Transplant. 2014. 29(1): p. 56-64.
98. Tiranathanagul, K., et al., Tissue engineering of an implantable bioartificial hemofilter. ASAIO J. 2007. 53(2): p. 176-86.
99. Fissell, W.H. and S. Roy, The implantable artificial kidney. Semin Dial, 2009. 22(6): p. 665-70.
100. Fissell, W.H., et al., Development of continuous implantable renal replacement: past and future. Transl Res. 2007. 150(6): p. 327-36.
101. Badylak, S.F., D. Taylor, and K. Uygun, Whole-organ tissue engineering: decellularization and recellularization of three-dimensional matrix scaffolds. Annu Rev Biomed Eng. 2011. 13: p. 27-53.
102. Bonandrini, B., et al., Recellularization of well-preserved acellular kidney scaffold using embryonic stem cells. Tissue Eng Part A. 2014. 20(9-10): p. 1486-98.

103. Sullivan, D.C., et al., Decellularization methods of porcine kidneys for whole organ engineering using a high-throughput system. Biomaterials. 2012. 33(31): p. 7756-64.
104. Orlando, G., et al., Discarded human kidneys as a source of ECM scaffold for kidney regeneration technologies. Biomaterials. 2013. 34(24): p. 5915-25.
105. Nakayama, K.H., et al., Decellularized rhesus monkey kidney as a three-dimensional scaffold for renal tissue engineering. Tissue Eng Part A. 2010. 16(7): p. 2207-16.
106. Burgkart, R., et al., Decellularized kidney matrix for perfused bone engineering. Tissue Eng Part C Methods. 2014. 20(7): p. 553-61.
107. Ross, E.A., et al., Embryonic stem cells proliferate and differentiate when seeded into kidney scaffolds. J Am Soc Nephrol. 2009. 20(11): p. 2338-47.
108. Kusaba, T., et al., Differentiated kidney epithelial cells repair injured proximal tubule. Proc Natl Acad Sci U S A. 2014. 111(4): p. 1527-32.
109. Smeets, B., et al., Proximal tubular cells contain a phenotypically distinct, scattered cell population involved in tubular regeneration. J Pathol. 2013. 229(5): p. 645-59.
110. Guthrie, K., et al., Potency evaluation of tissue engineered and regenerative medicine products. Trends Biotechnol. 2013. 31(9): p. 505-14.

SUPPLEMENTARY DATA

Table S4.1 – Unsuccessful ECM coating used with HK-2 and HPTC

Coating type and concentration	Cells used	source	Surface material	Seeding density (cells/cm^2)	ZO-1	Ref.
Poly-D-Lysine (100 µg/ml)	HK-2	NM	24-wells plate polystyrene	1.4 . 10^5	2	(34)
Poly-L-Lysine (10 µg/ml)	HPTC	NM	24-wells plate polystyrene	1.4 . 10^5	1	(34)
Pronectin F (NM)	HPTC	NM	24-wells plate polystyrene	1.4 . 10^5	-	(34)
Collagen I (750 µg/ml)	HPTC	murine	PES/PVP	1x10^5 cultivated for up to four weeks	-	(28)
Collagen IV (150 µg/ml)	HPTC	human	PES/PVP	1x10^5 cultivated for up to four weeks	-	(28)
Collagen IV (150 µg/ml)+ Laminin (100 mg/ml)	HPTC	human	PES/PVP	1x10^5 cultivated for up to four weeks	-	(28)

Optimal monolayer formation and cell attachment can be studied by the ZO-1 staining using a scoring system ranging from 1 to 5, accordance to Zhang et al. (28) The ZO-1 pattern scores are here reported in relation with different ECM coatings and surface materials used until now.

Chapter 5

DEVELOPMENT OF A LIVING MEMBRANE COMPRISING OF A FUNCTIONAL HUMAN RENAL PROXIMAL TUBULE CELL MONOLAYER ON POLYETHERSULFONE POLYMERIC MEMBRANE

Schophuizen CMS[1,2,3]*, De Napoli IE[4]*, Jansen J[1,2,3], Teixeira S[4], Wilmer MJ[3], Hoenderop JGJ[2], van den Heuvel LP[15], Masereeuw R[3], Stamatialis D[4]

Acta Biomaterialia,14, 22–32, 2015

Departments of [1]Pediatric Nephrology, [2]Physiology, and [3] Pharmacology and Toxicology, Radboudumc, Nijmegen, The Netherlands.
Department of [4]Biomaterials Science and Technology, MIRA Institute for Biomedical Technology and Technical Medicine, University of Twente, The Netherlands
Department of Pediatrics[5], Catholic University Leuven, Leuven, Belgium.

* Authors contributed equally

ABSTRACT

The need for improved renal replacement therapies is a stimulance for innovative research for the development of a cell based bioartificial kidney, or so called Renal Assist Device (RAD). A key requirement for such device is the formation of a "living membrane" consisting of a tight kidney cell monolayer with preserved functional organic ion transporters, on suitable artificial membrane surfaces. In this work, we applied a unique conditionally immortalized proximal tubule epithelial cell (ciPTEC) line with an optimized coating strategy on polyethersulfone (PES) membranes to develop a "living membrane" with a functional proximal tubule epithelial cell layer. PES membranes were coated with combinations of 3,4-dihydroxy-L-phenylalanine and human Collagen IV (Coll IV). The optimal coating time and concentrations were determined to achieve retention of vital blood components while preserving high water transport and optimal ciPTEC adhesion. The ciPTEC monolayers obtained were examined through immunocytochemistry to detect zona occludens-1 (ZO-1) tight junction proteins. Reproducible monolayers were formed when using a combination of 2 mg/ml L-DOPA (4 min coating, 1 h dissolution) and 25 µg/ml Coll IV (4 min coating). The successful transport of ^{14}C-creatinine through the developed "living membrane" system was used as an indication for organic cation transporter functionality. Addition of metformin or cimetidine significantly reduced the creatinine transepithelial flux, indicating active creatinine uptake in ciPTEC, most likely mediated by the organic cation transporter, OCT2 (*SLC22A2*).

In conclusion, this study shows the successful development of a "living membrane" consisting of a reproducible ciPTEC monolayer on PES membranes, an important step towards the development of a bioartificial kidney.

INTRODUCTION

The number of patients with end-stage renal disease (ESRD) is progressively increasing and the need for renal replacements therapies is rising (1). Worldwide, over 2 million patients suffer from ESRD and each year that number grows by 5%. Since transplant options are limited (2), approximately 70% of patients receive (hemodialysis or peritoneal) dialysis treatment. While dialysis therapy has already prolonged many ESRD patients' lives, the treatment cannot completely replace renal function. Mortality (15-20% per year) and morbidity of these patients remain high, whereas their quality of life is generally low. Hemodialysis (HD) therapy removes mainly small, unbound substances from the circulation, while leaving large, compartmentalized and protein-bound uremic retention solutes untouched (3). Although the introduction of high-flux (HF) or hemodiafiltration (HDF) therapy promotes enhanced removal of middle molecular weight solutes, the removal of protein-bound retention solutes remains limited (4,5).

Since renal secretion of such protein-bound compounds is predominantly mediated by the proximal tubule epithelial cells (PTEC) (6,7), the need for improved renal replacement therapy has stimulated innovative research into the development of a bioartificial kidney, or so called Renal Assist Devices (RAD) (8). These innovative devices aim to complement the hemodialysis treatment, by coupling artificial membranes with functional kidney cells. To achieve efficient clearance of uremic retention solutes, proximal tubular epithelial cells need to be seeded on the inner surface of hollow fiber membranes. This situation is comparable to the native tubule, where the basement membrane separates proximal tubule cells from the circulation. While the patients' blood flows over the outer surface, the uremic retention solutes can bind to the transport proteins present on the basolateral surface of human PTEC, facilitating their subsequent secretion into the hemodialysis filtrate. This approach could provide a means to further diminish the systemic accumulation of uremic retention solutes, reduce the incidence of secondary morbidities in patients, and shorten dialysis duration or frequency, thereby improving the quality of life in ESRD.

The development of a RAD brings along very specific biotechnological challenges, as was recently reviewed by Jansen et al. 2014 (9). First of all, an important challenge in the development of a RAD is the limited availability of reliable and well characterized human proximal tubule cells

capable of transepithelial excretion of uremic retention solutes. This "living membrane" should consist of tight cellular monolayers maintaining their typical polarity and functionality. Second, one side of the membrane to be used in a RAD needs to be suitable for blood contact (low cell adhesion), whilst the other side should facilitate cellular adhesion. Surface topography was identified as an important feature affecting cell adhesion and membrane hemocompatibility, the two properties being favored by higher surface roughness and smoothness, respectively (10). Several studies, which attempted to create "living membranes" with renal epithelial cells, have used existing membranes (mostly hollow fibers) used in dialysis and / or blood purification. Polyethersulfone (PES), polysulfone (PSF), polyacrylonitrile (PAN) and cellulose acetate membranes, were evaluated for their ability to support monolayer growth of renal epithelial cells (11-13). Since these membranes are designed for low cell adhesion, and maximum hemocompatibility during blood filtration, it is necessary to apply a coating consisting of extracellular matrix components. This actually describes the third challenge in RAD development; the optimization of coating conditions. In some cases, coatings have been reported to improve the attachment of renal tubule epithelial cells, but often coatings failed to maintain trans-monolayer transport activity and monolayer integrity (14-18). Human collagen type IV (Coll IV) based coatings are promising for attachment and functional culture of proximal tubule cells (15), since Coll IV is endogenously present in the basal lamina and promotes mesenchymal cell differentiation towards the epithelial lineage (19). However, it is necessary to improve its adhesion to the artificial membrane. The treatment of polymeric surfaces with biomolecules via covalent reactions is generally inconvenient given the susceptibility of different activated groups to hydrolysis, which can lead to low efficiency of surface biofunctionalization (20). An easy two-step water based biofunctionalization method has been proposed that promotes the formation of a thin adherent polydopamine (PDA) film (10,17,21) using self-polymerizing 3,4-dihydroxy-L-phenylalanine (L-DOPA); and exploits the reactivity of the PDA film to covalently bind the biomolecule Coll IV on the membrane surface (10,20). However, in these earlier studies, the application of the coatings was not optimized with regard to membrane transport characteristics (high water permeance and retention of vital proteins such as BSA and IgG).

The selection of renal cell lines suitable for RAD application poses another challenge. The use of animal cell models, such as porcine (primary or LLC-PK1), monkey (JTC-12) and canine (MDCK) renal epithelial cells, provides insight in

the functionality of a RAD, both *in-vitro* as well as *in-vivo* (13,16,22-25). However, their clinical application is highly restricted. Moreover, species differences in renal proximal tubule physiology are in favor of a renal cell line of human origin (26,27). Studies using freshly isolated primary human proximal tubule cells in a RAD have shown promising results (10,28,29). However, their limited availability, low proliferative capacity, and donor-to-donor variation, severely restrict the use of these cells. The utilization of a functional human proximal tubule epithelial cell line overcomes these drawbacks. Previously, some of the co-authors of this study have developed a human conditionally immortalized proximal tubule epithelial cell (ciPTEC) line, with intact proximal tubular characteristics and endogenous expression of various functional transport proteins (30,31). Among the advantages of this cell line is the switch between a proliferative state at 33 °C to a differentiation state at 37 °C, permitted by transduction with the temperature sensitive Simian virus 40 (SV40) large T antigen. The genetic switch allows for cell proliferation arrest when the cells are confluent and fully differentiated, promoting the formation of tight and functional monolayers (30).

In this work, we show for the first time the development of a stable, functional "living membrane" by culturing ciPTEC on PES based membranes with a molecular weight cut off 50 kDa. This cut off prevents albumin leakage, blocks possible immunoglobulin transfer, and avoids the loss of vital blood component in case of cell monolayer integrity failure. The membranes were coated with a double coating consisting of L-DOPA and Coll IV on the more porous rough membrane side to maximize the beneficial effect of both membrane topography and coating on cell adhesion. This coating was carefully optimized to preserve high membrane permeability and create a tight cell monolayer. The selective active transport of creatinine through the "living membranes" was investigated in the presence and absence of specific inhibitors, and compared to a commercially available polyester Transwell® system.

MATERIALS AND METHODS

Membrane coatings

Flat polyethersulfone membranes (Sartorius, Goettingen, Germany), which showed good hemocompatibility properties (32), with a molecular weight cut off of 50 kDa (indicated, as PES - 50) were coated with a double layer

of 3,4-dihydroxyl-L-phenylalanine (L-DOPA) (D9628, Sigma Aldrich, Zwijndrecht, The Netherlands) and human collagen IV (Coll IV, C6745, Sigma Aldrich, Zwijndrecht, The Netherlands) L-DOPA solutions with concentrations ranging from 1 to 2 mg/ml in Tris buffer 10 mM (pH 8.5) were prepared and dissolved at 37°C. Complete dissolution was obtained after 1 h, followed by filter sterilization. Subsequently, the L-DOPA solution was used to either coat the membranes immediately after powder dissolution, with minimum polymerization degree (referred to as L-DOPA (1 h)), or left to polymerize for 2 more hours (referred to as L-DOPA (3 h)) before coating the membranes. For the sake of simplicity, we defined the dissolution time as the time that the L-DOPA is kept in solution before coating the membrane. The membranes were first pre-incubated in Hanks' balanced salt solution (HBSS; Life Technologies, Bleiswijk, the Netherlands) for 10 min. Next, the L-DOPA solutions were applied to the membrane surface. The solution was aspirated, and the membranes were left to dry for 5 min. Then, a Coll IV solution (25 µg/ml or 50 µg/ml) in HBSS was used for the second step of the coating. After fluid aspiration and drying, the membranes were washed three times in HBSS to remove any remaining solvent or unbound compound. Diverse L-DOPA dissolution times (1 and 3h) and coating times of membranes (1 and 4 min) were tested and their effects on membranes properties were evaluated in terms of membrane morphology and pure water permeance. An overview of the coating conditions tested is given in Figure 5.1. The PES-50 membrane has an asymmetric structure: one membrane side is denser (and therefore determines the transport properties) and smooth, while the other membrane side is more porous and rough. The double coating was performed on the more porous membrane side, under static conditions, by contacting the coating solution with the membrane surface. To obtain single sided coating of the flat PES membranes, the coating solution was first poured in glass Petri dishes and the membrane was gently placed on the top of the solutions with the porous side in contact with the liquid. The selection of final concentrations, dissolution times and coating times for both the L-DOPA and the Coll IV solution was based on cell adhesion, cell monolayer formation and tight junction expression. Reproducibility of the coating was investigated in terms of water and protein transport properties. For cell culturing, polyester Corning (Corning Costar, NY, USA) custom Transwell® supports were used. In these Transwells (12mm in diameter), the polyester cell membrane was replaced by PES - 50 membrane used for the double coating development. Here, membrane coating was performed on one side of the membrane by applying the solutions to the apical (cell-facing) side of the Transwell®.

Since the PES membrane is sealed on the perimeter to the plastic holder, the basolateral side of the membrane did not come into direct contact with the coating solution. Supplemental figure 5.A1 provides a schematic overview of a coated Transwell® membrane. As a reference, we employed double-coated (positive control) polyester Transwell® membranes, which are frequently used for *in-vitro* PTEC culture (30,33).

Membrane morphological and surface composition analysis

Membrane morphology was determined by scanning electron microscopy (FEI/Philips XL30 FEG ESEM). Surface samples were prepared and kept overnight at 30°C and gold sputtered before examination by SEM at a voltage of 5 kV. The membrane surface chemical structures and composition of the coated and uncoated PES-50 were characterized using an Attenuated total reflection-Fourier transform infrared spectra (ATR-FTIR) (Spectrum two,, Perkin Elmer, Waltham, USA) instrument. Elementary analysis of the membrane composition was performed by Energy Dispersive Spectroscopy analysis (EDS -EDAX Apollo X for ESEM, New Jersey, USA).

Membrane transport properties

Pure water, bovine serum albumin (BSA, A2153, Sigma Aldrich, Zwijndrecht, the Netherlands) and immunoglobulin G (IgG, I9640, Sigma Aldrich, Zwijndrecht, the Netherlands) solution permeance was determined using an air-pressurized dead end 'Amicon type' ultrafiltration cell (hosting 4 cm Ø membrane samples) and ultrapure water. The flux (J) of water and protein solution through the membranes at each pressure was determined by collecting the mass of the permeated liquid over time and correlating it to the membrane unit surface area. The permeance (L, in L m^{-2} h^{-1} bar^{-1}) of water or protein solution was estimated by normalizing the water or protein solution flux (J, in L m^{-2} h^{-1}) by the applied transmembrane pressure (ΔP, in bar). The permeance is, in fact, calculated from the slope of the linear part of the flux vs. transmembrane pressure relationship:

$$L = \frac{J}{\Delta P} \quad (1)$$

Clean water permeation tests were performed by using ultrapure water (MilliQ 18 MΩ.cm, Millipore; Billerica, MA, U.S.A) solutions inside stirred Amicon cells (Millipore; Billerica, MA, U.S.A), where the membranes were placed with the thin layer facing the feed solution. Automatic collection of permeate mass

during time was performed by means of a Labview based software, the mass was converted to volume given the water density equal to 998 kg. m^{-3} at 20°C (34). Uncoated flat membranes were tested after immersing them in pure water for 1 hour to remove preservatives added during the manufacturing process. Membranes double coated with L-DOPA and Coll IV were immersed in HBSS buffer for 30 min before they were used. Subsequently, the membranes were subject to a flushing step with ultrapure water at the highest working pressure (0.75 bar). Then, down to up pressure cycles were applied to each membrane.

The extent of protein transport through the membrane was evaluated by estimating the apparent sieving coefficient (SC_a).

$$SC_a = \frac{C_p}{C_b} \quad (2)$$

Where C_p is the protein concentration in the permeate and C_b is the protein concentration in the feed protein solution. SC_a=1 means that the protein passes freely through the membrane, while SC_a=0 means that the membrane rejects the protein completely.

Phosphate buffered saline (PBS) containing BSA or IgG, were used at a concentration of 1 mg/ml and 0.02 mg/ml, respectively. Three different pressures (0.25, 0.50, 0.75 bar) were applied and sample collection occurred every 15 minutes for 1 hour. The protein solution was continuously mixed at the top of the membrane surface to prevent polarization concentration effect and delay membrane fouling. BSA and IgG concentration was evaluated by spectrophotometric analysis in quartz cuvettes at 280 nm.

Cell culture

A previously developed ciPTEC cell line (30) was used for functional testing of the coated membranes. In short, this immortal cell line was developed by transducing primary human proximal tubule epithelial cells, obtained from urine samples of healthy volunteers, with a SV40t, and hTERT gene. SV40t stimulates cellular proliferation at 33°C, while it is silenced by culturing the cells in a 37°C environment. As a consequence, at 37°C the cells are able differentiate and form a tight monolayer. The hTERT ensures the cellular quality, by keeping the length of the telomeres intact during proliferation. We have previously evaluated the characteristics of this cell line, on a morphological and functional level (7,31). CiPTEC were cultured in Dulbecco's modified eagle medium DMEM-HAM's F12 (Lonza; Basel, Switzerland)

containing 10% v/v fetal calf serum (FCS) (Greiner Bio-One; Alphen a/d Rijn, the Netherlands), 5 µg/ml insulin, 5 µg/ml transferrin, 5 ng/ml selenium, 36 ng/ml hydrocortisone, 10 ng/ml epidermal growth factor and 40 pg/ml tri-iodothyronine, all purchased from Sigma-Aldrich Co. (Zwijndrecht, the Netherlands). Culture media were phenol-red and antibiotic free. To prevent de-differentiation of ciPTEC during regular culturing, cells were used in experiments up to a maximum of 40 passages, during which proximal tubular characteristics remained unaltered (30). Proliferating ciPTEC were seeded onto the polyester or PES membrane Transwell® inserts at a density of 133.000 cells/cm^2. To promote initial cellular attachment and proliferation, ciPTEC were cultured for 24 h at 33°C 5% (v/v) CO_2 and after this time period the temperature was changed to 37°C for 7 days to promote the formation of a differentiated monolayer.

Immunocytochemistry

To investigate morphological characteristics and monolayer integrity of matured ciPTEC cultured on polyester (30,33) and PES-50 Transwell® inserts, immunocytochemistry was performed and after 7 days the expression of the tight junction protein, ZO-1 (zonula occludens – 1), was studied. Matured ciPTEC were fixed using 2% (w/v) paraformaldehyde in HBSS supplemented with 2% (w/v) sucrose for 5 min and permeabilized in 0.3% (v/v) Triton X-100 in HBSS for 10 min. To prevent non-specific binding of antibodies, cells were exposed to block solution containing 2% (w/v) bovine serum albumin fraction V (Roche, Woerden, the Netherlands) and 0.1% (v/v) Tween-20 in HBSS for 30 min. Cells were incubated with antibodies diluted in block solution against the tight junction protein zonula occludens 1 (ZO-1, 1:50 dilution, Invitrogen, Carlsbad, CA) for 1 h, followed by incubation with goat-anti-rabbit-Alexa488 conjugate (1:200, Life Technologies Europe BV, Bleiswijk, the Netherlands) for 30 min. Finally, DAPI nuclei staining (300 nM, Life Technologies Europe BV) was performed for 5 min. Protein expression and localization were examined using the Olympus FV1000 Confocal Laser Scanning Microscope (Olympus, Tokyo, Japan) and images were captured using the Olympus software FV10-ASW version 1.7. To semi-quantify the fluorescent staining of ZO-1, a grid of 8.5 µm^2 was placed on top of the confocal images using ImageJ software (ImageJ 1.46r, NIH, USA) (35). The number of intersections between the grid and the ZO-1 signal was determined for each condition.

Transepithelial transport measurements

Transepithelial transport of (^{14}C)-creatinine by matured ciPTEC monolayers cultured on either polyester or PES Transwell® inserts was measured using a Transwell® culture system. A schematic overview of the set-up, is provided in the supplemental file (Figure 5.A1). Polyester Transwells® (diameter 12mm, pore size 0,4µm) were coated with L-Dopa alone or in combination with Coll IV (25 mg/ml, for 2 hours), and compared to double coated polyester or PES-50 Transwells®. Mature cell monolayers were washed in modified Krebs-Henseleit buffer (Sigma-Aldrich, Zwijndrecht, The Netherlands) including 10mM Hepes (pH 7.4). Subsequently, all membranes tested were pre-incubated for 2 h at 37°C, 5% (v/v) CO_2 in Krebs-Henseleit-Hepes buffer (0.5 mL apically, 1.5 mL basolaterally). Transport was initiated by the basolateral addition of either (^{14}C)-creatinine (0.75 µM, 2 µCi/ml) or (^{3}H)-inulin (0.45 µM, 20 µCi/ml) with or without cimetidine (100 µM) or metformin (100 µM) as competitors for OCT2 transport (Sigma-Aldrich Co., Zwijndrecht, the Netherlands). At the start of the measurement, a 20 µL reference sample was taken from the basolateral exposure compartment. After 30 min of incubation with gentle agitation at 37°C a 200 µL sample was removed from the apical chamber. The activity of (^{3}H) and (^{14}C) in the samples was determined by liquid scintillation counting (Beckman). Fluxes of (^{14}C)-creatinine or (^{3}H)-inulin were determined for each separate Transwell®. The flux of (^{3}H)-inulin was used as an internal leakage marker. The basolateral to apical flux (J) was calculated with:

$$J = \frac{dQ}{S * dt} \tag{3}$$

Where dQ = amount transported (pmol); dt = duration of transport (minutes); S = surface area (cm^2).

Data analysis

Water, BSA and IgG transport measurements in each experiment were performed at least in triplicates (N≥3 for each coating condition). Results are presented as mean ± standard deviation. Statistical analysis was performed with the Microsoft Excel® software (Microsoft Corporation, Seattle, USA) using a one-way ANOVA or a Student's T-test when appropriate.

Quantification of ZO-1 staining on Transwell® polyester or PES membranes was performed in triplicates for each coating condition. The results are presented as mean ± sem. Results were normalized by taking the double coated Polyester Transwell® as 100% reference. One-way ANOVA followed by

a Dunnett's post-test, was performed using GraphPad Prism version 6.00 for Windows, (GraphPad Software, La Jolla California USA).

For basolateral creatinine transport experiments in the commercially available polyester Transwells® the experiments were performed at least in triplicate in three independent experiments. The custom PES Transwells® were tested in duplicate in three independent experiments. Results are presented as mean ± sem. Statistical analysis was performed with GraphPad Prism, using a two way ANOVA combined with a Bonferroni's post-test.

RESULTS – DISCUSSION

The biofunctionalization strategy of flat PES-50 membranes was optimized first to develop functional ciPTEC monolayers. Artificial membranes should provide a solid base for cells to form tight monolayers and facilitate active transepithelial solute transport. In the nephron, the proximal tubule is responsible for the reabsorption of 65% of all the water filtered by the glomerulus; the very high permeability of the tissue was estimated to be about $1x10^5$ L m^{-2} h^{-1} bar^{-1} (36). The hydraulic permeability of native PES-50 membrane is 2 orders of magnitude lower than the value reported for natural tissue, the membrane was chosen on the base of its capacity to retain vital blood components, consistent with other research in the field (22). For this reason, water transport through the coated membranes was one of the main parameters to optimize, in order to preserve the highest permeance possible. A recent study proposed the application of an overnight double coating (10). However, when we applied such a coating, a significant decrease in membrane water permeance, (39 ± 23 L m^{-2} h^{-1} bar^{-1}) was detected in comparison to uncoated membranes (738 ± 110 L m^{-2} h^{-1} bar^{-1}). Further reduction of the permeance was expected when applying the second coating layer consisting of Coll IV. To avoid significant transport limitations, we investigated shorter L-DOPA dissolution times. In a first attempt, L-DOPA was used for the coating immediately after the dissolution step (L-DOPA (1 h)). The average value of water permeance did not change significantly (654 ± 70 L m^{-2} h^{-1} bar^{-1}) with respect to uncoated membrane values (Figure 5.1, I). After applying the Coll IV coating on top of the L-DOPA layer (Figure 5.1, II), the average value of water permeance decreased to 347± 151 L m^{-2} h^{-1} bar^{-1}.

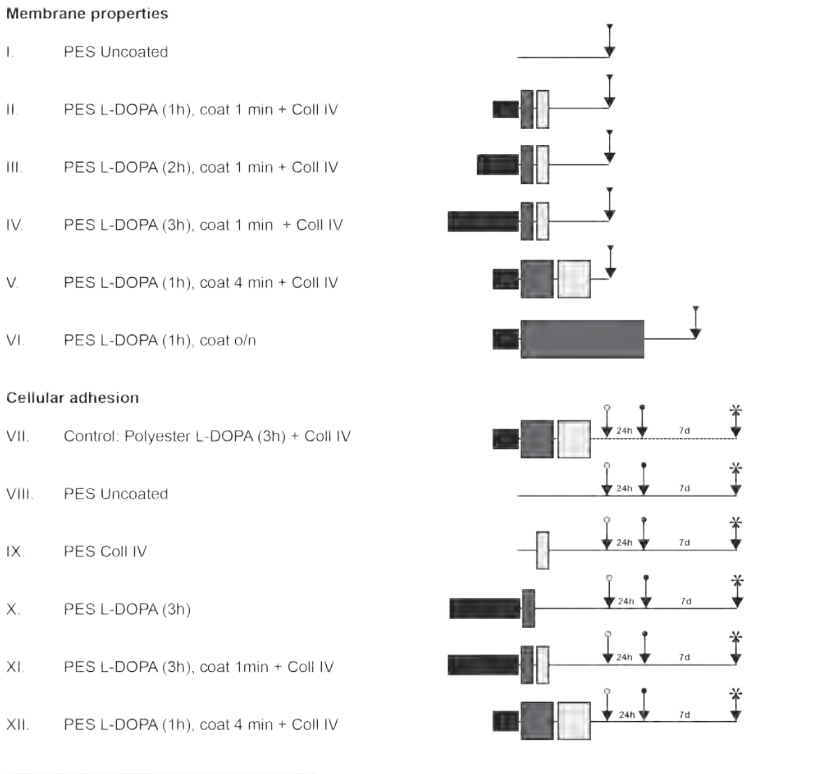

Figure 5.1 Schematic overview of the coating conditions evaluated for their membrane properties and cell adhesion.
See text for further details and abbreviations.

However, the high coefficient of variation (0.44) indicated a non-reproducible coating. These results indicate that short coating times do not cause significant changes, whilst overnight coating results in a dramatic reduction in membrane transport properties. Since the variable "time" plays a central role in the macroscopic transport properties of the coated membrane, we compared the effects of prolongation of the L-DOPA dissolution time (Figure 5.1; II, III and IV), to prolongation of the coating time to L-DOPA and Coll IV from 1 to 4 min (Figure 5.1; II, V).

When applying L-DOPA coating alone, prolongation of the L-DOPA dissolution time slightly increases the average membrane water permeance, although this effect was not significantly different from the non-coated PES-50 membranes (dark symbols, Figure 5.2a). Literature reports that L- DOPA coating can increase the membrane hydrophilicity due to the coexistence of carboxylic and amino groups in the L- DOPA molecule (37). In fact, the effect of L-DOPA coating on hydrophilization of different materials has been shown by the reduction of water contact angle under the same experimental conditions used in the present study (pH, Tris buffer molarity and L-DOPA concentration) (21,37,38) we therefore expect that our membranes are slightly hydrophilized, too. Nevertheless, the application of L-DOPA to porous membranes can reduce the membrane transport properties. This decrease mostly occurs to UF membranes where the pore dimensions allow migration of L-DOPA monomers and oligomers inside the membrane structure with consequent reduction or blockage of the inner porosity (39,40). The transport properties of reverse osmosis (RO) and microfiltration (MF) membranes was reported to be less affected by L-DOPA coatings, due to the different pore size (40). Since we used PES-50 UF membranes, the coating time as well as the L-DOPA dissolution time required optimization to avoid complete suppression of the membrane permeance.

The Coll IV coating on top of the L-DOPA layer (Figure 5.1, conditions I – IV) decreased the membrane water permeance significantly (open symbols in Figure 5.2a). The permeance for the double coated membranes with L-DOPA (3 h) and Coll IV for 1 min was 194 ± 35 L m^{-2} h^{-1} bar^{-1}, which is significantly lower than the uncoated membranes. However, when compared to overnight L-DOPA coating (Figure 5.1; VI), the membrane permeance improved markedly. Furthermore, prolongation of L-DOPA dissolution to 3 h enhanced the coating reproducibility, as demonstrated by the low standard deviation of the permeance values. Figure 5.2b presents the optimization procedure

of the double coating using different coating times of L-DOPA (1h) (Figure 5.1; II, V and VI). The water permeance for double-coated membranes with 4 min coating was A 2.7 fold higher (146 ± 10 L m^{-2} h^{-1} bar^{-1}) than for overnight L-DOPA (only) coating. Prolongation of coating time to 4 min also improved the double coating reproducibility, as demonstrated by the low standard deviation of the permeance results. These results indicate that optimization of the L-DOPA dissolution, and coating times significantly improves the membrane permeance and coating reproducibility, when compared to overnight coating.

The progressive reduction of membrane water permeance correlated with the observed morphological changes at the porous side of the membrane surface where the double coating was applied. Figure 5.3 presents SEM images of uncoated, only L-DOPA and double coated membranes surfaces. The single L-DOPA coating slightly affected the porous layer morphology (data not shown). After application of L-DOPA (3h), an estimated 40% reduction in the macroporosity visible at the upper surface of the flat membranes could be observed compared with the original membranes (Figure 5.3b). Application of Coll IV to the L-DOPA coating resulted in complete occlusion of membrane surface pores as compared to membranes coated with L-DOPA only, for all L-DOPA dissolution times tested (Figure 5.3c). The lack of visible differences in surface morphology in the presence of the single L-DOPA coating in comparison with native membranes was consistent with the average rate of PDA layer deposition (2 nm/h) reported in previous studies for the same experimental conditions (L-DOPA concentration, temperature, pH and Tris buffer molarity) (21,41). The analysis of membrane surface chemical composition confirmed that the thickness of the coating was in the nm range, as the beam penetration for both EDAX and FT-IR analysis was deeper than the single or double coating applied. In fact for both the FT-IR spectrum and the elementary composition, the underlying PES material is still dominant (Figure 5.4). Dopamine monomers and small oligomers have previously been demonstrated to play a primary role in the initiation of the PDA deposition and its consequent polymerization at the membrane surface (21,40,41). In these studies, maximal monomer deposition rate was observed during the first hours after L-DOPA dissolution. This finding may explain why, in our case, a short coating time was sufficient to modify the PES-50 membranes, providing good collagen IV adhesion and reproducibility of transport properties.

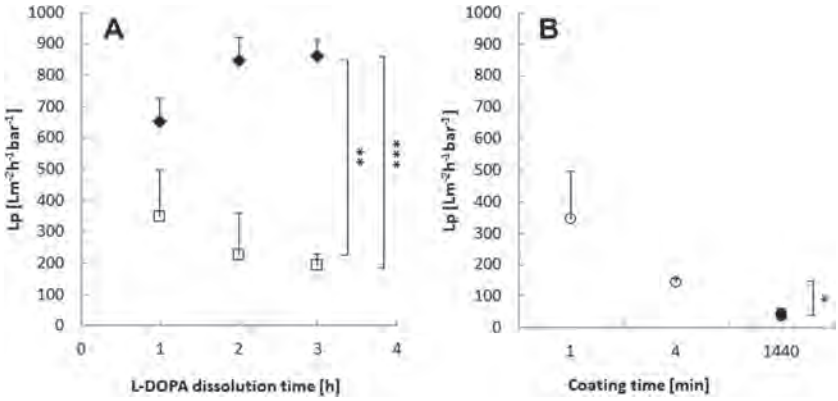

Figure 5.2 Pure water permeance of PES-50 membranes coated with L-DOPA (2 mg/ml) and Coll IV (25 µg/ml) as a function of: a) L-DOPA dissolution time for PES membranes coated for 1 min with L-DOPA solution only (◆), or L-DOPA followed by Coll IV (□); b) double coating with L-DOPA followed by Coll IV with varying coating times (○), or L-DOPA solution after overnight coating (●). Data are presented as mean ± standard error, * $p<0.05$; ** $p<0.01$; *** $p<0.005$; N≥3 for each experimental point.

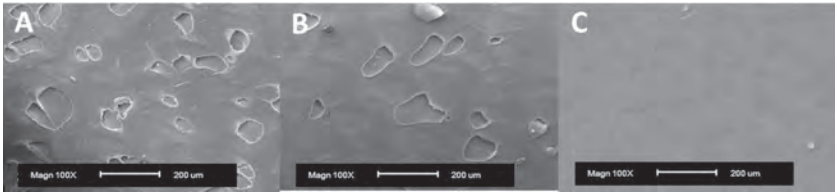

Figure 5.3 Representative Scanning Electron Microscopy analysis of PES-50 membranes porous side surface morphology with L-DOPA (2 mg/ml) and Coll IV (25 µg/ml) with different L-DOPA dissolution times: a) uncoated; b) 1 min coating with L-DOPA (3h) only; c) 4 min coating with L-DOPA (1h) and Coll IV. Magnification 100X. At least three independent membranes were examined for each condition.

The optimized coatings were tested further for optimal cell monolayer formation by ZO-1 tight junction protein expression, a marker that indicates monolayer integrity and polarity of epithelial cells. The tested coating conditions are described schematically in Figure 5.1, under the cellular adhesion heading (Figure 5.1; conditions VII-XII). Standard double coated polyester Transwell® inserts, were used as a positive control (Figure 5.5a). Uncoated PES-50 membranes provided poor cell adhesion of ciPTEC (Figure 5.5b) while single coating with Coll IV (25mg/ml) or L-DOPA (2mg/ml) did not improve this (Figure 5.5c,d). After application of the double coating, cellular adhesion and the expression of ZO-1 improved (Figure 5.5e-f). The observed clear ZO-1 expression indicates polarization of the monolayer, improving epithelial characteristics (42) and limits paracellular leakage. No significant difference in monolayer formation and ZO-1 expression was detected between conditions XI and XII (Figure 5.5e,f), which varied either the coating or dissolution time. Furthermore, quantification of the ZO-1 has indicated that ciPTEC expressed ZO-1 protein in a similar fashion on both double coated PES-50 as on polyester Transwells®, which are considered the golden standard in ciPTEC transepithelial studies (Figure 5.5g). Lowering the concentration of L-DOPA reduced the reproducibility of cellular adhesion, even in the presence of a higher Coll IV concentration, thus suggesting the importance of a good L-DOPA layer to foster Coll IV membrane coating. Furthermore, increasing the Coll IV concentration to 50 µg/ml after 2 mg/ml L-DOPA coating did not improve monolayer quality with respect to 25 µg/ml Coll IV (supplemental Figure 5.A2).

The coatings were investigated further in terms of protein rejection and fouling phenomena during protein solution permeance. Table 5.1 shows a comparison of transport properties of uncoated and membranes with optimized coatings (Figure 5.1; conditions I, IV and V). The permeance of IgG and BSA solutions for the uncoated PES-50 membranes is 53 ± 11 and 57 ± 7 L m^{-2} h^{-1} bar^{-1}, respectively, about 96% lower than the water permeance through the same membranes (P<0.05). There was no significant difference in protein solution permeance for the coated membranes, as values ranged from 37 ± 27 L m^{-2} h^{-1} bar^{-1} to 65 ± 24 L m^{-2} h^{-1} bar^{-1}. Both BSA (66 kDa) and IgG (150 kDa) were almost completely rejected by both uncoated and coated membranes: the SC < 0.1, consistently to what is expected for a 50 kDa membrane.

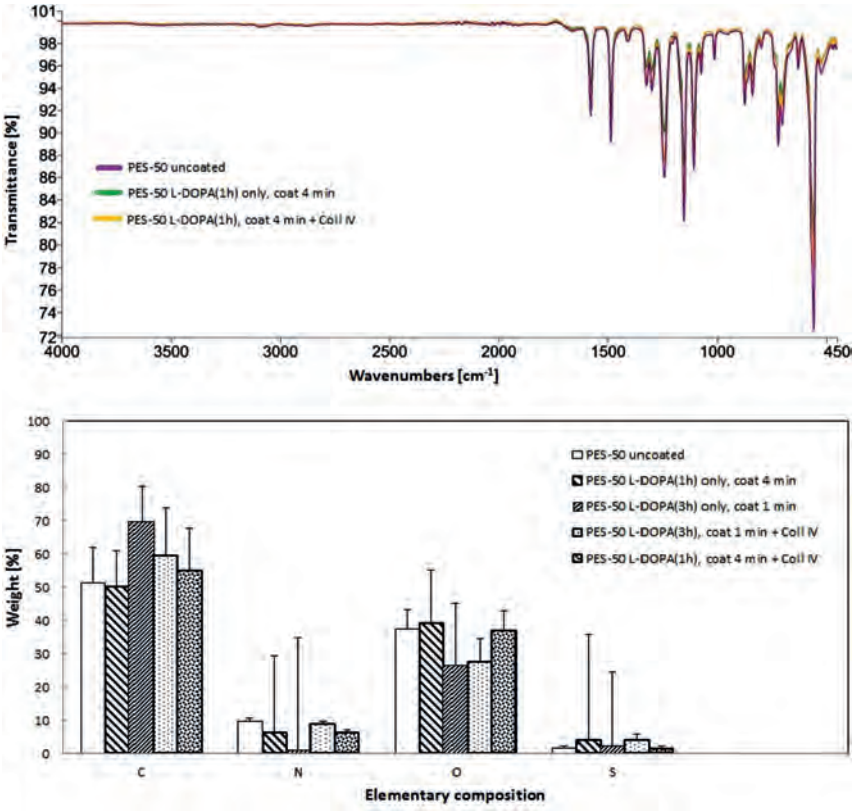

Figure 5.4 Surface chemical composition of PES-50 membranes uncoated and coated with L-DOPA (2 mg/ml) and Coll IV (25 µg/ml).

Above ATR-FTIR spectra for: purple) uncoated PES-50; green) 4 min coating with L-DOPA (1h) only; yellow) 4 min coating with L-DOPA (1h) and Coll IV. Below EDAX analysis of (from left to right: uncoated PES-50; 4 min coating with L-DOPA (1h) only; 1 min coating with L-DOPA (3h) only; 1 min coating with L-DOPA (3h) and Coll IV; 4 min coating with L-DOPA (1h) and Coll IV.

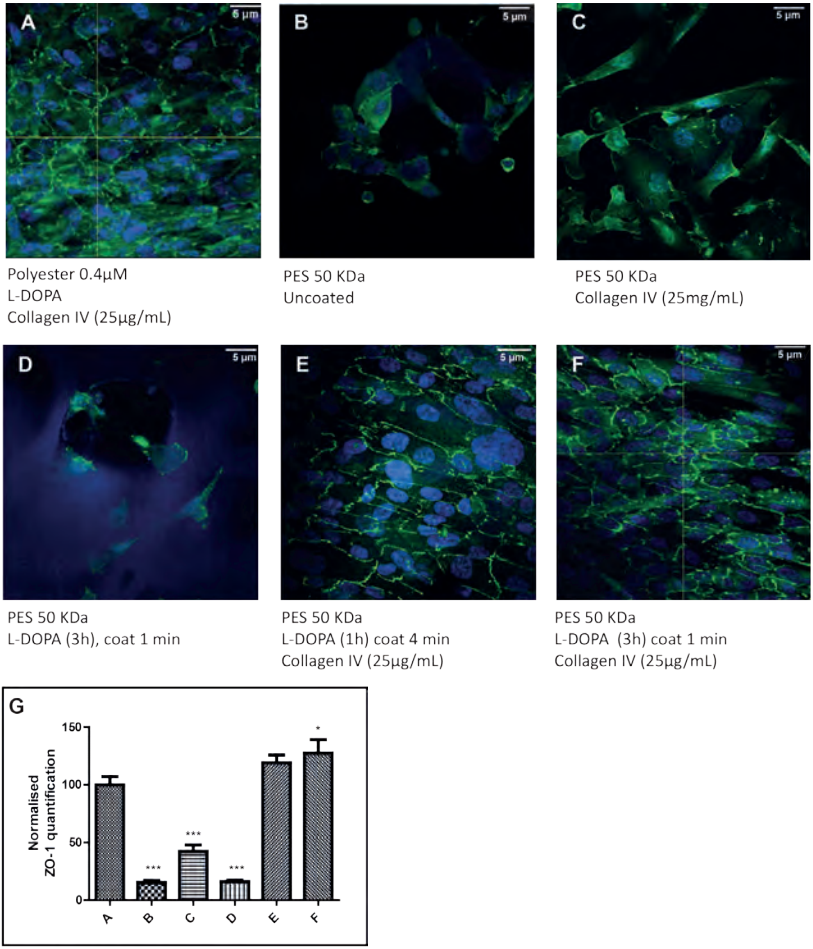

Figure 5.5 Representative images of immunocytochemical analysis of the ZO-1 tight junction protein (green) and nuclei (blue) in ciPTEC monolayers cultured on membranes with varying coating times.

a) L-DOPA (2 mg/ml) and Coll IV (25 µg/ml) double coated Polyester Transwell® inserts; b) uncoated PES - 50 Transwell® insert; c) Coll IV (25 µg/ml) coated PES-50 Transwell® inserts d) L-DOPA (2 mg/ml) coated PES - 50 insert; e) PES-50 Transwell® inserts coated for 4 min with L-DOPA (1h) and Coll IV; f) PES-50 Transwell® inserts coated for 1 min with L-DOPA (3h) and Coll IV. G) ZO-1 abundance in ciPTEC monolayers compared to double coated Polyester Transwell® inserts. At least three independent membranes were examined for each condition. ***p<0.005 Magnification 60x.

		Uncoated	1 min L-DOPA (3 h) + 1 min Coll IV	4 min L-DOPA (1 h) + 4 min Coll IV
Pure water permeance	(L m^{-2} h^{-1} bar^{-1})	738 ± 110	194 ± 35	146 ± 10
BSA solution permeance	(L m^{-2} h^{-1} bar^{-1})	57 ± 7	44 ± 8	37 ± 27
IgG solution permeance	(L m^{-2} h^{-1} bar^{-1})	53 ± 11	65 ± 24	51 ± 12
BSA $SC_a = C_P/C_b$	(–)	0.03 ± 0.01	0.06 ± 0.02	0.02 ± 0.01
IgG $SC_a = C_P/C_b$	(–)	0.02 ± 0.01	0.05 ± 0.03	0.04 ± 0.03

Table 5.1 Comparison of the transport properties of uncoated PES-50 membrane and coated with L-DOPA (2 mg/ml) and Coll IV (25 µg/ml) with two approaches: 1) 1 min coating with L-DOPA (3h) and 1 min Coll IV; 2) 4 min coating with L-DOPA (1h) and 4 min Coll IV.

Given the similarity between the transport properties and the similar cell behavior for the membranes with the optimized coatings, the transport of inulin and creatinine was measured on membranes coated with the coating which required the shortest experimental time: L-DOPA (1h) with a coating time of 4 min for both L-DOPA and Coll IV (Figure 5.1, XII). Transepithelial transport of (^{14}C)-creatinine was measured in presence and absence of transporters substrates, acting as competitors to inhibit uptake. In the kidney, approximately 20% of creatinine is actively transported by organic cation transport proteins (43). The functionality of the basolateral cation uptake by organic cation transporters (OCTs) in ciPTEC has previously been demonstrated (7). Here, Figure 5.6 presents the transmembrane flux of (^{14}C)-creatinine (0.75 µM, Figure 5.6 a, b, c) and (^{3}H)-inulin (0.45 µM, Figure 5.6 d, e, f) by ciPTEC cell monolayers, cultured on double coated PES-50, polyester Transwell® membranes or Coll IV coated polyester Transwell® membranes. The paracellular leakage of (^{3}H)-inulin across the monolayer was used as an indicator of passive diffusion, hence, monolayer tightness, since active transcellular transport has not been reported for this compound (44). In all cases, the inulin leakage was very low, indicating that a tight monolayer was achieved. The observed average leakage of 0.8 ± 0.1 pmol min^{-1} cm^{-2} (0.1% of the total inulin amount) is comparable to observations made in previous studies that utilized MDCK or LCC-PK cells (45). In accordance, the organic cation transport inhibitors, metformin and cimetidine, did not affect inulin transport across the cell monolayers. The creatinine flux through the double-coated "living" PES-50 membranes (2.8 ± 0.1 pmol min^{-1} cm^{-2}) was 3.5 times

higher than the inulin flux (0.8 ± 0.03 pmol min^{-1} cm^{-2}). Importantly, the creatinine flux was significantly decreased by the inhibitors, metformin (24 ± 6% decrease, $P<0.05$) and cimetidine (18 ± 0.2% decrease, $P<0.05$), indicating that the developed "living" membrane actively secretes creatinine. The results of the "living" PES-50 membranes were comparable to those obtained for cells cultured on the golden standard Polyester - Coll IV Transwell® system (see Figure 5.6 and supplemental Figure 5.A3 which compare the permeance of inulin and creatinine through the various membranes).

Various studies have used cellular over-expression models to demonstrate transepithelial creatinine transport. We currently show this trans-epithelial secretory pathway is endogenously present and functional in ciPTEC. Limited data are available for creatinine fluxes in human renal cells. Brown et al. 2008 reported transepithelial creatinine fluxes for primary human proximal tubule epithelial cells (46). Although we observed lower creatinine fluxes in ciPTEC, the transport capacity is maintained for up to 40 passages (unpublished data). This underscores the robustness of this model and its potential application in a RAD. The use of an immortal cell line provides unlimited proliferative capacity, providing the option to expand the surface area of the living membrane necessary to reach the required clearance levels.

Previous studies have shown that the proximal tubule cell can take up free L-DOPA through the organic cation transport system, thereby influencing cellular processes (47,48). However, since the L-DOPA coating was fully polymerized before application of Coll IV, and several additional pre-culture washing steps had been applied, no free L-DOPA is expected to be present when culturing the cells. This is supported by the finding that no detrimental effect of the coating was observed for either transepithelial ^{14}C-creatinine transport or for the morphology of ciPTEC.

Although we focused here on creatinine transport as a marker for endogenous secretion processes in ciPTEC, creatinine is not the only substance that has to be cleared from the blood. Many cationic and anionic waste products, including indoxyl sulfate, hippuric-acid, kynurenic acid, polyamines and guanidines, are retained in patients suffering from uremia (49). Previously, we reported that ciPTEC functionally express various membrane transport proteins that are involved in the uptake and excretion of uremic toxins (UTs) (7,30,50). Therefore a device based on cultured monolayers of ciPTEC grown on modified PES-50 surfaces could provide the ideal tool in the removal of these compounds.

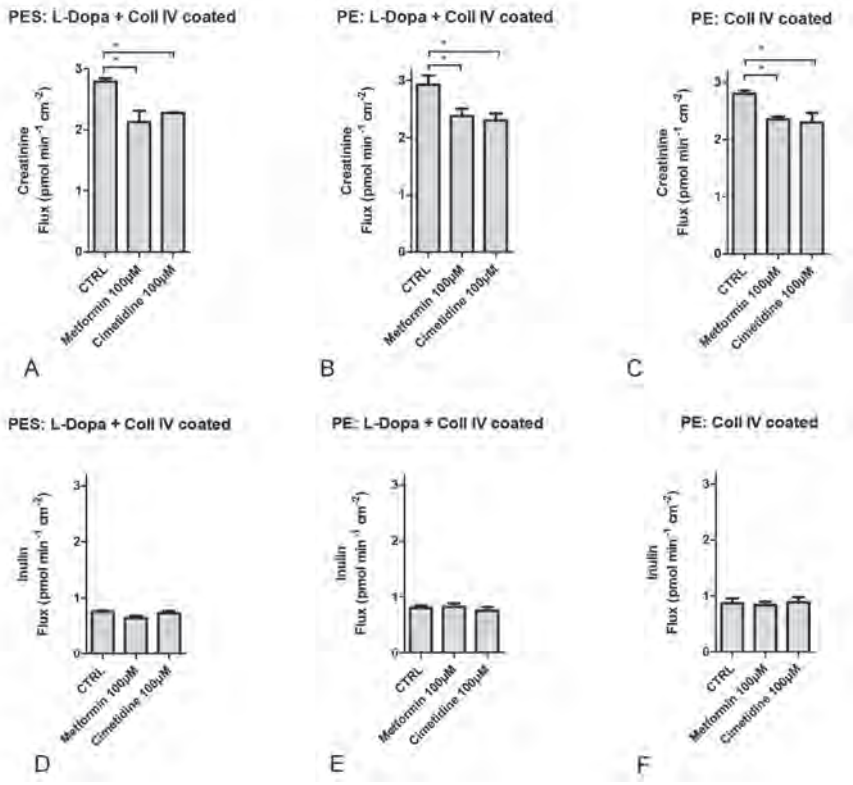

Figure 5.6 Basolateral to apical fluxes of (a,b,c) (^{14}C)-creatinine (0.75 µM) and (d,e,f) (^{3} ^{h})-inulin (0.45 µM) across ciPTEC monolayers. Measurements were performed in the presence or absence of the inhibitors metformin (100 µM) or cimetidine (100 µM). Depicted are ciPTEC monolayers cultured on: (a,d) PES-50 Transwell® inserts coated with L-DOPA(1h) and Coll IV; (b,e) Polyester Transwell® membranes coated with L-DOPA(1h) and Coll IV; (c,f) Polyester Transwell® membranes coated with Coll IV only. All coatings were applied for 4 minutes at the following concentration: L-Dopa 2mg/ml, Coll IV 25mg/mL. Data are presented as mean ± standard error, N=3 *P<0.05.

The use of sophisticated bioanalysis techniques such as LC-MS/MS might provide more opportunities for the transepithelial transport measurements of these toxic compounds by ciPTEC monolayers (51). As a next step in RAD development, long term stability and preservation of functionality in ciPTEC monolayers should be evaluated. Furthermore, the introduction of dynamic culture conditions could improve both the formation of tight junctions and cellular transport properties (52). Recent work suggests beneficial effects of shear stress on renal epithelia, leading to increased endocytosis (45) and sodium reabsorption by the NHE3 receptor (53,54). Evaluation of the shear stress on the functionality of a transporting ciPTEC monolayer would provide valuable information for the development of a bioartificial device.

Conclusions - outlook

In this study, we showed the proof of concept for creating a "living membrane" by combining functional ciPTEC with PES-50 membranes coated with L-DOPA and Coll IV. The coating was optimized to achieve retention of vital blood components whilst preserving high water permeance and optimal cell monolayer formation. The transport of creatinine through the developed "living membrane" was comparable to golden standard systems for studying transepithelial transport across proximal tubule monolayers *in-vitro*. The results reported here are promising for the development of a bioartificial kidney. Further investigations are required to establish the long-term stability of these functional renal cell monolayers. Future studies will be directed towards producing "living membranes" on hollow fiber PES-based membranes and to evaluate up-scaling in a bioreactor system to develop a clinically relevant device.

Acknowledgment

This research forms part of the Project P3.01 BioKid of the research program of the BioMedical Materials institute, co-funded by the Dutch Ministry of Economic Affairs. The financial contribution of the Dutch Kidney Foundation is gratefully acknowledged.

REFERENCES

1. USRDS. 2014 Annual Data Report: Epidemiology of Kidney Disease in the United States. National Institutes of Health, National Institute of Diabetes and Digestive and Kidney Diseases. Bethesda, MD,, 2014;
2. Wolfe RA, Ashby VB, Milford EL, Ojo AO, Ettenger RE, Agodoa LY, Held PJ, Port FK. Comparison of mortality in all patients on dialysis, patients on dialysis awaiting transplantation, and recipients of a first cadaveric transplant. N Engl J Med. 341: 1725-1730, 1999.
3. Vanholder R, De Smet R, Glorieux G, Argiles A, Baurmeister U, Brunet P, Clark W, Cohen G, De Deyn PP, Deppisch R, et al. Review on uremic toxins: classification, concentration, and interindividual variability. Kidney Int. 63: 1934-1943, 2003.
4. Meyer TW, Walther JL, Pagtalunan ME, Martinez AW, Torkamani A, Fong PD, Recht NS, Robertson CR, Hostetter TH. The clearance of protein-bound solutes by hemofiltration and hemodiafiltration. Kidney Int. 68: 867-877, 2005.
5. Krieter DH, Hackl A, Rodriguez A, Chenine L, Moragues HL, Lemke HD, Wanner C, Canaud B. Protein-bound uraemic toxin removal in haemodialysis and post-dilution haemodiafiltration. Nephrol Dial Transplant. 25: 212-218, 2010.
6. El-Sheikh AA, Masereeuw R, Russel FG. Mechanisms of renal anionic drug transport. Eur J Pharmacol. 585: 245-255, 2008.
7. Schophuizen CM, Wilmer MJ, Jansen J, Gustavsson L, Hilgendorf C, Hoenderop JG, van den Heuvel LP, Masereeuw R. Cationic uremic toxins affect human renal proximal tubule cell functioning through interaction with the organic cation transporter. Pflugers Arch. 465: 1701-1714, 2013.
8. Humes HD, Buffington D, Westover AJ, Roy S, Fissell WH. The bioartificial kidney: current status and future promise. Pediatr Nephrol. 29: 343-351, 2014.
9. Jansen J, Fedecostante M, Wilmer MJ, van den Heuvel LP, Hoenderop JG, Masereeuw R. Biotechnological challenges of bioartificial kidney engineering. Biotechnol Adv. 32: 1317-1327, 2014.
10. Oo ZY, Deng R, Hu M, Ni M, Kandasamy K, bin Ibrahim MS, Ying JY, Zink D. The performance of primary human renal cells in hollow fiber bioreactors for bioartificial kidneys. Biomaterials 32: 8806-8815, 2011.
11. Fey-Lamprecht F, Gross U, Groth TH, Albrecht W, Paul D, Fromm M, Gitter AH. Functionality of MDCK kidney tubular cells on flat polymer membranes for biohybrid kidney. J Mater Sci. Mater. Med. 9: 711-715, 1998.
12. Fey-Lamprecht F, Groth T, Albrecht W, Paul D, Gross U. Development of membranes for the cultivation of kidney epithelial cells. Biomaterials 21: 183-192, 2000.

13. Sato Y, Terashima M, Kagiwada N, Tun T, Inagaki M, Kakuta T, Saito A. Evaluation of proliferation and functional differentiation of LLC-PK1 cells on porous polymer membranes for the development of a bioartificial renal tubule device. Tissue Eng. 11: 1506-1515, 2005.
14. Kanai N, Fujita Y, Kakuta T, Saito A. The effects of various extracellular matrices on renal cell attachment to polymer surfaces during the development of bioartificial renal tubules. Artif Organs 23: 114-118, 1999.
15. Zhang H, Tasnim F, Ying JY, Zink D. The impact of extracellular matrix coatings on the performance of human renal cells applied in bioartificial kidneys. Biomaterials 30: 2899-2911, 2009.
16. Fujita Y, Kakuta T, Asano M, Itoh J, Sakabe K, Tokimasa T, Saito A. Evaluation of Na+ active transport and morphological changes for bioartificial renal tubule cell device using Madin-Darby canine kidney cells. Tissue Eng. 8: 13-24, 2002.
17. Ip TK, Aebischer P, Galletti PM. Cellular control of membrane permeability. Implications for a bioartificial renal tubule. ASAIO Trans. 34: 351-355, 1988.
18. van der Aa MA, Helmerhorst TJ, Siesling S, Riemersma S, Coebergh JW. Vaginal and (uncommon) cervical cancers in the Netherlands, 1989-2003. Int J Gynecol Cancer. 20: 638-645, 2010.
19. Oliver JA, Barasch J, Yang J, Herzlinger D, Al-Awqati Q. Metanephric mesenchyme contains embryonic renal stem cells. Am J Physiol Renal Physiol 283: F799-F809, 2002.
20. Lee H, Rho J, Messersmith PB. Facile conjugation of biomolecules onto surfaces via mussel adhesive protein inspired coatings. Adv Mater. 21: 431-434, 2009.
21. Lee H, Dellatore SM, Miller WM, Messersmith PB. Mussel-inspired surface chemistry for multifunctional coatings. Science 318: 426-430, 2007.
22. Humes HD, MacKay SM, Funke AJ, Buffington DA. Tissue engineering of a bioartificial renal tubule assist device: in vitro transport and metabolic characteristics. Kidney Int. 55: 2502-2514, 1999.
23. Fissell WH, Lou L, Abrishami S, Buffington DA, Humes HD. Bioartificial kidney ameliorates gram-negative bacteria-induced septic shock in uremic animals. J Am Soc Nephrol. 14: 454-461, 2003.
24. Inagaki M, Yokoyama TA, Sawada K, Duc VM, Kanai G, Lu J, Kakuta T, Saito A. Prevention of LLC-PK(1) cell overgrowth in a bioartificial renal tubule device using a MEK inhibitor, U0126. J Biotechnol. 132: 57-64, 2007.
25. Terashima M, Fujita Y, Sugano K, Asano M, Kagiwada N, Sheng Y, Nakamura S, Hasegawa A, Kakuta T, Saito A. Evaluation of water and electrolyte transport of tubular epithelial cells under osmotic and hydraulic pressure for development of bioartificial tubules. Artif Organs 25: 209-212, 2001.
26. Shitara Y, Horie T, Sugiyama Y. Transporters as a determinant of drug clearance and tissue distribution. Eur J Pharm Sci. 27: 425-446, 2006.

27. Tahara H, Kusuhara H, Endou H, Koepsell H, Imaoka T, Fuse E, Sugiyama Y. A species difference in the transport activities of H2 receptor antagonists by rat and human renal organic anion and cation transporters. J Pharmacol Exp Ther. 315: 337-345, 2005.
28. Fissell WH, Manley S, Westover A, Humes HD, Fleischman AJ, Roy S. Differentiated growth of human renal tubule cells on thin-film and nanostructured materials. ASAIO J. 52: 221-227, 2006.
29. Humes HD, Weitzel WF, Bartlett RH, Swaniker FC, Paganini EP, Luderer JR, Sobota J. Initial clinical results of the bioartificial kidney containing human cells in ICU patients with acute renal failure. Kidney Int. 66: 1578-1588, 2004.
30. Wilmer MJ, Saleem MA, Masereeuw R, Ni L, Van Der Velden TJ, Russel FG, Mathieson PW, Monnens LA, Van Den Heuvel LP, Levtchenko EN. Novel conditionally immortalized human proximal tubule cell line expressing functional influx and efflux transporters. Cell Tissue Res. 339: 449-457, 2010.
31. Jansen J, Schophuizen CM, Wilmer MJ, Lahham SH, Mutsaers HA, Wetzels JF, Bank RA, van den Heuvel LP, Hoenderop JG, Masereeuw R. A morphological and functional comparison of proximal tubule cell lines established from human urine and kidney tissue. Exp Cell Res. 323: 87-99, 2014.
32. Tijink M, Janssen J, Timmer M, Austen J, Aldenhoff Y, Kooman J, Koole L, Damoiseaux J, Van Oerle R, Henskens Y, et al. Development of novel membranes for blood purification therapies based on copolymers of N-vinylpyrrolidone and n-butylmethacrylate. J Mater Chem B 1: 6066-6077, 2013.
33. Sweet DH, Miller DS, Pritchard JB. Basolateral localization of organic cation transporter 2 in intact renal proximal tubules. Am J Physiol Renal Physiol. 279: F826-834, 2000.
34. Green D, Perry R. Perry's Chemical Engineers' Handbook, Eighth Edition. McGraw-Hill Education: 2007; ISBN: 9780071593137.
35. Schneider CA, Rasband WS, Eliceiri KW. NIH Image to ImageJ: 25 years of image analysis. Nat Methods. 9: 671-675, 2012.
36. Kokko JP, Burg MB, Orloff J. Characteristics of NaCl and water transport in the renal proximal tubule. J Clin Invest. 50: 69-76, 1971.
37. Azari S, Zou L. Using zwitterionic amino acid l-DOPA to modify the surface of thin film composite polyamide reverse osmosis membranes to increase their fouling resistance. J Membr Sci. 401-402: 68-75, 2012.
38. Azari S, Zou L, Cornelissen E, Mukai Y. Facile fouling resistant surface modification of microfiltration cellulose acetate membranes by using amino acid L-DOPA. Water Sci Technol. 68: 901-908, 2013.
39. Cheng C, Li S, Zhao W, Wei Q, Nie S, Sun S, Zhao C. The hydrodynamic permeability and surface property of polyethersulfone ultrafiltration membranes with mussel-inspired polydopamine coatings. J Membr Sci. 417–418: 228-236, 2012.

40. McCloskey BD, Park HB, Ju H, Rowe BW, Miller DJ, Chun BJ, Kin K, Freeman BD. Influence of polydopamine deposition conditions on pure water flux and foulant adhesion resistance of reverse osmosis, ultrafiltration, and microfiltration membranes. Polymer. 51: 3472-3485, 2010.
41. Bernsmann F, Ponche A, Ringwald C, Hemmerle J, Raya J, Bechinger B, Voegel JC, Schaaf P, Ball V. Characterization of dopamine-melanin growth on silicon oxide. J Phys Chem C 113: 8234-8242, 2009.
42. Ito K, Suzuki H, Horie T, Sugiyama Y. Apical/basolateral surface expression of drug transporters and its role in vectorial drug transport. Pharm Res. 22: 1559-1577, 2005.
43. Ciarimboli G, Lancaster CS, Schlatter E, Franke RM, Sprowl JA, Pavenstadt H, Massmann V, Guckel D, Mathijssen RH, Yang W, et al. Proximal tubular secretion of creatinine by organic cation transporter OCT2 in cancer patients. Clin Cancer Res. 18: 1101-1108, 2012.
44. Perrone RD. Means of clinical evaluation of renal disease progression. Kidney Int Suppl. 36: S26-32, 1992.
45. Raghavan V, Rbaibi Y, Pastor-Soler NM, Carattino MD, Weisz OA. Shear stress-dependent regulation of apical endocytosis in renal proximal tubule cells mediated by primary cilia. Proc Natl Acad Sci. U. S. A. 111: 8506-8511, 2014.
46. Brown CD, Sayer R, Windass AS, Haslam IS, De Broe ME, D'Haese PC, Verhulst A. Characterisation of human tubular cell monolayers as a model of proximal tubular xenobiotic handling. Toxicol. Appl. Pharmacol. 233: 428-438, 2008.
47. Grundemann D, Koster S, Kiefer N, Breidert T, Engelhardt M, Spitzenberger F, Obermuller N, Schomig E. Transport of monoamine transmitters by the organic cation transporter type 2, OCT2. J Biol Chem. 273: 30915-30920, 1998.
48. Pinto-do OP, Soares-da-Silva P. Studies on the pharmacology of the inward transport of L-DOPA in rat renal tubules. Br J Pharmacol. 118: 741-747, 1996.
49. Duranton F, Cohen G, De Smet R, Rodriguez M, Jankowski J, Vanholder R, Argiles A, European Uremic Toxin Work G. Normal and pathologic concentrations of uremic toxins. J Am Soc Nephrol. 23: 1258-1270, 2012.
50. Mutsaers HA, Wilmer MJ, van den Heuvel LP, Hoenderop JG, Masereeuw R. Basolateral transport of the uraemic toxin p-cresyl sulfate: role for organic anion transporters? Nephrol Dial Transplant. 26: 4149, 2011.
51. Mutsaers HA, Engelke UF, Wilmer MJ, Wetzels JF, Wevers RA, van den Heuvel LP, Hoenderop JG, Masereeuw R. Optimized metabolomic approach to identify uremic solutes in plasma of stage 3-4 chronic kidney disease patients. PLoS ONE 8: e71199, 2013.
52. Weinbaum S, Duan Y, Satlin LM, Wang T, Weinstein AM. Mechanotransduction in the renal tubule. Am J Physiol Renal Physiol. 299: F1220-1236, 2010.

53. McDonough AA. Mechanisms of proximal tubule sodium transport regulation that link extracellular fluid volume and blood pressure. Am J Physiol Regul Integr Comp Physiol. 298: R851-861, 2010.
54. Wang T. Flow-activated transport events along the nephron. Curr Opin Nephrol Hypertens. 15: 530-536, 2006.

SUPPLEMENTARY DATA

Figure 5.A1 Transwell® set up.
Schematic overview of the Transwell® set up used for creatinine and inulin transmembrane transport across ciPTEC monolayers. Indicated on the left are the basolateral and apical compartments. On the right side the ciPTEC monolayer and the L-DOPA Coll-IV double coating have been schematically represented.

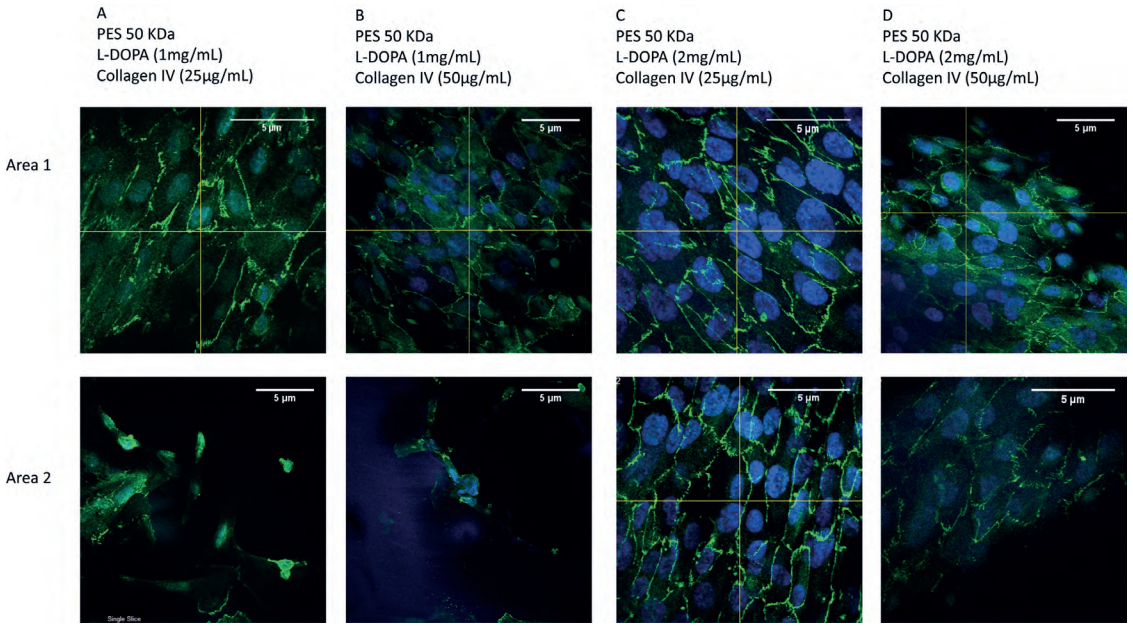

Figure 5.A2 Effect of double coating concentration on cell adhesion.
The effect of two different L-DOPA and Coll IV concentrations on cell adhesion (by using optimized coating with 3 h L-DOPA dissolution and 1 min coating for both L-DOPA and collagen IV) was tested. Uniformity was evaluated upon visual inspection with confocal microscopy, for which two representative membrane areas of each sample were analyzed (see Figure 5.A2). The most uniform monolayer on the complete membrane surface was obtained when double coating of 2 mg/ml L-DOPA and 25 µg/ml Coll IV was applied (Figure 5.A2,c). Thus, no differences in coating concentration were introduced by the optimization performed with respect to previously published data (10).

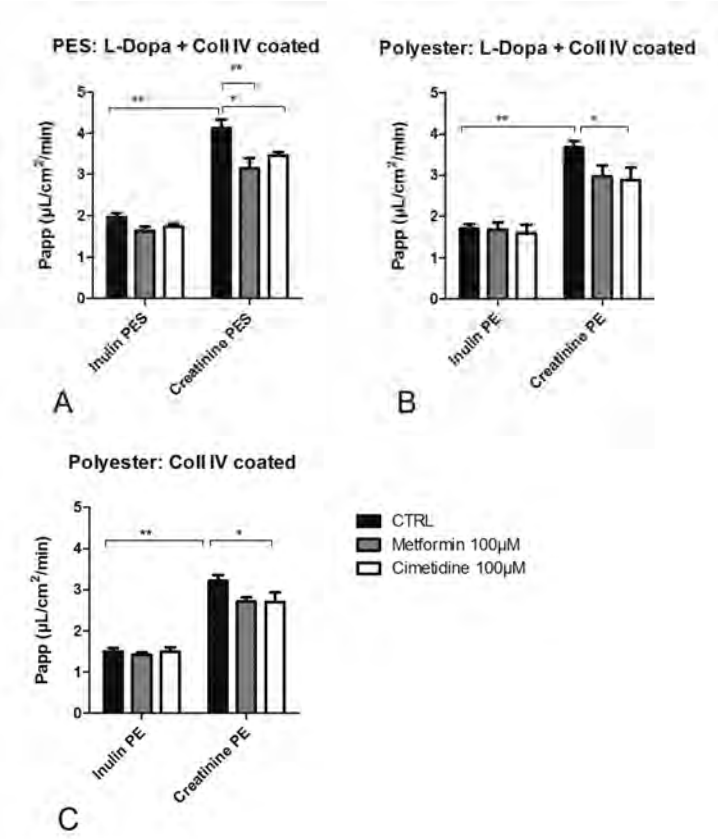

Figure 5.A3 basolateral to apical creatinine transport.
The basolateral to apical Inulin diffusion, and creatinine apparent permeability (P_{app}) was calculated with the following equation:

$$P_{\text{app}} = \frac{J}{C_{\text{b}} - C_{\text{a}}}$$

Where J = flux; C_b = initial concentration in the basolateral compartment; C_a = initial concentration in the apical compartment. For the double coated PES-50 and polyester membranes the transepithelial transport levels were 2.2 ± 0.4 and 1.97 ± 0.3 µL cm^{-2} min^{-1}, respectively. For the standard polyester Transwells® coated with Coll IV this value was 1.8 ± 0.3 µL cm^{-2} min^{-1}. Data are presented as mean ± standard error, N=3 in duplicates, *P<0.05 **P<0.01 ***P<0.001

Chapter 6

HUMAN PROXIMAL TUBULE EPITHELIAL CELLS CULTURED ON HOLLOW FIBERS: LIVING MEMBRANES THAT ACTIVELY TRANSPORT ORGANIC CATIONS

Jansen J[123], De Napoli IE[4], Fedecostante M[123], Schophuizen CMS[123], Chevtchik NV[4], Wilmer MJ[1], van Asbeck AH[5], Croes HJ[6], Pertijs JC[1], Wetzels JFM[7], Hilbrands LB[7], van den Heuvel LP[3,8], Hoenderop JG[2], Stamatialis D[4], Masereeuw R[19]

Nature Scientific Reports, 5, 16702, 2015

Department of [1]Pharmacology and Toxicology, [2]Physiology, [5]Biochemistry and [6]Cell Biology, Radboud university medical center, Radboud Institute for Molecular Life Sciences, Nijmegen, The Netherlands.
Department of [3]Pediatrics and [7]Nephrology, Radboud university medical center, Nijmegen, The Netherlands.
Department of [4]Biomaterials Science and Technology, MIRA Institute for Biomedical Technology and Technical Medicine, University of Twente, The Netherlands.
Department of [8]Pediatric Nephrology & Growth and Regeneration, Catholic University Leuven, Leuven, Belgium.
Div. [9]Pharmacology, Department of Pharmaceutical Sciences, Utrecht University, The Netherlands

ABSTRACT

The bioartificial kidney (BAK) aims at improving dialysis by developing 'living membranes' for cells-aided removal of uremic metabolites. Here, unique human conditionally immortalized proximal tubule epithelial cell (ciPTEC) monolayers were cultured on biofunctionalized MicroPES (polyethersulfone) hollow fiber membranes (HFM) and functionally tested using microfluidics. Tight monolayer formation was demonstrated by abundant zonula occludens-1 (ZO-1) protein expression along the tight junctions of matured ciPTEC on HFM. A clear barrier function of the monolayer was confirmed by limited diffusion of FITC-inulin. The activity of the organic cation transporter 2 (OCT2) in ciPTEC was evaluated in real-time using a perfusion system by confocal microscopy using 4-(4-(dimethylamino)styryl)-N-methylpyridinium iodide (ASP^+) as a fluorescent substrate. Initial ASP^+ uptake was inhibited by a cationic uremic metabolites mixture and by the histamine H2-receptor antagonist, cimetidine. In conclusion, a 'living membrane' of renal epithelial cells on MicroPES HFM with demonstrated active organic cation transport was successfully established as a first step in BAK engineering.

BACKGROUND

The development of biotechnological platforms to aid uremic syndrome treatment is of high interest world-wide. Current treatment strategies, such as hemo- or peritoneal dialysis, demonstrate a poor clearance of small lipid soluble and protein-bound uremic metabolites and the mortality rate in patients suffering from renal disease remains high (1). The uremic syndrome is characterized by the retention of metabolites due to an attenuated filtration capacity of the glomerulus and a loss of function of proximal tubule epithelial cells (PTEC), which are responsible for active metabolite secretion. Elevated levels of retention solutes contribute to competitive inhibition of drug transporters and thereby alter the metabolic environment as well as drug disposition in the kidney (2, 3). The accumulation of uremic metabolites (i.e. uremic toxins) in the human body may contribute to further progression of renal disease and the association of chronic kidney disease with cardiovascular morbidity (4-6).

A cell-aided device containing stable living membranes, which enable active transport of uremic metabolites would be a major breakthrough in the field of regenerative nephrology. Nowadays, various research groups are focussed on the development of a bioartificial kidney (BAK), containing PTEC to improve current treatment strategies (7-9). In uremic animals and patients suffering from acute kidney injury (AKI) encouraging results have been obtained with respect to enhanced survival in BAK treated subjects by reduction of the inflammatory status, but further extensive research is required to obtain stable and functional cell-aided devices for chronic use (9-13). A crucial step in the development of functional devices relates to advanced functionalization of the hollow fiber membranes (HFM) to stimulate monolayer formation. *In vivo*, the extracellular matrix (ECM) is key in inter- and intracellular signaling, regeneration, and support (14, 15). Mimicking this complex matrix to obtain well-differentiated PTEC monolayers *in vitro* is essential in BAK engineering. Successful PTEC monolayer formation was obtained using combinations of laminin, gelatin, matrigel, collagen IV and L-3,4-dihydroxydiphenylalanine (L-DOPA) ECM coatings on biomaterials (16-18). However, active transport of uremic metabolites mediated by PTEC specific transporters on hollow fiber membranes to aid renal replacement therapy has, as of yet, not been demonstrated.

In addition to glomerular filtration, the renal excretion of endo- and xenobiotics is advanced by active tubular secretion, a process mediated by PTEC, which are equipped with a broad range of transporters. One of the main PTEC transporters involved in the uptake of cationic uremic metabolites and drugs, such as cimetidine, metformin and cisplatin (19-21), is the basolateral organic cation transporter - 2 (OCT2; *SLC22A2*). Various cationic uremic metabolites, including guanidino compounds and polyamines, were found to interact with this transporter as well (30). Guanidino compounds are derived from the arginine metabolism and are small, water-soluble cations and not bound to proteins (4). However, the effective removal of guanidines is hampered in uremic conditions particularly due to their large distribution volume (22). Guanidines are known neurotoxins (23), but more recently the pro-inflammatory effects on the expression of leukocyte surface molecules and thus the possible interference of leukocytes with endothelial cells resulting in cardiovascular events was demonstrated as well (24, 25). Polyamines, derived from cellular lysine, arginine or ornithine catabolism, were identified in the late '70s as putative cationic uremic metabolites by Campbell *et al.* (26). More recent work elucidated further that the polyamines cadaverine, putrescine, spermine, spermidine and their breakdown product acrolein accumulate in uremic patients and are associated with cytotoxicity, through damage to proteins, DNA and other cellular components (27-29).

In our laboratory, a unique conditionally immortalized PTEC model (ciPTEC) derived from human urine was established and thoroughly characterized (31, 32). These cells contain the temperature sensitive vector SV40tsA58, allowing proliferation at 33°C and differentiation in mature PTEC at 37°C. In addition, cells were transfected with human telomerase (hTERT) limiting replicative senescence by telomere length maintenance, improving further the unlimited availability of ciPTEC. This model presents a broad range of PTEC-specific functions, including the transporters associated with uremic toxin secretion along with drug metabolism enzymes (30, 31, 47). In the present study, ciPTEC monolayer function when cultured on MicroPES HFM was investigated as a crucial element of a renal assist device. To this end, permeability properties of (biofunctionalized) membranes, monolayer formation and epithelial functional characteristics were investigated. The latter included OCT2 activity assessment using a microfluidic system with real-life imaging in the presence or absence of OCT2 inhibitors as well as a cationic uremic metabolites mixture of guanidines and polyamines.

METHODS

Brief methods are given. For details, the reader is referred to Supplementary information.

Chemicals and cell culture materials

Chemicals were purchased from Sigma-Aldrich (Zwijndrecht, The Netherlands) unless stated otherwise. MicroPES type TF10 hollow fiber capillary membranes (wall thickness 100 µm, inner diameter 300 µm, max pore size 0.5 µm) were obtained from Membrana GmbH (Wuppertal, Germany). Cell culture plates were purchased from Greiner Bio-One (Monroe, NC).

Hollow fiber sterilization and double coating

MicroPES (polyethersulfone) hollow fiber membranes were sterilized using 70% (v/v) EtOH incubation for 30 min. The primary coating component L-DOPA (L-3,4-dihydroxyphenylalanine, 2 $mg.ml^{-1}$) was dissolved in 10 mM Tris buffer (pH 8.5), as described previously by Ni et al. (16), at 37°C for 45 min. Next, the solution was filter sterilized prior to incubation of the horizontally placed fibers for 5 hours at 37°C. The L-DOPA coated fibers were exposed to the second coating component human collagen IV (C6745-1ml, 25 $\mu g.ml^{-1}$) for 1 hour at 37°C. The collagen IV solution was aspirated afterwards and the fibers were washed thoroughly in HBSS buffer prior to cell seeding.

Scanning electron microscopy of cell-free hollow fiber membranes

Membrane topography of uncoated and coated HFM was determined using scanning electron microscopy (SEM) analysis (Philips XL-30 ESEM, Amsterdam, the Netherlands). In short, HFM were prepared using liquid nitrogen fracture to enable cross section analysis. Samples were incubated at 37°C overnight and gold sputtered before examination by SEM (3 kV and 5 kV).

Transport properties of cell-free hollow fibers membranes

The transport of pure water (Merck MilliPore, Billerica, MA), bovine serum albumin (BSA) and immunoglobulin G (IgG) solutions through the uncoated and coated cell-free HFMs were measured at various transmembrane pressures using a KrosFlo Research IIi Tangential Flow Filtration system (Spectrum laboratories, Wurzburg, Germany). The membrane permeability

of H_2O was plotted as the slope of the flux versus the transmembrane pressure. The membrane sieving coefficient (SC) was calculated by dividing the concentration of the BSA and IgG in the permeate by the concentration of the feed protein solution.

Culture of ciPTEC on double coated hollow fiber membranes

Proliferating ciPTEC (32) were seeded on double-coated fibers (length 2cm) using 1.5 x 10^6 cells per 1.5 ml. The cell suspension was added to an eppendorf tube containing the fiber and incubated at 33°C, 5% (v/v) CO_2, for 4 hours. Every hour the tube was turned 90° in order to stimulate cell adhesion to the whole surface. Next, fibers with adhered cells were removed from the suspension and transferred to a 6 well plate with PTEC culture medium and were cultured as previously described by Jansen et al. (31).

Immunocytochemistry

The expression of OCT2, zonula occludens-1 (ZO-1) and the ECM component collagen IV in ciPTEC monolayers on hollow fibers were investigated using the immunocytochemistry methodology as previously described by Jansen et al. (31). The expression and localization of the proteins of interest were examined using the Olympus FV1000 Confocal Laser Scanning Microscope (Olympus, Tokyo, Japan) and images were captured using the Olympus software FV10-ASW version 1.7.

Transmission- and scanning electron microscopy

The morphology of ciPTEC and its organelles was investigated using transmission electron microscopy (TEM) and SEM. In short for TEM, cells were fixed and dehydrated using series of chemical solutions and finally embedded in Epon and polymerized at 60°C. After ultrathin sectioning and contrasting with uranyl acetate and lead citrate, sections were analyzed using a transmission electron microscope JEOL JEM 1010 (Jeol, Akishima Tokyo, Japan). For SEM purposes, cells were fixed and dehydrated using various chemical solutions and finally critical point dried. Samples were gold sputtered prior to SEM analysis (JEOL JSM-6340F, Tokyo, Japan).

Transepithelial barrier function

Paracellular permeability was determined in the living membrane by endpoint quantification of inulin-fluorescein isothiocyanate (FITC) (0.1 $mg.ml^{-1}$ in Krebs-Henseleit buffer) supplemented with HEPES (10 mM; KHH buffer))

diffusion when perfused (6 ml.h^{-1}, in close agreement with previously applied flow rates (8)) using a custom-made microfluidic system (supplemental figure S6.1) connected to a syringe pump (Terumo STC-521, Terumo Europe N.V., Leuven, Belgium) for 13 min at 37°C. As a control, the inulin-FITC diffusion in coated HFM in the absence of cells was investigated in similar conditions. Fluorescence was detected by measuring samples and a standard range (0.0005 – 0.1 mg/ml, including a final blank sample (KHH buffer) 100 µl) at excitation wavelength 485 nm and emission wavelength 535 nm, using a Victor^{TM} X3 multilabel platereader (Perkin-Elmer, Groningen, The Netherlands). Blank data were subtracted from all arbitrary fluorescence units measured and the corrected AFU data of the standard range were used to calculate the inulin-FITC concentration of the samples (mg/ml). Next, the flux (J) was calculated according to:

$J = ((((C / Mw) * V) * 10^9) / t) / A = pmol \cdot min^{-1} \cdot cm^{-2}$

Where C is the calculated concentration (mg/ml), Mw the average inulin-FITC molar mass in mg/mmol (4500 mg/mmol), V the volume present in the apical compartment of the perfusion chamber (0.3 ml), t the perfusion time (13 min) and A the fiber surface (0.13 cm^2).

Functional organic cation transport

The activity of OCT2 in ciPTEC cultured on HFM was examined real-time by perfusing the hollow fiber basolaterally (inner HFM, (6 ml.h^{-1}, (8))) with the fluorescent OCT2 substrate 4-(4-(dimethylamino)styryl)-N-methylpyridinium iodide (ASP$^+$, 10 µM) in KHH buffer, when assembled in a microfluidic system. The assay was performed in the presence or absence of a cationic uremic toxin mix (UTmix; 10 times uremic plasma concentrations reported in literature - spermidine 6.7 μ M, spermine 0.9 μ M, cadaverine 2.1 μ M, putrescine 8.8 μ M, acrolein 14.2 μ M, guanidine 21.8 μ M and methylguanidine 76.6 μ M) (30) or cimetidine (100 µM), for 13 min at 37°C, 5% (v/v) CO_2. Imaging was performed using the Zeiss LSM510 META microscope (Zeiss, Oberkochen, Germany). Semi-quantification of real-time data was performed using Image J software (version 1.40g). Of each fiber in time spanning 1 - 13 min (800 scans), four cells present in the focal plane were used to extract mean ASP$^+$ pixel intensities and background was subtracted using pixel intensities form ASP$^+$ perfused non-cell double-coated fibers. Next, data were normalized according to:

$Y_t / x^m_t * 100$

Where Y_t is the pixel intentsity at time point t of a condition (ASP^+ only, ASP^+ + UTmix or ASP^+ + cimetidine) divided by X^m_t , which is the average pixel intensity (m) of only ASP^+ condition at that similar time point (t). This value was multiplied by 100 and the obtained relative data were fitted according to One-phase exponential association using nonlinear regression analysis. To compare ASP^+ uptake in different conditions, slopes were extracted from min 1 - 8 and compared. In detail, of each fiber from min 1 - 8 (428 scans), four cells present in the focal plane were used to extract mean ASP^+ pixel intensities and were background corrected. Average pixel intensities from these four cells per fiber were plotted and six slopes derived from six fibers per condition were calculated using linear regression analysis and compared to ASP^+ uptake using two-way ANOVA analysis followed by Bonferroni post-test.

Data analysis

All data are expressed as mean ± S.E.M of multiple replicates. Nonlinear curve fitting and statistical analysis of functional organic cation data were performed with GraphPad Prism version 5.02 (La Jolla, CA). A two-way ANOVA analysis followed by Bonferroni post-test or, when appropriate, an unpaired t test was applied. A p-value of <0.05 was considered significant.

RESULTS

Modified HFM maintain membrane permeability

The surface of MicroPES HFM was functionalized via a double coating to enable tight homogeneous cell monolayer formation. The coating was successfully developed in 2D by our group using Transwell® membrane supports (18). Here, this was optimized further in 3D. The membrane surface and cross sections of uncoated and coated HFM in the absence of cells were investigated using SEM (figure 6.1A-B). In agreement with our previous study (18), the coatings applied were thin and did not differ between fibers, consistent with their transport properties. The coated HFM should facilitate transepithelial transport of protein-bound uremic toxins, with retained solute permeability. As shown in figure 6.1C, the H_2O permeability was preserved in double coated HFM ($(16.4 \pm 0.7) \cdot 10^3$ L m^{-2} $h^{-1}bar^{-1}$) compared to uncoated HFM ($(17.0 \pm 0.3) \cdot 10^3$ L m^{-2} $h^{-1}bar^{-1}$). In addition, both IgG and BSA passed almost freely through the membrane as demonstrated by the sieving coefficient (SC) close to 1 for both coated (0.90 ± 0.01 and 0.97 ± 0.02, respectively; $p<0.01$) and uncoated HFM (0.97 ± 0.02 and 0.98 ± 0.01, respectively) (figure 6.1D).

Obviously, the final composition of coated HFM with a tight cell monolayer should form a true barrier and prevent the loss of essential components such as IgG and albumin into the dialysate.

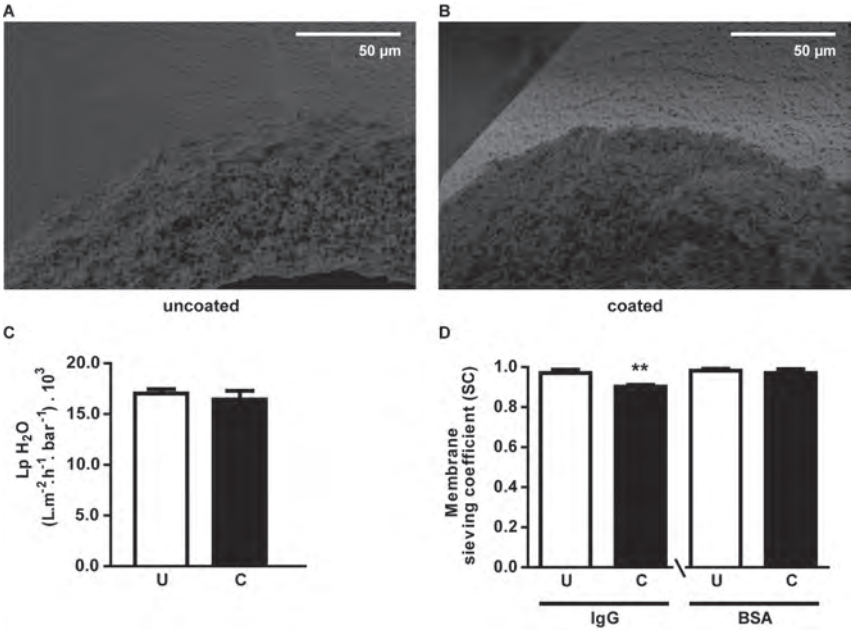

Figure 6.1. HFM topography and flux of essential compounds.
(a-b) Representative SEM images of uncoated and coated MicroPES HFM are shown. No microscopic differences were observed and topography was preserved in coated HFM. (c) The water permeance of uncoated and coated HFM was highly similar in both conditions (U: (17.0 ± 0.3) . 10^3 Lm^{-2} $h^{-1}bar^{-1}$) *vs.* C: (16.4 ± 0.7) . 10^3 Lm^{-2} $h^{-1}bar^{-1}$, respectively). (d) The SC of IgG was slightly less in coated HFM (C: 0.90 ± 0.01, $p<0.01$) compared to uncoated HFM (U: 0.97 ± 0.02), whereas BSA passed almost freely through the membrane as demonstrated by the SC close to 1 for coated (C: 0.97 ± 0.02) and uncoated HFM (U: 0.98 ± 0.01). Data are shown as mean ± S.E.M. of three independent experiments performed in duplicate ** = $p<0.01$ using an unpaired *t* test.

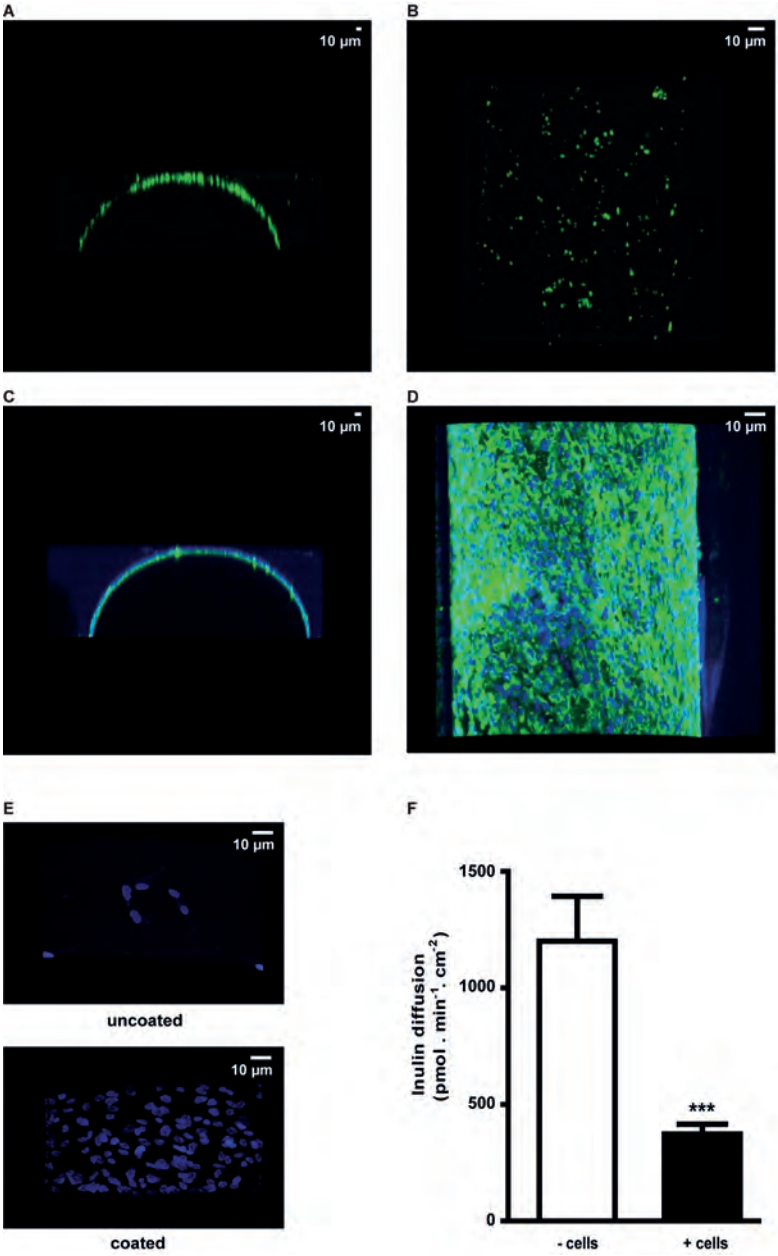
A
10 µm
B
10 µm
C
10 µm
D
10 µm
E
10 µm
uncoated
10 µm
coated
F
Inulin diffusion
(pmol . min-1. cm-2)
1500
1000
500
0
***
- cells
+ cells

Figure 6.2 Extracellular matrix, cellular adhesion and paracellular permeability. Representative confocal images of collagen IV (green) in y-z (a and c) and x-y (b and d) planes are shown. (a-b) A heterogeneous collagen IV ECM pattern was detected on coated HFM without cells. (c-d) Nuclei were stained using DAPI (blue) in matured ciPTEC cultured on coated HFM. A homogenous and abundant distribution of collagen IV (green) was detected in the presence of matured ciPTEC. (e) Representative images of adhered cells (matured ciPTEC) are shown by nuclei staining (dapi; blue). A limited number of cells were present when cultured on uncoated HFM whereas numerous cells adhered to the coated HFM surface. (f) The transepithelial barrier function was examined in the presence or absence of matured ciPTEC by inulin-FITC perfusion and the flux across the HFM was quantified. Data are shown as mean ± S.E.M. of three independent experiments performed in triplicate or duplicate. *** = $p<0.001$ using an unpaired *t* test.

Extracellular matrix, cellular adhesion and paracellular permeability

Collagen IV is a non-fibrillar collagen and is known to assist in cell differentiation towards renal lineages from various stem cell populations (33). The presence of a collagen IV matrix after the coating procedure was confirmed, as shown in figure 6.2A and B, though a heterogeneous pattern was observed. Interestingly, in the presence of matured ciPTEC, a nice homogeneous collagen IV matrix was visible (figure 6.2C and D). Moreover, cell adhesion clearly improved upon surface modification, as shown in figure 6.2E, suggesting biofunctionalization. Hardly any nuclei (i.e. cells) were detected when cultured on uncoated HFM, whereas a uniform distribution of nuclei was observed after double coating. Furthermore, the transepithelial barrier function was quantified by inulin-FITC diffusion after perfusion of HFM in the presence or absence of matured ciPTEC. As shown in figure 6.2F, matured ciPTEC formed a true barrier compared to coated HFM in the absence of cells (373 ± 42 pmol · min^{-1} · cm^{-2}; 1200 ± 193 pmol · min^{-1} · cm^{-2}, respectively, $p<0.001$). In addition, cell adhesion of ciPTEC to PES HFM was found to be related to the curvature of the membrane. Similar double coating procedures applied to PES HCO 1100 membranes with an inner diameter of 215 µm resulted in poor ciPTEC adherence (supplemental figure S6.2), in contrast to double coated MicroPES HFM with an inner diameter of 300 µm (figure 6.2).

Intact cellular organelles and numerous microvilli

Matured ciPTEC cultured on HFM retained intact cellular organelle morphology as observed by TEM (figure 6.3A). The presence of numerous mitochondria indicated that the cell monolayer consists of viable and

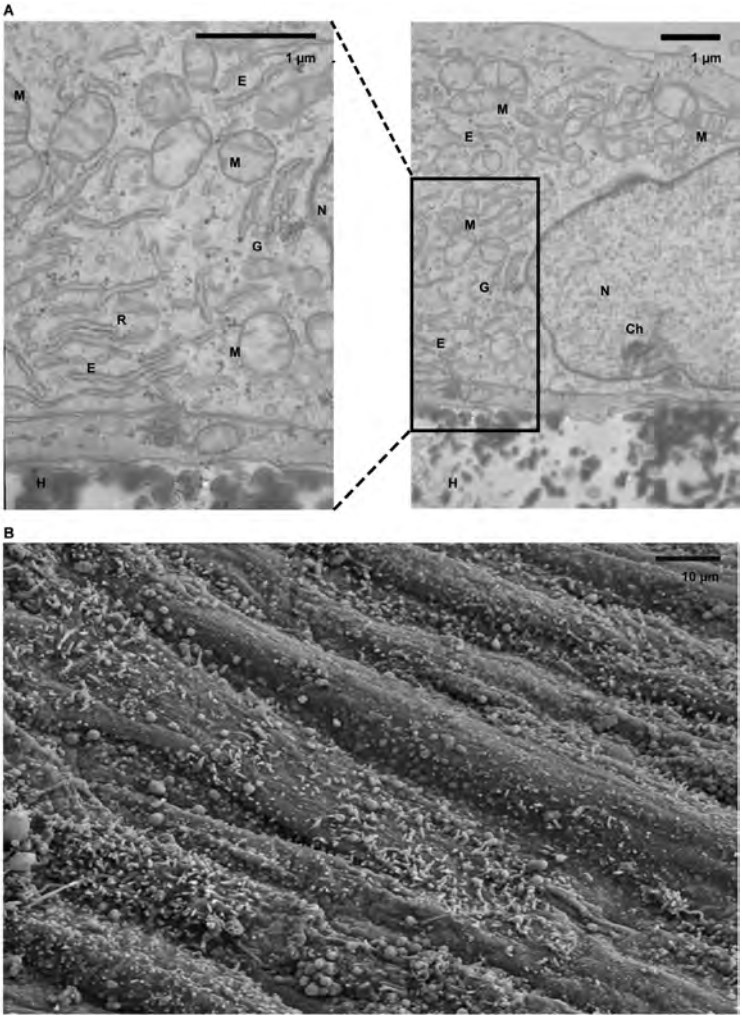

Figure 6.3 Cellular organelles and surface characteristics.
(a) The morphology of organelles in matured ciPTEC cultured on HFM (H) was investigated by transmission electron microscopy and intact cells were detected. Next to numerous well-developed mitochondria, the nucleus (N) containing the chromatin (Ch), the endoplasmatic reticulum (E), ribosomes (R) and the Golgi apparatus could be nicely detected. (b) The surface of matured ciPTEC was visualized using scanning electron microscopy. At the apical membrane microvilli were observed, as expected for proximal tubule epithelial cells, though a heterogeneous distribution was detected.

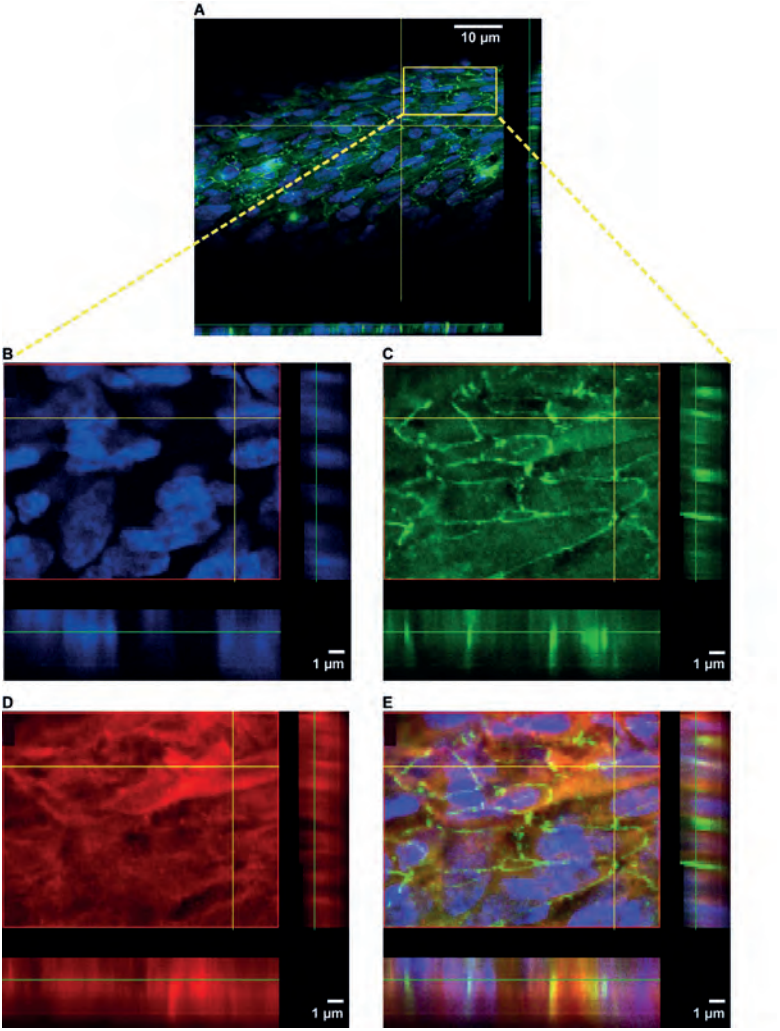

Figure 6.4 ZO-1 and OCT2 protein expression.
Representative confocal images of ZO-1 (green), OCT-2 (red) and nuclei (blue) in matured ciPTEC cultured on HFM are shown in x-y and y-z planes. (a-b-c-e) The ZO-1 expression was abundantly present along the cell boundaries within a tight and homogenous cell monolayer. (d-e) The endogenous OCT-2 protein expression in ciPTEC was observed heterogeneously in the membranes, moreover, some signal was detected in the cytoplasm.

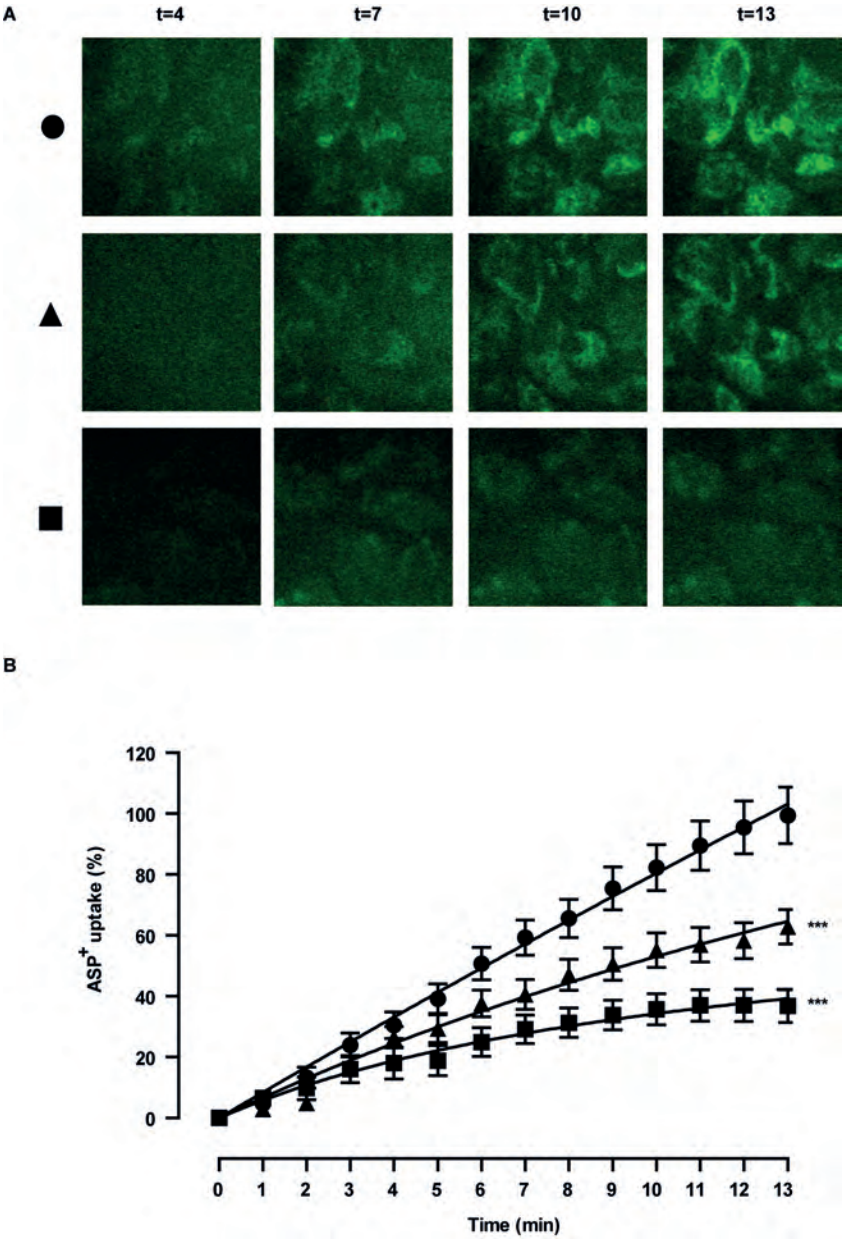
A
t=4
t=7
t=10
t=13
B
ASP+ uptake (%)
120
100
80
60
40
20
0
***
***
0 1 2 3 4 5 6 7 8 9 10 11 12 13
Time (min)

Figure 6.5 Functional organic cation transporter - 2 transport.
(a) Representative real-time images and (b) semi-quantification of ASP^+ uptake (10 μM, green) are shown, a model substrate for OCT-2, in the absence (circle) or presence of specific inhibitors (triangle: cationic uremic toxin mix (UTmix), square: cimetidine (100 μM)) in matured ciPTEC cultured on HFM. Data were normalized against ASP^+ uptake in the absence of inhibitors and were fitted according to One-phase exponential association using nonlinear regression analysis. (a - circle) After 4 min, intracellular ASP^+ signal could be visualized and further increased until 13 min. (a - triangle) In the presence of UTmix the ASP^+ uptake was less pronounced during the complete uptake experiment compared to perfusion with only ASP^+. (a - square) The ASP^+ uptake was clearly attenuated in the presence of cimetidine and hardly any further increase in fluorescent ASP^+ uptake was detected after 7 min. (b) Semi-quantification of ASP^+ uptake data in the absence (10 μM, circle) or presence of specific inhibitors (triangle: cationic uremic toxin mixture (UTmix, (10X)), square: cimetidine (100 μM) in matured ciPTEC cultured on HFM are shown. A clear fluorescent intracellular signal in ciPTEC indicated an active OCT-2 mediated basal ASP^+ uptake started at 1 min. Initial uptake was significantly inhibited by the UT mixture and cimetidine. Data are shown as mean ± S.E.M. of three independent experiments performed in duplicate. Slopes extracted from min 1 - 8 of the ASP^+ uptake in different conditions were compared and applied for statistical analysis. *** = $p<0.001$ using two-way ANOVA analysis followed by Bonferroni post-tests.

metabolically active PTEC (34). Moreover, other essential cellular components, including the Golgi apparatus, endoplasmatic reticulum, ribosomes, the nucleus and its chromatin, could be determined. The brush border membrane of ciPTEC is reasonably well-developed, containing many microvilli to enlarge the apical surface and to stimulate intensive reabsorption, as observed with SEM (figure 6.3B).

Homogenous cell monolayers represent ZO-1 and OCT2 expression

The presence of the tight junction protein ZO-1 in cell monolayers emphasizes cell polarity and monolayer tightness. In addition, tight junction proteins contribute to fluid and ion homeostasis mediated by paracellular transport (35). A tight homogeneous cell monolayer was observed for ciPTEC on HFM with ZO-1 abundantly expressed along the cell boundaries as shown in representative z-scans (figure 6.4A and C). Moreover, the endogenous expression of the influx transporter OCT2 was demonstrated to be expressed basolaterally (figure 6.4D), although some cytoplasmic staining was visible as well, suggesting ongoing posttranslational OCT2 modifications as previously suggested (53). The OCT2 antibody was validated in paraffin embedded

human kidney tissue using immunohistochemistry and positive staining at the basolateral membrane of PTEC was observed (data not shown).

ciPTEC on HFM show functional OCT2 transport

The activity of basolaterally expressed OCT2 in matured ciPTEC cultured on coated HFM was determined by real-time fluorescent ASP^+ uptake measurements, and shown in figure 6.5. The experiments were performed in the presence or absence of a cationic toxin mix or cimetidine, which are known inhibitors of OCT2-mediated ASP^+ transport (30). In figure 6.5A, representative real-time uptake images of the various conditions are shown for the time frame of 4 - 13 min. In the absence of inhibitors, a clear intracellular fluorescent ASP^+ signal was visible after 4 min of perfusion, which increased up to 13 min. In the presence of the cationic uremic toxin mixture of guanidine and polyamine compounds, the basal uptake of ASP^+ was still detectable and augmented over time, though the uptake was less pronounced compared to fiber perfusion in absence of the mixture. In the presence of cimetidine, the ASP^+ uptake was even further attenuated. Semi-quantification of these data (figure 6.5B) confirmed the observed differences in ASP^+ uptake per condition. The slopes from the linear part (min 1 - 8) of ASP^+ uptake curves in the presence of the cationic toxin mix or cimetidine were significantly altered compared to control uptake ($25 \pm 16\%$, $p<0.001$ and $62 \pm 12\%$, $p<0.001$, respectively)

DISCUSSION

In this study, ciPTEC were successfully cultured on optimally coated HFM with maintained functionality. The coating and membrane curvature showed to be crucial for the formation of a homogenous cell monolayer with a clear epithelial barrier function, without affecting transport properties of H_2O or albumin. Epithelial cell polarity and organelle morphology were retained when cultured on HFM. In addition, the epithelial and polarized characteristics of ciPTEC were demonstrated further by the expression of ZO-1 and the basolaterally expressed OCT2. Transport activity was confirmed by specific uptake in ciPTEC monolayers, demonstrating the establishment of a living membrane suitable for BAK development.

The MicroPES membranes used in this study are hydrophilized fibers used predominantly for plasma separation and have rather large pores allowing the

transport of proteins including BSA and IgG. The membranes are designed for having low interaction with blood, plasma and proteins. To apply a uniform cell monolayer, the outer membrane of HFM had to be biofunctionalized by ECM components. The native ECM is a dynamic network consisting of various types of collagen, glycosaminoglycans, laminin and fibronectin connected to integrins present in the plasma membrane. The ECM is a key factor in cell adhesion, differentiation and regeneration, as well as in intercellular signalling (14, 15). Oo *et al.* demonstrated a successful coating on PES membranes consisting of the combination of L-DOPA and collagen IV to culture primary human renal cells (36). Upon polymerization, when exposed to light and oxygen, the L-DOPA layer becomes negatively charged and will attract the positively charged collagen IV that is applied subsequently. In our laboratory, this coating was first applied on flat PES membranes and optimal conditions for ciPTEC adhesion and differentiation were established (18). Maintained membrane permeability, as well as homogenous cell monolayers and creatinine transport were demonstrated in ciPTEC on double coated PES flat membranes. Based on these encouraging results, the coating was adapted for HFM biofunctionalization. Both L-DOPA and collagen IV coating times were extended to hours instead of minutes to stimulate cell adhesion and tight cell monolayer formation. Next to an optimized ECM, the membrane curvature is an important parameter for maintaining cellular functions (51). The culture of ciPTEC on MicroPES HFM with a slightly lower membrane curvature compared to the HCO 1100 HFM had a positive effect on cell adhesion, most likely related to a more optimal organization of the cytoskeleton and its membrane composition. The almost unrestricted permeability of H_2O, IgG and albumin in coated MicroPES HFM indicated the need for a tight cell monolayer with a true barrier function to avoid significant blood components loss from the host. Hence, the free permeability of albumin across coated HFM is essential, as a large number of uremic toxins are protein-bound and need to be delivered in close proximity to the cells in order to be eliminated. Possible immunogenic effects due to contact between the host blood components and cell monolayers will be studied thoroughly in future research.

The morphological characteristics of tight cell monolayers on HFM were examined, as well as the epithelial barrier functions. *In vivo*, the proximal tubule epithelium is known as a leaky epithelium and paracellular transport is mediated along the tight junctions and lateral inter-cellular spaces (34). The reabsorption of glucose, amino acids, H_2O and electrolytes is partly facilitated by paracellular transport and occurs in a passive manner. The abundant

expression of the tight junction protein ZO-1 in the monolayers emphasized the epithelial character of the ciPTEC when cultured on HFM. Moreover, the epithelial barrier function was confirmed by demonstrating limited inulin-FITC diffusion. Since technical aspects of fiber handling when placed in the perfusion chamber will affect the tightness of the cell layer, the barrier restriction measured, as shown here, is most likely an underestimation. To prevent monolayer disturbance caused by technical aspects in future research, cell culture on HFM could be performed in disposable perfusion chambers. In this way, the cells on HFM will mature while already present in the system and will be ready-to-use for any perfusion experiment. Vital PTEC possess a high number of mitochondria to facilitate active processes (e.g. elimination of waste products) and a well-developed brush border membrane containing microvilli to enlarge the apical surface (34). The morphology of ciPTEC reflected the presence of intact organelles and a substantial number of mitochondria. The microvilli at the apical surface were visible when ciPTEC were cultured on HFM, but showed a heterogeneous pattern. Further optimization of culture conditions in disposable perfusion chambers, including medium flow across the apical membrane, could improve the uniformity of the ciPTEC brush border membrane (49).

The application of a cell-aided device, such as the BAK, for the removal of cationic metabolites can improve current renal replacement therapies. In this study, active OCT2 transport was demonstrated in living membranes of human PTEC when cultured on HFM for BAK purposes. Uptake via the OCT2 transporter is the first step in the renal secretion of various cationic endogenous metabolites or other xenobiotics, including drugs (54). Upon transport failure, accumulation of cationic metabolites, such as guanidines occurs. This is associated with cardiovascular implications, induced by, amongst others, activated leukocytes and microinflammation (24, 25). Here, OCT2-mediated ASP^+ uptake was inhibited in the presence of a polyamine and guanidino cationic uremic toxin mixture, as well as in the presence of cimetidine, a well-known and extensively studied renal OCT substrate and inhibitor (37, 38). These findings indicate functional OCT2 transport in ciPTEC on HFM, in concordance with recently described observations by Schophuizen *et al.*, where the cationic toxin mixture competed with OCT2-mediated ASP^+ uptake in a ciPTEC cell suspension (30). In addition, Kimura and Winter *et al.* demonstrated interference of guanidino compounds and putrescine, a polyamine, with OCT2 using human embryonic kidney cell line (HEK293) overexpressing the transporter (39, 40). The application of functional ciPTEC

cultured on HFM opens a promising avenue in the clearance of cationic metabolites in patients suffering from renal disorders. Future research is required to quantify transepithelial transport of uremic metabolites in up-scaled multifiber bioreactors. As (cationic) uremic toxins compete for the same system, their accumulation may also hamper efficient removal. Therefore, in-depth kinetic studies are needed to investigate the clearance capacity of our bioartificial tubule over time, and to predict their performance *in vivo*. In addition, other aspects, such as the balance between the number of ciPTEC and the duration per dialysis cycle required for efficient removal of waste products in human patients, have to be investigated.

The development of a functional and stable BAK device is a complex interplay between advanced biomaterials and renal epithelial cells. Beneficial effects were demonstrated in uremic animals and enhanced survival of patients suffering from multi-organ failure and AKI in a phase II clinical trial. However, a phase IIb clinical trial failed predominantly due to hampered cell performance (9-13, 41). In the late '90s, Humes *et al.* cultured porcine proximal tubule epithelial cells (LLC-PK1) in a multi-fiber bioreactor and demonstrated metabolically active cells, capable of ammoniagenesis, glutathione metabolism and 1,25-dihydroxyvitamin D_3 synthesis (42). However, next to its non-human origin, porcine cells have limited transport functionality (e.g. lack of essential transporters (43, 44)) and are not preferred for use in a BAK device. Only a few human-derived cell models are available with endogenous transporter expression and functional capacity. A well-distributed cell line is HK2, which was developed by recombinant retroviral transduction (humanpapillomavirus 16 E6/E7 genes) of human primary renal cortex cells (45), though a lack of functional transporters emphasizes the limitations of this model for studying renal transport in pharmacological and physiological studies (46). The thoroughly characterized cell model ciPTEC, as used in this study, was isolated from human urine and immortalized using retroviral hTERT and SV40 large T antigen transduction (32). The cell model displays diverse functional endogenous in- and efflux transporters relevant in the secretion of endo- and xenobiotics (31, 32). In addition, UDP-glucuronosyltransferases (UGT) and mitochondrial succinate dehydrogenase enzyme activity was confirmed and altered in uremic conditions that might affect drug disposition during CKD (47). Similar to HK-2, no organic anion transporter (OAT) expression could be detected in ciPTEC, a known phenomenon of immortal renal cells in culture and a drawback of renal cell line applications (48). Nevertheless, the stable functionality of other relevant transporters and metabolic enzymes in ciPTEC

upon prolonged culturing illustrate that these cells may prove a valuable tool in regenerative nephrology. Furthermore, this model may serve as a predictive model for drug toxicity screening in drug development processes.

To treat patients suffering from CKD or end-stage renal disease (ESRD), an efficient removal of protein-bound uremic toxins by a BAK is a prerequisite to diminish systemic disease progression (50). The active transport of cationic uremic toxins mediated by ciPTEC, as shown here, is an important contribution for future BAK engineering. However, future research is required to study the maintenance of functional cationic and anionic toxin transport in an up-scaled BAK system, as well as multi-factorial safety aspects, as described by the European medicines agency in the European guidelines for advanced therapy medicinal products enabling the applications of GMO in medicinal products (52).

In conclusion, a successful cell monolayer formation was established on biofunctionalized MicroPES HFM and matured ciPTEC represented clear epithelial characteristics with barrier and active transporter function. To the best of our knowledge, for the first time active organic cationic transport in PTEC monolayers on HFM was demonstrated. The combination of a unique human cell model with biofunctionalized MicroPES HFM is a valuable tool in regenerative nephrology and further development may contribute in future BAK engineering.

Acknowledgments

This research was performed as part of the Project P3.01 BioKid of the research program of the BioMedical Materials institute, co-funded by the Dutch Ministry of Economic Affairs. Furthermore, the financial contribution of the Dutch Kidney Foundation is gratefully acknowledged (IK08.03 and KJPB 11.0023), as well as the Netherlands Institute for Regenerative Medicine (NIRM, grant no. FES0908), the Netherlands Organization for Scientific Research (016.130.668) and the Marie Curie ITN project: BIOART (grant no. EU-FP7-PEOPLE-ITN-2012). The authors would like to gratefully thank V. Verweij and H.J. Jansen for technical support regarding perfusion chamber development, U.M. Kreuser for her contribution in the schematic presentation of the perfusion chambers and M. Wijers-Rouw for technical assistance in transmission electron microscopy.

Author contributions

J.J. performed literature search, experimental design, data collection, analysis and interpretation, created figures and wrote the paper. I.E.D.N. and N.V.C. contributed to data collection and analysis of cell-free membrane properties. M.F. contributed to data collection and analysis of extracellular matrix and cellular adhesion properties. C.M.S.S. contributed to coating optimization and initiated OCT2-activity assay in 2D, which could be translated into HFM approaches. M.J.W., L.P.H, J.G.H. and D.S. contributed to experimental design, data interpretation and manuscript writing. A.H.A. developed the microfluidic chamber using 3D printing. H.J.C. contributed to the setup of real-time imaging experiments using a microfluidic chamber. J.C.P. contributed to data collection and analysis of transmission electron microscopy samples. J.F.M.W. and L.B.H. contributed to data interpretation from a clinical point of view and manuscript writing. R.M. contributed to literature search, experimental design, data interpretation and manuscript writing.

Additional information

The experiments described in this article comply with the current laws of the country in which they were performed (the Netherlands). The authors declare that they have no conflict of interest.

REFERENCES

1. Vanholder, R., et al. Chronic kidney disease as cause of cardiovascular morbidity and mortality. Nephrol Dial Transplant. 20, 1048-56 (2005).
2. Masereeuw, R., et al. The kidney and uremic toxin removal: glomerulus or tubule? Semin Nephrol. 34, 191-208 (2014).
3. Sun, H., Frassetto, L., Benet, L.Z. Effects of renal failure on drug transport and metabolism. Pharmacol Therapeut. 109, 1-11 (2006).
4. Neirynck, N., et al. An update on uremic toxins. Int Urol Nephrol. 45, 139-50 (2013).
5. Vanholder, R., Schepers, E., Pletinck, A., Nagler, E.V., Glorieux, G. The uremic toxicity of indoxyl sulfate and p-cresyl sulfate: a systematic review. J. Am Soc Nephrol. 25, 1897-907 (2014).
6. Poveda, J., et al. p-cresyl sulphate has pro-inflammatory and cytotoxic actions on human proximal tubular epithelial cells. Nephrol Dial Transplant. 29, 56-64 (2014).
7. Humes, H.D., Buffington, D., Westover, A.J., Roy, S., Fissell, W.H. The bioartificial kidney: current status and future promise. Ped Nephrol. 29, 343-51 (2014).
8. Oo, Z.Y., Kandasamy, K., Tasnim, F., Zink, D. A novel design of bioartificial kidneys with improved cell performance and haemocompatibility. J. Cell Mol Med. 17, 497-507 (2013).
9. Saito, A., et al. Evaluation of bioartificial renal tubule device prepared with lifespan-extended human renal proximal tubular epithelial cells. Nephrol Dial Transplant. 27, 3091-9 (2012).
10. Humes, H.D., et al. Metabolic replacement of kidney function in uremic animals with a bioartificial kidney containing human cells. Am J Kidney Dis. 39, 1078-87 (2002).
11. Humes, H.D., et al. Initial clinical results of the bioartificial kidney containing human cells in ICU patients with acute renal failure. Kidney Int. 66, 1578-88 (2004).
12. Tumlin, J., et al. Efficacy and safety of renal tubule cell therapy for acute renal failure. J. Am Soc Nephrol. 19, 1034-40 (2008).
13. Westover, A.J., et al. A bio-artificial renal epithelial cell system conveys survival advantage in a porcine model of septic shock. J. Tissue Eng Regen Med. DOI 10.1002/term.1961 (2014).
14. Combes, A.N., Davies, J.A., Little, M.H. Cell-cell interactions driving kidney morphogenesis. Curr Top Dev Biol. 112, 467- 508 (2015).
15. Kruegel, J., Rubel, D., Gross, O. Alport syndrome – insights from basic and clinical research. Nat Rev Nephrol. 9, 170-178 (2013).
16. Ni, M., et al. Characterization of membrane materials and membrane coatings for bioreactor units of bioartificial kidneys. Biomaterials. 32, 1465-76 (2011).
17. Zhang, H., Tasnim, F., Ying, J.Y., Zink, D. The impact of extracellular matrix coatings on the performance of human renal cells applied in bioartificial kidneys. Biomaterials. 30, 2899-911 (2009).

18. Schophuizen, C.M., et al. Development of a living membrane comprising a functional human renal proximal tubule cell monolayer on polyethersulfone polymeric membrane. Acta Biomater. 14, 22-32 (2014).
19. Kimura, N., et al. Metformin is a superior substrate for renal organic cation transporter OCT2 rather than hepatic OCT1. Drug Metab Pharmacokinet. 20, 379-86 (2005).
20. Pietig, G., et al. Properties and regulation of organic cation transport in freshly isolated human proximal tubules. J. Biol Chem. 276, 33741-46 (2001).
21. Ciarimboli, G., et al. Cisplatin nephrotoxicity is critically mediated via the human organic cation transporter 2. Am J Pathol. 167, 1477-84 (2005).
22. Eloot, S., et al. Impact of hemodialysis duration on the removal of uremic retention solutes. Kidney Int. 73, 765-70 (2008).
23. D'Hooge, R., et al. Involvement of voltage- and ligand-gated Ca2+ channels in the neuroexcitatory and synergistic effects of putative uremic neurotoxins. Kidney Int. 63, 1764-75 (2003).
24. Glorieux, G.L., et al. In vitro study of the potential role of guanidines in leukocyte functions related to atherogenesis and infection. Kidney Int. 65, 2184-92 (2004).
25. Schepers, E., et al. Guanidino compounds as cause of cardiovascular damage in chronic kidney disease: an in vitro evaluation. Blood Purif. 30, 277-87 (2010).
26. Campbell, R.A., Grettie, D.P., Bartos, F., Bartos, D., Marton, L.J. Uremic polyamine dysmetabolism. Proc Clin Dial Transplant Forum. 8, 194-8 (1978).
27. Dhondt, A., Vanholder, R., Van Biesen, W., Lameire, N. The removal of uremic toxins. Kidney Int Suppl. 76, S47-59 (2000).
28. Igarashi, K., Ueda, S., Yoshida, K., Kashiwagi, K. Polyamines in renal failure. Amino acids. 31, 477-83 (2006).
29. Pegg, A.E. Toxicity of polyamines and their metabolic products. Chem Res Toxicol. 26, 1782-800 (2013).
30. Schophuizen, C.M., et al. Cationic uremic toxins affect human renal proximal tubule cell functioning through interaction with the organic cation transporter. Pflug Arch: Eur J Phy. 465, 1701-14 (2013).
31. Jansen, J., et al. A morphological and functional comparison of proximal tubule cell lines established from human urine and kidney tissue. Exp Cell Res. 323, 87-99 (2014).
32. Wilmer, M.J., et al. Novel conditionally immortalized human proximal tubule cell line expressing functional influx and efflux transporters. Cell Tissue Res. 339, 449-57 (2010).
33. Bonandrini, B., et al. Recellularization of well-preserved acellular kidney scaffold using embryonic stem cells. Tissue Eng Part A. 20, 1486-98 (2014).
34. Giebisch, G., Windhager, E. The urinary system in Medical Physiology (eds Boron, W.F., et al.) 743-4 (Saunders 2003).

35. Kirk, A., Campbell, S., Bass, P., Mason, J., Collins, J. Differential expression of claudin tight junction proteins in the human cortical nephron. Nephrol Dial Transplant. 25, 2107-19 (2010).
36. Oo, Z.Y., et al. The performance of primary human renal cells in hollow fiber bioreactors for bioartificial kidneys. Biomaterials. 32, 8806-15 (2011).
37. Urakami, Y., Akazawa, M., Saito, H., Okuda, M., Inui, K. cDNA cloning, functional characterization, and tissue distribution of an alternatively spliced variant of organic cation transporter hOCT2 predominantly expressed in the human kidney. J. Am Soc Nephrol. 13, 1703-10 (2002).
38. Kido, Y., Matsson, P., Giacomini, K.M. Profiling of a prescription drug library for potential renal drug-drug interactions mediated by the organic cation transporter 2. J Med Chem. 54, 4548-58 (2011).
39. Kimura, N., Masuda, S., Katsura, T., Inui, K. Transport of guanidine compounds by human organic cation transporters, hOCT1 and hOCT2. Biochem Pharm. 77, 1429-36 (2009).
40. Winter, T.N., Elmquist, W.F., Fairbanks, C.A. OCT2 and MATE1 provide bidirectional agmatine transport. Mol Pharm. 8, 133-42 (2011).
41. Humes, H.D., Buffington, D.A., MacKay, S.M., Funke, A.J., Weitzel, W.F. Replacement of renal function in uremic animals with a tissue-engineered kidney. Nature biotechnol. 17, 451-5 (1999).
42. Humes, H.D., MacKay, S.M., Funke, A.J., Buffington, D.A. Tissue engineering of a bioartificial renal tubule assist device: in vitro transport and metabolic characteristics. Kidney Int. 55, 2502-14 (1999).
43. Kuteykin-Teplyakov, K., Luna-Tortos, C., Ambroziak, K., Loscher, W. Differences in the expression of endogenous efflux transporters in MDR1-transfected versus wildtype cell lines affect P-glycoprotein mediated drug transport. Br J Pharmacol. 160, 1453-63 (2010).
44. Takada, T., Suzuki, H., Sugiyama, Y. Characterization of polarized expression of point- or deletion-mutated human BCRP/ABCG2 in LLC-PK1 cells. Pharm Res. 22, 458-64 (2005).
45. Ryan, M.J., et al. HK-2: an immortalized proximal tubule epithelial cell line from normal adult human kidney. Kidney Int. 45, 48-57 (1994).
46. Jenkinson, S.E., et al. The limitations of renal epithelial cell line HK-2 as a model of drug transporter expression and function in the proximal tubule. Pflug Arch: Eur J Phy. 464, 601-11 (2012).
47. Mutsaers, H.A., et al. Uremic toxins inhibit renal metabolic capacity through interference with glucuronidation and mitochondrial respiration. Biochim Biophys Acta. 1832, 142-50 (2013).

48. Miller, J.H. Sodium-sensitive, probenecid-insensitive p-aminohippuric acid uptake in cultured renal proximal tubule cells of the rabbit. Proc Soc Exp Biol Med. 199, 298-304 (1992).
49. Jang, K.J., et al. Human kidney proximal tubule-on-a-chip for drug transport and nephrotoxicity assessment. Integr Biol (Camb). 5, 1119-29 (2013).
50. Jansen, J., et al. Biotechnological challenges of bioartificial kidney engineering. Biotech Adv. 32, 1317-27 (2014).
51. McMahon, H.T., Boucrot, E. Membrane curvature at a glance. J. Cell Sci. 6, 1065-1070 (2015).
52. European medicines agency: committee for advanced therapies, Classification of advanced therapy medicinal products. Reflection paper. (2012) Available at: http://www.ema.europa.eu/docs/en_GB/document_library/Scientific_guideline/2012/12/WC500136422.pdf. (Accessed: 7th December 2012).
53. Guckel, D., Ciarimboli, G., Pavenstadt, H., Schlatter, E. Regulation of organic cation transport in isolated mouse proximal tubules involves complex changes in protein trafficking and substrate affinity. Cell Physiol Biochem. 1, 269-81 (2012).
54. Pelis, R.M., Wright, S.H. SLC22, SLC44, and SLC47 transporters-oganic anion and cation transporters: molecular and cellular properties. Curr Top Membr. 73, 233-261 (2014).

SUPPLEMENTARY INFORMATION

Methods

Hollow fiber sterilization and double coating

MicroPES (polyethersulfone) hollow fiber membranes were sterilized using 70% (v/v) EtOH incubation for 30 min. Subsequently, membranes were washed thoroughly in Hank's balanced salt solution (HBSS) buffer containing $CaCl_2$ (1.26 mM), MgCl (0.49 mM), $MgSO_4$ (0.41 mM), KCl (5.33 mM), KH_2PO_4 (0.44 mM), $NaHCO_3$ (4.17 mM), NaCl (137.93 mM), Na_2HPO_4 (0.34 mM) and D-Glucose (5.56 mM). The primary coating component L-DOPA (L-3,4-dihydroxyphenylalanine, 2 mg.ml^{-1}) was dissolved in 10 mM Tris buffer (pH 8.5), as described previously by Ni et al. (16). To dissolve the coating, the solution was incubated at 37°C for 45 min. Next, the solution was filter sterilized prior to incubation of the horizontally placed fibers for 5 hours at 37°C. Every hour the fiber was turned 90°. Next, the L-DOPA solution was aspirated and the fibers were washed once with HBSS buffer. The L-DOPA coated fibers were exposed to the second coating component human collagen IV (C6745-1ml, 25 µg.ml^{-1}) for 1 hour at 37°C. After 30 min, the tube was turned 180° and incubated for the remaining time. The collagen IV solution was aspirated afterwards and the fibers were washed thoroughly in HBSS buffer prior to cell seeding.

Transport properties of cell-free hollow fibers membranes

The transport of pure water (Merck MilliPore, Billerica, MA), bovine serum albumin (BSA) and immunoglobulin G (IgG) solutions through the uncoated and coated cell-free HFMs were measured at various transmembrane pressures using a KrosFlo Research IIi Tangential Flow Filtration system (Spectrum laboratories, Wurzburg, Germany). Prior to the experiment, HFMs were incubated at 37°C in phosphate buffered saline, (PBS, pH 7.4; Life technologies, Breda, The Netherlands) for 1 hour. Next, the HFMs were assembled in one-membrane module using bi-component polyurethane potting glue (Intercol BV, Ede, The Netherlands), push-in fittings (Festo, Brussels, Belgium) and polyethylene tubing (Festo, Brussels, Belgium). The BSA and IgG were dissolved in PBS at concentrations of 1 mg.ml^{-1} and 0.02 mg.ml^{-1}, respectively (feed solutions). The pressure (0.10, 0.15 and 0.20 bar) was applied from the luminal side towards the abluminal side of the HFM. As described previously by Schophuizen *et al.* (18), the flux through the HFM at each pressure was determined by collecting the mass of the permeated liquid over time correlated to the HFM surface area. BSA and

IgG samples were collected at each pressure after 15 min and concentrations were determined by spectrophotometric analysis (Cary 300 UV-Vis system, Agilent Technologies, Amstelveen, The Netherlands) at 280 nm and 276 nm wavelengths, respectively.

Culture of ciPTEC on double coated hollow fiber membranes

Proliferating ciPTEC (32) were seeded on double-coated fibers (length 2cm) using 1.5 x 10^6 cells per 1.5 ml. The cell suspension was added to an eppendorf tube containing the fiber and incubated at 33°C, 5% (v/v) CO_2, for 4 hours. Every hour the tube was turned 90° in order to stimulate cell adhesion to the whole surface. Next, fibers with adhered cells were removed from the suspension and transferred to a 6 well plate with PTEC culture medium: phenol-red free DMEM-HAM's F12 medium (catalogue number 11039, Lonza, Basel, Switzerland) containing 10% (v/v) FCS (Greiner Bio-One, Monroe, NC), 5 µg/ml insulin, 5 µg/ml transferrin, 5 ng/ml selenium, 36 ng/ml hydrocortisone, 10 ng/ml EGF and 40 pg/ml tri-iodothyronine. The incubation period was prolonged at 33°C, 5% (v/v) CO_2, for additional 48 hours. Subsequently, the proliferating cells on fibers were transferred to 37°C, 5% (v/v) CO_2 to mature for 7 days. Cells upon passage 42 were applied in this study.

Immunocytochemistry

The expression of OCT2 and zonula occludens-1 (ZO-1) in ciPTEC monolayers on hollow fibers were investigated using the immunocytochemistry methodology as previously described by Jansen et al. (31). The ZO-1 (Invitrogen, Carlsbad, CA) and OCT2 primary antibodies were diluted (1:50) in block solution (HBSS buffer supplemented with 2% (w/v) BSA, 2% (v/v) fetal calf serum and 0.001% (v/v) Tween-20 to prevent aspecific binding), followed by incubation with goat-anti-mouse-Alexa488 conjugate or goat-anti-rabbit-Alexa568 conjugate (1:200, Life Technologies), respectively. The expression of the ECM component collagen IV was investigated using the primary anti-type IV collagen antibody (1:50, Southern Biotech (Birmingham, AL)) followed by incubation with donkey-anti-goat-Alexa 488 conjugate ((1:200, Life Technologies).

Transmission- and scanning electron microscopy

The morphology of ciPTEC and its organelles was investigated using transmission electron microscopy (TEM) and SEM. In short for TEM, cells were primary fixed using 2% (w/v) glutaraldehyde, postfixated in 1% (w/v) osmiumtetroxide supplemented with 1% (w/v) potassium ferrocyanide, all

dissolved in 0.1 M sodium cacodylatebuffer at room temperature (rT) for 1 hour. Next, samples were dehydrated through a graded series of ethanol and finally embedded in Epon and polymerized at 60°C. After ultrathin sectioning and contrasting with uranylacetate and leadcitrate, sections were analyzed using a transmission electron microscope JEOL JEM 1010 (Jeol, Akishima Tokyo, Japan) at an accelerating voltage of 60 kV and images were captured using a Kodak Megaplus camera (San Diego, CA). For SEM purposes, cells were washed twice in 0.1M sodiumcacodylate buffer supplemented with 3% (w/v) sucrose (SCS) and primary fixed using 2% (w/v) glutaraldehyde in SCS at rT for 1 hour. Next, cells were washed three times in SCS and secondly fixed in 1% (w/v) osmiumtetroxide in SCS at rT for 2 hours. After this, cells were incubated using 1% (w/v) tannic acid in SCS at rT for 1 hour. Subsequently, samples were washed three times, processed to 70% (v/v) ethanol and incubated in 5% (w/v) uranyl acetate dissolved in 70% (v/v) EtOH at rT overnight. Samples were dehydrated trough a graded series of ethanol (70%-80%-96%-100% (v/v)) and critical point dried. Finally, samples were gold sputtered prior to SEM analysis (JEOL JSM-6340F, Tokyo, Japan).

Transepithelial barrier function

Paracellular permeability was determined in the living membrane by endpoint quantification of inulin-fluorescein isothiocyanate (FITC) (0.1 $mg.ml^{-1}$ in Krebs-Henseleit buffer (containing $MgSO_4$ (0.14 g/L), KCl (0.35 g/L), KH_2PO_4 (0.16 g/L), NaCl (6.9 g/L), $CaCl_2$ (0.37 g/L), $NaHCO_3$ (2.1 g/L) and D-Glucose (2.0 g/L)) supplemented with HEPES (10 mM; KHH buffer)) diffusion when perfused (6 $ml.h^{-1}$) using a syringe pump (Terumo STC-521, Terumo Europe N.V., Leuven, Belgium) for 13 min at 37°C. The inulin-FITC diffusion in coated HFM in the absence of cells was investigated in similar conditions. During the experiment, the HFM was connected to a separated in- and outlet glass cannula (inner diameter 120 – 150 µm; DMT Trading, Aarhus, Denmark) assembled in a custom-made 3D printed cytocompatible polyester device (figure S6.1) to enable a separated basolateral (inner HFM, perfusion channel) and apical compartment (outer HFM, containing 300 µl KHH buffer). The inlet cannula was connected to a tubing system and a syringe pump, whereas the outlet cannula was connected to a tubing system and a depot to collect perfusate. First, the HFM was rinsed once using KHH buffer. Next, the inulin-FITC was perfused and 100 µl sample was collected in the apical compartment after 13 min.

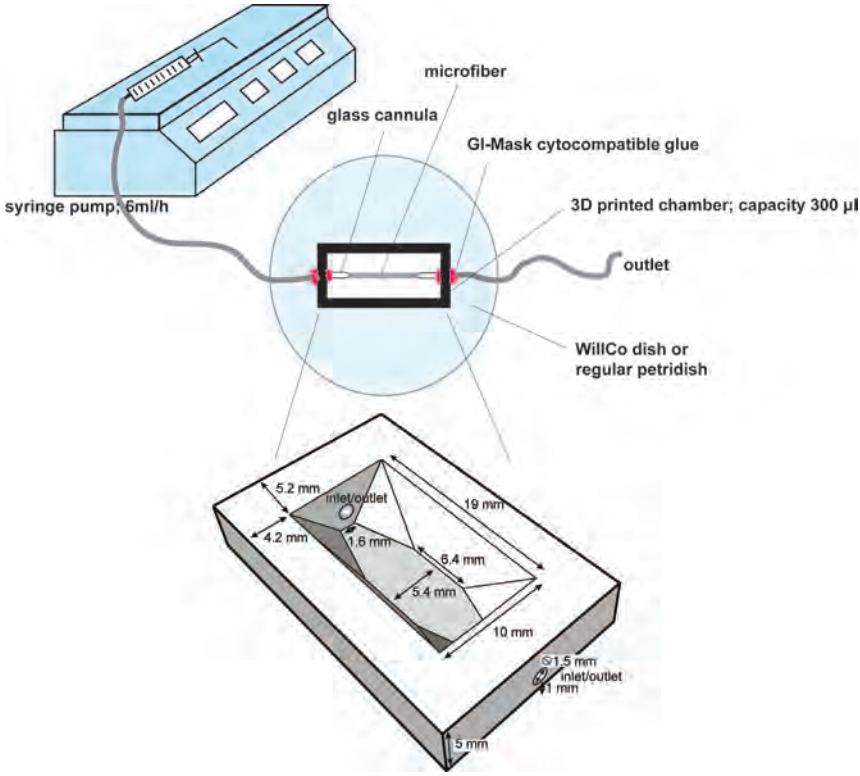
microfiber
glass cannula
GI-Mask cytocompatible glue
syringe pump; 6ml/h
3D printed chamber; capacity 300 µl
outlet
WillCo dish or
regular petridish
5.2 mm
inlet/outlet
19 mm
4.2 mm
1.6 mm
6.4 mm
5.4 mm
10 mm
1.5 mm
inlet/outlet
1 mm
5 mm

Supplemental figure S6.1 Schematic presentation of a flow experiment setup including a 3D-printed microfluidic chamber.
The microfiber was connected to a separated in- and outlet glass cannula assembled in a custom-made 3D printed cytocompatible polyester device. The chamber was printed using a calibrated ROBO 3D beta R1 printer (Robo3D LLC, San Diago, CA) and the cytocompatible acrylonitril butadiene styrene (ABS) polymer. The ABS print temperature was 215°C on a heated bed of 90°C and the thickness of each layer was 100 µm, using a nozzle diameter of 0.3 mm. Dimensions as shown in the figure were optimized to have a stable system for fiber assembly and a low inner volume of 300 µl buffer, which enabled detection of inulin-FITC. Obviously, the buffer covered the fiber completely. For imaging purposes, the chamber was connected to a WillCo dish (WillCo Wells B.V., Amsterdam, The Netherlands) with a glass bottom using GI-MASK cytocompatible glue (Dental Union, Nieuwegein, The Netherlands) to prevent leakage from the chamber. During the experiment the system was closed using a cabinet in which 5% (v/v) CO_2 was present and the temperature was controlled at 37°C. The real-time imaging was performed using a 40x magnification water lens of the confocal microscope. To test paracellular permeability using inulin-FITC, the chamber was connected to a regular petridish and the temperature was controlled at 37°C during the experiment using a heating plate. In both types of experiments a flow rate of 6 $ml.h^{-1}$ was used for 13 min, using a syringe pump.

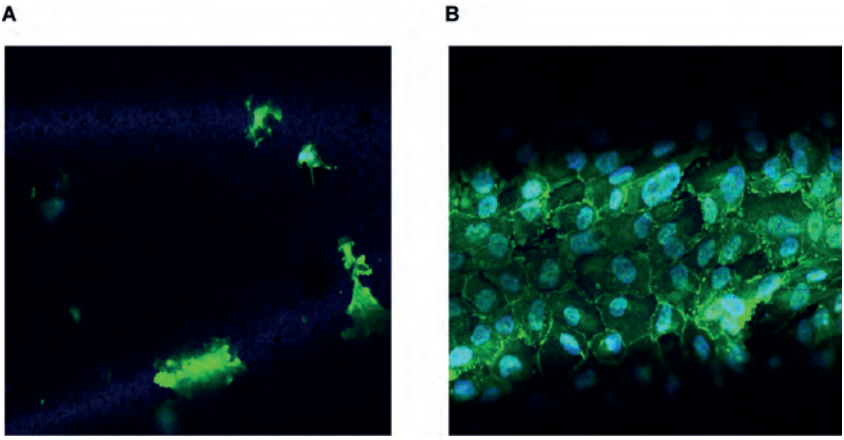

Supplemental figure S6.2 Representative images of ciPTEC performance on HCO 1100 and MicroPES HFM.
(a) A poor cell adhesion was observed (i.e. no nuclei (blue)) when ciPTEC were cultured on double coated PES HCO 1100 HFM (inner diameter 215 µm). (b) Using a similar double coating procedure and the same batch of cells as used for HCO 1100 HFM, optimal cell adhesion and a tight monolayer formation with abundant ZO-1 expression (green) was detected using MicroPES HFM (inner diameter 300 µm).

Chapter 7

BIOENGINEERED KIDNEY TUBULES EFFICIENTLY EXCRETE UREMIC TOXINS

Jansen J[1,2,3,4*], Fedecostante M[1,2,3,4*], Wilmer MJ[1], Peters JG[1], Kreuser UM[1], van den Broek PH[1], Mensink RA[5], Boltje TJ[5], Stamatialis D[6], Wetzels JF[7], van den Heuvel LP[3,8], Hoenderop JG[2], Masereeuw R[4]

Nature Scientific Reports, 6, 26715, 2016

Department of [1]Pharmacology and Toxicology and [2]Physiology, Radboud university medical center, Radboud Institute for Molecular Life Sciences, Nijmegen, The Netherlands.
Department of [3]Pediatrics and [7]Nephrology, Radboud university medical center, Nijmegen, The Netherlands.
Division of [4]Pharmacology, Utrecht Institute for Pharmaceutical Sciences, Utrecht, The Netherlands.
Cluster for [5]Molecular Chemistry, Institute for Molecules and Materials, Radboud University, Nijmegen, The Netherlands.
Department of [6]Biomaterials Science and Technology, MIRA Institute for Biomedical Technology and Technical Medicine, University of Twente, The Netherlands.
Department of [8]Pediatric Nephrology & Growth and Regeneration, Catholic University Leuven, Leuven, Belgium.

* Authors contributed equally

ABSTRACT

The development of a biotechnological platform for the removal of waste products (e.g. uremic toxins), often bound to proteins in plasma, is a prerequisite to improve current treatment modalities for patients suffering from end stage renal disease (ESRD). Here, we present a newly designed bioengineered renal tubule capable of active uremic toxin secretion through the concerted action of essential renal transporters, *viz.* organic anion transporter-1 (OAT1), breast cancer resistance protein (BCRP) and multidrug resistance protein-4 (MRP4). Three-dimensional cell monolayer formation of human conditionally immortalized proximal tubule epithelial cells (ciPTEC) on biofunctionalized hollow fibers with maintained barrier function was demonstrated. Using a tailor made flow system, the secretory clearance of human serum albumin-bound uremic toxins, indoxyl sulfate and kynurenic acid, across the renal tubule was confirmed. These functional bioengineered renal tubules are promising entities in renal replacement therapies and regenerative medicine, as well as in drug development programs.

BACKGROUND

Chronic renal failure (CRF) is a severe health problem with a high morbidity and mortality rate as adequate therapy is currently not available. Impaired renal function results in the accumulation of various endogenous uremic metabolites (i.e. uremic toxins), which are associated with a broad range of pathologies that constitute the uremic syndrome (1-3). The preferred treatment option for end-stage renal disease (ESRD) is organ transplantation, however, the worldwide organ shortage is profound and many patients experience graft failure (4, 5). Chronic dialysis (hemodialysis or peritioneal dialysis) is currently the best alternative treatment option, which is widely applied and efficient in removal of small water-soluble and middle molecular weight molecules, but it insufficiently removes larger and protein-bound uremic toxins (6, 7). The latter class comprises end-metabolites that originate from dietary breakdown amino acids, such as tyrosine, phenylalanine and L-tryptophan, for which their pathological role in the progression of the uremic syndrome has gained substantial interest in the last decade (6).

The majority of dietary protein derived L-tryptophan is metabolized to L-kynurenine, which in turn can be converted into kynurenic acid. Accumulation of kynurenic acid was found to correlate with several symptoms of uremia, including neurological disturbances, lipid metabolism disorder and anemia (8). Tryptophan can also be metabolized by intestinal bacteria into indoles, which are processed further in the liver into indoxyl sulfate, indole-3 acetic acid and indoxyl-β-D-glucuronide (9). Indoxyl sulfate as well as the tyrosine end-metabolites *p*-cresyl sulfate and *p*-cresyl glucuronide are associated with cardiovascular disease development via the activation of leukocytes, ROS production and their interaction with the vascular endothelium (10-12). Furthermore, the *p*-cresol derivates demonstrated cytotoxicity and a pro-inflammatory response in renal epithelial cells (13), possibly contributing to CRF progression. Also, drug disposition is altered in patients with CRF, not only because of diminished kidney function but also due to a direct inhibition of drug transporters and drug-metabolism enzymes by uremic toxins (14, 15). The residual renal function in ESRD patients is not only associated with the remaining glomerular filtration capacity, but also the ability of the proximal nephron segment to actively secrete protein-bound uremic toxins into the pro-urine (16, 17). To this end, proximal tubule epithelial cells (PTEC) are equipped with a broad range of transport proteins that accept a wide range of xenobiotics, including exogenous compounds such as drugs, and

endogenous (waste) metabolites. At the basolateral membrane the organic anion transporters 1 (OAT1; *SLC22A6*) and -3 (OAT3; *SLC22A8*) of the solute carrier family (SLC), are highly efficient in the uptake of the anionic uremic toxins such as the L-tryptophan, tyrosine and phenylalanine end-metabolites, shifting their protein binding to the free fraction (8, 18, 19). At the luminal side, the ATP binding cassette (ABC) transporters breast cancer resistance protein (BCRP; *ABCG2*) and the multidrug resistance-associated proteins 2 and -4 (MRP2/4; *ABCC2/4*) are involved in their urinary secretion (20).

As the removal of protein-bound uremic toxins via PTEC is associated with better patients survival, the engineering of a bioartificial kidney (BAK) containing PTEC cultured on hollow fiber membranes (HFM) could be a promising platform to advance uremic toxin clearance. This was the focus of the current study using human conditionally immortalized PTEC (ciPTEC), expressing endogenously a broad range of functional transporters associated with uremic toxin handling (21, 22). Recently, complemented with OAT1 and -3 that are generally lost in PTEC upon culturing(23). The cells carry the temperature-sensitive mutant U19tsA58 of SV40 large T antigen (SV40T) and the essential catalytic subunit of human telomerase (hTERT), allowing the cells to proliferate at the permissive low temperature of 33°C and differentiate to mature PTEC at 37°C, and maintenance of telomere length preventing replicative senescence, respectively. This resulted in stable cell lines that could be maintained over a long period of time, and a valuable tool for studying renal clearance processes as required for BAK engineering.

In the present study, we demonstrate the development of functional bioengineered renal tubules that efficiently clear protein-bound anionic uremic toxins. First, the essential role of in- and efflux transporters in the removal of uremic toxins was studied in flat monolayers. Subsequently, three dimensional, polarized, ciPTEC monolayers on biofunctionalized polyethersulfone hollow fiber membranes were developed. Finally, as a crucial next step in BAK engineering, the secretory clearance of human serum albumin-bound indoxyl sulfate and kynurenic acid was confirmed.

METHODS

Brief methods are given. For details, the reader is referred to Supplementary information.

Chemicals and cell culture materials

Chemicals were purchased from Sigma-Aldrich (Zwijndrecht, The Netherlands) unless stated otherwise. The uremic toxins *p*-cresylsulfate and *p*-cresyl-glucuronide were synthesized by the Institute for Molecules and Materials, Radboud University, Nijmegen, The Netherlands. MicroPES type TF10 hollow fiber capillary membranes (wall thickness 100 µm, inner diameter 300 µm, max pore size 0.5 µm) were obtained from Membrana GmbH (Wuppertal, Germany). Cell culture plates were purchased from Greiner Bio-One (Monroe, NC).

Cell culture of ciPTEC-OAT1 and -OAT3

The transduction of OAT1 and OAT3 in ciPTEC (22) was performed as previously described by Nieskens *et al.* (23) and cells were cultured in supplemented PTEC culture media as described by Jansen *et al.*(21) Fibers were coated and seeded as described by Jansen *et al.* (27).

Fluorescein inhibition assay

The potency of a panel of eight anionic uremic toxins to inhibit OAT1- and OAT3-mediated fluorescein uptake was investigated in flat monolayers using an inhibition assay as previously described by Nieskens *et al.* (23). Blank fluorescence data were subtracted and relative data compared to control were plotted.

Uptake of indoxyl sulfate and kynurenic acid by ciPTEC-OAT1

In short, active OAT1-mediated uptake of indoxyl sulfate and kynurenic acid was investigated using two concentrations of toxins (3 and 30 µM) in the presence or absence of probenecid (100 µM), kynurenic acid (100 µM) or indoxyl sulfate (100 µM). Intracellular toxin concentrations were analyzed using a LC-MS/MS system (Thermo scientific, Breda, The Netherlands) following the method described by Mutsaers *et al.* (14). Data processing was performed using the Thermo Xcaliber software (Thermo scientific, version 2.1) and absolute data were plotted.

Cell viability assay

An MTT (3-(4,5-dimethylthiazol-2-yl)-2,5-diphenyltetrazolium bromide) cell proliferation assay was performed as previously described by Nieskens *et al.* (23). Background values were subtracted and normalized data were plotted.

Monolayer polarization and transepithelial barrier function

To investigate the barrier function of matured ciPTEC-OAT1 cultured on HFM, fibers were perfused with FITC-inulin (0.1 mg/ml in Krebs-Henseleit buffer supplemented with 10mM Hepes (KHH, pH 7.4)) and diffusion was measured in real-time. From each single replicate 4 different regions in focus were analyzed. Semi-quantification of real-time data was performed using Image J software (version 1.40g) and normalized data were plotted. To determine the polarization of the ciPTEC-OAT1 monolayer on HFM, the expression of tight junction protein zonula occludens-1 (ZO-1) was investigated according to the protocol as previously described by Jansen *et al. (27)*.

Detection of OAT1, BCRP and MRP4 mRNA expression

The mRNA expression of OAT1, BCRP and MRP4 was examined in ciPTEC-OAT1 when cultured in flat monolayers and as bioartificial renal tubules as previously described by Jansen *et al.* (21). Gene expression levels were normalized to expression levels of the reference gene GADPH and were expressed as fold increase compared to matured cells in well plates.

Fluorescein assay

To determine the OAT1 as well as BCRP and MPR4 transport activity in matured ciPTEC-OAT1 cultured on HFM, the fibers were connected to a similar perfusion set-up as was used for the barrier function assay. To measure active fluorescein uptake in real-time, fibers were perfused using 1 µM fluorescein in KHH in the presence or absence of specific drug transporter inhibitors or uremic toxins. Background corrected data were normalized against fluorescein uptake in the absence of inhibitors and were fitted according to one-site total binding saturation curve using non-linear regression analysis. In addition, V_{max} values (i.e. the maximum initial rate of a reaction) were calculated from the corrected AFU data according to Michaelis-Menten kinetics using non-linear regression analysis.

Transepithelial transport of indoxyl sulfate and kynurenic acid

Transepithelial transport of indoxyl sulfate and kynurenic acid through the HFM with matured ciPTEC was studied using a similar perfusion set-up as was used for the barrier function assay. First, fibers were pre-incubated using efflux pump EP inhibitors (5 µM) or probenecid (100 µM) for 15 min. Next, the fibers were perfused using 100 µM IS or 30 µM KA in the presence or absence of inhibitors for 10 min and samples from the apical compartment were collected (100 µl). To determine the ability of ciPTEC to initiate a shift from the toxin protein-bound fraction to a free fraction for transport, similar conditions were investigated in the presence of human serum albumin ((HSA), 1mM). The binding efficiency of IS and KA to HSA was determined an ultrafiltration technique with a 30 kDA cut-off filter (Merck Millipore, Amsterdam, the Netherlands). The mixture was centrifuged for 15 min at 6,500 x rcf at rT and the ultrafiltrate containing the free toxin fraction was collected. The percentage albumin-bound (C_{bound}) of indoxyl sulfate and kynurenic acid was calculated according to equation 1:

$$C_{bound} = ((C_{total} - C_{free}) / C_{total}) * 100 \quad (1)$$

Where C_{total} is the total concentration of toxin solution and C_{free} the free toxin concentration present in ultrafiltrate, both in µmol/l. All samples collected from the binding analysis and the apical compartment after the transport experiment were analyzed using a LC-MS/MS system as described earlier.

In vitro clearance values of the transepithelial transport of both toxins were calculated according to equation 2:

$$Cl = (U * V) / P \quad (2)$$

Where U is the apical concentration in µmol/ml, V the volume in the apical compartment in ml and P the basolateral concentration in µmol/ml.

Next, the *in vitro* clearance was calculated according to equation 3:

$$Cl_{in\ vitro} = (Cl / T) / A \quad (3)$$

Where Cl is the calculated clearance, T is the time in min and A the surface of the fiber in cm^2.

All toxin samples were analyzed using a LC-MS/MS system as described earlier in this section.

Endocytosis-mediated albumin uptake in bioengineered renal tubules

Matured renal tubules were assembled in our custom-made flow system and perfused with BSA-FITC (25 µg / ml) for 30 min at 37°C. In the next condition, fibers were perfused with KHH buffer and BSA-FITC (25 µg / ml) was added apically and exposed for 30 min at 37°C. As a control, the apical exposure was also performed at 4°C in order to inhibit endocytosis. After the uptake was arrested, tubules were fixed using 2% (w/v) PFA for 5 min at room temperature. Finally, tubules were mounted using Prolong Gold Antifade Reagent with DAPI (Cell Signaling Technology, Leiden, The Netherlands) and BSA-FITC localization in the cells was examined using the Leica SPE-II – DM14000 (Leica Microsystems, Rijswijk, The Netherlands) and images were captured using the Leica Microsystems LAS-AF software version 1.00.71.

Data analysis

All data are expressed as mean ± S.E.M of multiple replicates. Inhibition data were fitted according to one-site total binding saturation curve using non-linear regression analysis and Vmax values were calculated according to Michaelis-Menten kinetics using non-linear regression analysis. Statistical analysis was performed using one-way ANOVA analysis followed by Dunnett's or Tukey's multiple comparison test, or, when appropriate, an unpaired t test with GraphPad Prism version 5.02 (La Jolla, CA). A p-value of <0.05 was considered significant.

RESULTS

Uremic toxins inhibit OAT1 and OAT3 activity at clinically relevant concentrations

To evaluate the role of uptake transporters in uremic toxin handling, a panel of eight anionic uremic toxins was selected to study their affinity to inhibit OAT1- and OAT3-mediated uptake in ciPTEC. These toxins were selected based on their structure and potential PTEC-mediated urinary secretion, and their previously suggested association with complications of CRF (13-15, 19). The OAT1 and -3 model substrate fluorescein was used to evaluate transporter function (23). A concentration-dependent inhibition of fluorescein uptake was shown for all anionic uremic toxins tested (Fig. 7.1), with most potent interactions found for kynurenic acid and hippuric acid (Fig. 7.1D and F, table 7.1, resp.). The inhibitory potencies of the toxins, as reflected by their IC_{50} values (Table 7.1), were higher for OAT1 compared to OAT3, except for *p*-cresylglucuronide.

The renal excretion of indoxyl sulfate and kynurenic acid is OAT1-, BCRP- and MRP4-mediated

Indoxyl sulfate and kynurenic acid were selected for further studies using the ciPTEC-OAT1 model, as both showed a strong OAT1-mediated inhibition and have been associated severely with ESRD progression and its related complications (8, 15, 24, 25). Next to their inhibitory potency, we studied active PTEC transport processes. A dose-dependent uptake of indoxyl sulfate by ciPTEC-OAT1 monolayers was observed (Fig. 7.2A, 1.2 ± 0.1 and 6.7 ± 0.9 pmol.min^{-1}.cm^{-2}, at 3 and 30 µM respectively), which was sensitive to probenecid inhibition (by 83 ± 6 and 63 ± 5 % for 3 and 30 µM, respectively; $p < 0.001$), a classical OAT inhibitor (26). Indoxyl sulfate uptake was also inhibited by kynurenic acid (100 µM; by 64 ± 13 and 61 ± 5 % for 3 and 30 µM, respectively; $p < 0.001$), while kynurenic acid uptake by OAT1 was not significantly affected by indoxyl sulfate (100 µM), most likely due to a higher affinity of kynurenic acid for the transporter than indoxyl sulfate (8). But dose-dependent kynurenic acid uptake (Fig. 7.2B, 2.7 ± 0.3 and 5.9 ± 0.5 pmol.min^{-1}.cm^{-2} for 3 and 30 µM, respectively) in ciPTEC-OAT1 was also sensitive to probenecid (53 ± 10 and 52 ± 12 % inhibition, respectively; $p < 0.05$).

Using a vesicular transport assay for evaluating the activities of BCRP and MRP4 (14), Mutsaers *et al.* showed previously that indoxyl sulfate and kynurenic acid are potent inhibitors of both efflux pumps. Moreover, the

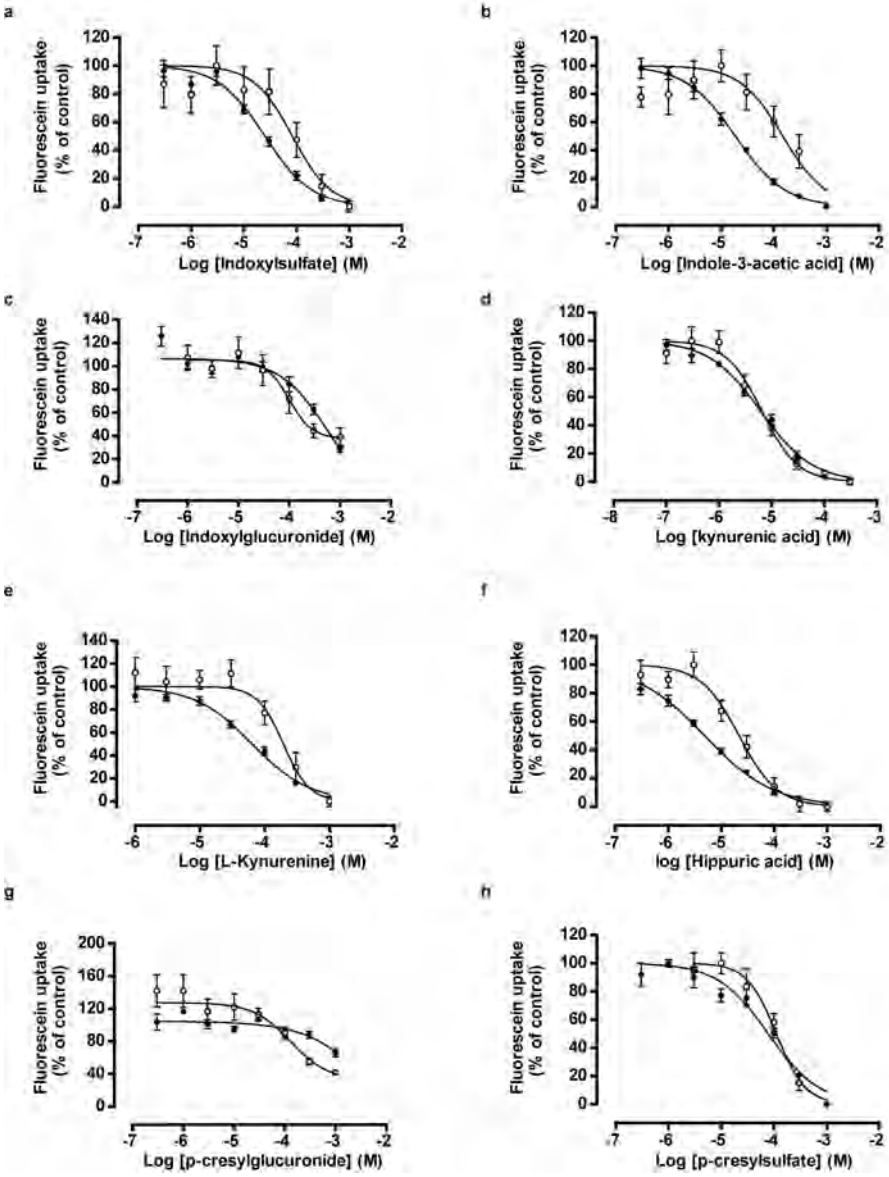
a
Fluorescein uptake (% of control)
Log [Indoxylsulfate] (M)
b
Fluorescein uptake (% of control)
Log [Indole-3-acetic acid] (M)
c
Fluorescein uptake (% of control)
Log [Indoxylglucuronide] (M)
d
Fluorescein uptake (% of control)
Log [kynurenic acid] (M)
e
Fluorescein uptake (% of control)
Log [L-Kynurenine] (M)
f
Fluorescein uptake (% of control)
log [Hippuric acid] (M)
g
Fluorescein uptake (% of control)
Log [p-cresylglucuronide] (M)
h
Fluorescein uptake (% of control)
Log [p-cresylsulfate] (M)

Figure 7.1 Concentration-dependent inhibition of OAT1- and OAT3-mediated fluorescein uptake by anionic uremic toxins.
(a-h) A concentration range of eight uremic toxins were exposed to matured ciPTEC-OAT1 (•) and -OAT3 (°) in the presence of 1 µM fluorescein, a known OAT model substrate. The intracellular fluorescent signal was detected by measuring samples at excitation wavelength 485 nm and emission wavelength 535 nm. Blank data were subtracted and data were normalized to control (absence of uremic toxin). Nonlinear regression analysis was performed using Graphpad Prism 5.02. Data are shown as mean ± S.E.M. of three independent experiments performed, at least, in duplicate.

Table 7.1 Uremic toxins inhibit OAT1- and OAT3-mediated fluorescein uptake.

Uremic toxin	C_m (µM) in ESRD patients[1]	ciPTEC-OAT1 (IC_{50} - µM)	R square	ciPTEC-OAT3 (IC_{50} - µM)	R square
Indoxyl sulfate	110	25 ± 4	0.92	83 ± 41	0.42
L-Kynurenine	6	65 ± 8	0.92	219 ± 66	0.54
Kynurenic acid	1	6 ± 1	0.95	6 ± 1	0.83
Indole-3-acetic acid	4	19 ± 2	0.93	148 ± 60	0.49
Hippuric acid	398	5 ± 1	0.95	22 ± 9	0.78
Indoxyl-β-glucuronide	9	492 ± 68	0.67	527 ± 218	0.55
p-Cresylglucuronide	44	2650 ± 922	0.28	588 ± 81	0.36
p-Cresylsulfate	675	79 ± 14	0.84	112 ± 19	0.80

The eight tested anionic uremic toxins inhibit OAT1- and OAT3-mediated fluorescein uptake in a concentration-dependent manner. Mean plasma levels of uremic toxins in ESRD patients were extracted from Duranton *et al.* (6). R square: goodness of fit values extracted from non-linear regression analysis.

intrinsic PTEC toxicity of the uremic toxins was demonstrated by their ability to reduce renal metabolic capacity and to increase free radical production in proximal tubule epithelial cells (15, 19). Here, the role of BCRP and MRP4 in indoxyl sulfate and kynurenic acid detoxification was studied further using a cell viability assay (Fig. 7.2C and D). CiPTEC showed to be slightly more sensitive to both uremic toxins when BCRP and MRP4 were inhibited by KO143 and MK571 (resp.), as demonstrated by decreased TC_{50} values (indoxyl sulfate: 2.0 ± 0.7 mM; kynurenic acid: 9.0 ± 3.0) compared to the TC_{50} values in the absence of inhibitors, though not significant (Indoxyl sulfate: 3.6 ± 0.6 mM; Kynurenic acid: not applicable). To support the importance of the combined effort of in- and efflux transport pathways especially in indoxyl sulfate detoxification, parent ciPTEC models lacking OAT1 demonstrated enhanced resistance against indoxyl sulfate in the presence of efflux pump inhibitors (TC_{50} 3.0 ± 0.5 mM).

The bioengineered renal tubule shows a three dimensional, tight and differentiated epithelial monolayer

Further development of a biotechnological platform for the removal of protein-bound waste products requires an optimal three-dimensional configuration, as a two-dimensional system poorly predicts renal xenobiotic handling. We recently successfully developed a three-dimensional bioengineered tubule system (27), which we here optimized and determined monolayer integrity by analyzing paracellular diffusion prior to transport experiments. The transepithelial barrier function was measured using a custom-made flow system and inulin as a leakage marker labeled with fluorescein isothiocyanate (FITC), allowing live imaging of hollow fiber membranes (HFM). Differentiated ciPTEC-OAT1 on double-coated HFM were compared to unseeded coated HFM (Fig. 7.3A). Within 1 min of perfusion, unseeded-HFM showed a sustained leakage compared to the fully PTEC covered HFM (Fig. 7.3B-C, no cells: 89 ± 4 % vs. cells: 10 ± 3 %; $p<0.001$). This effect remained stable until the end of the perfusion experiment, thereby confirming the formation of a three-dimensional, efficient and stable transepithelial barrier by ciPTEC-OAT1 on HFM. To further elucidate polarization characteristics of ciPTEC-OAT1 monolayers when cultured in a 3D HFM environment, the barrier function was also evaluated in 2D monolayers cultured on Transwell® filter inserts. When exposed to FITC-inulin, monolayers on inserts showed a limited barrier function of 20 ± 4% ($p= 0.08$) compared to unseeded filters (Fig. S7.1), confirming poor monolayer formation of ciPTEC-OAT1 using 2D systems in

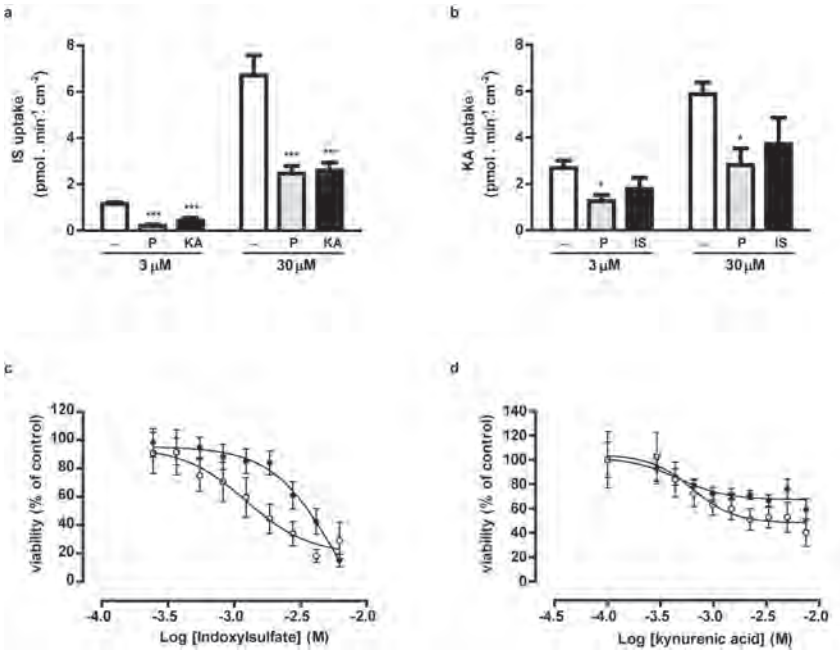

Figure 7.2 Handling of indoxyl sulfate and kynurenic acid by OAT1, BCRP and MRP4 in flat monolayers.

In matured ciPTEC-OAT1, a concentration-dependent uptake of (a) IS and (b) KA (white) was shown using LC-MS/MS analysis of the uremic toxins. In the presence of probenecid (P, grey), the uptake of both toxins was attenuated. Moreover, the IS uptake was inhibited in the presence of KA (100 µM; black), and vice versa. The role of BCRP and MRP4 in the efflux of IS and KA was shown using an MTT assay. The experiment was performed in the absence (•) or presence (◦) of efflux pump inhibitors (KO143 (10 µM) and MK571 (5 µM)). Nonlinear regression analysis was performed using Graphpad Prism 5.02. Data are shown as mean ± S.E.M. of three independent experiments performed in triplicate. *= $p<0.05$, ***= $p<0.001$ using one-way ANOVA analysis followed by Dunnett's multiple comparison test.

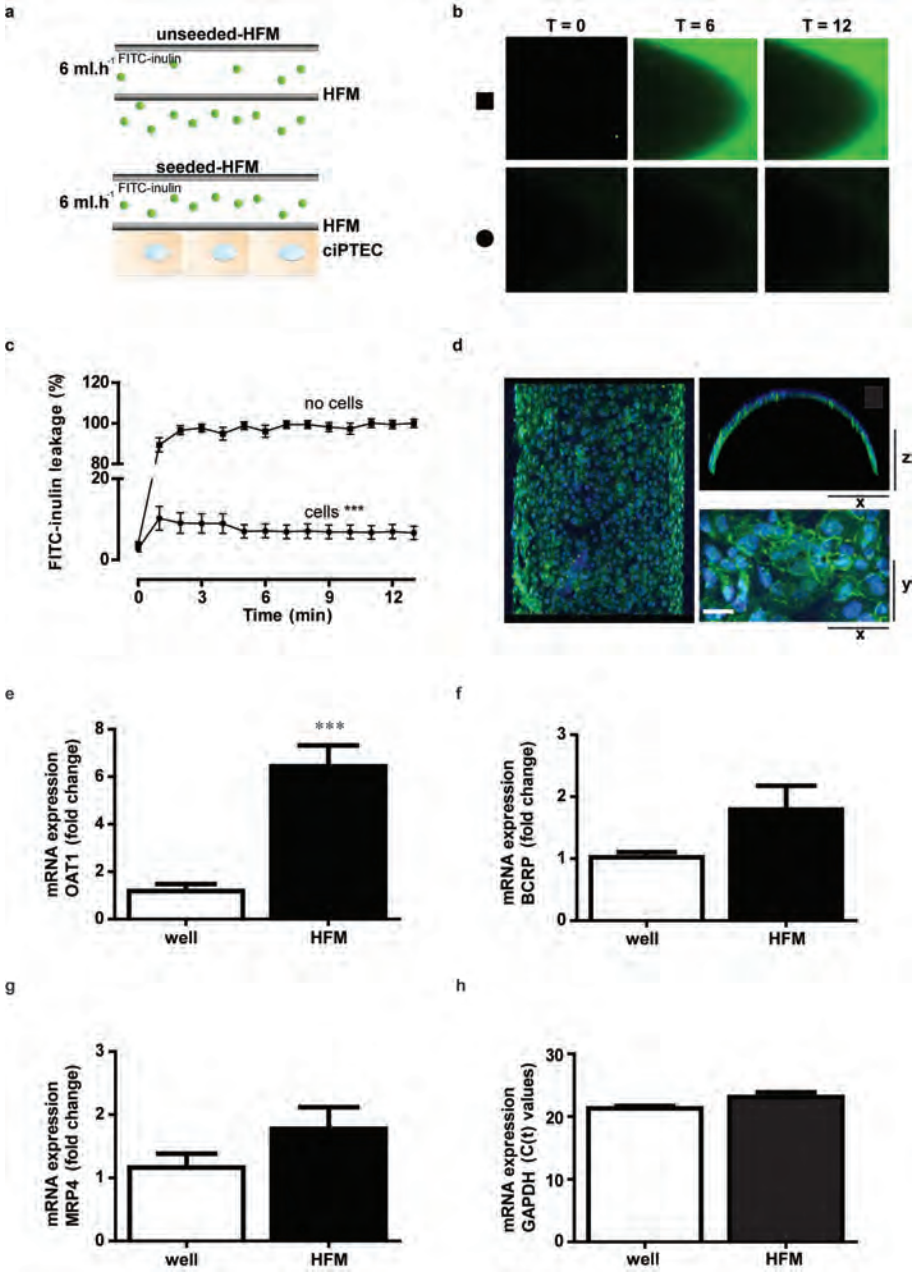
a
unseeded-HFM
6 ml.h-1
FITC-inulin
HFM
seeded-HFM
6 ml.h-1
FITC-inulin
HFM
ciPTEC
b
T = 0
T = 6
T = 12
c
FITC-inulin leakage (%)
120
100
80
20
0
no cells
cells ***
0
3
6
9
12
Time (min)
d
z
x
y
x
e
mRNA expression OAT1 (fold change)
***
8
6
4
2
0
well
HFM
f
mRNA expression BCRP (fold change)
3
2
1
0
well
HFM
g
mRNA expression MRP4 (fold change)
3
2
1
0
well
HFM
h
mRNA expression GAPDH (C(t) values)
30
20
10
0
well
HFM

Figure 7.3 Bioengineered renal tubules show transepithelial barrier function and polarized characteristics.
FITC-inulin leakage was measured in matured ciPTEC-OAT1 seeded on coated HFM. (a) Schematic presentation of the experimental set-up in the absence (upper panel) or presence (lower panel) of cells. (b) Representative eal-time images of the two different conditions are shown; unseeded (square) and seeded (circle) HFM. In the absence of cells, a bright green fluorescent signal was detected at the apical membrane, whereas in the presence of cells the signal was clearly attenuated. Representative real-time images of the two different conditions were shown. (c) Semi-quantification of FITC-inulin diffusion in the absence (square) and the presence of ciPTEC-OAT1 (circle) on HFM. Seeded HFM showed significantly less FITC-inulin leakage demonstrating monolayer tightness. From each single replicate 4 different regions in focus were analyzed. (d) The expression of ZO-1 (green) was demonstrated in a homogenous cell monolayer cultured on HFM. Scale bar: 10 µm. (e-g) The OAT1, BCRP and MRP4 mRNA expression levels were investigated in matured ciPTEC-OAT1 cultured in well plates and on HFM. Gene expression levels were normalized to expression levels of the reference gene GADPH (h) and were expressed as fold increase when cultured on HFM (black) compared to matured cells in well plates (white). Data are shown as mean ± S.E.M. of three independent experiments performed, at least, in duplicate. *** = $p < 0.001$, using an unpaired *t* test.

contrast to the 3D HFM environment. The presence of the tight junction protein ZO-1 along the boundaries of the cells (Fig. 7.3D) further endorsed the epithelial character of a homogenous and polarized cell monolayer on HFM. In addition to monolayer polarization, the expression of OAT1, BCRP and MRP4 in ciPTEC was compared between 2D and 3D cultures. Interestingly, significantly increased expression levels of OAT1 were observed (Fig. 7.3E) as compared to flat monolayers and a trend towards an increase in BCRP and MRP4 (Fig. 7.3F – G) was shown, respectively. These data assume that a 3D environment induces membrane transporter expression, which might be the result of an improved epithelial character in 3D.

Bioengineered renal tubules show organic anion transport activity

To study the activity of OAT1, BCRP and MRP4 in the bioengineered renal tubules, we used the substrate fluorescein and life confocal imaging (Fig. 7.4A-B). Perfusion of the tubes with fluorescein solely (I) resulted in an in intracellular fluorescent signal, which increased significantly in the presence of efflux pumps inhibitors (II). In the presence of indoxyl sulfate (III) and kynurenic acid (IV), the fluorescein uptake was inhibited resulting in a less intense intracellular fluorescent signal. In the final condition (V), fluorescein

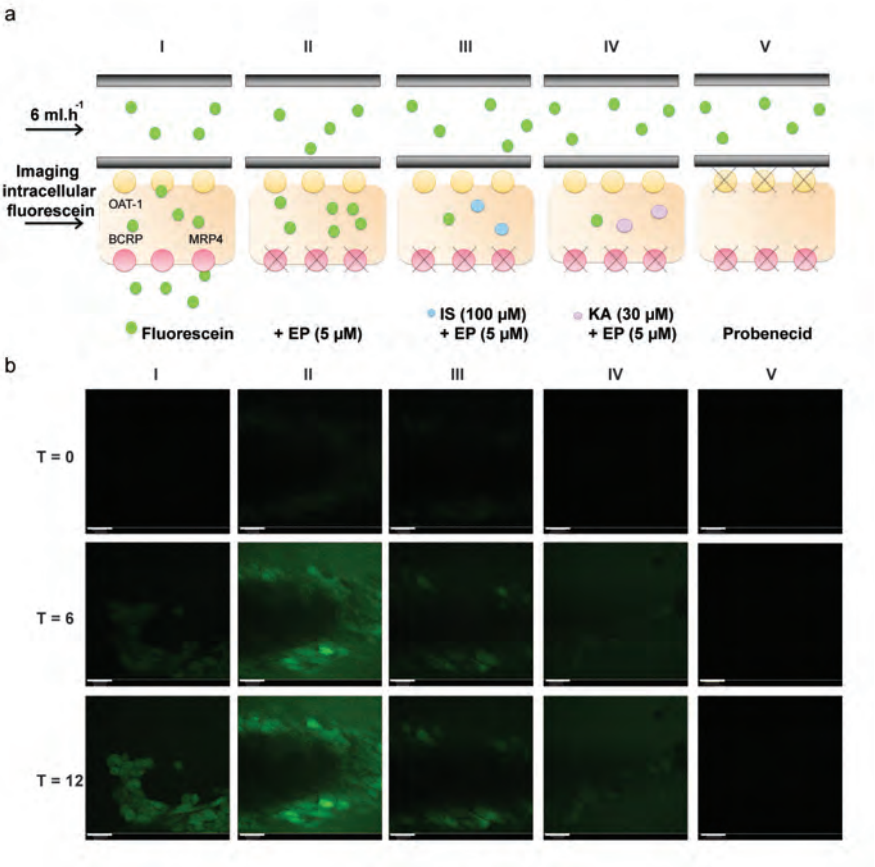

Figure 7.4 OAT1-mediated fluorescein uptake in bioengineered renal tubules.
Fluorescein was used as a model substrate in an advanced fiber perfusion system. (a) Schematic presentation of the experimental set-up: I. Fluorescein perfusion, II. Fluorescein perfusion in the presence of efflux pump inhibitors (EP; (5 µM)), III and IV. Fluorescein perfusion in the presence of efflux pump inhibitors and indoxyl sulfate (III; 100 µM) or kynurenic acid (IV; 30 µM), V. Fluorescein perfusion in the presence of probenecid (P; 100 µM). (b) Representative real-time images of the five different conditions. Scale bare: 10 µm. (c) Semi-quantification of fluorescein uptake data in the absence or presence of the efflux pumps inhibitors solely, in combination with IS and KA, and in the presence of probenecid. From each single replicate 4 different regions

Figure 7.4 Continued

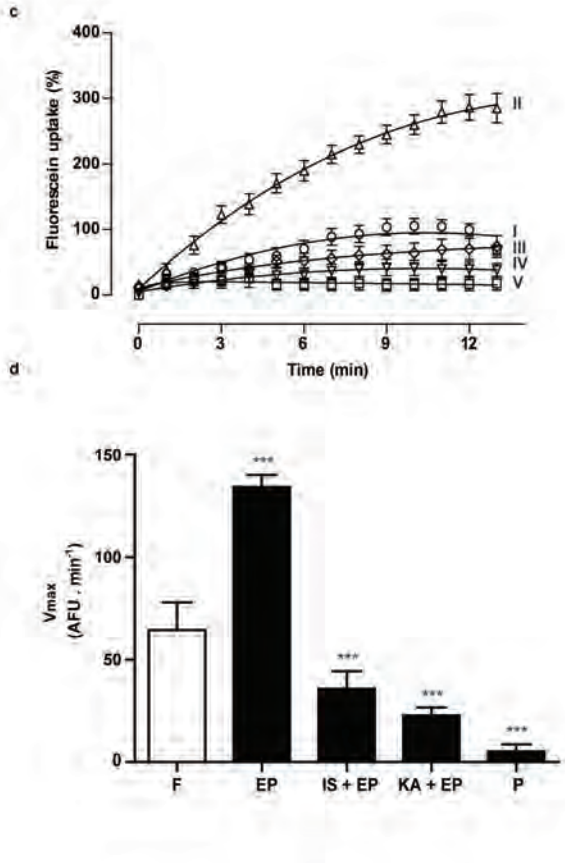

in focus were analyzed. Data were fitted according to one-site total binding saturation curve using non-linear regression analysis. (d) Vmax values from all conditions were calculated from the corrected AFU data according to michaelis-menten kinetics using non-linear regression analysis. For statistical analysis, the Vmax values obtained from condition EP and P where compared to only fluorescein uptake (F). Conditions IS + EP and KA + EP were compared to EP. Data are shown as mean ± S.E.M. of three independent experiments performed in duplicate. *** = $p<0.001$, using one-way ANOVA followed by Dunnett's multiple comparison test.

Figure 7.5

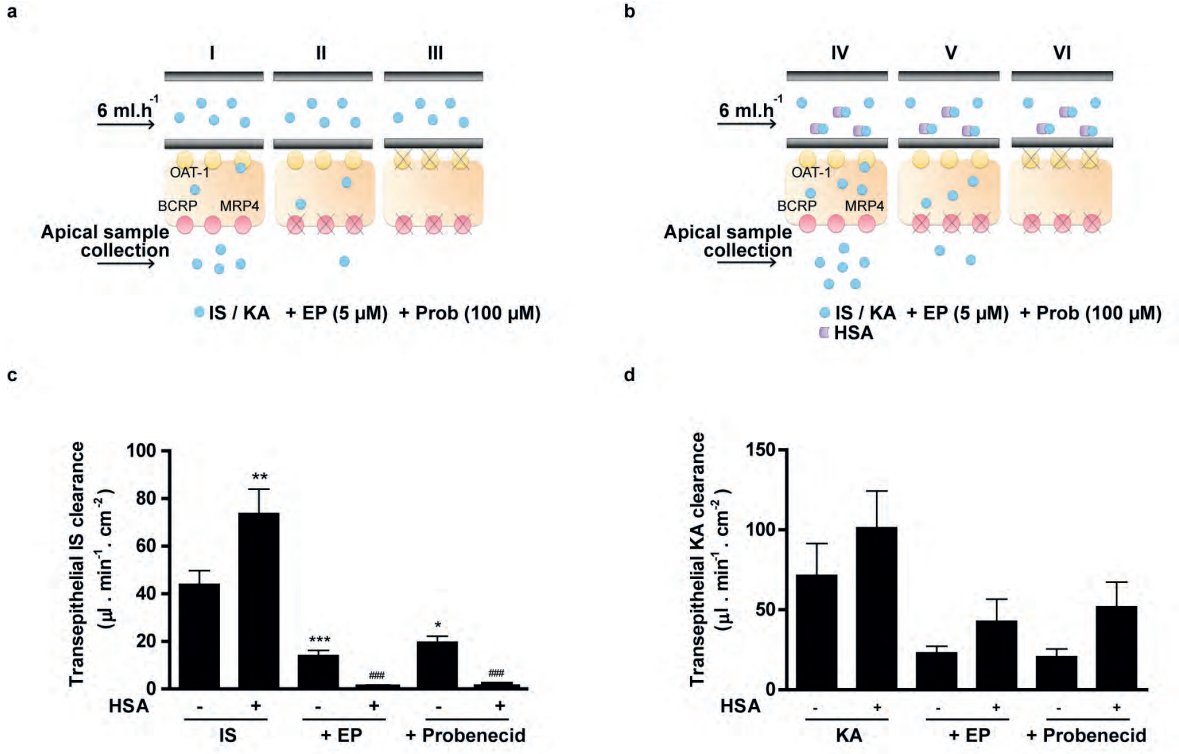
a
I
II
III
6 ml.h-1
OAT-1
BCRP
MRP4
Apical sample collection
IS / KA + EP (5 µM) + Prob (100 µM)
b
IV
V
VI
6 ml.h-1
OAT-1
BCRP
MRP4
Apical sample collection
IS / KA + EP (5 µM) + Prob (100 µM)
HSA
c
Transepithelial IS clearance (µl . min-1 . cm-2)
100
80
60
40
20
0
**
***
###
*
###
HSA
-
+
-
+
-
+
IS
+ EP
+ Probenecid
d
Transepithelial KA clearance (µl . min-1 . cm-2)
150
100
50
0
HSA
-
+
-
+
-
+
KA
+ EP
+ Probenecid

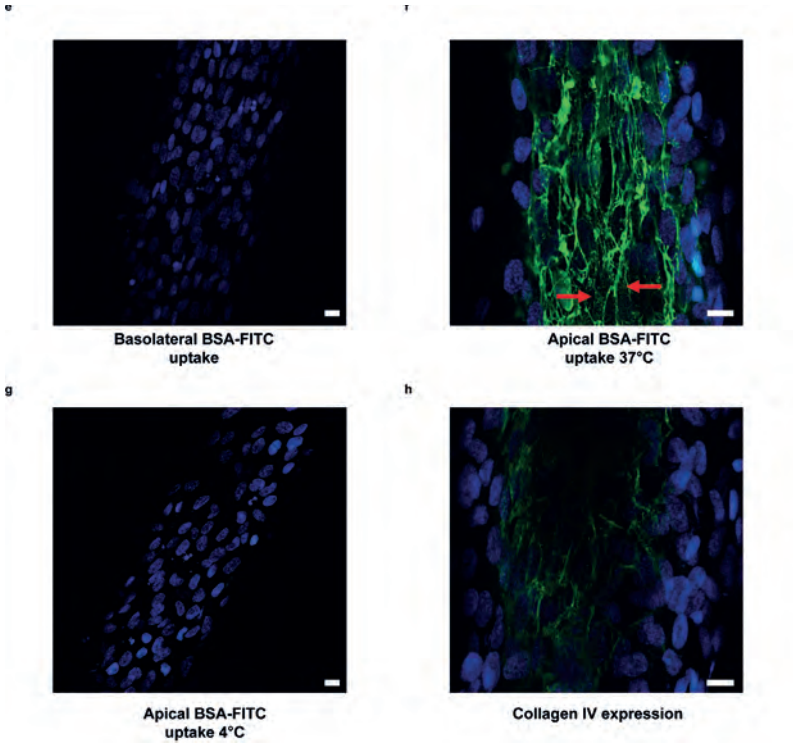

Figure 7.5 Transepithelial clearance of indoxyl sulfate and kynurenic acid in the presence of human serum albumin, and albumin-FITC handling in bioengineered renal tubules.

a-d. Transepithelial clearance of indoxyl sulfate and kynurenic acid. Schematic presentation of the experimental set up of IS and KA transepithelial transport in the absence (a) or presence (b) of HSA is reported. Quantification of IS (c) and KA (d) clearance in the absence (-) or presence (+) of HSA. The protein bound fraction of IS was 73 ± 5 % and 63 ± 8 % of KA was bound to albumin. Data are shown as mean ± S.E.M. of three independent experiments performed in duplicate. *= $p<0.05$, **= $p<0.01$ compared to IS in the absence of HSA, ###= $p<0.001$ compared to IS in the presence of HSA. Statistical analysis was performed using one-way ANOVA followed by Tukey's multiple comparison test. (e-g) Endocytosis-mediated albumin uptake in bioengineered renal tubules. Cellular BSA-FITC uptake (green) in renal tubules (nuclei: blue) after 30 min exposure from the (e) basolateral compartment at 37°C (f) apical compartment at 37°C and (g) apical compartment at 4°C. Active uptake was detected solely when BSA-FITC uptake was performed at 37°C, as indicated by the red arrows. (h) Collagen IV expression (green) in renal tubules showed a highly similar pattern as BSA-FITC uptake as shown in b. Scale bare: 10 µm.

uptake was studied in the presence of probenecid, a blocker of OAT1, which resulted in a strongly diminished uptake. Semi-quantification of the normalized time-lapse experiment is presented in Figure 7.4C. For statistical analysis, maximum uptake (V_{max}) values were calculated from background corrected AFU data (Fig. 7.4D). A significant increased fluorescein uptake was detected when studied in the presence of efflux pumps inhibitors (208 ± 10 %; $p<0.001$). Again, this was inhibited by indoxyl sulfate (45 ± 13 %; $p<0.001$) and kynurenic acid (83 ± 3 %; $p<0.001$). In the presence of probenecid, fluorescein uptake was clearly attenuated as well (96 ± 3 %; $p<0.001$). These findings are compatible with the formation of a functionally active bioengineered renal tubule.

Bioengineered renal tubules facilitate uremic toxin secretion despite protein binding

Lastly, we investigated the capability of the bioengineered renal tubules to actively secrete protein bound uremic toxins. Active clearance of indoxyl sulfate and kynurenic acid in the absence of human serum albumin was studied by perfusing the tubules with 100 μM of the uremic toxin and measuring transport into the apical compartment. This revealed a clearance of 44 ± 6 $\mu l.min^{-1}.cm^{-2}$ and 72 ± 20 $\mu l.min^{-1}.cm^{-2}$ for indoxyl sulfate and kynurenic acid, respectively (Fig. 7.5C-D). This secretion was attenuated by probenecid (by 55 ± 6, $p<0.05$ and 71 ± 7 %, respectively) and by the efflux pumps inhibitors (68 ± 5, $p<0.001$; 68 ± 6 %, respectively), indicating active transepithelial transport of both uremic solutes across the epithelial cell monolayer. In a separate experiment we observed that clearance of the uremic toxins was fully restored after the probenecid treatment, when the bioengineered tubules were re-perfused with the toxins (data not shown). These findings confirmed that the cell monolayer is still viable after multiple treatments, including probenecid incubation, and that probenecid has an inhibitory effect on transport protein level solely. To further mimic the physiological situation, the ability of the bioengineered tubules to facilitate protein-bound toxin transport was shown. In this setup, we achieved a protein binding of indoxyl sulfate slightly lower than previously reported (73 ± 3 %) (28) in the presence of 1 mM HSA. Under the same conditions, kynurenic acid showed a protein binding of 63 ± 5 %. Interestingly, the clearance of protein-bound indoxyl sulfate (74 ± 10 $\mu l.min^{-1}.cm^{-2}$, $p<0.01$) and kynurenic acid (101 ± 23 $\mu l.min^{-1}.cm^{-2}$, ns) was enhanced when compared to the clearance of both toxins in the absence of albumin. Again, transport was attenuated by probenecid (99.4 ± 0.2, $p<0.001$; 49 ± 15 %, respectively) and by the efflux pumps inhibitors (98.9 ± 0.2, $p<0.001$; 58 ± 14

%, respectively). These findings suggest that protein binding positively affects the renal tubular clearance of the uremic toxins.

To study in more detail the mechanism of protein bound uremic toxin handling, we not only performed a basolateral perfusion with FITC-albumin, but also studied the uptake of FITC-albumin from the apical site. Wilmer and Jansen *et al.* previously reported on the presence of a megalin-mediated albumin reabsorption mechanism in ciPTEC, located at the PTEC apical membrane (21-22). Figure 7.5E-G shows BSA-FITC uptake in renal tubules after basolateral or apical exposures. Upon basolateral perfusion, intracellular BSA-FITC could not be detected (Fig. 5E). This observation is in agreement with the retention of albumin in the blood compartment under physiological conditions to prevent protein loss (52). Figure 7.5F shows that active uptake of BSA-FITC was detectable when exposed to the apical compartment at 37°C, thereby confirming that reabsorption is functional in renal tubules (red arrows). Importantly, this uptake was highly reduced when apical exposure took place at 4°C (Fig. 7.5G), thereby further confirming the presence of an active endocytosis process in the bioengineered kidney tubules. Note that the BSA-FITC reabsorbed at 37°C binds to collagens present in the tubules (27). As described by Rueth *et al.*, albumin is known to bind hydrophobic compounds like collagen (48). Concurrently, the pattern observed in ciPTEC upon BSA-FITC reabsorption indeed showed high similarities to the pattern observed when stained against collagen IV (Fig. 7.5H). As a consequence, the typical endocytosis BSA-FITC particles, which are usually detected in this reabsorption mechanism, are less clear in this setting. Nevertheless, these data show that albumin is actively reabsorbed by the apical membrane and not transported along with uremic toxins from the basal compartment across renal tubules.

Discussion

The renal clearance of organic anions, including protein bound endogenous metabolites, highly depends on active secretion, which is confined to the tubular system. In ESRD, this function is severely compromised resulting in the accumulation of these metabolites in patients. Current dialysis therapies insufficiently remove the protein bound uremic toxins, which contributes to the high morbidity and mortality rates of the disease (29), therefore, alternative treatment strategies are warranted. In this study, a

bioengineered renal tubule was successfully developed and transepithelial transport of albumin-bound uremic toxins was demonstrated. Key in this process is the concerted action between (basolateral) uptake and (apical) efflux performed by transporters with designated membrane localization. In exchange for intracellular α-ketoglutarate, the OATs efficiently translocate organic anions from the blood compartment into the intracellular space against an electrochemical gradient. The efflux pumps belonging to the ABC family of transmembrane transporters then couple ATP hydrolysis to their urinary excretion in a unidirectional fashion. Using a unique, robust and complete human cell model, we first identified eight anionic uremic toxins for their interaction with OAT1- and OAT3-mediated transport in flat cell monolayers. Next, the essential role of the ABC transporters BCRP and MRP4 in cellular detoxification through efflux was demonstrated. Finally, a three-dimensional bioengineered tubule containing a polarized cell monolayer with a clear epithelial barrier function was developed. These human bioengineered tubules demonstrated active clearance of albumin-bound anionic uremic toxins as a next step in BAK engineering. Note that the formation of a cellular barrier is not unique for ciPTEC but also found for intestinal epithelial cells when cultured on HFM (data not shown).

The concept of BAK engineering was initiated in the late 80's of last century by Aebischer *et al.* with non-human cell models (*i.e.* the canine derived MDCK or pig originating LLC-PK1 cells) cultured on HFM (30). Follow-up studies by Humes and co-workers used cells of human origin, but with a major focus on the immunomodulatory effects for treatment of critically ill patients suffering from acute kidney injury (31-33). Phase I and II clinical trials showed reduced cytokine levels and long-term survival improvement compared to the non-treated group. However, a follow-up clinical phase IIb trial failed due to difficulties in the manufacturing process of the BAK and the clinical study design (34). One of the challenges to successfully develop a BAK is a suitable cell source to replace transport functions of the kidneys (32, 35). Primary renal epithelial cells show a high batch-to-batch variability in quality and function and dedifferentiation upon prolonged cultivation, and therefore hamper reproducibility. Moreover, to obtain a sufficient number of primary renal epithelial cells for a BAK approach is another hurdle to overcome (35). Recent advances in the application of stem cells (i.e. of embryonic origin or induced pluripotent cells) into a PTEC-like phenotype is a promising alternative (36-38) , but this has not been characterized sufficiently nor their capability to maintain the OATs in culture has been proven. Human renal

cells loose the expression of these essential transport proteins and (in part) their proximal tubular phenotype upon culturing (21, 39). This phenomenon has already been described in 1990 (40) and has, as of yet, not been solved, however, stable expression of OATs in renal cell lines is a prerequisite for renal functional replacement therapies as emphasized in a BAK. Here, we applied a recently optimized, robust and translational human renal cell model that endogenously expresses a panel of renal xenobiotic transporters successfully complemented with the OATs (21-23). This appeared to be an asset, as we demonstrated for the first time active renal tubular secretion of the protein-bound uremic toxins indoxyl sulfate and kynurenic acid.

Using a conventional two-dimensional approach, the potency of eight uremic toxins to inhibit basolateral OAT1 and -3 mediated transport at clinically relevant concentrations was demonstrated (6, 20). The inhibitory potencies are in good agreement with previously published data obtained in animal models or in transfected cell systems expressing OAT1 or OAT3 (18, 20). We selected two uremic toxins because of the highest inhibitory potency (kynurenic acid, this study) and widely described associations with uremic syndrome complications (indoxyl sulfate)(8, 11). Indoxyl sulfate has been considered to be a causative factor in CRF progression (41), with most likely a dominant role of hOAT1 as its affinity for this transporter is at least 3-fold higher as compared to OAT3 (this study and (18)). Parent ciPTEC, lacking OAT1, were more resistant against indoxyl sulfate, but in ciPTEC-OAT1 a concentration-dependent reduction in cell viability was found. This effect was amplified when inhibitors of the efflux transporters, BCRP and MRP4, were applied, confirming the concerted action of uptake and efflux transporters in uremic toxin handling. Kynurenic acid showed a lower intrinsic toxicity as compared to indoxyl sulfate, despite its higher affinity for OAT1 (this study), BCRP and MRP4 (14). The molecular mechanisms through which both uremic toxins exert their cytotoxic potential are largely unrevealed.

The high affinity of kynurenic acid for OAT1, BCRP and MRP4 was demonstrated further by the higher bioengineered renal tubular clearance as compared to the elimination of indoxyl sulfate, either in the presence or absence of albumin. Moreover, it was shown that albumin itself is not taken up by ciPTEC from the basolateral site, but actively reabsorbed from the apical compartment. Interestingly, in the presence of albumin the transport of indoxyl sulfate and kynurenic acid was enhanced, which emphasizes the ability of ciPTEC to shift the protein-binding and allow for active secretion of the free fraction. These

data support that albumin may stimulate transport of organic anions, as was suggested earlier in the 80's of last century by Besseghir and Depner *et al.* They showed that albumin facilitated para-aminohippurate uptake in isolated rabbit proximal tubules and rat kidney slices (42, 43). Moreover, Pichette *et al.* demonstrated altered dynamics of furosemide in hypoalbuminaemic rabbits (44, 45). Furosemide is a known diuretic agent, and organic anion, which targets the Na^+-K^+-Cl^- cotransporter-2 (NKCC2) located downstream the proximal segment in the apical membrane of the thick ascending limb of Henle's loop. Furosemide is highly protein bound (approx. 98%, (44)) and actively secreted via the proximal tubules into the apical compartment. In hypoalbuminaemic rabbits, higher furosemide doses were required to achieve a similar diuretic effect as in control rabbits (44), supporting the important role of albumin in facilitating active transport of the organic anion. This may be the result of electronegative to -neutral transition of the compounds when bound to albumin and/or post-translational modifications of albumin when toxins are bound (46, 47). The tertiary structure of albumin may also stimulate the binding and transport of metabolites across the capillary wall into the interstitial compartments. As shown recently, the binding capacity of albumin was demonstrated to be diminished in CRF patients, most likely due to post-translational guanidylation of albumin sites (48). The attenuated albumin binding capacity in CRF patients will probably contribute to less efficient transport of uremic toxins by PTEC, thus resulting in elevated plasma levels and their known consequences. Note that the double-coated HFM used in our bioengineered renal tubules allow albumin to reach the target transporters, emphasizing further the potential of the device in BAK applications. Future research should elucidate the impact of modified albumin as observed in uremic patients in the removal of uremic toxins using a BAK platform.

Altogether, a successful bioartifical renal tubule was established which presented a clear barrier function and facilitated transepithelial transport of protein-bound indoxyl sulfate and kynurenic acid. This provides an innovative basis for regenerative nephrology through advanced function replacement and paves the way to progress towards potential clinical applications focusing at: i) optimization and up-scaling of the system with the aim of maintaining the best possible cell function under sterile conditions for extended time periods; ii) *in vitro* validation of the bioreactor with respect to uremic toxin kinetics; iii) the safety aspects as ciPTEC are classified as GMO's, for which thorough research in agreement with European guidelines for advanced therapy medicinal products (European Medicines Agency) is needed to enable

the applications of GMO in medicinal products (49); iv) preclinical validation of the model, and v) prediction of uremic toxin clearance by the bioengineered system in clinical settings, for which research should be directed at building a physiologically-based computational model. This allows predicting the capacity needed for treatment of uremia and defining the most suitable application strategies in function of solute kinetics. Hence, such model would not only apply to uremia treatment, but can be used for mimicking 3D scenarios of kidney disease modeling as well as for drug- toxicity and -efficacy testing.

Acknowledgments

This research was performed as part of the Netherlands Institute for Regenerative Medicine (NIRM, grant no. FES0908), funded by the Dutch Ministry of Economic Affairs. Furthermore, the financial contribution of the Dutch Kidney Foundation is gratefully acknowledged (KJPB 11.0023), as well as the Netherlands Organization for Scientific Research (016.130.668) and the Marie Curie ITN project: BIOART (grant no.316690, EU-FP7-PEOPLE-ITN-2012). The authors declare that they have no conflict of interest.

Author contributions

J.J. and M.F. performed literature search, experimental design, data collection, analysis and interpretation, created figures and wrote the paper. U.M.K. and J.G.P. contributed to data collection and analysis of transport assays in flat monolayers and bioengineered renal tubules. A.B. contributed to uremic toxin LC/MS-MS measurements. M.J.W. contributed to experimental design, data interpretation and manuscript writing. R.A.M. and T.J.B. contributed to compound synthesis and manuscript writing. J.F.M.W. contributed to data interpretation from a clinical point of view and manuscript writing. D.S., L.P.H and J.G.H. contributed to experimental design, data interpretation and manuscript writing. R.M. contributed to literature search, experimental design, data interpretation and manuscript writing.

Competing financial interest

The authors declare no competing financial interests. The experiments described in this article comply with the current laws of the country in which they were performed (the Netherlands).

REFERENCES

1. Ortiz, A., et al. Epidemiology, contributors to, and clinical trials of mortality risk in chronic kidney failure. Lancet. 383, 1831-1843 (2014).
2. Vanholder, R., et al. A bench to bedside view of uremic toxins. J Am Soc Nephrol. 19, 863-870 (2008).
3. Go, A.S., Chertow, G.M., Fan, D., McCulloch, C.E., Hsu, C.Y. Chronic kidney disease and the risks of death, cardiovascular events, and hospitalization. N Engl J Med. 351, 1296-1305 (2004).
4. Roodnat, J.I., et al. 15-year follow-up of a multicenter, randomized, calcineurin inhibitor withdrawal study in kidney transplantation. Transplantation. 98, 47-53 (2014).
5. Segev, D.L. Innovative strategies in living donor kidney transplantation. Nat Rev Nephrol. 8, 332-338 (2012).
6. Duranton, F., et al. Normal and pathologic concentrations of uremic toxins. J Am Soc Nephrol. 23, 1258-1270 (2012).
7. Deltombe, O., et al. Exploring Protein Binding of Uremic Toxins in Patients with Different Stages of Chronic Kidney Disease and during Hemodialysis. Toxins (Basel). 7, 3933-3946 (2015).
8. Uwai, Y., Honjo, H., Iwamoto, K. Interaction and transport of kynurenic acid via human organic anion transporters hOAT1 and hOAT3. Pharmacol Res. 65, 254-260 (2012).
9. Lin, C.J., et al. Indoxyl sulfate predicts cardiovascular disease and renal function deterioration in advanced chronic kidney disease. Arch Med Res. 43, 451-456 (2012).
10. Pletinck, A., et al. Protein-bound uremic toxins stimulate crosstalk between leukocytes and vessel wall. J Am Soc Nephrol. 24, 1981-1994 (2013).
11. Barreto, F.C., et al. Serum indoxyl sulfate is associated with vascular disease and mortality in chronic kidney disease patients. Clin J Am Soc Nephrol. 4, 1551-1558 (2009).
12. Itoh, Y., Ezawa, A., Kikuchi, K., Tsuruta, Y., Niwa, T. Protein-bound uremic toxins in hemodialysis patients measured by liquid chromatography/tandem mass spectrometry and their effects on endothelial ROS production. Anal Bioanal Chem. 403, 1841-1850 (2012).
13. Poveda, J., et al. p-cresyl sulphate has pro-inflammatory and cytotoxic actions on human proximal tubular epithelial cells. Nephrol Dial Transplant. 29, 56-64 (2014).
14. Mutsaers, H.A., et al. Uremic toxins inhibit transport by breast cancer resistance protein and multidrug resistance protein 4 at clinically relevant concentrations. PLoS One. 6, e18438 (2011).
15. Mutsaers, H.A., et al. Uremic toxins inhibit renal metabolic capacity through interference with glucuronidation and mitochondrial respiration. Biochim Biophys Acta. 1832, 142-150 (2013).

16. Lowenstein, J. The anglerfish and uremic toxins. FASEB J. 25, 1781-1785 (2011).
17. Eloot, S., et al. Does the adequacy parameter Kt/V(urea) reflect uremic toxin concentrations in hemodialysis patients? PLoS One. 8, e76838 (2013).
18. Deguchi, T., et al. Characterization of uremic toxin transport by organic anion transporters in the kidney. Kidney Int. 65, 162-174 (2004).
19. Motojima, M., Hosokawa, A., Yamato, H., Muraki, T., Yoshioka, T. Uraemic toxins induce proximal tubular injury via organic anion transporter 1-mediated uptake. Br J Pharmacol. 135, 555-563 (2002).
20. Masereeuw, R., et al. The kidney and uremic toxin removal: glomerulus or tubule? Semin Nephrol. 34, 191-208 (2014).
21. Jansen, J., et al. A morphological and functional comparison of proximal tubule cell lines established from human urine and kidney tissue. Exp Cell Res. 323, 87-99 (2014).
22. Wilmer, M.J., et al. Novel conditionally immortalized human proximal tubule cell line expressing functional influx and efflux transporters. Cell Tissue Res. 339, 449-457 (2010).
23. Nieskens, T.T.G.P., et al. A human renal proximal tubule cell line with stable organic anion transporter 1 and 3 expression predictive for antiviral-induced toxicity. AAPS J. 2016; 18:465-75.
24. Neirynck, N., et al. Review of protein-bound toxins, possibility for blood purification therapy. Blood Purif. 35, 45-50 (2013).
25. Dankers, A.C., et al. Hyperuricemia influences tryptophan metabolism via inhibition of multidrug resistance protein 4 (MRP4) and breast cancer resistance protein (BCRP). Biochim Biophys Acta. 1832, 1715-1722 (2013).
26. Vanwert, A.L., Bailey, R.M., Sweet, D.H. Organic anion transporter 3 (Oat3/Slc22a8) knockout mice exhibit altered clearance and distribution of penicillin G. Am J Physiol Renal Physiol. 293, F1332-1341 (2007).
27. Jansen, J., et al. Human proximal tubule epithelial cells cultured on hollow fibers: living membranes that actively transport organic cations. Sci Rep. 5, 16702 (2015).
28. Viaene, L., et al. Albumin is the main plasma binding protein for indoxyl sulfate and p-cresyl sulfate. Biopharm Drug Dispos. 34, 165-175 (2013).
29. Sirich, T.L., Meyer, T.W., Gondouin, B., Brunet, P., Niwa, T. Protein-bound molecules: a large family with a bad character. Semin Nephrol. 34, 106-117 (2014).
30. Aebischer, P., Ip, T.K., Panol, G., Galletti, P.M. The bioartificial kidney: progress towards an ultrafiltration device with renal epithelial cells processing. Life Support Syst. 5, 159-168 (1987).
31. Humes, H.D., et al. Initial clinical results of the bioartificial kidney containing human cells in ICU patients with acute renal failure. Kidney Int. 66, 1578-1588 (2004).
32. Tasnim, F., et al. Achievements and challenges in bioartificial kidney development. Fibrogenesis Tissue Repair. 3, 14 (2010).

33. Tumlin, J., et al. Efficacy and safety of renal tubule cell therapy for acute renal failure. J Am Soc Nephrol. 19, 1034-1040 (2008).
34. Humes, H.D., Buffington, D., Westover, A.J., Roy, S., Fissell, W.H. The bioartificial kidney: current status and future promise. Pediatr Nephrol. 29, 343-351 (2014).
35. Jansen, J., et al. Biotechnological challenges of bioartificial kidney engineering. Biotechnol Adv. 32, 1317-1327 (2014).
36. Takasato, M., et al. Kidney organoids from human iPS cells contain multiple lineages and model human nephrogenesis. Nature. 526, 564-568 (2015).
37. Morizane, R., et al. Nephron organoids derived from human pluripotent stem cells model kidney development and injury. Nat Biotechnol. 33, 1193-1200 (2015).
38. Lawrence, M.L., Chang, C.H., Davies, J.A. Transport of organic anions and cations in murine embryonic kidney development and in serially-reaggregated engineered kidneys. Sci Rep. 5, 9092 (2015).
39. Van der Hauwaert, C., et al. Expression profiles of genes involved in xenobiotic metabolism and disposition in human renal tissues and renal cell models. Toxicol Appl Pharmacol. 279, 409-418 (2014).
40. Miller, J.H. Sodium-sensitive, probenecid-insensitive p-aminohippuric acid uptake in cultured renal proximal tubule cells of the rabbit. Proc Soc Exp Biol Med. 199, 298-304 (1992).
41. Niwa, T., Ise, M. Indoxyl sulfate, a circulating uremic toxin, stimulates the progression of glomerular sclerosis. J Lab Clin Med. 124, 96-104 (1994).
42. Besseghir, K., Mosig, D., Roch-Ramel, F. Facilitation by serum albumin of renal tubular secretion of organic anions. Am J Physiol. 256, F475-484 (1989).
43. Depner, T.A. Suppression of tubular anion transport by an inhibitor of serum protein binding in uremia. Kidney Int. 20, 511-518 (1981).
44. Pichette, V., Geadah, D., du Souich, P. The influence of moderate hypoalbuminaemia on the renal metabolism and dynamics of furosemide in the rabbit. Br J Pharmacol. 119, 885-890 (1996).
45. Pichette, V., Geadah, D., du Souich, P. Role of plasma protein binding on renal metabolism and dynamics of furosemide in the rabbit. Drug Metab Dispos. 27, 81-85 (1999).
46. Fanali, G., et al. Human serum albumin: from bench to bedside. Mol Aspects Med. 33, 209-290 (2012).
47. Ghuman, J., et al. Structural basis of the drug-binding specificity of human serum albumin. J Mol Biol. 353, 38-52 (2005).
48. Rueth, M., et al. Guanidinylations of albumin decreased binding capacity of hydrophobic metabolites. Acta Physiol (Oxf). 215, 13-23 (2015).

49. European medicines agency: committee for advanced therapies. Classification of advanced therapy medicinal products. http://www.ema.europa.eu/docs/en_GB/document_library/Scientific_guideline/2012/12/WC500136422.pdf. (2012).
50. Feigenbaum J, Neuberg CA. Simplified Method for the Preparation of Aromatic Sulfuric Acid Esters. J Am Chem Soc. 63, 3529-3530 (1941).
51. Desai RN, Blackwell LF. TEMPO-mediated regiospecific oxidation of glucosides to glucuronides. Synlett. 13, 1981-1984 (2003).
52. Tojo, A. and S. Kinugasa. Mechanisms of glomerular albumin filtration and tubular reabsorption. *Int J Nephrol.* **2012**, 481520 (2012).

SUPPLEMENTARY INFORMATION

Methods

Chemicals and cell culture materials

The uremic toxin p-cresylsulfate (pCS) was synthesized *via* a modified literature procedure (50). NaOH was used instead of KOH to afford pCS as its sodium salt. ^{1}H-NMR (500 MHz, D_2O) δ 7.10 (d, *J* = 8.0 Hz, 1H), 6.78 (d, *J* = 8.0 Hz, 1H), 2.22 (s, 1H). ^{13}C-NMR (126 MHz, D_2O) δ 148.85, 136.49, 130.17, 121.33, 19.95. *p*-Cresylglucuronide (pCG) was synthesized according to a procedure by Desai and Blackwell *et al.* using a modified workup (51). The crude product was purified by silica flash column chromatography (gradient: 0-15% H_2O/MeCN), after which the appropriate fractions were combined and concentrated *in vacuo*. The purified product was subsequently freeze dried to afford pCG as a white solid (60.5%). ^{1}H- and ^{13}C-NMR spectra matched the reported data.

Cell culture of ciPTEC-OAT1 and -OAT3

In standard cell culture approaches, cells were seeded in well plates or Transwell inserts using a density of 63,000 cells/cm^2 or 110,000 cells/cm^2 for ciPTEC-OAT1, respectively, and 82,000 cells/cm^2 for ciPTEC-OAT3 and were cultured for 24 h at 33°C, 5 % (v/v) CO_2, to proliferate and subsequently transferred to 37°C, 5 % (v/v) CO_2 for 7 days to mature.

Prior to ciPTEC-OAT1 seeding on the outside of HFM (1.0 x 10^6 cells/ml), fibers were biofunctionalized using a coating combination consisting out of 3,4-Dihydroxy-L-phenylalanine (L-DOPA; 2 mg/ml) and collagen IV (25 µg/ml), as previously described by Jansen *et al.* (27), and cells were seeded and cultured accordingly.

Fluorescein inhibition assay

Briefly, a concentration range (mM – nM) of indoxylsulfate, indole-3-acetic acid, indoxyl glucuronide, L-kynurenine, kynurenic acid, hippuric acid, p-cresylglucuronide and p-cresylsulfate were exposed to ciPTEC-OAT1 and -OAT3 cells in the presence of a known OAT substrate, fluorescein (1 µM), for 10 min at 37°C, 5 % (v/v) CO_2. After uptake arrest, intracellular fluorescence was detected at excitation wavelength 485 nm and emission wavelength 535 nm, using a Victor™ X3 multilabel platereader (Perkin-Elmer, Groningen, The Netherlands).

Uptake of indoxyl sulfate and kynurenic acid by ciPTEC-OAT1

Active OAT1-mediated uptake of indoxyl sulfate and kynurenic acid was investigated using two concentrations of toxins. Prior to the uptake, matured cells cultured in 48-well plates were pre-incubated using krebs-henseleit buffer supplemented with 10 mM Hepes (KHH buffer, pH 7.4) in the presence or absence of probenecid (100 µM), kynurenic acid (100 µM) or indoxyl sulfate (100 µM) for 30 min at 37°C, 5 % (v/v) CO_2. Next, the cells were exposed to either indoxyl sulfate (3 and 30 µM) or kynurenic acid (3 and 30 µM) for 10 min at 37°C, 5 % (v/v) CO_2 and the uptake was arrested using ice-cold KHH buffer. Finally, cells were lysed using perchloric acid (3.3 % (v/v)) for 1h at room temperature (rT) and were ready for analysis.

Cell viability assay

Matured ciPTEC-OAT1 were exposed to a concentration range (mM - µM) of indoxyl sulfate or kynurenic acid in serum-free culture medium in the presence or absence of the BCRP and MRP4 efflux pump inhibitors, KO143 (10 µM) and MK571 (5 µM), for 24h at 37°C, 5 % (v/v) CO_2. After 4 hours of incubation, the intracellular accumulated precipitate was detected by measuring samples at a wavelength of 570 nm from which the background was subtracted, using a Benchmark Plus plate reader (Bio-rad Laboratories, Veenendaal, The Netherlands).

Monolayer polarization and transepithelial barrier function

To investigate the barrier function of matured ciPTEC-OAT1 cultured on HFM, the fibers were mounted on a separated inlet and outlet glass cannula (DMT Trading, Aarhus, Denmark) stabilized by a frame glued to a petri-dish, forming a separated basolateral (inner HFM) and apical compartment (outer HFM), containing KHH buffer (pH 7.4). A syringe pump (Terumo STC-521, Terumo Europe N.V., Leuven, Belgium) was connected to the inlet cannula by tubing, whereas the outlet cannula was connected by tubing to a depot to collect the perfusate. The chamber was installed on the Zeiss LSM510 META microscope (Zeiss, Oberkochen, Germany). Double coated HFM in the presence or absence of matured ciPTEC were perfused with FITC-inulin (0.1 mg/ml in KHH buffer) and diffusion was measured real-time for 13 min at 37°C, 5 % (v/v) CO_2.

Fixed and permeabilized cell monolayers were blocked and subsequently incubated against ZO-1(1:50 dilution in block solution; Invitrogen, Carlsbad, CA) for 1h at room temperature (rT). Next, cells were incubated with goat-

anti-rabbit-Alexa488 conjugate (1:200, Abcam, Cambridge, UK) and finally nuclei were stained using DAPI (300 nM, Life Technologies) for 5 min at rT. Images were captured using the Olympus FV1000 Confocal Laser Scanning Microscope (Olympus, Tokyo, Japan) and the Olympus software FV10-ASW version 1.7.

Detection of OAT1, BCRP and MRP4 mRNA expression

To extract RNA from matured cells cultured on fibers, the RNAqueous® Micro Kit (Ambion, Carlsbad, CA) was used. RNA extraction from cells cultured in well plates was performed using the RNeasy® Mini Kit (Qiagen, Venlo, Netherlands), both kits were used according to the manufacturer's protocol. Subsequently, cDNA was synthesized using the M-MLV reverse transcriptase kit (Invitrogen, Carlsbad, CA). The mRNA expression levels of ciPTEC transporter genes were detected using gene specific primer-probe sets (Table S7.1) and TaqMan Universal PCR Master Mix (Applied Biosystems, Branchburg, NJ). The quantitative PCR reactions were performed using the CFX96 Real Time PCR system (Bio-Rad Laboratories, Veenendaal, Netherlands) and data were analyzed using the CFX Manager software (Bio-Rad Laboratories, Veenendal, Netherlands).

Fluorescein assay

To measure active fluorescein uptake, the fibers were perfused using 1 µM fluorescein in KHH in the presence or absence of specific drug transporter inhibitors (OAT1 inhibitor probenecid (100 µM), and efflux pump (EP) inhibitors KO143 (5 µM, to block BCRP), PSC833 (5 µM, to block any minor P-gp contribution) (Tocris Bioscience, Minneapolis, MN) and MK571 (5 µM, to block MRP4)) for 13 min at 37°C, 5 % (v/v) CO_2. Prior to fluorescein perfusion, fibers were pre-incubated using similar concentrations of inhibitors in KHH for 5 min at 37°C, 5 % (v/v) CO_2. To investigate the interaction of fluorescein (1 µM) and the uremic toxins indoxyl sulfate and kynurenic acid in ciPTEC cultured on HFM, fibers were exposed to indoxyl sulfate (100 µM) or kynurenic acid (30 µM) in combination with EP inhibitors for 13 min at 37°C, 5 % (v/v) CO_2. The fluorescein uptake was examined in real-time and imaging was performed using the Zeiss LSM510 META microscope (Zeiss, Oberkochen, Germany). Semi-quantification of real-time data was performed using Image J software (version 1.40g). From each single replicate 4 different cellular regions in focus were analyzed.

Methods to figure S7.1

Transepithelial barrier function of ciPTEC-OAT1 monolayers in 2D

To investigate the barrier function of matured ciPTEC-OAT1 cultured on 2D Transwell inserts, both compartments were washed once using KHH prior to FITC-inulin (0.1 mg/ml in KHH buffer) exposure basolaterally for 1h at 37°C, 5% (v/v) CO_2. Fluorescence was detected by measuring samples (75 µl) at excitation wavelength 485 nm and emission wavelength 535 nm, using a Victor™ X3 multilabel platereader. Blank data were subtracted and normalized data were plotted.

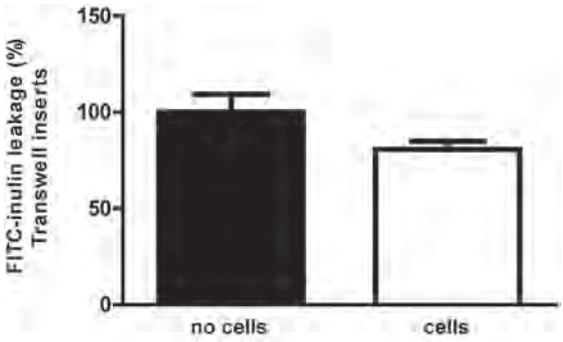

Figure S7.1 FITC-inulin diffusion in matured ciPTEC-OAT1 monolayers cultured in 2D systems.

The FITC-inulin leakage was measured in matured ciPTEC-OAT1 seeded on coated Transwell© filter inserts. A limited transepithelial barrier function was observed in the presence of cells (white) compared to unseeded Transwell filters (black) after 13 min. Data are shown as mean ± S.E.M. of three independent experiments performed in triplicate.

Table S7.1: Taqman primer-probe sets.

Gene	Catalogue number
OAT1 (*SLC22A6*)	Hs00537914_m1
BCRP (*ABCG2*)	Hs00184979_m1
MRP4 (*ABCC4*)	Hs00195260_m1
GAPDH	Hs99999905_m1

Chapter 8

GENERAL DISCUSSION

GENERAL DISCUSSION

The kidneys play a pivotal role in the homeostasis of many physiological processes in the human body (1). As such, the removal of waste products by proximal tubule epithelial cells from blood into the pro-urine is of major importance to maintain a healthy balance. Disease onset is often multi-causal and an abrupt loss or a severe decline in kidney function will contribute to the development of the uremic syndrome and its associated complications (2, 3). To substitute kidney function, patients have to be treated with renal replacement therapies such as hemodialysis. However, hemodialysis is not adequate in the removal of waste products (i.e. uremic toxins) and as organ transplants are scarce, the development of new treatment modalities is warranted. Therefore, this thesis aimed to develop innovative approaches to replace or improve the proximal tubule function. In this chapter, the knowledge obtained in this thesis, in particular with respect to bioartificial kidney engineering, is being discussed in the current context of regenerative nephrology.

In vitro models to facilitate bioengineering and disease modeling

To date, numerous proximal tubule epithelial cell models have been characterized and applied in bioartificial kidney (BAK) engineering (4). Initially, animal-derived models such as the porcine Lilly Laboratories Cell Porcine Kidney proximal tubular cells (LLC-PK1) or dog Madin-Darby Canine Kidney (MDCK) cell lines, with limited transporter function, were applied in cell-based approaches, as human models were not available. Nowadays, human primary renal epithelial cell models as well as immortalized cell systems are widely used for BAK purposes. Although primary cells reflect most closely the physiological demands, a high batch-to-batch variability in function as well as the isolation of a sufficient number of cells hampered the implementation of primary renal epithelial cells in a BAK (4). As such, Humes and co-workers developed the Bioartificial Renal Epithelial Cell System (BRECS) (5). The BRECS was designed to maintain a dense population of primary adult human renal epithelial cells grown on coated carbon disks within the system. After the cells reach an optimal density, the BRECS can be cryopreserved, transported, and stored, thereby reducing many practical limitations previously encountered by cell-based therapies using primary cells. Although metabolic activity like oxygen consumption and the epithelial character was demonstrated by zona occludens 1 (ZO-1) and aminopeptidase-N expression in BRECS monolayers,

the presence of essential proximal tubule epithelial cell (PTEC) transporters has, as of yet, not been demonstrated nor any active excretion of uremic toxins (6, 7). Hence, the proof-of-concept with BRECS for BAK purposes to treat uremia still needs to be demonstrated. As such, a crucial step in the validation of BRECS is to determine anionic and cationic transport activities and compare functionality to other PTEC models as described in chapter 2 and 4 of this thesis.

The concerted action of organic anion and cation in- and efflux transporters is an essential characteristic for a suitable BAK model. It was shown that ciPTEC encompass a broad range of PTEC-specific transporters which are essential in studying renal transport of pharmaceutical and physiological entities as compared to other human renal cell models, such as the widely distributed HK-2 cell line which lacks OCTs, OATs and BCRP (4). Initially the endogenous expression of the organic anion influx transporters OAT1 and OAT3 was absent in the ciPTEC models, which is a known phenomenon of renal cells in culture (8). However, both organic anion transporters were recently successfully incorporated in ciPTEC, as described by Nieskens *et al.* (9). Such, more complete ciPTEC model is a promising tool in BAK engineering, but the cell line appears to be suitable for other applications as well, like drug- toxicity and - efficacy testing and for kidney disease modeling. The latter subject was addressed in Chapter 3, where ciPTEC was used as an experimental inflammatory model to mimic septic acute kidney injury *in vitro* and to study molecular processes upon therapeutic interventions. This was demonstrated with dexamethasone, for which the molecular mechanism involving a mitochondrial target was unravelled. Altogether, ciPTEC models represent a broad range of essential drug transporters concerted by a high metabolic activity ((10, 11) and this thesis).

Another interesting finding in this thesis is the fact that cells isolated from urine demonstrated comparable physiological characteristics with respect to functional proteins (e.g. drug transporters, endocytosis receptors) when compared to kidney tissue-derived cell models (12). Differences found between the cell sources were predominantly related to ECM proteins. A possible explanation for a reduced capability of urine cells to excrete ECM proteins might be the reason to be exfoliated from the renal epithelium, which includes the release from the basement membrane followed by urinary excretion. As the ECM has a concerted role in cell monolayer formation and intracellular signaling pathways (13), one could argue that tissue derived cell

lines are more preferred models to apply in BAK applications. Nevertheless, using cells originating from urine for BAK applications remains an interesting source, especially as this material is easy accessible and urine-derived PTEC maintain transport function.

Biofunctionalized scaffolds; the backbone of a successful BAK

Defined biomaterials mimicking the native basement membrane and ECM composition are a prerequisite to achieve a successful BAK approach, which warrant preserved PTEC phenotype and function. Importantly, the composition of the scaffold should reflect cyto- as well as hemocompatible properties. Furthermore, it should facilitate the transport of albumin-bound toxins to come in close proximity to the PTEC monolayer to enable clearance of waste products. The hollow fiber membranes, as applied in this thesis, are the commercially available MicroPES® capillary membranes, which consist of a balanced mixture between PES and PVP. The controlled and well-characterized composition of these two components allow for optimal hydrophilic and biocompatible properties (e.g. anti-fouling) for dialysis purposes (14). Although MicroPES membranes demonstrate hemocompatible characteristics, unmodified MicroPES membranes reflect poor cytocompatible properties as was shown in Chapters 6. The biofunctionalization of these membranes required a thorough investigation to maintain the balance between the permeance of molecules and a polarized cell monolayer that form a selective barrier. Various research groups provided insight in ECM applications for BAK purposes over the past years (15, 16). From these, collagen IV appeared to be a crucial component to compromise PTEC monolayer formation and differentiation. In addition, Ni *et al.* showed that the combination of 3,4-dihydroxy-L-phenylalanine (L-DOPA) followed by collagen IV treatment was the most successful combination (15). Upon polymerization, L-DOPA becomes negatively charged and, consequently, will attract the positively charged collagen IV. Consequently, the charged collagen layer will attract cells with their negative membrane potential and will facilitate epithelial differentiation. In addition, membrane hydrophilicity will increase after L-DOPA coating due to coexistence of carboxylic and amino groups in the L-DOPA molecule, and therefore will further stimulate collagen IV adhesion (17, 18). This coating application was optimized for ciPTEC in flat cell monolayers (Chapter 5) and consequently for 3D bioartificial renal tubules (Chapter 6 and 7). Although coating composition (i.e. L-DOPA (2 mg/ml) and collagen IV (25 µg/ml)) remained similar for flat and tubule configurations,

the coating times were extended from minutes to hours to obtain polarized cell monolayers on tubules. Most likely, the advanced 3D configuration of tubules requires a more thorough surface modification to stimulate cell adhesion as compared to flat monolayers. In flat membranes, gravity will allow the majority of the seeded cells to sink and subsequently adhere to the coated membrane present at the bottom of the compartment. In contrast, the adhesion of cells on the outside of a curved fiber with an inner diameter of 300 microns is a more challenging configuration than a flat membrane. Moreover, only a minor fraction of the cells present in the suspension will adhere to the fiber as a large fraction of the cells will not come in contact with the fiber present in the test tube at all. Altogether, a tubule configuration requires a comprehensive coating approach to achieve adherence and, subsequently, a polarized cell monolayer.

Next to biological approaches, like L-DOPA/collagen IV as used in the majority of our studies, synthetic polymers, so called supramolecular polymers, are being developed to mimic the native basement membrane of renal epithelial cells (19, 20). These offer a well-controlled approach and have potentially an unrestricted accessibility. Synthetic polymers can be mixed with peptides based on cell-binding epitopes of ECM proteins to develop a bioactive mesh. Subsequently, using electrospinning techniques hierarchical fibrous nano-microscale membranes can be processed. This was successfully demonstrated with HK-2 cell monolayers, however, for ciPTEC poor cell adhesion and monolayer development were observed (unpublished data). Still, it would be worthwhile to invest in the development a ciPTEC-compatible synthetic mesh to further facilitate the bioartificial *in vitro* environment in future research.

Finally, native ECM components isolated from pigs or discarded human kidneys might be an interesting source to apply for fiber biofunctionalization. Nowadays, native ECM scaffolds are under investigation in the field of whole organ engineering (21-24). This pioneering research focusses on the decellularization of the kidney followed by recellularization in order to induce tissue regeneration (21-23). Decellularized ECM scaffolds preserve innate architecture, support cell growth when recellularized and demonstrate angiogenic capacity to stimulate vasculature (24). Using acellular porcine kidney scaffolds, Abolbashari and co-workers injected primary porcine renal cells into the cortical region of decellularized kidneys (21). This resulted in promising outcomes with respect to cell proliferation into tubular structures, gamma-glutamyl transpeptidase (GGT) activity, sodium uptake and,

predominantly, aquaporin-1 expression (21). In addition, murine embryonic stem cells (mES) have been used to recellularize acellular rat kidneys (25). Bonandrini *et al.* demonstrated that perfusion of stem cells through the renal artery system resulted in a uniform distribution of the vascular network and glomerular capilliaries but only a few cells reached the tubular compartment (25). The differentiation of mES towards an endothelial-like phenotype was confirmed by the expression of CD31 and Tie-2 after 24h, indicating that decellularized kidney scaffolds indeed preserve native ECM structures to support cell adhesion and differentiation. Most likely, using the renal artery as well as the ureter for seeding purposes, an improved proliferation of cells in the tubular compartment might be stimulated (26). Moreover, the recellularized organs should be cultured under flow conditions to supply nutrients and oxygen to cells in order to maintain cell viability and functional properties (e.g. hyperfiltration, active transport of waste products) upon prolonged applications (25). Altogether, using (m)ES as a source to recellularize kidney scaffolds is interesting as the pluripotent character of these cells allow for differentiation into multiple renal lineages (27). However, ethical concerns and tumor formation might hamper the potential of this source for clinical applications (21). To overcome these limitations, a promising cell source encompass induced pluripotent stem cells (iPSC), which are reprogrammed fibroblast and their potential to differentiate into different renal lineages has already been shown (28, 29). Moreover, iPS technologies allow for autologous applications and will, most likely, be tolerated by the host immune system. Although these initial whole organ engineering studies are promising, the kidney architecture is highly complex and, therefore, developing cell seeding procedures to repopulate acellular kidneys with different renal cell types (endothelial and epithelial cell types) in a homogenous manner is a large hurdle to take (21, 25, 26). Nevertheless, the knowledge obtained in these studies with respect to the role of the native ECM in stimulating renal cell differentiation is valuable for BAK purposes as well. Hence, investigating the effect of native ECM-coated fibers on ciPTEC adhesion and transport properties would be worthwhile to test in future research.

Mechanosensing stimulates PTEC differentiation

One could argue that tubular formation in a 3D environment like hollow fiber membranes or decellularized kidneys better resembles the *in vivo* nephron structure than flat culture conditions and would stimulate cell adhesion and differentiation. As shown in chapter 6 and 7, cell monolayer polarization was indeed enhanced in 3D configurations when compared to flat monolayers.

As a consequence, the transepithelial transport of anionic uremic toxins in bioengineered renal tubules could be nicely demonstrated. The effect of curved biomaterials was also studied by Shen *et al.* (30). Hollow fiber membranes with an inner diameter of 400 microns enhanced renal characteristics such as brush border enzyme activity, glucose transport and cell viability when compared to flat membranes. It has been shown that membrane curvature has an important effect on mechanosensitive molecules such as integrins and focal adhesion proteins, followed by a signal transduction towards the cytoskeleton where it will influence organelle shape and enzyme and protein activation (31, 32). As the *in vivo* nephron has a diameter of approximately 50 microns, one would assume additional improvement of PTEC transport function when membrane curvature will further increase. Conversely, poor monolayer formation was observed when ciPTEC were cultured on coated PES/PVP tubules with an increased curvature (HCO1100 fibers: inner diameter of 215 microns) when compared to MicroPES fibers (inner diameter of 300 microns). This indicates that, next to curvature, also other parameters like membrane topography and physico-chemical properties will influence cell adhesion and subsequent functional characteristics *in vitro* (33, 34). Related to membrane topography, MicroPES membranes contain relatively large asymmetric pore structures as they are applied for plasmapheresis purposes and therefore allow free passage of molecules such as albumin and IgG. The HCO1100 dialyzers have a molecular weight cut-off close to the native glomerulus (~65 kDa) and hence display different membrane topography with smaller pores. It has been shown that different biomaterial surface topographies can influence cell adhesion, morphology and even differentiation of human kidney-2 (HK-2) cells, a PTEC cell line, and human stem cells towards different lineages (33-35). To further elucidate the role of membrane properties in PTEC adhesion and differentiation, similar topography compositions with varying curvatures could be investigated or vice versa.

Next to membrane topography, fluid flow is a crucial factor that induces mechanosignaling and modifies PTEC differentiation via subsequent cytoskeleton rearrangements (36-40). *In vivo*, the apical surface of PTEC is exposed to fluidic shear stress of 0.2 dyne. cm^{-2} due to a constant flow of the glomerular filtrate, and flow sensors such as cilia or microvilli induce signaling towards the intracellular microenvironment (36, 40). Frohlich *et al.* demonstrated that a certain membrane topography in combination with fluid-induced shear stress resulted in a more physiologically relevant *in vitro* PTEC model. The expression of the tight junction protein ZO-1 was clearly

enhanced when both conditions were applied as compared to a modified surface topography solely (33). In addition, Jang *et al.* compared physiological as well as toxicological responses between primary PTEC cultured in a 2D micro-fluidic device exposed to an apical shear stress of 0.2 dyne. cm^{-2} versus static 2D Transwell insert cultures (38). They found that various PTEC characteristics such as cell height, Na^+/K^+-ATPase and aquaporin 1 expression, the number of ciliated cells and alkaline phosphate activity were clearly enhanced when cultured in the microfluidice device using flow conditions. Moreover, clear differences with respect to albumin reabsorption as well as cisplatin-induced toxicity were observed between fluidic *vs.* static culture. It was postulated that the drug transporter OCT2, which is involved in the renal handling of cisplatin, is more tightly regulated due to flow as cellular differentiation improved (38). A next step would be the implementation of continuous flow in a 3D culture environment like hollow fibers. As such, membrane characteristics as well as flow would synergistically stimulate the mechanosensory system. In an initial study performed by Ng *et al.*, primary PTEC were cultured in fibrin-coated hollow fibers (inner diameter of 500 microns) and were connected to a bioreactor with an apical flow of 200 µl. min^{-1} (41). Though tight cell monolayers as well as apical uptake of solutes were observed under flow conditions, a comparison between static conditions *vs.* flow in fibers on the reabsorption and secretion of solutes was not investigated thoroughly in this study. In our studies, as presented in chapter 6 and 7, tubules consisting of a cell monolayer on the outer surface of fibers were cultured under static conditions and flow was only applied through the fiber during experiments. As the experimental settings were in terms of minutes and not in days, the effect of flow in our setup is most likely negligible. Culturing bioartificial renal tubules under continuous flow conditions should become feasible as soon as bioreactors will be introduced. These systems allow for sterile and controlled multi-fiber culture environments and will be our next important step in BAK engineering.

The transition from a single renal tubule towards a full device

The bioartificial renal tubules (figure 8.1), as shown in this thesis, demonstrate promising functional characteristics for further development towards a full BAK device. Obviously, a direct translation from a single tubule towards a full extracorporeal device containing numerous HFM would not be realistic, therefore bioreactors containing 10 - 20 fibers would be an appropriate follow-up model. The group of Zink and co-workers demonstrated successful cell

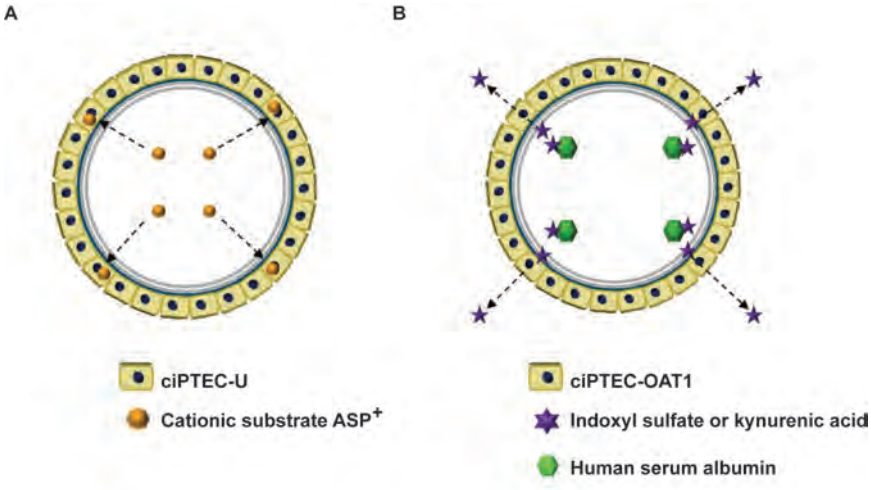

Figure 8.1 Schematic presentation of assays performed in bioengineered renal tubules to demonstrate functional drug transporters. (a) The OCT2 activity in ciPTEC-U monolayers was measured using the cationic substrate 4-(4-(dimethylamino) styryl)-N-methylpyridinium iodide (ASP^+). In chapter 6 it was demonstrated that ASP^+ uptake could be inhibited by a cationic uremic metabolites mixture and by the histamine H2-receptor antagonist, cimetidine, thereby confirming active OCT2-mediated transport. (b) The secretory clearance of protein-bound indoxyl sulfate and kynurenic acid across the renal tubule was confirmed in chapter 7. Transepithelial transport of both toxins was mediated by OAT1, BCRP and MRP4 and clearance could be reduced using specific inhibitors. To this end, active anionic transport processes in our bioengineered renal tubules were confirmed. In conclusion, the results obtained in this thesis are important milestone to pave way towards a successful bioartificial kidney device to treat uremia in ESRD patients.

monolayer formation when primary cells were cultured on the outer surface of medium-sized bioreactors containing 25 HFM and large-sized bioreactors containing 250 HFM (inner diameter 215 microns) at a flow rate of 80 µl/min for 7 days (42). Moreover, cytokine production and organic anion transport of a fluorescent model substrate was shown in monolayers cultured in medium-sized bioreactors. Based on these encouraging results, primary cells were cultured on commercially available bioreactors, a PrismafleX HF20 dialyzer from Gambro GmbH, containing approximately 2600 HFM. The dense packing of HFM resulted in compromised cell performance as monolayers

were disrupted. Although culturing cells on outer surfaces of HFM allow for relatively easy monitoring of monolayer formation and function, the possible mechanical stress between cells in a densely packed dialyzer might hamper monolayer maintenance. In the past, various research groups including Humes, Saito and also Zink, cultured cells on inner HFM surfaces to study the endocrine, metabolic and immunomodulatory effects of primary cells (43-46). Nevertheless, it is known that monolayer formation on the inner surface of HFM is a major challenge to achieve (42). Technical hurdles such as clogging of cells which will result in non-homogenous monolayer formation throughout the HFM should be solved, but also sheer stress during injection of cells into the narrow HFM should be minimized to avoid loss of function. Once successful, monolayers in multi-fiber bioreactors can be expected to be more stable as mechanical stress between cell layers will be avoided. In addition, the inner seeding configuration might better resemble the *in vivo* nephron architecture and could positively affect mechanosensitive molecules like integrins and focal adhesion proteins (31), resulting in improved ciPTEC monolayer differentiation and function. Hence, this application will be investigated in the near future in our laboratory and the effect on cell performance will be studied.

The balance between membrane curvature, topography and coating in combination with flow conditions should finally result in an optimal environment for ciPTEC to achieve an efficient clearance of albumin bound uremic toxins within a reasonable time span. As current dialysis sessions are performed three times a week and already take approximately 4h per session, the clearance capacity of a BAK should be sufficient to maintain or preferably shorten the current time span of a dialysis session. Based on the *in vitro* clearance of indoxyl sulfate and kynurenic acid detected in bioengineered renal tubules as shown in Chapter 7, a rough estimation can be calculated with respect to the time required to achieve a clinically relevant clearance of both toxins. As calculated in the table below (table 1), it would take approximately 30 min for both metabolites, using a commercially available dialyzer with a membrane surface of 1.8 m^2 and using a flow rate of 200 $ml.min^{-1}$, to achieve normal plasma concentrations (table 1; C_N) of indoxyl sulfate or kynurenic acid.

Although the estimated treatment time for these two uremic toxins seems promising, the *in vivo* uremic milieu consists of a myriad of factors that could reduce PTEC-mediated clearance in a BAK and, thus, will extend treatment

Table 8.1 Clearance time calculations to achieve a clinically relevant removal of uremic toxins using a BAK

	Indoxyl sulfate	Kynurenic acid
Plasma concentrations[a] (pMol . μl^{-1})	C_N: 13; C_U: 129	C_N: 0.05; C_U: 1
Clearance in bioengineered tubules[b] ($\mu l . min^{-1} . cm^{-2}$)	73	101
Amount of nMol cleared (Plasma C_U x Clearance) (IS: nmol . $min^{-1} . cm^{-2}$, KA: pmol . $min^{-1} . cm^{-2}$)	9.4	101
Surface BAK (cm^2)	180	180
Total clearance using a BAK (Amount of cleared nMol * surface BAK) (IS: $\mu mol . min^{-1}$, KA: nmol . min^{-1})	1.7	18.2
Dialysis flow rate (ml . min^{-1})	200	200
Amount of uremic toxin passing the membrane per min (flow rate x C_U) (IS: $\mu mol . min^{-1}$; KA nmol . min^{-1})	26	200
Reduction rate (total clearance using a BAK / amount of toxin passing the membrane)	0.07	0.09
Clearance time required to achieve normal plasma concentrations of a uremic toxin ($C_N=C_U*((1-R)^t)$) (min)	31	28

[a] C_N: normal plasma concentrations found in healthy volunteers (47); C_U: uremic plasma concentrations found in ESRD patients (47). [b] clearance values extracted from Chapter 7. R: reduction rate.

time. For example, as described by members of the EUToX workgroup (www.uremic-toxins.org), over 100 solutes have been characterized as uremic toxins in renal failure (48, 49) and, nowadays, many of these uremic toxins are known substrates and compete for similar PTEC transporter pathways (47, 50-53). Moreover, next to uremic toxins also hormones, like endothelin-1, and drugs like cimetidine and metformin impair PTEC-mediated transport function (53-55). In addition, it is known that the albumin binding of endo- and xenobiotics is decreased in ESRD patients, which is caused by factors such as hypoalbuminaemia, competitive binding of substances and conformational changes (guanidinylations) in the albumin molecule leading to less available binding sites (56-58). As a consequence, attenuated protein binding of compounds and metabolites will contribute to an altered pharmacodynamic profile, as was demonstrated by Pichette et al. (59, 60) and also in chapter 7 of this thesis. Altogether, the active uremic toxin clearance via essential renal transporter pathways present in our bioengineered renal tubules, which

has, as of yet, never been demonstrated by any other BAK before, provides a promising platform for future BAK engineering. Obviously, future research demands *in vitro* validation of an up-scaled bioreactor system using uremic plasma. These outcomes will gain insight in the actual uremic toxins kinetics and will further elucidate the clearance efficacy and efficiency of our BAK. Based on these outcomes, a physiologically-based computational model to mimic uremic milieus in different renal patients populations could be established and allow for a concise prediction of the capacity required for ESRD treatment.

Following *in vitro* preclinical validation, the efficacy and efficiency of extracorporeal BAK approaches should be further evaluated using *in vivo* models. For example, Saito and Humes tested the endocrine and metabolic function of a BAK containing porcine or human renal cells in uremic goats and dogs suffering from acute kidney injury (46, 61, 62). Testing a BAK using uremic pigs might be a more preferable model in translational medicine as the anatomy and physiology of these animals resemble human physiology (63). Recently, Humes investigated the immunomodulatory effects of an advanced artificial kidney in uremic pigs (64). In the Netherlands, pig models are also operational and could be applied in the *in vivo* preclinical testing of a ciPTEC-containing BAK (65). One could argue that testing human cells as an experimental treatment platform in other species could result in an immunological response. This could also occur in humans as ciPTEC are a non-autologous cell source. However, the membrane of the hollow fiber with an appropriate composition and molecular weight cut-off should prevent direct contact between host immune factors and cells in a BAK. Still, small immunological factors such as soluble human leukocyte antigens (HLA), which are members of the MHC class I molecules (66), could be released from ciPTEC, subsequently end up in the patients' plasma and exert an immune response. Another critical note is the application of immortal cells in a therapeutic entity. To date, the Food and Drug Administration (FDA) only approved primary renal epithelial cells for clinical evaluation (67). Therefore, as ciPTEC are genetically engineered cells, a thorough risk and safety management plan should be conducted based on the guidelines for advanced therapy medicinal products (ATMPs) developed by the European Medicines Agency in collaboration with the European parliament and the Council prior to any clinical testing (68, 69). These guidelines describe detailed aspects of pharmacovigilance, risk management planning, safety and efficacy follow-up of authorized ATMPs and aspects of clinical follow-up of patients treated with ATMPs.

Important risk parameters to test first in a preclinical environment is the possible release of soluble factors by ciPTEC and the possible loss of ruptured cells which might end up in the patients' blood. To prevent such adverse effects, membrane modifications and filters should be implemented to capture substances and avoid host contact. Another option could be the development of a cell model using hTERT immortalization without the proto-oncogene SV40 large T, as was successfully developed by Wieser *et al.* (70). This strategy was tested during cell model development as described in Chapter 2, however, this immortalization strategy led to impaired renal cell morphology with numerous intracellular 'vacuole-like' structures. Therefore, we excluded these cells for further characterization. Another safety option could be to introduce a so called genetically engineered 'kill-switch' in the ciPTEC model which is activated after the administration of a specific drug and induces elimination of ciPTEC if ended up in a patient (71). Altogether, a thorough risk and safety assessment should demonstrate the feasibility of using immortal cells as a treatment modality. Currently, a preclinical safety evaluation is performed within the EU-FP7 Marie Curie International Training Network BioArt project. If promising outcomes are being obtained, this device might have the potential to achieve approval of the Dutch Ministry of Welfare, Health and Cultural Affairs for clinical testing of a BAK containing ciPTEC.

Alternative strategies to remove protein-bound uremic toxins

Next to bioartificial platforms, there is an increasing interest in advanced artificial renal replacement therapies to aid uremic toxins removal (figure 8.2). For example, the effect of a modified dialysate composition in the currently applied hemodialyzers is under investigation (72). Recently, Bohringer *et al.* studied the effect of a hypertonic dialysis buffer on the release of uremic toxins from albumin, in order to stimulate the removal of waste products. It was postulated that the ionic strength of the dialysate stimulates the removal of the charged free fraction from the patients' blood and, subsequently, contributes to a continuous release of the albumin bound uremic toxins to maintain the equilibrium between bound and unbound uremic toxins. *In vitro* dialysis under hypertonic conditions indeed resulted in an increased release of phenylacetic acid, indoxyl sulfate and *p*-cresyl sulfate from albumin and improved clearance rates were observed (72). However, it is known that hypertonic conditions contribute to volume depletion, cell stress and damage and predominantly affect renal cells but also adverse effects on macrophages, endothelial cells and neurons have been observed (73). Though healthy

mammalian cells can survive a moderated hypertonic environment, using hypertonic conditions in patients suffering from ESRD might be harmful. Therefore, thorough future research is required to develop a safe though efficient dialysis environment to stimulate protein-bound uremic toxin removal.

In addition, a new generation of hollow fiber membranes were developed in the field of artificial kidney engineering to adsorb uremic toxins from the patients' blood. The fibers are dual-layered mixed matrix membranes (MMM) and consist of a porous macro-void free polymeric inner membrane layer to improve hemocompatibilty, which is connected to the activated carbon containing outer MMM layer (74, 75). Activated carbon is a known sorbent for blood purification and is also a strong uremic toxin's adsorbent (76, 77). As carbon has poor biocompatible properties and thus hamper clinically safe applications, the carbon-particle free layer in the MMM at the blood side should prevent the release of carbon particles into the patients' blood. Interestingly, the majority of the free fraction of the protein-bound uremic toxins tested, *viz. p*-cresyl sulfate, indoxyl sulfate and hippuric acid, was removed after 4h exposure of plasma to the MMM. Moreover, plasma pH values and electrolyte concentrations were maintained during the experiment (74). However, albumin partially passed through the membranes and, furthermore, binding specificity of end-metabolites should be investigated further as a possible loss of essential amino acids such as tryptophan should be prevented. In addition, although an artificial kidney with adsorptive characteristics can be efficient in the removal of the available pre-dialysis free fraction, the ability to restore the bound and free fraction equilibrium during dialysis to achieve continuous free toxin adsorption might be a challenge (78, 79). In contrast, a bioartificial kidney, of which a proof of principle was shown in chapter 7, might be able to restore the equilibrium and enable a continuous removal of albumin-bound toxins into the dialysate via active transport processes. Still, the development of advanced artificial kidneys is an interesting research field as cell-based therapies require stringent safety regulations to become clinically approved.

Charcoal adsorbent is also available as oral applications, known as AST-120, and its putative efficacy in uremic toxins removal has been widely studied. This drug consists of spheroid carbon particles and has a high affinity to adsorb organic compounds like indoles, p-cresol and advanced glycation end-products in the gastrointestinal lumen (80, 81). As a result, precursor molecules will not enter the liver and the hepatic biosynthesis of end-

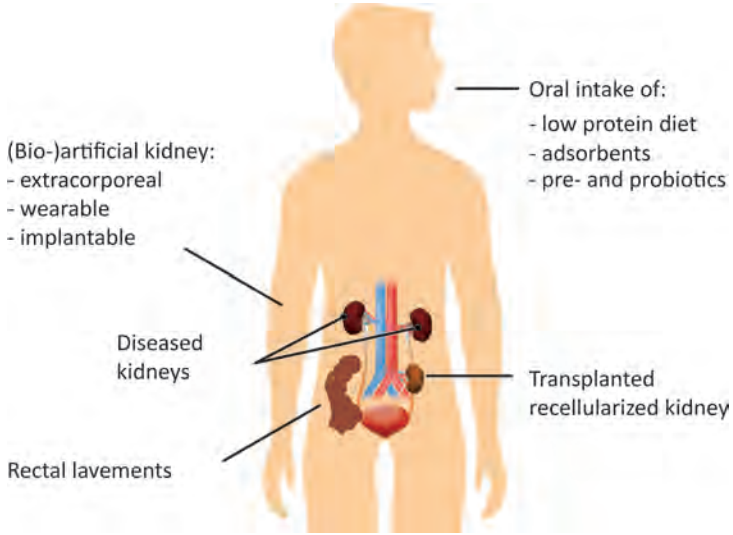

Figure 8.2 Advanced therapeutic interventions to treat uremia in ESRD patients. An overview of current and future treatment strategies to reduce uremia in ESRD patients is shown.

metabolites such as indoxyl sulfate and *p*-cresyl sulfate will be diminished. Several clinical trials were conducted in different patient populations, but the actual efficacy of AST-120 in the attenuation of CKD progression is still debatable (82). Where previously conducted trials showed promising results with respect to a reduction in serum indoxyl sulfate levels and lowering CKD progression (83-86), recent multinational randomized placebo-controlled trials showed no beneficial effects of AST-120 (82). Differences in the quality of study design, dialysis environment, data analysis and interpretation of total or subpopulations might result in the discrepancies observed in these studies. A thorough systematic analysis of all available data could provide more insight in the actual efficacy of AST-120 as a therapeutic intervention to reduce CKD progression.

Another interesting target to reduce uremic toxin levels in CKD patients is the colon and in particular the composition of the intestinal microbiome (87). Under healthy conditions, the microbial flora influence pathways involved in energy metabolism, inflammatory response and to a lesser

extent electrolyte homeostasis (87, 88). Ramezani and Vaziri *et al.* observed an altered gut microbiome composition in CKD rats and ESRD patients (88, 89). In particular, a disbalance between saccharolytic and proteolytic bacteria was observed in this study. Proteolytic bacteria produce the enzyme L-tryptophanase that mediates the formation of uremic toxin precursors like indole from tryptophan (90). Upon CKD progression, the biochemical environment of the gut alters due to urea influx and secretion of uric acid and oxalate by the colonic epithelium and, as a consequence, modifies the microbial flora. In addition, antibiotics, iron supplementation or phosphate-binding substances as well as dietary restrictions of high-fiber products may contribute to an altered microbiome (91). Moreover, a clinical complication often observed in ESRD patients is constipation and undigested proteins in the colon that further stimulates proliferation of proteolytic bacteria (91). Various therapeutic interventions have been proposed to modulate the gut microbiome of patients suffering from kidney disease. The effects of prebiotics (non-digestable food ingredient) and probiotics (living micro-organisms) to regenerate symbiosis in the intestine flora have been studied in hemodialysis populations and CKD rats but showed variable successes (89, 91). The microbial flora consists of a complex (>1000 bacterial species (92)) and dynamic environment, therefore, to establish an optimal intervention using pre- or probiotics is a major challenge. In addition, uremic toxin plasma levels in colectomized dialysis patients have been studied (93). In patients without colons, indoxyl sulfate and *p*-cresyl sulfate plasma levels were almost absent (93). Based on these findings, one could argue that studying the effect of a regularly performed rectal lavement, likely in combination with pre- and probiotics, could be a promising intervention to reduce plasma levels of colonic-derived uremic toxins.

The future of bioartificial kidney engineering

The cell-based therapies currently under development to replace renal function are promising entities in field of regenerative nephrology. To date, the scope of BAK research is predominantly focused on the implementation of one cell type, namely PTEC, and studying its function and beneficial effects in ESRD or AKI. Likely, BAK cell monolayer integrity and transport function might be further improved by applying more than one cell type within a device. The combination of proximal tubular cells with endothelial cells or epithelial cells from down-stream nephron segments might be favorable as it is postulated that paracrine factors secreted might maintain or improve PTEC function in uremia (4, 102). Preliminary results in our laboratory

showed a significantly enhanced transepithelial electrical resistance and less inulin diffusion when ciPTEC where co-cultured in the presence of human conditionally immortalized glomerular endothelial cells (kindly provided by the group of van der Vlag, dept. of Nephrology, Nijmegen) using Transwell® filter inserts (unpublished data). Moreover, the expression of the tight junction protein ZO-1 was more homogenous in co-culture conditions when compared to monocultures. These results suggest an improvement of PTEC monolayer integrity possibly induced by paracrine factors secreted by endothelial cells. In future studies, techniques like metabolomics could identify these factors and this knowledge can be translated further towards BAK development.

In addition, opportunities to combine cell therapy with a wearable or implantable artificial system to enable home-dialysis are being investigated. Roy and co-workers designed a miniaturized wearable hemodialysis system, which vascular access is based on the principle of peritoneal dialysis (94). The efficacy of this artificial device was tested in pigs suffering from AKI and in human subjects treated with hemodialysis to perform a proof-of-concept validation. However, technical hurdles like clotting of the extracorporeal circuit hampered further development and more advanced systems were designed. In collaboration with Humes, a system containing the combination of a silicon nanoporous carbon filter to fulfill ultrafiltration and adsorption of solutes with a bioreactor containing renal epithelial cells to replace partly the metabolic and reabsorptive functions was developed (95). Still, the cell system as developed by Humes and co-workers did not show any beneficial effects with respect to albumin-bound uremic toxin clearance so far (5, 6, 43). As the researchers aim to develop a bioengineered system to treat patients suffering from ESRD, the clearance capacity of albumin-bound uremic toxins using this system should definitely be demonstrated *in vitro* prior to any further clinical validation. Obviously, an implantable bioartificial system would be a major breakthrough in the field of regenerative nephrology and, next to ameliorated health conditions, would improve patients' socio-economic life significantly. However, many challenges like BAK immune tolerance, safety and clearance efficiency and efficacy of a miniaturized system should be critically evaluated.
A promising new era in the field of regenerative nephrology is the differentiation of autologous stem cells into renal lineages. Extrarenal sources, such as bone marrow-derived, embryonic or amniotic fluid stem cells, but also CD133+ multipotent stem cells isolated from kidney tissue itself, have been differentiated into cells with renal characteristics (5, 27, 96, 97). However, limited accessibility, the risk of tumor formation and ethical concerns hamper

future research and applications of these sources. Nowadays, cells isolated from skin tissue have been successfully reprogrammed into human induced pluripotent stem cells (iPSCs) and allow for autologous applications (98-100). It has been shown that engineered stem cells can give rise to kidney-like cells and, therefore, iPSC-derived renal cell models might be promising platforms to aid autologous BAK engineering (28, 29, 99, 101). Obviously, approaches containing autologous cell sources would likely be beneficial to enhance BAK immune tolerance. As soon as differentiation processes become well-controlled and functional active transport is confirmed in engineered kidney cells, an autologous BAK application may become feasible. Recently, engineered human kidney cells have been successfully cultured into 3D self-organizing kidneys, called organoids. The expression of various proteins originating from multiple renal lineages showed high similarities with first trimester human embryonic kidney development (29). Moreover, specific maturation of proximal tubule epithelial cells in organoids was confirmed as demonstrated by active endocytosis and toxicity response to a known nephrotoxic agent cisplatin (29). In concert, murine organoids reconstitute active organic cationic as well as anionic transport as was shown using known fluorescent model substrates in the presence or absence of specific inhibitors (28). Obviously, organoids are miniaturized kidneys-in-a-dish and the development of fully grown kidneys for transplantation will require many more years of research. For BAK engineering purposes, it will be a challenge to isolate a sufficient number of proximal tubule cells from organoids, for which immortalization strategies might be unavoidable. Organoids may, however, also be a valuable tool for safety screening of new pharmaceutical entities, kidney disease modeling and personalized medicine. But this also holds true for the bioengineered renal tubules as developed in Chapter 7.

As discussed, the development of innovative renal replacement therapies is challenging (figure 8.2), and the implementation of many of these platforms into clinical practice will require in depth future research. Based on my current knowledge, the development of novel renal replacement therapies to diminish the uremic syndrome will, most likely, demand a multifaceted therapeutic intervention. A well-defined balance between BAK applications with nutritional and drug treatment regimes could attenuate uremic toxin plasma levels in patients and alleviate the uremic syndrome and its associated complications. Moreover, physiologically-based *in silico* models can become useful tools to predict the adequacy of BAK treatment in order to achieve a clinically relevant clearance of uremic toxins in ESRD patients. Obviously,

to successfully establish a reliable *in silico* model, thorough in vitro and preclinical validations should be performed.

In conclusion, the work presented in this thesis is one of the first steps to pave the way towards a promising renal replacement therapy to treat ESRD patients. The established bioengineered renal tubules facilitate the secretion of protein-bound uremic toxins, which is mediated by the concerted action of essential in- and efflux transporters. Altogether, our findings will contribute to the expansion of novel bioengineered platforms to replace PTEC function.

REFERENCES

1. Boron WF, Boulpaep EL. Medical Physiology. 2003. p. 743-44.
2. Lameire NH, Bagga A, Cruz D, De Maeseneer J, Endre Z, Kellum JA, et al. Acute kidney injury: an increasing global concern. Lancet. 2013;382:170-9.
3. Vanholder R, De Smet R. Pathophysiologic effects of uremic retention solutes. J Am Soc Nephrol. 1999;10:1815-23.
4. Jansen J, Fedecostante M, Wilmer MJ, van den Heuvel LP, Hoenderop JG, Masereeuw R. Biotechnological challenges of bioartificial kidney engineering. Biotechnol Adv. 2014;32:1317-27.
5. Buffington DA, Pino CJ, Chen L, Westover AJ, Hageman G, Humes HD. Bioartificial Renal Epithelial Cell System (BRECS): A Compact, Cryopreservable Extracorporeal Renal Replacement Device. Cell Med. 2012;4:33-43.
6. Humes HD, MacKay SM, Funke AJ, Buffington DA. Tissue engineering of a bioartificial renal tubule assist device: in vitro transport and metabolic characteristics. Kidney Int. 1999;55:2502-14.
7. Humes HD, Weitzel WF, Bartlett RH, Swaniker FC, Paganini EP, Luderer JR, et al. Initial clinical results of the bioartificial kidney containing human cells in ICU patients with acute renal failure. Kidney Int. 2004;66:1578-88.
8. Miller JH. Sodium-sensitive, probenecid-insensitive p-aminohippuric acid uptake in cultured renal proximal tubule cells of the rabbit. Proc Soc Exp Biol Med. 1992;199:298-304.
9. Nieskens TT, Peters JG, Schreurs MJ, Smits N, Woestenenk R, Jansen K, et al. A Human Renal Proximal Tubule Cell Line with Stable Organic Anion Transporter 1 and 3 Expression Predictive for Antiviral-Induced Toxicity. AAPS J. 2016; 18:465-75.
10. Mutsaers HA, Wilmer MJ, Reijnders D, Jansen J, van den Broek PH, Forkink M, et al. Uremic toxins inhibit renal metabolic capacity through interference with glucuronidation and mitochondrial respiration. Biochim Biophys Acta. 2013;1832:142-50.
11. Peters E, Geraci S, Heemskerk S, Wilmer MJ, Bilos A, Kraenzlin B, et al. Alkaline phosphatase protects against renal inflammation through dephosphorylation of lipopolysaccharide and adenosine triphosphate. Br J Pharmacol. 2015;172:4932-45.
12. Jansen J, Schophuizen CM, Wilmer MJ, Lahham SH, Mutsaers HA, Wetzels JF, et al. A morphological and functional comparison of proximal tubule cell lines established from human urine and kidney tissue. Exp Cell Res. 2014;323:87-99.
13. Nony PA, Schnellmann RG. Interactions between collagen IV and collagen-binding integrins in renal cell repair after sublethal injury. Mol Pharmacol. 2001;60:1226-34.
14. Membrana GmbH. Available from: http://www.membrana.com/healthcare/products/products-for-new-therapies/micropes.

15. Ni M, Teo JC, Ibrahim MS, Zhang K, Tasnim F, Chow PY, et al. Characterization of membrane materials and membrane coatings for bioreactor units of bioartificial kidneys. Biomaterials. 2011;32:1465-76.
16. Zhang H, Tasnim F, Ying JY, Zink D. The impact of extracellular matrix coatings on the performance of human renal cells applied in bioartificial kidneys. Biomaterials. 2009;30:2899-911.
17. Schophuizen CM, De Napoli IE, Jansen J, Teixeira S, Wilmer MJ, Hoenderop JG, et al. Development of a living membrane comprising a functional human renal proximal tubule cell monolayer on polyethersulfone polymeric membrane. Acta Biomater. 2015;14:22-32.
18. Azari S, Zou L, Cornelissen E, Mukai Y. Facile fouling resistant surface modification of microfiltration cellulose acetate membranes by using amino acid L-DOPA. Water Sci Technol. 2013;68:901-8.
19. Mollet BB, Bogaerts ILJ, van Almen GC, Dankers PYW. A bioartificial environment for kidney epithelial cells based on a supramolecular polymer basement membrane mimic and an organotypical culture system. J Tissue Eng Regen Med. 2015; DOI: 10.1002/term.2080.
20. Mollet BB, Comellas-Aragones M, Spiering AJH, Sontjens SHM, Meijer EW, Dankers PYW. A modular approach to easily processable supramolecular bilayered scaffolds with tailorable properties. J Mater Chem B. 2014;2:2483-93.
21. Abolbashari M, Agcaoili SM, Lee MK, Ko IK, Aboushwareb T, Jackson JD, et al. Repopulation of porcine kidney scaffold using porcine primary renal cells. Acta Biomater. 2016;29:52-61.
22. Peloso A, Ferrario J, Maiga B, Benzoni I, Bianco C, Citro A, et al. Creation and implantation of acellular rat renal ECM-based scaffolds. Organogenesis. 2015;11:58-74.
23. Katari R, Peloso A, Zambon JP, Soker S, Stratta RJ, Atala A, et al. Renal bioengineering with scaffolds generated from human kidneys. Nephron Exp Nephrol. 2014;126:119.
24. Orlando G, Booth C, Wang Z, Totonelli G, Ross CL, Moran E, et al. Discarded human kidneys as a source of ECM scaffold for kidney regeneration technologies. Biomaterials. 2013;34:5915-25.
25. Bonandrini B, Figliuzzi M, Papadimou E, Morigi M, Perico N, Casiraghi F, et al. Recellularization of well-preserved acellular kidney scaffold using embryonic stem cells. Tissue Eng Part A. 2014;20:1486-98.
26. Ross EA, Williams MJ, Hamazaki T, Terada N, Clapp WL, Adin C, et al. Embryonic stem cells proliferate and differentiate when seeded into kidney scaffolds. J Am Soc Nephrol. 2009;20:2338-47.

27. Lam AQ, Freedman BS, Morizane R, Lerou PH, Valerius MT, Bonventre JV. Rapid and efficient differentiation of human pluripotent stem cells into intermediate mesoderm that forms tubules expressing kidney proximal tubular markers. J Am Soc Nephrol. 2014;25:1211-25.
28. Lawrence ML, Chang CH, Davies JA. Transport of organic anions and cations in murine embryonic kidney development and in serially-reaggregated engineered kidneys. Sci Rep. 2015;5:9092.
29. Takasato M, Er PX, Chiu HS, Maier B, Baillie GJ, Ferguson C, et al. Kidney organoids from human iPS cells contain multiple lineages and model human nephrogenesis. Nature. 2015;526:564-568.
30. Shen C, Meng Q, Zhang G. Increased curvature of hollow fiber membranes could up-regulate differential functions of renal tubular cell layers. Biotechnol Bioeng. 2013;110:2173-83.
31. Ingber DE. Tensegrity-based mechanosensing from macro to micro. Progr Biophys Mol Bio. 2008;97:163-79.
32. McMahon HT, Boucrot E. Membrane curvature at a glance. J Cell Sci. 2015;128:1065-70.
33. Frohlich EM, Zhang X, Charest JL. The use of controlled surface topography and flow-induced shear stress to influence renal epithelial cell function. Integr Biol. 2012;4:75-83.
34. Hulsman M, Hulshof F, Unadkat H, Papenburg BJ, Stamatialis DF, Truckenmuller R, et al. Analysis of high-throughput screening reveals the effect of surface topographies on cellular morphology. Acta Biomater. 2015;15:29-38.
35. McBeath R, Pirone DM, Nelson CM, Bhadriraju K, Chen CS. Cell shape, cytoskeletal tension, and RhoA regulate stem cell lineage commitment. Dev cell. 2004;6:483-95.
36. Du Z, Duan Y, Yan Q, Weinstein AM, Weinbaum S, Wang T. Mechanosensory function of microvilli of the kidney proximal tubule. Proc Natl Acad Sci. 2004;101:13068-73.
37. Duan Y, Gotoh N, Yan Q, Du Z, Weinstein AM, Wang T, et al. Shear-induced reorganization of renal proximal tubule cell actin cytoskeleton and apical junctional complexes. Proc Natl Acad Sci. 2008;105:11418-23.
38. Jang KJ, Mehr AP, Hamilton GA, McPartlin LA, Chung S, Suh KY, et al. Human kidney proximal tubule-on-a-chip for drug transport and nephrotoxicity assessment. Integr Biol. 2013;5:1119-29.
39. Duan Y, Weinstein AM, Weinbaum S, Wang T. Shear stress-induced changes of membrane transporter localization and expression in mouse proximal tubule cells. Proc Natl Acad Sci. 2010;107:21860-5.
40. Nauli SM, Alenghat FJ, Luo Y, Williams E, Vassilev P, Li X, et al. Polycystins 1 and 2 mediate mechanosensation in the primary cilium of kidney cells. Nat Gen. 2003;33:129-37.

41. Ng CP, Zhuang Y, Lin AWH, Teo JCM. A Fibrin-Based Tissue-Engineered Renal Proximal Tubule for Bioartificial Kidney Devices: Development, Characterization and In Vitro Transport Study. Int J Tissue Eng. 2013;2013:10.
42. Oo ZY, Kandasamy K, Tasnim F, Zink D. A novel design of bioartificial kidneys with improved cell performance and haemocompatibility. J Cell Mol Med. 2013;17:497-507.
43. Humes HD, Weitzel WF, Fissell WH. Renal cell therapy in the treatment of patients with acute and chronic renal failure. Blood Purif. 2004;22:60-72.
44. Sanechika N, Sawada K, Usui Y, Hanai K, Kakuta T, Suzuki H, et al. Development of bioartificial renal tubule devices with lifespan-extended human renal proximal tubular epithelial cells. Nephrol Dial Transplant. 2011;26:2761-9.
45. Oo ZY, Deng R, Hu M, Ni M, Kandasamy K, bin Ibrahim MS, et al. The performance of primary human renal cells in hollow fiber bioreactors for bioartificial kidneys. Biomaterials. 2011;32:8806-15.
46. Saito A, Sawada K, Fujimura S, Suzuki H, Hirukawa T, Tatsumi R, et al. Evaluation of bioartificial renal tubule device prepared with lifespan-extended human renal proximal tubular epithelial cells. Nephrol Dial Transplant. 2012;27:3091-9.
47. Mutsaers HA, van den Heuvel LP, Ringens LH, Dankers AC, Russel FG, Wetzels JF, et al. Uremic toxins inhibit transport by breast cancer resistance protein and multidrug resistance protein 4 at clinically relevant concentrations. PloS One. 2011;6:e18438.
48. Duranton F, Cohen G, De Smet R, Rodriguez M, Jankowski J, Vanholder R, et al. Normal and pathologic concentrations of uremic toxins. J Am Soc Nephrol. 2012;23:1258-70.
49. Neirynck N, Vanholder R, Schepers E, Eloot S, Pletinck A, Glorieux G. An update on uremic toxins. Int Urol Nephrol. 2013;45:139-50.
50. Lowenstein J. Competition for organic anion transporters in chronic renal disease. Kidney international. 2012;82:1033; author reply
51. Masereeuw R, Mutsaers HA, Toyohara T, Abe T, Jhawar S, Sweet DH, et al. The kidney and uremic toxin removal: glomerulus or tubule? Sem Nephrol. 2014;34:191-208.
52. Mutsaers HA, Caetano-Pinto P, Seegers AE, Dankers AC, van den Broek PH, Wetzels JF, et al. Proximal tubular efflux transporters involved in renal excretion of p-cresyl sulfate and p-cresyl glucuronide: Implications for chronic kidney disease pathophysiology. Toxicol In Vitro. 2015;29:1868-77.
53. Schophuizen CM, Wilmer MJ, Jansen J, Gustavsson L, Hilgendorf C, Hoenderop JG, et al. Cationic uremic toxins affect human renal proximal tubule cell functioning through interaction with the organic cation transporter. Pflugers Archiv. 2013;465: 1701-14.
54. Schophuizen CM, Hoenderop JG, Masereeuw R, Heuvel LP. Uremic Toxins Induce ET-1 Release by Human Proximal Tubule Cells, which Regulates Organic Cation Uptake Time-Dependently. Cells. 2015;4:234-52.

55. Jansen J, De Napoli IE, Fedecostante M, Schophuizen CM, Chevtchik NV, Wilmer MJ, et al. Human proximal tubule epithelial cells cultured on hollow fibers: living membranes that actively transport organic cations. Sci Rep. 2015;5:16702.
56. Meijers BK, Bammens B, Verbeke K, Evenepoel P. A review of albumin binding in CKD. Am J Kidney Dis. 2008;51:839-50.
57. Klammt S, Wojak HJ, Mitzner A, Koball S, Rychly J, Reisinger EC, et al. Albumin-binding capacity (ABiC) is reduced in patients with chronic kidney disease along with an accumulation of protein-bound uraemic toxins. Nephrol Dial Transplant. 2012;27:2377-83.
58. Rueth M, Lemke HD, Preisinger C, Krieter D, Theelen W, Gajjala P, et al. Guanidinylations of albumin decreased binding capacity of hydrophobic metabolites. Acta Physiol. 2015;215:13-23.
59. Pichette V, Geadah D, du Souich P. The influence of moderate hypoalbuminaemia on the renal metabolism and dynamics of furosemide in the rabbit. Br J Pharmacol. 1996;119:885-90.
60. Pichette V, Geadah D, du Souich P. Role of plasma protein binding on renal metabolism and dynamics of furosemide in the rabbit. Drug Metab Dispos. 1999;27:81-5.
61. Fissell WH, Lou L, Abrishami S, Buffington DA, Humes HD. Bioartificial kidney ameliorates gram-negative bacteria-induced septic shock in uremic animals. J Am Soc Nephrol. 2003;14:454-61.
62. Humes HD, Fissell WH, Weitzel WF, Buffington DA, Westover AJ, MacKay SM, et al. Metabolic replacement of kidney function in uremic animals with a bioartificial kidney containing human cells. Am J Kidney Dis. 2002;39:1078-87.
63. Klymiuk N, Seeliger F, Bohlooly YM, Blutke A, Rudmann DG, Wolf E. Tailored Pig Models for Preclinical Efficacy and Safety Testing of Targeted Therapies. Toxicol Pathol. 2016;44:346-57.
64. Pino CJ, Farokhrani A, Lou L, Smith PL, Johnston K, Buffington DA, et al. Selective cytopheretic inhibitory device with regional citrate anticoagulation and portable sorbent dialysis. Artif Organs. 2013;37:203-10.
65. Verloop WL, Hubens LE, Spiering W, Doevendans PA, Goldschmeding R, Bleys RL, et al. The Effects of Renal Denervation on Renal Hemodynamics and Renal Vasculature in a Porcine Model. PloS One. 2015;10:e0141609.
66. Misra MK, Pandey SK, Kapoor R, Sharma RK, Kapoor R, Prakash S, et al. HLA-G gene expression influenced at allelic level in association with end stage renal disease and acute allograft rejection. Human Immun. 2014;75:833-9.
67. Humes HD, Buffington D, Westover AJ, Roy S, Fissell WH. The bioartificial kidney: current status and future promise. Pediatric Nephrol. 2014;29:343-51.

68. European Medicines Agency. Reflection paper on classification of advanced therapy medicinal products 2012. Available from: http://www.ema.europa.eu/docs/en_GB/document_library/Scientific_guideline/2012/12/WC500136422.pdf.
69. European Medicines Agency. Guideline on safety and efficacy follow-up - risk management of advanced therapy medicinal products 2008. Available from: http://www.ema.europa.eu/docs/en_GB/document_library/Regulatory_and_procedural_guideline/2009/10/WC500006326.pdf.
70. Wieser M, Stadler G, Jennings P, Streubel B, Pfaller W, Ambros P, et al. hTERT alone immortalizes epithelial cells of renal proximal tubules without changing their functional characteristics. Am J Physiol Renal Physiol. 2008;295:F1365-75.
71. Davies JA. Synthetic Biology: Rational Pathway Design for Regenerative Medicine. Gerontology. 2015. DOI: 10.1159/000440721
72. Bohringer F, Jankowski V, Gajjala PR, Zidek W, Jankowski J. Release of uremic retention solutes from protein binding by hypertonic predilution hemodiafiltration. ASAIO J. 2015;61:55-60.
73. Alfieri RR, Petronini PG. Hyperosmotic stress response: comparison with other cellular stresses. Pflugers Arch. 2007;454:173-85.
74. Tijink MS, Wester M, Glorieux G, Gerritsen KG, Sun J, Swart PC, et al. Mixed matrix hollow fiber membranes for removal of protein-bound toxins from human plasma. Biomaterials. 2013;34:7819-28.
75. Tijink MS, Wester M, Sun J, Saris A, Bolhuis-Versteeg LA, Saiful S, et al. A novel approach for blood purification: mixed-matrix membranes combining diffusion and adsorption in one step. Acta Biomater. 2012;8:2279-87.
76. Dinh DC, Recht NS, Hostetter TH, Meyer TW. Coated carbon hemoperfusion provides limited clearance of protein-bound solutes. Artif Organs. 2008;32:717-24.
77. Meyer TW, Peattie JW, Miller JD, Dinh DC, Recht NS, Walther JL, et al. Increasing the clearance of protein-bound solutes by addition of a sorbent to the dialysate. J Am Soc Nephrol. 2007;18:868-74.
78. Deltombe O, Van Biesen W, Glorieux G, Massy Z, Dhondt A, Eloot S. Exploring Protein Binding of Uremic Toxins in Patients with Different Stages of Chronic Kidney Disease and during Hemodialysis. Toxins. 2015;7:3933-46.
79. Eloot S, Van Biesen W, Axelsen M, Glorieux G, Pedersen RS, Heaf JG. Protein-bound solute removal during extended multipass versus standard hemodialysis. BMC Nephrol. 2015;16:57.
80. Goto S, Yoshiya K, Kita T, Fujii H, Fukagawa M. Uremic toxins and oral adsorbents. Ther Apher Dial. 2011;15:132-4.
81. Yamagishi S, Nakamura K, Matsui T, Inoue H, Takeuchi M. Oral administration of AST-120 (Kremezin) is a promising therapeutic strategy for advanced glycation end product (AGE)-related disorders. Med Hypotheses. 2007;69:666-8.

82. Schulman G, Berl T, Beck GJ, Remuzzi G, Ritz E, Arita K, et al. Randomized Placebo-Controlled EPPIC Trials of AST-120 in CKD. J Am Soc Nephrol. 2015;26:1732-46.
83. Hatakeyama S, Yamamoto H, Okamoto A, Imanishi K, Tokui N, Okamoto T, et al. Effect of an Oral Adsorbent, AST-120, on Dialysis Initiation and Survival in Patients with Chronic Kidney Disease. Int J Nephrol. 2012;2012:376128.
84. Shoji T, Wada A, Inoue K, Hayashi D, Tomida K, Furumatsu Y, et al. Prospective randomized study evaluating the efficacy of the spherical adsorptive carbon AST-120 in chronic kidney disease patients with moderate decrease in renal function. Nephron Clin Pract. 2007;105:c99-107.
85. Yorioka N, Kiribayashi K, Naito T, Ogata S, Yokoyama Y, Kyuden Y, et al. An oral adsorbent, AST-120, combined with a low-protein diet and RAS blocker, for chronic kidney disease. J Nephrol. 2008;21:213-20.
86. Schulman G, Agarwal R, Acharya M, Berl T, Blumenthal S, Kopyt N. A multicenter, randomized, double-blind, placebo-controlled, dose-ranging study of AST-120 (Kremezin) in patients with moderate to severe CKD. Am J Kidney Dis. 2006;47:565-77.
87. Poesen R, Meijers B, Evenepoel P. The colon: an overlooked site for therapeutics in dialysis patients. Sem Dial. 2013;26:323-32.
88. Vaziri ND, Wong J, Pahl M, Piceno YM, Yuan J, DeSantis TZ, et al. Chronic kidney disease alters intestinal microbial flora. Kidney Int. 2013;83:308-15.
89. Ramezani A, Raj DS. The gut microbiome, kidney disease, and targeted interventions. J Am Soc Nephrol. 2014;25:657-70.
90. Sasaki-Imamura T, Yano A, Yoshida Y. Production of indole from L-tryptophan and effects of these compounds on biofilm formation by Fusobacterium nucleatum ATCC 25586. Appl Environ Microbiol. 2010;76:4260-8.
91. Wing MR, Patel SS, Ramezani A, Raj DS. Gut microbiome in chronic kidney disease. Exp Physiol. 2016;101:471-77.
92. Manichanh C, Reeder J, Gibert P, Varela E, Llopis M, Antolin M, et al. Reshaping the gut microbiome with bacterial transplantation and antibiotic intake. Genome Res. 2010;20:1411-9.
93. Aronov PA, Luo FJ, Plummer NS, Quan Z, Holmes S, Hostetter TH, et al. Colonic contribution to uremic solutes. J Am Soc Nephrol. 2011;22:1769-76.
94. Fissell WH, Roy S, Davenport A. Achieving more frequent and longer dialysis for the majority: wearable dialysis and implantable artificial kidney devices. Kidney Int. 2013;84:256-64.
95. Roy SF, W.; Humes, H.D. Artificial kidney research gets a boost 2015. Available from: http://universityofcalifornia.edu/news/artificial-kidney-research-gets-boost.
96. Qian H, Yang H, Xu W, Yan Y, Chen Q, Zhu W, et al. Bone marrow mesenchymal stem cells ameliorate rat acute renal failure by differentiation into renal tubular epithelial-like cells. Int J Mol Med. 2008;22:325-32.

97. Rota C, Imberti B, Pozzobon M, Piccoli M, De Coppi P, Atala A, et al. Human amniotic fluid stem cell preconditioning improves their regenerative potential. Stem Cells Dev. 2012;21:1911-23.
98. Takahashi K, Tanabe K, Ohnuki M, Narita M, Ichisaka T, Tomoda K, et al. Induction of pluripotent stem cells from adult human fibroblasts by defined factors. Cell. 2007;131:861-72.
99. Takasato M, Maier B, Little MH. Recreating kidney progenitors from pluripotent cells. Pediatric Nephrol. 2014;29:543-52.
100. Howden SE, Maufort JP, Duffin BM, Elefanty AG, Stanley EG, Thomson JA. Simultaneous Reprogramming and Gene Correction of Patient Fibroblasts. Stem Cell Rep. 2015;5:1109-18.
101. Freedman BS, Brooks CR, Lam AQ, Fu H, Morizane R, Agrawal V, et al. Modelling kidney disease with CRISPR-mutant kidney organoids derived from human pluripotent epiblast spheroids. Nature Commun. 2015;6:8715.
102. Brown, C.D., et al., Characterisation of human tubular cell monolayers as a model of proximal tubular xenobiotic handling. Toxicol Appl Pharmacol. 2008;233:428-38.

Chapter 9

SUMMARY
SAMENVATTING

SUMMARY

The kidneys consist of approximately 2 million nephrons, which all together fulfill the homeostatic regulation of the human body. An important task of the kidneys is the removal of waste products from blood into the (pro-) urine. The proximal tubule epithelial cells (PTEC) present in each nephron are equipped with a broad range of transporter proteins that facilitate the removal of many solutes from the systemic circulation. During renal failure, among others, PTEC function is impaired and the removal of waste products is diminished. Consequently, these products accumulate with adverse effects on the organism's homeostasis. Disorders like sepsis, cardiovascular or immune disease as well as diabetes mellitus and exposure to nephrotoxic agents are associated with the development of renal failure. In addition, inherited genetic diseases that primarily affect the kidneys have been described. Kidney function has to be replaced when an abrupt loss or a severe decline in kidney function (eGFR < 15ml/min/1.73m^2) is detected. Current renal replacement therapies, like hemodialysis, only replace renal function for approximately 20% and, as a result, waste products accumulate in the patient. The limited clearance capacity of waste products by dialysis treatment is caused by the chemical properties of these solutes that hamper their removal. To date, three classes of waste solutes have been characterized, comprising approximately 150 uremic solutes that accumulate in renal failure. The first and second class of uremic solutes consist of small water-soluble solutes (Molecular weight (MW) <500 Da) and middle molecules (MW >500 Da) and these classes can, to a certain extent, be removed using hemodialysis treatment. The third class, the albumin-bound uremic solutes, have a MW <500 Da but are difficult to remove by dialysis as they are bound to plasma proteins which greatly extents their MW. Detailed research showed that many of the uremic retention solutes interact negatively with various biological processes in the body and are, therefore, described as uremic toxins. The preferred option to replace renal function is kidney transplantation. However, as donor organs are scarce, the development of novel therapeutic strategies to improve or replace (preferentially PTEC) function are of high interest in the field of regenerative nephrology.

In a so-called bioartifical kidney (BAK), the implementation of PTEC in an extracorporeal device should enable the removal of albumin-bound uremic toxins from the patients' plasma. In this thesis, the handling of uremic toxins by PTEC was step-wisely studied. First, novel renal cell lines were developed

and transport processes of waste products across tight cell monolayers were studied in 2D flat cell monolayers. Next, the biofunctionalization of 3D hollow fiber membranes (HFM) to stimulate cell monolayer polarization was studied and elimination processes of uremic toxins mediated by bioengineered renal tubules were examined. Studying the clearance of waste products across vital PTEC monolayers will allow estimating the potency of a cell-based device to improve hemodialysis treatment.

A suitable cell model that reflects PTEC function is a prerequisite for successful bioartificial kidney development. In **Chapter 2**, we developed conditionally immortalized PTEC (ciPTEC) models with cells isolated from human urine and kidney tissue. Based on mRNA expression profiling of PTEC transporters, morphology and cell monolayer tightness, two out of twenty six kidney PTEC subclones were selected (ciPTEC-T1 and -T2) for detailed characterization. An extensive morphological and functional comparison of these cells models with a urine-derived model (ciPTEC-U) was set out. The selected cell models showed to form confluent and polarized cell monolayers when cultured on filter inserts as the expression of the tight junction protein ZO-1 was abundantly expressed along the boundaries of the cells. Remarkable, a larger diameter of kidney tissue-derived cells was observed when compared to urine-derived cells. In addition, also the expression profile of extracellular matrix (ECM) genes differed between sources. Where both tissue derived cell lines demonstrated a high abundance of collagen I and -IV α1, the cells isolated from urine showed a more pronounced expression of laminin V and fibronectin I. The endogenous expression and function of the uremic toxin transporters Organic Cation Transporter–2 (OCT2), Breast Cancer Resistance Protein (BCRP), Multidrug Resistance-associated Protein–4 (MRP_4) and P-glycoprotein (P-gp) were confirmed in all cell lines and only minor differences were observed. Moreover, active albumin- and phosphate-uptake was confirmed in the kidney-tissue derived cell lines, processes representative of tubular reabsorption. All together, these inexhaustible cell lines display robust functional PTEC characteristics and can be valuable tools to aid bioartificial kidney engineering. Moreover, these cell lines could be useful for the screening of novel pharmaceutical entities and are valuable for studying (patho)physiological processes in PTEC. The latter was demonstrated in **Chapter 3**, where PTEC were used to study the protective mechanism of dexamethasone, a drug that is often used to treat chronic inflammatory diseases, in experimental inflammation induced by the endotoxin lipopolysaccharide (LPS). In this study we showed that the

cellular alkalisation could be the initiating event underlying LPS-induced mitochondrial dysfunction. Upon dexamethasone treatment, pH was corrected and, consequently, the mitochondrial function was restored. This was shown by improved mitochondrial respiration and membrane potential, concerted by reduced ROS levels. In addition, we showed that an enhanced mitochondrial Complex V expression and activity act as a compensatory mechanism in the dexamethasone-induced acidified environment. Together, we nicely demonstrated in this chapter that ciPTEC can be valuable tools in studying metabolic pathways and, therefore, are suitable *in vitro* models for studying different renal processes in health and disease.

In **Chapter 4**, the current status of BAK engineering was reviewed. To date, the development of extracorporeal BAK platforms predominantly demonstrates immunomodulatory effects in order to reduce mortality in critically ill patients suffering from acute kidney injury (AKI). In the majority of the performed BAK studies, primary renal epithelial cells are being applied. These cell systems display a high batch-to-batch variability with respect to PTEC quality and function. Therefore, ciPTEC could be a promising alternative to aid BAK engineering as this system reflects a stable expression and function of PTEC transporters and metabolic activity. Another critical step in BAK engineering is that the native basement membrane and its extracellular matrix should be mimicked *in vitro*, in order to stimulate monolayer polarization to obtain a 'living membrane' which enables the removal of waste products. An overview of biomaterials and coatings applied for BAK purposes so far is summarized in this chapter. The natural compound 3,4-dihydroxy-L-phenylalanine (L-DOPA) in combination with collagen IV have shown to be a successful surface modification to stimulate the formation of a tight PTEC monolayer. In addition to the optimization of monolayer formation, thorough preclinical and safety evaluation should demonstrate the efficacy and efficiency of PTEC monolayers in a BAK to become a feasible approach to treat end-stage renal disease (ESRD) patients. Future research will, most likely, advance the development of an extracorporeal BAK into a wearable or implantable BAK. Concurrently, the possibilities to develop autologous cell-based therapies will be further explored in order to improve immune tolerance.

In vivo, the urinary excretion of uremic toxins from the blood into the pro-urine is mediated by PTEC in- and efflux transporters, a function that should be maintained *in vitro* for successful BAK development. As demonstrated in **Chapter 5**, we first developed a living membrane containing tight

ciPTEC monolayers on hemocompatbile PES/PVP flat membranes. The biofunctionalization of the membrane was studied thoroughly and the coating was optimized, which consisted of a well-defined combination of L-DOPA and collagen IV. Optimal cell adhesion and cell monolayer polarization was confirmed with ZO-1 expression, without a loss of membrane permeance as demonstrated by H_2O, albumin and IgG permeance. Consequently, the transepithelial clearance of creatinine, a known OCT2 substrate and uremic toxin, was confirmed in these cell monolayers. This creatinine flux was compared to transport rates observed across ciPTEC monolayers cultured on commercially available Transwell inserts. This system is regarded as a golden standard in cell culturing, though it has poor hemocompatible properties and is therefore not suitable for BAK applications. Interestingly, creatinine clearance rates were similar in both systems, confirming that ciPTEC transport properties are well preserved when cultured on PES/PVP biomaterials. In **Chapter 6**, this knowledge was translated into 3D PES/PVP membrane approaches. Hollow fiber membranes were coated with the same composition (L-DOPA and collagen IV), though coating time had to be extended to achieve a polarized cell monolayer, as shown by ZO-1 and OCT2 expressions. Importantly, the membrane permeance of H_2O and BSA were preserved allowing the free passage of albumin-bound uremic toxins through the membrane to come in close proximity with cells to enable transepithelial clearance. Obviously, the monolayer should maintain tight characteristics to avoid loss of host blood components. As a proof of concept, cell monolayers on HFM were functionally characterized in real-time using a perfusion system by measuring the transport of a fluorescent cationic model substrate 4-(4-(dimethylamino)styryl)-N-methylpyridinium-iodide (ASP^+). Initial ASP^+ uptake was inhibited by a cationic uremic metabolites mixture and by the histamine H2-receptor antagonist, cimetidine. These data confirmed a successfully established bioartificial renal tubule of PTEC on MicroPES HFM with active organic cation transport.

Many of the uremic toxins studied in literature are organic anions, therefore, the Organic Anion Transporter - 1 (OAT1) and -3 (OAT3)-mediated handling of a panel of eight anionic uremic toxins was investigated. In **Chapter 7**, we first designed 2D experiments and confirmed their potency to competitively inhibit OAT-mediated transport. Of these uremic toxins, indoxyl sulfate and kynurenic acid transport in PTEC was investigated further and active OAT1-mediated transport was demonstrated. We selected these two uremic toxins as both showed a strong OAT1-mediated inhibition and are associated

with ESRD progression and its related complications. Next, transepithelial clearance of indoxyl sulfate and kynurenic acid in the presence or absence of human serum albumin across polarized bioartificial renal tubules was shown. Interestingly, the clearance of both albumin-bound anionic uremic toxins was enhanced as compared to the clearance of toxins in the absence of albumin. This observation is nicely in line with literature where albumin is described as a carrier protein and stimulates transport processes.

In this thesis we aimed to develop new therapeutic entities to replace PTEC function, by studying elimination processes of cationic and anionic uremic toxins *in vitro* in flat cell monolayers and subsequently in 3D bioengineered renal tubules. In **Chapter 8**, the delineated knowledge obtained in this thesis was discussed within the current scope of regenerative nephrology and renal pharmacology. Moreover, future perspectives of the successfully established bioengineered renal tubules regarding (pre)clinical validation processes were discussed as well as promising opportunities to further aid regenerative nephrology. Altogether, this work may pave the way towards suitable approaches to aid ESRD and AKI treatment in the future.

SAMENVATTING

De nieren hebben een belangrijke rol in het handhaven van velerlei processen in het menselijk lichaam, zoals de regulatie van bloeddruk, hormoonproductie en de uitscheiding van afvalstoffen en urine productie. De nieren bestaan uit zo'n 2 miljoen filtratie buisjes, genaamd nefronen. Een nefron bestaat uit meer dan 20 verschillende celtypen met ieder een belangrijke rol in de homeostase van het interne milieu. Een belangrijk onderdeel daarvan is de uitscheiding van afvalstoffen door proximale tubulusepitheelcellen (PTEC). PTEC bevatten een variëteit aan transporterende eiwitten die afvalstoffen vanuit het bloed naar de (voor)-urine kunnen verplaatsen. Tijdens nierfalen verlopen diverse processen in de nier minder efficiënt wat leidt tot ophoping van afvalstoffen en een verstoorde homeostase van het lichaam, gevolgd door progressie van nierfalen uiteindelijk leidend tot het uremisch syndroom. Nierziekten kunnen secundair ontstaan door ziektes als sepsis, cardiovasculaire aandoeningen en auto-immuunziekten, maar ook diabetes mellitus en niertoxische medicijnen zijn bekende factoren die nierfalen kunnen veroorzaken. Daarnaast zijn er ook aangeboren genetische afwijkingen bekend welke leiden tot een verminderde nierfunctie. Patiënten waarvan de nierfunctie gedaald is tot minder dan 15% van de normale functie moeten behandeld worden met nierfunctie-vervangende therapieën, zoals hemodialyse. Echter, hemodialyse vervangt slechts zo'n 20% van de nierfunctie waardoor een belangrijk deel van de afvalstoffen in de patiënt niet verwijderd worden. De beperkte klaringscapaciteit van dialyse wordt veroorzaakt door de chemische eigenschappen van de afvalstoffen. De afvalstoffen in klasse I, de kleine, water oplosbare moleculen (MW < 500 Da), zijn wel middels dialyse te verwijderen. Met behulp van een meer poreus dialysefilter zijn ook de klasse II, de middelgrote moleculen (MW > 500 Da) tot op zekere hoogte te verwijderen. De metabolieten van klasse III zijn op zich niet groot (MW < 500 Da) maar doordat ze in het bloedplasma gebonden zijn aan eiwitten worden deze moleculen dermate groot en complex dat ze niet met behulp van een dialysemembraan verwijderd kunnen worden. Inmiddels zijn er zo'n 150 metabolieten geïdentificeerd die geassocieerd zijn met negatieve effecten op biologische systemen in het menselijk lichaam en daarom geclassificeerd als 'uremische toxine'. Van een aantal van deze toxines is bijvoorbeeld inmiddels bekend dat zij een directe bijdrage hebben aan de ontwikkeling van hart- en vaatziekten bij nierpatiënten, een veel voorkomende complicatie bij nierfalen. De meest effectieve wijze om nierfunctie te vervangen is het verkrijgen van een donororgaan via transplantatie, echter hiervoor geschikte organen

zijn schaars. Derhalve is er de behoefte aan de ontwikkeling van betere behandelmethoden zoals de biologische kunstnier (BAK) om de nierfunctie te kunnen vervangen of te verbeteren.

In een BAK zullen specifieke niercellen, namelijk PTEC, geïmplementeerd worden in een dialysesysteem om daarmee de uitscheiding van eiwitgebonden afvalstoffen te kunnen realiseren. In dit proefschrift is de wijze waarop PTEC *in vitro* omgaan met uremische toxines bestudeerd. Hiervoor zijn in eerste instantie 2-dimensionale cellagen gebruikt. Vervolgens is een methode ontwikkeld om een 3-dimensionaal systeem te maken dat de functie van een nierbuisje kan nabootsen. Hiertoe hebben we holle buisjes met een membraan bestaande uit synthetische polymeren voorbewerkt om daar vervolgens gepolariseerde PTEC cellagen op te kunnen kweken. Vervolgens is het transport van verschillende groepen afvalstoffen gefaciliteerd door deze zogenaamde bioartificiële nierbuisjes bestudeerd. Dit onderzoek geeft inzicht in de mogelijkheden om humane niercellen te gebruiken als een mogelijke therapeutisch platform en draagt hierdoor bij aan de realisatie van een klinisch-toepasbare BAK in de toekomst.

Voor de succesvolle ontwikkeling van een BAK is het cruciaal om een *in vitro* model toe te passen die de functie van de humane nier kan nabootsen. Daarom werden PTEC cellen geïsoleerd uit humaan nierweefsel en genetisch gemodificeerd om celdeling eigenschappen in stand te kunnen houden middels een temperatuurgevoelig systeem (conditionally immortalized PTEC; ciPTEC) en verder ontwikkeld tot twee stabiele cellijnen. Zoals beschreven in **hoofdstuk 2**, zijn deze modellen morfologisch en functioneel uitvoerig gekarakteriseerd en vergeleken met een cellijn ontwikkeld van cellen afkomstig uit humane urine. Alle drie de cellijnen gaven dichte monolagen waarin tevens het zonula occludens -1 (ZO1) eiwit kon worden aangetoond waarmee polarisatie werd bevestigd. Opmerkelijk was dat de cellijnen afkomstig uit nierweefsel bestonden uit beduidend grotere cellen dan de cellen uit urine. Bovendien vertoonden de niercellijnen op genniveau een ander extracellulaire matrix (ECM) profiel. ECM bestaat uit diverse eiwitstructuren, zoals collagenen en fibronectine, welke de verbinding tussen de cel en de basaalmembraan in stand houden. Bovendien is de ECM een belangrijk depot voor groeifactoren en stimuleert het mede het functioneren van en de communicatie tussen cellen. Collagen I en IV kwamen significant hoger tot expressie in de niercellijnen, daarentegen was de gen expressie van fibronectine I en laminine V hoger in de cellijn afkomstig van urine. Deze

bevindingen duiden op het feit dat de cellijn afkomstig uit urine deels het vermogen om ECM te produceren heeft verloren. Echter vertoonden de drie cellijnen wel overeenkomstige functionele eigenschappen met betrekking tot PTEC-specifieke transporteiwitten zoals de organische-kationtransporter - 2 (OCT2), P-glycoproteïne (P-gp), Multidrugresistentie-eiwit – 4 (MRP4) en het borstkankerresistentie-eiwit (BCRP). Alle cellijnen lieten bovendien albumine- en fosfaatreabsorptie zien, echter vertoonde een niercellijn beduidend meer albuminereabsorptie en de cellijn uit urine een groter vermogen om fosfaat te resorberen. Concluderend kan worden gesteld dat deze onuitputtelijke bron aan cellen PTEC-specifieke eigenschappen vertonen en ze derhalve toegepast zouden kunnen worden voor de ontwikkeling van een BAK. Bovendien zouden deze modellen geschikt kunnen zijn voor de screening van nieuwe medicijnen en de mogelijke effecten op nierfunctie, of voor het bestuderen van pathofysiologische processen in PTEC. Dit laatste wordt weergegeven in **hoofdstuk 3**, waarin ciPTEC werden behandeld met een endotoxine om vervolgens als een experimenteel ontstekingsmodel toegepast te kunnen worden. In deze studie werd het moleculaire mechanisme van dexamethasone als potentiële behandeling voor acuut nierfalen onderzocht. Cellen blootgesteld aan de endotoxine lipopolysaccharide (LPS) vertoonden een verhoging in mitochondrieël-geproduceerde zuurstofradicalen, wat door dexamethasone werd hersteld. Mitochondriële-zuurstofrespiratie en ook de membraanpotentiaal waren beduidend verlaagd in cellen blootgesteld aan LPS en ook dit kon worden hersteld door toediening van dexamethasone. De pH in cellen blootgesteld aan LPS bleek verhoogd te zijn, wat waarschijnlijk de afwijkende metabole activiteit verklaart. Door dexamethasone kon de intracellulare pH worden verlaagd en zelfs iets worden verzuurd ten opzichte van de controle. Als gevolg daarvan vond een toename in expressie en functie van complex V van het oxidatieve-fosforyleringssysteem plaats. Bovendien is het pH effect door dexamethasone behandeling waarschijnlijk de aanleiding voor het herstellen van de membraanpotentiaal en de mitochondriële activiteit. Onze studie toont hiermee aan dat ciPTEC, naast hun potentie als model voor BAK toepassingen, ook zeer geschikt zijn voor het bestuderen van metabole processen in niercellen.

In **hoofdstuk 4** wordt een overzicht gegeven van de huidige kennis met betrekking tot de ontwikkeling van de BAK. Tot op heden zijn door andere groepen voornamelijk immuun-modulerende effecten door BAK behandeling aangetoond in ernstig zieke patiënten die lijden aan acuut nierfalen. Hiervoor zijn met name primaire niercellen gebruikt, echter vertonen deze cellen per

batch een hoge variabiliteit in kwaliteit en functie. Vanuit dat oogpunt zouden ciPTEC lijnen veelbelovende modellen zijn voor BAK ontwikkeling gezien de functionele eigenschappen van specifieke transporteiwitten en hun metabole activiteit. Een ander belangrijk aspect is de keuze van het biomateriaal waar de cellen op gekweekt moeten worden. Er is reeds veel onderzoek verricht naar het simuleren van de *in vivo* basaalmembraan en de ECM voor *in vitro* applicaties. De combinatie van een geschikt poreus membraan en een biologische coating zou de vorming van een dichte en functionele niercellaag moeten stimuleren om uiteindelijk een zogenaamd 'levend membraan' te ontwikkelen dat in staat is om afvalstoffen uit te scheiden. In **hoofdstuk 4** wordt een overzicht gegeven van de tot op heden geteste biomaterialen en toegepaste coatings voor BAK doeleinden. Het is gebleken dat bijvoorbeeld de combinatie 3,4-dihydroxy-L-phenylalanine (L-DOPA) en collagen IV gunstig is voor cellaagvorming. Om de efficiëntie waarmee PTEC monolagen in een BAK afvalstoffen kunnen transporteren nader vast te stellen zijn er echter nog uitgebreide studies nodig. Bovendien zullen veiligheidsaspecten nauwkeurig onderzocht moeten worden om het gebruik van een BAK als therapeutische toepassing voor patiënten met nierfalen te kunnen realiseren. Daarnaast worden in dit hoofdstuk de mogelijkheden voor een draagbare of implanteerbare kunstnier en het gebruik van stamcel technologieën voor gepersonaliseerde BAK toepassingen als mogelijk toekomstige toepassingen geëvalueerd.

In de nier wordt de klaring van uremische toxinen vanuit het bloed naar de voorurine gemedieerd door PTEC specifieke in- en efflux transporteiwitten. Deze uitscheidingsprocessen dienen ook plaats te vinden in een BAK om daarmee de huidige hemodialyse technieken te kunnen verbeteren. In **hoofdstuk 5** wordt de klaring van het kationische creatinine door ciPTEC cellagen gekweekt in 2D op gecoate biomaterialen bestudeerd. Eerst is een coating, bestaande uit L-DOPA en collagen IV, dermate geoptimaliseerd dat er een balans ontstond waarin de permeabiliteit van de PES/PVP membraan gehandhaafd werd en er tevens een dichte cellaag ontstond met een homogene ZO1 expressie. Het transport van creatinine is bestudeerd in ciPTEC cellagen op gemodificeerde PES/PVP membranen en vergeleken met cellagen op Transwell inserts. Deze inserts zijn commerciële kweeksystemen welke de gouden standaard zijn voor het bestuderen van cellulaire (transport) processen. Deze systemen zijn echter niet geschikt zijn voor BAK toepassingen vanwege de beperkte hemocompatibele eigenschappen. Het transport van creatinine door ciPTEC cellagen gekweekt op gemodificeerd PES/PVP was

niet verschillend van dat op Transwell inserts. Dit betekent dat ciPTEC functie gehandhaafd blijft op hemocompatibele PES/PVP biomaterialen. In **hoofdstuk 6** is deze kennis verkregen in 2D vertaald naar 3D door gebruik te maken van holle buisjes van PES/PVP membranen. Eenzelfde compositie van coating worden toegepast, echter was het wel noodzakelijk om de coatingtijd te verlengen om goede dichte cellagen te verkrijgen. Opnieuw is de membraanpermeabiliteit onderzocht en is de coating afgestemd op de passage van moleculen als H_2O en albumine, zodat uiteindelijk ook afvalstoffen gebonden aan albumine in nabijheid van de cellaag konden komen. Op buisjes gekweekte cellen vertoonden naast een gepolariseerd karakter, aangetoond middels ZO1 en OCT2 expressie, ook intacte celorganellen en een PTEC-specifieke apicaalmembraan met microvilli. De functionaliteit van deze buisjes is onderzocht door gebruik te maken van geavanceerde fluorescentie microscopie in combinatie met een perfusie systeem om het opname proces van een model substraat 4-(4-(dimethylamino)styryl)-N-methylpyridinium-iodide (ASP^+) in de tijd te kunnen volgen. De opname van ASP^+ kon worden geremd door een mengsel van kationische uremische metabolieten en door het geneesmiddel en bekend OCT substraat, cimetidine. Deze bevindingen geven aan dat kationische transportprocessen aanwezig zijn in ciPTEC gekweekt op holle buisjes en bevestigd daarmee de succesvolle ontwikkeling van een functioneel bioartificieel nierbuisje. Naast kationische toxinen spelen met name ook anionische uremische toxinen een prominente rol in de progressie van het uremisch syndroom. Hiertoe is in **hoofdstuk 7** de interactie van anionische uremische toxinen op niertransport in 2D onderzocht, en vervolgens het uitscheidingsproces in bioartificiele nierbuisjes bestudeerd. Een groep van acht uremische toxinen was in meer of minder mate in staat om het transport van een organisch-aniontransporter – 1 (OAT1) en - 3 (OAT3) modelsubstraat op een competitieve manier te remmen. Uit deze groep zijn indoxylsulfaat en kynureninezuur geselecteerd voor nader onderzoek, aangezien deze stoffen een hoge potentie vertoonden om OAT-gemedieerd transport te beïnvloeden en geassocieerd zijn met diverse uremische complicaties. Het transport van beide toxinen door OAT1 kon worden bevestigd in 2D cellagen. Vervolgens is voor beide stoffen de uitscheiding door de bioartificiële nierbuisjes bestudeerd. Actieve uitscheiding kon worden bevestigd en bovendien werd door de aanwezigheid van albumine aangetoond dat eiwit-binding een gunstig effect heeft op deze uitscheiding.

Het doel van dit proefschrift was de ontwikkeling van nieuwe therapeutische interventies om PTEC functie te vervangen tijdens eindstadium nierfalen,

door de uitscheiding van kationische alsmede anionische uremische toxinen in 2D en vervolgens in bioartificiële nierbuisjes te bestuderen. In **hoofdstuk 8** worden de resultaten verkregen in dit proefschrift bediscussieerd. Daarnaast wordt noodzakelijk toekomstig (pre)klinisch onderzoek naar de verkregen bioartificiële nierbuisjes nader toegelicht en worden de mogelijkheden met betrekking tot gepersonaliseerde regeneratieve nefrologie beschreven. Samenvattend kan gesteld worden dat dit proefschrift bijdraagt aan een eerste stap in de richting van nieuwe nierfunctievervangende therapieën voor de toekomstige behandeling van eindstadium nierfalen.

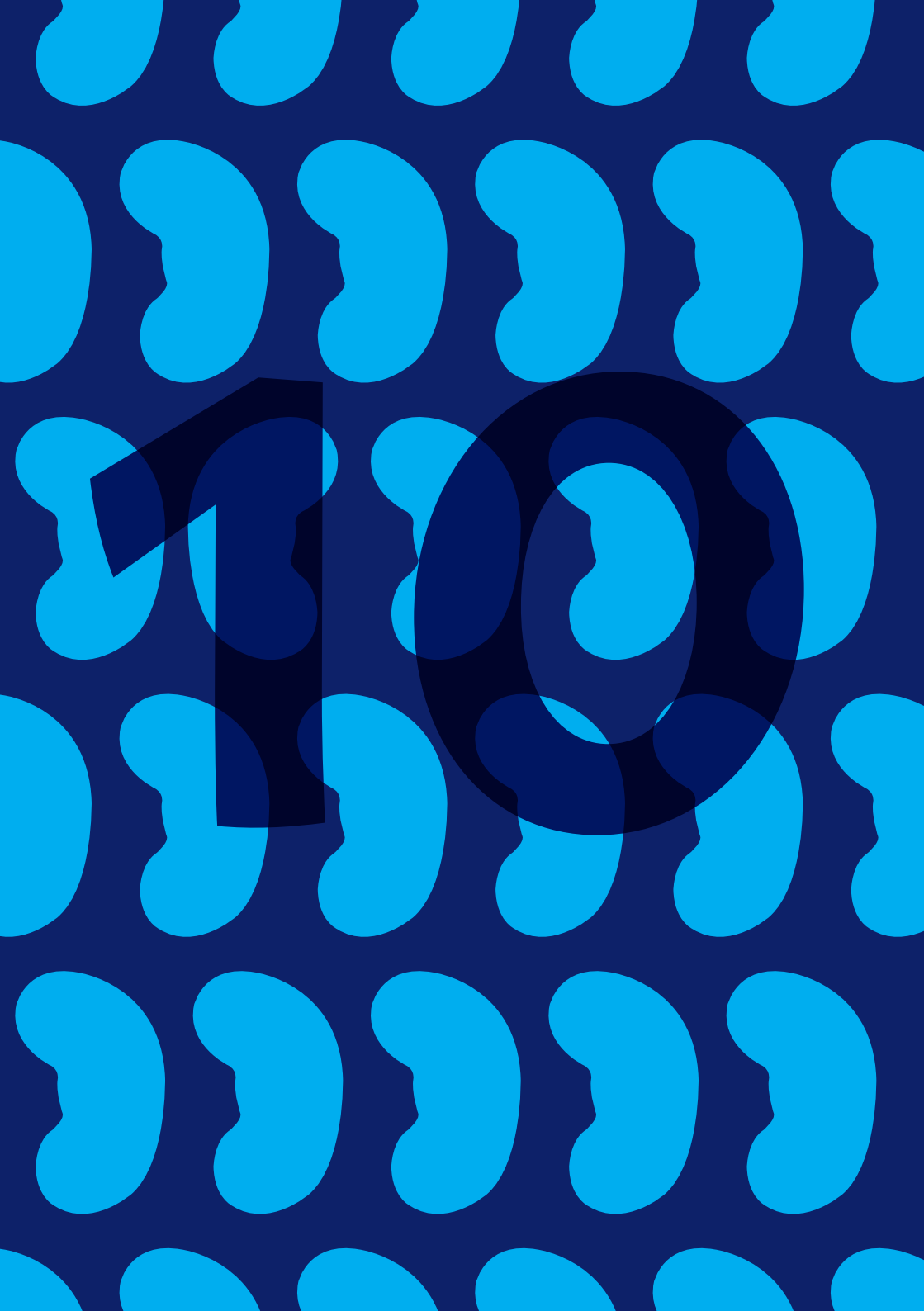
10

Chapter 10

LIST OF ABBREVIATIONS
CURRICULUM VITAE
BIBLIOGRAPHY & AWARDS
RIMLS PORTFOLIO

LIST OF ABBREVIATIONS

ABC	ATP-binding cassete
AKI	Acute kidney injury
ASP^+	4-(4-(dimethylamino)styryl)-N-methylpyridinium-iodide
ATMPs	Advanced therapy medicinal products
ADP	Adenosine diphosphate
ATP	Adenosine triphosphate
BAK	Bioartificial Kidney
BCECF	2',7'-Bis-(2-Carboxyethyl)-5-(and-6)-carboxyfluorescein acetoxy methyl ester
BCRP	Breast cancer resistance protein
BM	Basement membrane
BRECS	Bioartificial renal epithelial cell system
BSA	Bovine serum albumin
CiPTEC-U	Conditionally immortalized proximal tubule epithelial cell, urine origin
CiPTEC-T1	Conditionally immortalized proximal tubule epithelial cell, tissue origin 1
CiPTEC-T2	Conditionally immortalized proximal tubule epithelial cell, tissue origin 2
CKD	Chronic kidney disease
CM-H_2DCFDA	5-(and-6)-Chloromethyl-2',7'-dichlorodihydrofluorescein diacetate, acetyl ester
Coll IV	Collagen IV
COX	Cytochrome c oxidase
CI-V	Mitochondrial respiratory complex I-V
kDa	Kilodalton
ECM	Extra cellular matrix
ESCs	Embryonic stem cells
ESRD	End stage renal disease
EUtox	European uremic toxin (work group)
FCS	Fetal calf werum
G3PDH	Glycerol-3-phosphate dehydrogenase
G418	Geneticin
GAGs	Glycosaminoglycans
GC(R)	Glucocorticoid (receptor)
GFR	Glomerular filtration rate

GGT	γ-Glutamyltransferase
GRE	Glucocorticoid responsive element
HBSS	Hanks' balanced salt solution
HEK	Human embryonic kidney
HFM	Hollow fiber membranes
HGF	Hepatocyte growth factor
HK-2	Human kidney-2
HPTC	Human primary tubular cell cultures
HSA	Human serum albumin
hTERT	Essential catalytic subunit of human telomerase
HUVEC	Human umbilical vein endothelial cells
IC50	Half maximal inhibitory concentration
ICU	Intensive care unit
IgG	Immunoglobulin G
IL-6/-8	Interleukin-6 / -8
iNOS	Inducible nitric oxide synthase
iPSCs	Induced pluripotent stem cells
J	Flux
L-DOPA	3,4-Dihydroxy-L-phenylalanine
LLC-PK	Lilly laboratories cell porcine kidney proximal tubular cells
LPS	Lipopolysaccharide
MATE	Multidrug and toxin extrusion protein
MDCK	Madin-darby canine kidney cells
MMM	Mixed matrix membranes
MRP2/-4	Multidrug resistance protein -2 / -4
mTOR	Mammalian target of rapamycin
MTT	(3-(4,5-Dimethylthiazol-2-yl)-2,5-diphenyltetrazoliumbromide
MW	Molecular weight
NAD	Nicotinamide adenine dinucleotide
NBC-1	Sodium-bicarbonate co-transporter -1
NF-κB	Nuclear factor kappa bèta
NHE-3	Sodium-proton exchanger-3
NO	Nitric oxide

(i)NOS	(Inducible) nitric oxide synthase
OA	Organic anion
OAT	Organic anion transporter
OATP	Organic anion transporting polypeptide
OC	Organic cation
OCT	Organic cation transporter
OCTN	Carnitine/organic cation transporter
OXPHOS	Oxidative phosphorylation system
PBS	Phosphate buffered saline
PBS-T	Phosphate buffered saline - tween
PES	Polyethersulfone
PGC-1α	Peroxisome proliferator –activated receptor (PPAR) gamma coactivator - 1α
P-gp	P-glycoprotein
PG	Proteoglycan
P:O	Phosphate : oxygen
PSF	Polysulfone
PTEC	Proximal tubule epithelial cell
RAD	Renal assist device
ROS	Reactive oxygen species
SC	Sieving coefficient
SDS-PAGE	Sodium sodecyl sulfate polyacrylamide gel electrophoresis
SEM	Standard error of the mean
SEM image	Scanning electron microscope image
SLC	Solute carrier
SM	Stromal matrix
SV40-T	Simian virus 40 large T antigen
TEER	Trans-epithelial electric resistance
TMRM	Tetramethylrhodamine methyl ester
TNF-α	Tumor necrosis factor-α
TPA	Tetrapentylammoniumchloride
UGT	UDP-glucuronosyltransferases
Upy	Ureido-pyrimidinone
URAT	Urate reuptake transporter

UT(s)	Uremic toxin(s)
V/V	Volume/volume
W/V	Weight/volume
WAK	Wearable artificial kidney
ZO-1	Zona occludens 1

CURRICULUM VITAE

Jitske Jansen werd geboren op 14 maart 1984 te Beek (Montferland). In 2001 behaalde zij haar HAVO-diploma, profiel Natuur en Gezondheid, aan het Liemers College te Zevenaar. In hetzelfde jaar begon zij aan de Hogere Laboratorium opleiding aan de Hogeschool van Arnhem en Nijmegen. Tijdens haar opleiding tot Medische Microbiologisch analist liep ze twee stages binnen dit vakgebied (Slingeland ziekenhuis, Doetinchem en Canisius Wilhelmina Ziekenhuis, Nijmegen). In 2005 behaalde zij haar HLO-diploma en in datzelfde jaar begon ze aan de opleiding Biologie aan de Radboud Universiteit Nijmegen. Na enkele maanden werd deze studie beëindigd en begon zij haar loopbaan als medisch microbiologisch analist in het Canisius Wilhelmina Ziekenhuis te Nijmegen, afdeling Medische Microbiologie. Na 2,5 jaar begon zij in 2007 als analist bij QM Diagnostics in het RadboudUMC te Nijmegen, waarna zij vervolgens binnen het UMC de overstap maakte naar de afdeling kindergeneeskunde. Daar ging zij aan de slag bij de DNA diagnostiek onder leiding van Prof. Dr. L.P.W.J. van den Heuvel en Ing. W. Heys. Zij verrichte genetische analyses om mutaties op te sporen in het oxidatieve fosforyleringssysteem van mitochondriën alsmede DNA onderzoek naar genen gerelateerd aan het atypische hemolytisch uremisch syndroom. In het najaar van 2010 begon zij als research analist op het zogenaamde Biologische Kunstnier project (BioKid P3.01) onder leiding van Prof. Dr. R. Masereeuw, Prof. Dr. J.G.J. Hoenderop en Prof. Dr. L.P.W.J. van den Heuvel. Dit project maakte onderdeel uit van het onderzoeksprogramma van het BioMedical Materials Institute, mede gefinancierd door het ministerie van Economische Zaken en ondersteund door de Nierstichting. In dit project werkte zij nauw samen met de toenmalige promovendus C.M.S. Schophuizen. Na 2 jaar succesvol als research analist gewerkt te hebben, begon zij oktober 2012 haar promotieonderzoek naar de ontwikkeling van de Biologische Kunstnier onder leiding van Prof. Dr. R. Masereeuw, Prof. Dr. J.G.J. Hoenderop, Prof. Dr. L.P.W.J. van den Heuvel en Dr. M.J. Wilmer. Haar onderzoek maakte deel uit van het Netherlands Institute for Regenerative Medicine, mede gefinancierd door het ministerie van Economische Zaken en ondersteund door de Nierstichting. Jitske heeft meerdere studenten begeleid, haar werk gepresenteerd op nationale en internationale congressen en ze heeft verschillende prijzen in ontvangst mogen nemen. Haar onderzoek heeft geleid tot meerdere gepubliceerde artikelen en dit proefschrift. Jitske zet haar wetenschappelijke carrière voort in de regeneratieve nefrologie en is momenteel werkzaam als post-doctoraal onderzoeker aan de Universiteit Utrecht, departement Farmaceutische Wetenschappen, afdeling Farmacologie, onder leiding van Prof. Dr. R. Masereeuw.

BIBLIOGRAPHY

Full papers

Jansen J*, Fedecostante M*, Kreuser UM, JG Peters, A Bilos, Wilmer MJ, Mensink RA, Boltje TJ, Stamatialis D, Wetzels JFM, van den Heuvel LP, Hoenderop JG, Masereeuw R. Bioengineered kidney tubules efficiently excrete uremic toxins. Nature Scientific Reports. 2016; 6:26715.

Chevtchik NV, Fedecostante M, Jansen J, Mihajlovic M, Wilmer M, Rüth M, Masereeuw R, Stamatialis D. Upscaling of a living membrane for bioartificial kidney device. Eur J Pharmacol. 2016, in press

Jansen J, De Napoli IE, Fedecostante M, Schophuizen CMS, Chevtchik NV, Wilmer MJ, van Asbeck AH, Croes HJ, Pertijs JC, Wetzels JFM, Hilbrands LB, van den Heuvel LP, Hoenderop JG, Stamatialis D, Masereeuw R. Human proximal tubule epithelial cells cultured on hollow fibers: living membranes that actively transport organic cations. Nature Scientific Reports. 2015; 5:16702.

Schophuizen CM*, De Napoli IE*, Jansen J, Teixeira S, Wilmer MJ, Hoenderop JG, Van den Heuvel LP, Masereeuw R, Stamatialis D. Development of a living membrane comprising a functional human renal proximal tubule cell monolayer on polyethersulfone polymeric membrane. Acta Biomaterialia. 2015;14:22-32.

Poesen R, Mutsaers HA, Windey K, van den Broek PH, Verweij V, Augustijns P, Kuypers D, Jansen J, Evenepoel P, Verbeke K, Meijers B, Masereeuw R. The Influence of Dietary Protein Intake on Mammalian Tryptophan and Phenolic Metabolites. PloS One. 2015;10(10):e0140820.

Jansen J*, Schophuizen CM*, Wilmer MJ, Lahham SH, Mutsaers HA, Wetzels JF, Bank RA, van den Heuvel LP, Hoenderop JG, Masereeuw R. A morphological and functional comparison of proximal tubule cell lines established from human urine and kidney tissue. Experimental cell research. 2014;323(1):87-99.

Jansen J*, Fedecostante M*, Wilmer MJ, van den Heuvel LP, Hoenderop JG, Masereeuw R. Biotechnological challenges of bioartificial kidney engineering. Biotechnology Advances. 2014;32(7):1317-27.

Schophuizen CM*, Wilmer MJ*, Jansen J, Gustavsson L, Hilgendorf C, Hoenderop JG, van den Heuvel LP, Masereeuw R. Cationic uremic toxins affect human renal proximal tubule cell functioning through interaction with the organic cation transporter. Pflugers Archiv.: European Journal of Physiology. 2013;465(12):1701-14.

Mutsaers HA, Wilmer MJ, Reijnders D, Jansen J, van den Broek PH, Forkink M, Schepers E, Glorieux G, Vanholder R, van den Heuvel LP, Hoenderop JG, Masereeuw R. Uremic toxins inhibit renal metabolic capacity through interference with glucuronidation and mitochondrial respiration. Biochimica et Biophysica Acta. 2013;1832(1):142-50.

Jonckheere AI, Huigsloot M, Lammens M, Jansen J, van den Heuvel LP, Spiekerkoetter U, von Kleist-Retzow JC, Forkink M, Koopman WJ, Szklarczyk R, Huynen MA, Fransen JA, Smeitink JA, Rodenburg RJ. Restoration of complex V deficiency caused by a novel deletion in the human TMEM70 gene normalizes mitochondrial morphology. Mitochondrion. 2011;11(6):954-63.

Westra D, Volokhina E, van der Heijden E, Vos A, Huigen M, Jansen J, van Kaauwen E, van der Velden T, van de Kar N, van den Heuvel L. Genetic disorders in complement (regulating) genes in patients with atypical haemolytic uraemic syndrome (aHUS). Nephrology, Dialysis, Transplantation: 2010;25(7):2195-202.

Submitted

Caetano-Pinto P, Jansen J, Masereeuw R. The importance of Breast Cancer Resistance Protein to the kidneys excretory function and in chemotherapeutic resistance. 2016.

Schirris TJJ*, Jansen J*, Mihajlović M, van den Heuvel LP, Masereeuw R*, Russel FGM*. Mild intracellular acidification by dexamethasone attenuates mitochondrial dysfunction in a human inflammatory proximal tubule epithelial cell model. 2016.

Schirris TJJ, Rossell S, Manjeri GR, Renkema GH, Jansen J, Beyrath JD, Willems PHGM, Huijnen MA, Smeitink JAM, Russel FGM, Notebaart RA. Towards intervention of mitochondrial complex I-deficiency: elimination of electron excess via cholesterol biosynthesis as electron sink. 2016.

* both authors contributed equally

Blog

Jansen J. Let's raise awareness for kidney disease! AAPS J Blog in Current Perspectives. 2016; http://aapsblog.aaps.org/2016/03/09/lets-raise-awareness-for-kidney-disease/

Awards

Young Investigator Award of the Federation of European Pharmacology Societies (EPHAR) and the European Association for Clinical Pharmacology and Therapeutics (EACPT), Istanbul, Turkey, 2016.

One year full ERA-EDTA membership following two oral presentations during the EUtox meeting, Marseille, France, 2015.

Best poster award New Frontiers in regenerative medicine, October 2014, Nijmegen.

Van Noordwijk Stipendium prize (Battle of the Universities), October 2014, Eindhoven.

PHD PORTFOLIO

Institute for Molecular Life Sciences
Radboudumc

Name PhD candidate: J. Jansen	PhD period: 01-10-2012 – 31-12-2015
Department: Pharmacology & toxicology	Promotors:
Graduate School: Radboud Institute for Molecular Life Sciences	Prof. Dr. R. Masereeuw,
	Prof. Dr. J.G.J. Hoenderop,
	Prof. Dr. L.P.W.J. van den Heuvel
	Co-promotor: Dr. M.J. Wilmer

	Year(s)	ECTS
TRAINING ACTIVITIES		
Courses & Workshops		
- Winterschool Dutch Kidney Foundation	2013	1.75
- RIMLS Graduate School	2013	1.75
- Systematic review course – SYRCLE	2013	0.2
- Course 'How to write a medical scientific paper'	2013	0.2
- MIC user meeting – Leica SP8 intro	2014	0.1
- Nephrotools / BioArt workshop	2014	0.2
- RU workshop: 'Get Inspired'	2014	0.2
Seminars & lectures		
- Prof. Dr. R. Kleta – EAST syndrome	2012	0.1
- Technical Forum Tissue Engineering	2013	0.1
- Prof. Dr. D. Markovich - NaS1 and Sat1 transporters in PTEC	2013	0.1
- Noon-spotlight seminar: Chemical and Physical biology	2013	0.1
- Kidney Theme – Tissue engineering[b]	2013	0.35
- Prof. Dr. F. Ashcroft – ATP-sensitive K^+ channels and neonatal diabetes	2013	0.1
- Kidney Theme – Uremic toxins	2013	0.1
- Dr. R. Xavier- Biology in immunity	2013	0.1
- Prof. Dr. D. Humes	2013	0.1
- Dr. S. Tornroth – Structural basis for regulation of eukaryotic aquaporins	2013	0.1
- Noon-spotlight seminar: Zebrafish as a model system to study the function and pathology of new genes	2013	0.1
- Prof. Dr. R. Vanholder – An update on the Cinderella of protein-bound uremic toxins	2014	0.1
- Kidney Theme – Brainstorm session	2014	0.1
- Dr. B. Gloss – Trends in transcriptomics	2014	0.1
- Prof. Dr. R. Walker – Mechanisms of drug nephrotoxicity	2014	0.1
- Dr. C. Lee-Thedieck – The significance of material properties for stem cells	2014	0.1
- Radboud Research Rounds – Renal disorders	2014	0.1
- Prof. Dr. S. Dryer – Multimodal gating of podocyte TRPC6 channels and dysregulation in a rodent model of FSGS	2014	0.1
- Kidney Theme meeting	2014	0.1
- Kidney Theme meetings (8x)	2015	0.8
- Radboud Research Rounds Plus: Prof. Dr. M. Little - How to build a kidney: organogenesis to regeneration and back again.	2015	0.1

- Radboud Research Rounds Plus: Meet the Professor. Prof. Dr. M. Little	2015	0.1
- Dr. J. de Boer – Talking to cells: surface topography as a tool to evoke cellular responses	2015	0.1
Symposia & congresses		
- New Frontiers in Personal Genomics	2012	0.5
- IGMD Science Day[a]	2013	0.5
- Dutch Nephrology Days[a]	2013	0.75
- PLAN Day[b]	2013	0.35
- RIMLS PhD retreat	2013	0.5
- Spring meeting Dutch Society of Pharmacology	2013	0.25
- BMM annual meeting[b]	2013	0.5
- NIRM annual meeting[a]	2013	0.75
- REFORM symposium[b]	2013	0.5
- NCMLS PhD retreat[a]	2014	0.5
- Dutch Nephrology Days[b]	2014	0.5
- NfN Najaarssymposium[a]	2014	0.5
- New Frontiers in Regenerative Medicine[a]*	2014	0.75
- NIRM annual meeting[a]	2014	0.5
- ASN conference, Philadelphia, USA[a,b]	2014	2.25
- EUtox meeting Marseille, France[b,b]	2015	1.5
- Spring meeting Dutch Society of Pharmacology[a]	2015	0.5
- RIMLS PhD retreat[b]	2015	0.5
- Nephrotools conference, Liverpool, UK[a]	2015	1.0
- Radboud Frontiers in Cilia Medicine	2015	0.5
Other		
- Voorlichtingsdag Biomedische Wetenschappen[b]	2013	0.1
- Publieksavond 'Nier op maat'- Demo experimental setup	2014	0.2
- Van Noordwijk Stipendium – Battle of the Universities*	2014	0.5
- Co-organizer World Kidney Day 2015 event – Clean the Waal beach	2015	0.5
- Membership Renal Theme Board – Representative PhD students	2015	0.5
TEACHING ACTIVITIES		
Lecturing		
- Capita Selecta: De biologische kunstnier	2014	0.5
- Capita Selecta: De biologische kunstnier	2015	0.5
Supervision of internships / other		
- Supervision K. Jansen – lab intro excellent student programme	2013	0.1
- Supervision D. den Braanker – Master thesis	2013	0.05
- Supervision Y. van Deursen – Master internship	2013-14	2
- Supervision J. Stoop – Bachelor internship	2014	2
- Supervision I. Donderwinkel – Bachelor internship	2014	1
- Supervision BMW students – Writing a research paper (5AM08)	2014	0.1
TOTAL		29.3

[a] poster presentation, [b] oral presentation, * awarded.

Chapter 11

DANKWOORD

Acknowledgments

DANKWOORD

Promoveren. Of ik het traject ook ingegaan was als ik toen wist wat ik nu weet? Een volmondig JA! Dit overtuigende antwoord is te danken aan het team professionals om me heen en de mensen uit mijn privé omgeving. Daarom wil ik in dit dankwoord graag een aantal personen bedanken die een belangrijke bijdrage hebben gehad aan de totstandkoming van dit proefschrift.

Prof. dr. R. Masereeuw, beste **Roos**. Jouw bijdrage in mijn ontwikkeling van analist tot gepromoveerd onderzoeker is enorm geweest en ik wil je dan ook graag hartelijk danken voor al je ondersteuning en het vertrouwen in mij. Dat het ons is gelukt om functionerende nierbuisjes te ontwikkelen is fantastisch en jouw aandeel hierin is essentieel geweest. Jouw enthousiasme, kennis en doorzettingsvermogen ervaar ik dan ook als zeer inspirerend. Als we lastig interpreteerbare resultaten hadden wist jij altijd weer met een goede oplossing te komen zodat ik vol goede moed weer verder ging. Ondanks je drukke agenda vind je altijd weer even de tijd om mee te denken of een manuscript te reviewen. Dank daarvoor!
Maar zeker waardeer ik ook je oprechte en sociale karakter, waardoor je bij jou altijd met alles terecht kunt. Als er weer eens iets was met de honden, of voorheen met t paard dan werd dat net zo goed besproken als het experiment van de afgelopen week. Of gewoon gezellig een borrel op vrijdag middag, je deelname aan Döner-donderdag of een etentje bij je thuis, dit alles maakt je een bijzonder plezierig persoon om mee samen te werken. Ik ben dan ook dankbaar dat ik mijn wetenschappelijke carrière voort mag zetten onder jouw supervisie. De mogelijkheden die je mij geeft als postdoc binnen jouw onderzoeksgroep aan de Universiteit Utrecht bieden mij de kans om het avontuur in de onderzoekswereld verder aan te gaan, veel dank daarvoor! Ik hoop dat we samen nog veel wetenschappelijke hoogtepunten zullen bereiken (en vieren ☺)!

Prof. dr. J.G.J. Hoenderop, beste **Joost**. Ik begon als analist op het BioKid project bij jou op het lab en later als promovendus verhuisde ik naar farmacologie. Ik heb door de jaren heen altijd van jullie faciliteiten gebruik mogen maken (en de feestjes, gebak, etc. ☺) en was meer dan welkom. Ik heb daardoor de samenwerking tussen de verschillende afdelingen binnen mijn project dan ook als zeer positief ervaren. Dank daarvoor! Je kennis en gedrevenheid is enorm en de input die jij gaf tijdens onze BioKid werkbesprekingen waren zeer waardevol en vaak de trigger om experimenten nog net even iets verder

uit te werken. Jouw bijdrage heeft er mede voor gezorgd dat mijn onderzoek succesvol is geworden. En ik nu alle figuren in mijn presentaties uitlijn, even groot maak, zelfde kleur/stijl/font size toepas, etc. ☺ Behalve je professionele vaardigheden was je ook regelmatig in voor een geintje tussendoor (Martijn's introductieweek bij fysiologie bijvoorbeeld) of gewoon een praatje bij de koffiemachine. Naast het onderzoek gaf je me ook de mogelijkheid om me verder te ontwikkelen op meer organisatorisch vlak en beleidsniveau binnen het Nier thema. Ik wil je dan ook graag bedanken voor alle ondersteuning. En natuurlijk niet te vergeten de organisatie van World Kidney Day 2015 en 2016. We hebben samen twee succesvolle edities georganiseerd en wat mij betreft volgen er nog velen!

Prof. dr. L.P.W.J. van den Heuvel, beste **Bert**. Bij jou is het min of meer allemaal begonnen, toen ik als analist in de DNA-groep in aanraking met het wetenschappelijk onderzoek kwam. Na een paar jaar had ik de behoefte om me verder te ontwikkelen en je vertelde me iets over het BioKid project en dat er geld was voor een research analist. Na het sollicitatiegesprek met Roos en Joost kreeg ik het heuglijke nieuws dat ik aangenomen was en 'the rest is history'. Ik wil je dan ook bedanken voor de ondersteuning tijdens de afgelopen jaren. Naast het delen van je kennis over de nieren ben je ook altijd in voor een 'social talk'; even een update geven over de fopshop, je fobie voor vrijdag de 13e of de status van de door jou zelf in elkaar geknutselde auto, dit soort onderwerpen werden op vermakelijke wijze besproken. Het hoogtepunt was natuurlijk ons (jij, Marieke van Mullem en ik) karaoke optreden tijdens een labuitje van kindergeneeskunde. Vol overgave zongen we samen 'Maak me gek' van Gerard Joling. Top optreden. Bedankt voor de mooie tijd!

Dr. M.J. Wilmer, beste **Martijn**. Toen ik bij kindergeneeskunde kwam zat jij te zwoegen aan je proefschrift. Ik wist dat je iets met nieren deed, maar veel meer dan dat ook niet. En de term 'ciPTEC' kwam verdacht vaak voorbij, maar wat je daar aan had?! Verder was het duidelijk dat je als echte Limburger van een feestje hield en je in spraakmakende outfits carnaval vierde. Later raakte ook ik besmet met het 'ciPTEC-virus' en het werd zelfs een succesvolle besmetting. Ik heb veel van je geleerd en heb altijd prettig met je samengewerkt. Jij als ciPTEC-vader wist als geen ander hoe experimenten in te richten met deze cellen en je kennis was dan ook essentieel. Ik wil je hartelijk danken voor al je hulp, ondersteuning en ook de gezelligheid op feestjes. Je bent nu je wilde haren kwijt, gesetteld en zelfs vader; chapeau ☺!

Graag wil ik de leden van manuscript commissie, **Prof. dr. D.W. Swinkels**, **Dr. ir. W.F. Daamen** en **Prof. dr. M.C. Verhaar**, hartelijk danken voor de zorgvuldige beoordeling van mijn proefschrift. Ook wil ik graag de overige leden van de oppositie bedanken voor hun bereidheid zitting te nemen in de commissie voor de promotie.

Rachel en **Marthe**, mijn lieve paranimfen! Ik ben blij dat jullie aan mijn zijde staan tijdens het uur van de waarheid, bedankt dat jullie mijn paranimf willen zijn. Rachel, soms kom je mensen tegen in je leven waarbij je je vanaf minuut één op je gemak voelt en dat had ik bij jou. We verstaan elkaar moeiteloos, of het nu gaat om wetenschap, versieren van werkplekken of de passie voor honden en dat is bijzonder plezierig. Jouw doorzettingsvermogen, kennis en gedrevenheid zijn bewonderenswaardig en je hebt daarmee een mooie positie weten te vergaren in de groep van Prof. dr. D.W. Swinkels. Ik wil je bedanken voor je steun tijdens de afgelopen jaren en hoop dat we onze interesses nog lang mogen blijven delen! Marthe, bij kindergeneeskunde hebben we menig sequentie reactie samen ingezet en onze samenwerking verliep altijd bijzonder soepel. Daarnaast hadden we gemeenschappelijke passies en dus voldoende gespreksstof tijdens ons werk; namelijk de paarden en honden (en soms de mannen bij genetica ☺). Verder denk ik bij deze periode met plezier terug aan de Jillz-avond, al lust ik na die avond gek genoeg geen Jillz meer. Uiteindelijk gingen we beide een andere kant op, maar altijd hebben we nauw contact behouden. Het is fijn om een vriendin te hebben waarbij ik altijd terecht kan in voor- en tegenspoed, bedankt!

Het ontwikkelen van een biologische kunstnier is een uitdagende expeditie, hetgeen enkel succesvol kan worden in een goed draaiend team. Ik wil dan ook graag de Biokiddies bedanken voor hun samenwerking. **Carolien**, samen begonnen we aan de uitdaging om nierbuisjes te maken voor de biologische kunstnier, jij als promovendus en ik in eerste instantie als analist. Menig cellijn, PES-membraan, transportexperiment, potjes L-DOPA en collageen zijn door onze handen gegaan en al 't noeste arbeid heeft uiteindelijk geleid tot twee proefschriften. Ik wil je ontzettend bedanken voor de plezierige samenwerking, jouw geduld om zaken uit te zoeken en te regelen en je hulp bij het schrijven van het eerste artikel over de cellijnen. Daarnaast was je altijd bereid om te helpen met experimenten en dus weer, voor de zoveelste keer, met de step richting de toren te komen (en je ons dus ook even een update kon geven over je surf hunk ☺). Jouw aandeel in de totstandkoming van mijn proefschrift is essentieel geweest. Bedankt voor al je support en veel geluk voor de toekomst!

Rick M, 'Mister Uremic Toxin'. Toen Carolien en ik op het Biokid project begonnen was jij al even bezig om rol van niertransporters in uremie te onderzoeken. Samen met Martijn heb je mij ondergedompeld in de wondere wereld van de celkweek en mij de kneepjes van dit vak en de weg naar de Aesculaaf geleerd. Jouw kennis en creatieve houding zijn een waardevolle bijdrage geweest voor het Biokid project. Dank daarvoor! **Michèle** and **Miloš**, you were highly valuable members in the Nijmegen BioKid team, but I will acknowledge you in the Utrecht section ☺.

Prof. dr. D. Stamatialis, dear **Dimitrios**, I am very grateful for our enjoyable collaboration during the past years. Our vivid scientific discussions were really valuable to expand my (biomaterials) knowledge and to bring our research to the next level, but I also appreciated the social talks during meetings very much. Together we published several nice papers and hopefully that number will rise in the future. **Natalia**, **Ilaria** and **Sandra**, many thanks for the fruitful collaboration. I wish you all the best for the future!

Prof. dr. R.A. Bank, beste **Ruud**. Ik wil je hartelijk danken voor de prettige samenwerking tijdens het BioKid project. We hebben een mooi artikel over de cellijnen samen weten te publiceren, welke het fundament is geweest voor de ontwikkeling van de biologische kunstnier.

Prof. dr. L.B. Hilbrands en Prof. dr. J.F. Wetzels, beste **Luuk** en **Jack**, jullie klinische inbreng in dit project is zeer waardevol geweest. Jullie expertise en kritische noot heeft er mede voor gezorgd dat we er in zijn geslaagd om de nierbuisjes te publiceren in mooie vakbladen. Daarnaast was de toegang tot controle en uremisch plasma altijd binnen handbereik, hartelijk dank daar voor.

Tevens wil ik ook graag de overige projectleden van de **TU Eindhoven**, de **Nierstichting** en **PharmaCell** bedanken voor de prettige samenwerking.

Moreover, I would like to thank the **Renal Theme board members** for the inspiring meetings and the opportunity for me to learn more about regulatory, research and teaching affairs within the Renal Theme.

Tevens wil ik graag mijn mentor, Dr. J. van der Vlag, bedanken voor zijn begeleiding tijdens mijn promotietraject. Beste **Johan**, eens per jaar kwam ik met mijn RIMLS Trainings- and Supervision Plan onder mijn arm bij je langs

om de stand van zaken met betrekking tot mijn promotieonderzoek door te nemen. Het waren altijd prettige gesprekken en als ik je kamer verliet ging ik altijd met een gerust hart weer verder met mijn onderzoek. Tijdens ons laatste mentorgesprek, toen ik toch wat twijfelde over wat ik nou moest gaan doen na mijn PhD, gaf je me een helder advies. Ik heb dit advies dan ook opgevolgd, behalve dan dat ik het Radboud heb verlaten ☺. Ook wil ik je bedanken voor de mogelijkheid om jullie nierendotheelcellen te gebruiken in een aantal pilot studies, wie weet komen onze epitheelcellen en jullie endotheelcellen nog weer eens samen in de toekomst.

Daarnaast zijn er veel (oud-)collega's binnen de verschillende afdelingen die het werk tijdens mijn promotietraject bijzonder aangenaam hebben gemaakt. **Janny**, ik wil je bedanken voor je betrokkenheid en oprechte interesse in het onderzoek, maar ook de gezellige 'social talks' over niet-werk gerelateerde zaken. Als die ($%$!) fibers kuren hadden, wist je me altijd weer op te beuren. Daarnaast zorg jij er mede voor dat het lab goed draait en is het fijn om iemand op de werkvloer te hebben waarbij je altijd terecht kunt met praktische vragen en van op aan kunt. **Rick G** en **Karl**, onze Boer-Zoekt-Vrouw groepsapp gaat hopelijk ook in het nieuwe seizoen weer van start. Als nuchtere mede-achterhoekers verstonden we elkaar goed, bedankt voor jullie support en de gezelligheid binnen en buiten het lab! **Tom S.**, waar die ciPTECs niet allemaal goed voor zijn ☺. We hebben samen een mooi artikel bij elkaar gepipetteerd over de energiecentrales in niercellen. Je bent nu al een succesvol onderzoeker en tevens bijzonder goed in t prakken van kilo's koeienweefsel. Bon, bedankt voor de fijne samenwerking en veel succes in Cambridge! **Jelle** en **Tom N**, mede-ciPTECers die als geen ander weten hoe lastig het kan zijn om het de niercellen naar hun zin te maken. Onze samenwerking was altijd bijzonder soepel (en gezellig in de aesculaaf ☺) en daarvoor wil ik jullie hartelijk danken. Veel succes met jullie PhD projecten! **Esther**, mijn Philly-buddy, wat hebben we een coole week gehad tijdens de ASN in de US. Al waren we beide blij dat we weer veilig aan de grond stonden op Schiphol na die horrorvlucht. Bedankt voor je support tijdens mijn PhD-project en succes met de laatste loodjes van jouw boekje. **Ria**, bedankt voor je support tijdens mijn onderzoek en de gezellig tijd op t lab, tijdens pauzes, borrels, interesse in de honden etc. Veel succes met je onderzoek en houd die CDL mensen een beetje in toom! **Lindsey** en **Maarten**, ook voor jullie is de eindstreep van het promotietraject in zicht. Hoe fijn is dat ☺. Bedankt voor jullie gezelligheid, luidruchtigheid ☺ en de wijze les om constructen vooral kant-en-klaar te kopen. Helaas geen vierdaagsefeestjes meer op het balkon bij Lindsey.. **Jeroen**, mijn U-genoot en Mr. labguru,

bedankt voor de support in het lab (lekkere antilichamen ☺) en de social talks over van alles en nog wat. **Jeanne** en **Vivienne**, de eerste keer dat ik die minuscule glazen cannules zag dacht ik: hoe dan?! Maar nu een paar jaar later pruts ik zonder enige moeite een fiber aan zo'n cannule en heeft het al geleid tot twee mooie publicaties! Hartelijk dank voor jullie hulp en interesse tijdens mijn onderzoek! **Petra** en **Ab**, jullie analytisch vermogen is een belangrijke spil geweest in de analyse van de uremische toxines. Hartelijk dank voor jullie hulp! **Sanna**, **Hanneke**, **Anita**, **Elnaz**, **Sabrina**, **Marieke**, **Niels**, **Kim**, **Julien**-let's-cover-Karl's-bench-with-balloons-Beyrath ☺, **Wendy** (De liefste Bruce Springsteen-fan die ik ken!), **Bas, Robert**, **Jan**, **Gerard**, **Kees**, **Frans** and all other colleagues; many thanks for supporting my research and for celebrating the victories! It was a great pleasure to work with you in the department of Pharmacology & Toxicology. I wish you all the best for the future!

Annemieke, ik vind het erg leuk dat we altijd nog contact hebben en waardeer zeer je toewijding en support zoals ik die ervaren heb tijdens (maar ook voor en na ☺) mijn promotietraject. Dankjewel!

I also would like to thank **Sjoerd**, **Ellen**, **Liz**, **Omar**, **Lauriane, Andreas**, **Femke**, **Silvia, Kukiat, Mohammed**, **Paco, Claudia**, **Jenny**, **Sami**, **Sabina**, **Caro, Jeroen**, **Theun**, **Anne, Irene**, **Dennis**, **Prof. dr. P.M.T. Deen** and all other colleagues from the department of Physiology for the enjoyable time I had in the lab (and beyond ☺) and the nice discussions during the Friday lab meetings. Special thanks to Prof. dr. R.J.M. Bindels. Dear **René**, I admire your enthusiastic approach to science and would like to thank you for your advises and fruitful discussions during meetings but also the joyful time during dinners.

We shared the Pharmacology & Toxicology lab with the department of Biochemistry and I would like to thank **Lisanne**, **Marco, Jori**, **Herman**, **Marleen**, **Federica**, **Mina**, **Sander G**, **Sjenet**, **Dania**, **Hoa, Ganesh**, and all others for the nice interactions with you guys during the coffee breaks or in the cell culture. In het bijzonder wil ik Sander bedanken, **baron van Asbeck**. Dankzij jouw betrokkenheid is het gelukt een eerste generatie microfluidic te 3D printen waardoor wij onze transportexperimenten in de fibers hebben kunnen uitvoeren. Veel dank daarvoor! Maar zeker ook onze BCRP CRISPR/Cas expeditie mag er zijn, bedankt voor je behulpzaamheid en geduld. Uiteraard waren ook de chats over honden, vrouwen ☺ en andere niet-werkgerelateerde zaken altijd erg leuk. Nog even doorknallen en dan kom ik graag je verdediging bijwonen!

Huib en **Jack**, veel dank voor jullie hulp bij het imagen en het opzetten van de opstelling met de fibers. Als de Mic weer eens kuren had waren jullie altijd bereid mij uit de brand te helpen (1x zelfs bijna letterlijk ☺). Dank daarvoor!

De collega's van de afdeling kindergeneeskunde wil ik bedanken voor de leerzame en leuke tijd die ik heb gehad tijdens mijn periode als analist bij de DNA-groep, maar ook voor de samenwerking daarna tijdens mijn promotietraject. **Marieke**, wij zaten gelijktijdig op het HLO en later werden we collega's. Je enthousiaste en betrokken houding op de werkvloer zijn enorm plezierig en al snel groeide dit uit tot een mooie vriendschap. Etentjes zijn altijd erg gezellig en onder het genot van een wijntje worden alle 'ins and outs' besproken. Ook je medewerking aan 'het mooiste cadeau in het donker' en je hulp bij het maken van de knapzakjes voor de kerstmarkt in Keulen zal ik nooit vergeten ☺! Bedankt voor je betrokkenheid bij mijn promotieonderzoek, maar ook je oprechte interesse in huis-tuin-en-keuken onderwerpen waardeer ik zeer. **Roel** en **Edwin**, PCR-masters, jullie hebben mij alle kneepjes van het PCRen, sequencen etc. bijgebracht. Bedankt daarvoor! Ook werd mijn muziekkennis door jullie wat opgeschroefd en wist ik wat SV Hatert had gedaan na het weekend. Dit laatste natuurlijk mede door de bezoekjes aan het lab door Prof. Zegers. Beste **Frans**, jij kwam elke dag even langs om het laatste nieuws te bespreken, van sport tot en met je vakantie plannen naar Afrika. Je bracht altijd weer even wat schwung in het lab! Je gesigneerde shirt waarmee je kampioen bent geworden met SV Hatert heb ik altijd nog zorgvuldig bewaard. **Maaike Bras**, **Maaike Brink**, **Saskia**, **Inge**, **Paulien**, **Mariël**, **Maurice**, **Wilmien**, **Karin**, **Rutger**, **Cindy**, **Conny**, **Jessica**, **Thea**, **Annelies**, **Dineke**, **Irma**, **Jacqueline**, **Frans**, **'Spiergroep'**, **An**, **Richard** en alle andere collega's bedankt voor de samenwerking en de gezelligheid tijdens feestjes!

De oud-collega's van QM diagnostics wil ik bedanken voor de prettige tijd die ik bij jullie heb gewerkt (kort maar krachtig ☺). In het bijzonder wil ik **Marloes** bedanken, nadat ik vertrok bij QM hebben we altijd nog contact gehouden en spraken we af voor lunch om gezellig bij te kletsen of we gingen bij elkaar op bezoek. Bedankt voor je interesse en support gedurende mijn promotietraject en laten we vooral blijven afspreken ☺.

Als laatste wil ik de oud-collega's van het Canisius Wilhelmina Ziekenhuis en het Slingeland Ziekenhuis, afdeling Medische Microbiologie bedanken voor de leerzame en leuke tijd. Ik heb met veel plezier gewerkt op de afdeling serologie van het CWZ, tijdens de bepalingen werd het weekend doorgenomen, de

laatste nieuwtjes besproken, **Theo**, **Toon**, **Jack** en **Bert** die 'diepgaande' gesprekken hadden en **Bea**, **Mary**, **Dorine** en later **Fien** die de mannen een beetje in toom hielden. Ook op de afdelingen bacteriologie en moleculaire biologie (**Margret**, **Annet**, **Dirk**, **Jos**, **Sabrina**, **Maaike B**, **Sandra**, **Hanneke**, **Maaike** (DNA), **Corina**, **Kim**, **Bart**, **Theo**, e.v.a.) heb ik met veel plezier gewerkt, bedankt voor de fijne tijd! In het bijzonder wil ik **Romana** bedanken, nadat we beide vertrokken bij het CWZ hebben we altijd nog contact onder houden. Je bent een luisterend oor voor mij geweest en het is altijd gezellig als we elkaar weer zien. Vielen Dank Liebe Romana! De allereerste kneepjes van het microbiologisch vak zijn me bijgebracht door **Frits** Florestein en **Mariëtte** Nusselder onder leiding van Medisch Microbioloog **Ron Bosboom** en toenmalig labhoofd **Johan van der Elzen**, in het Slingeland ziekenhuis te Doetinchem. Ik wil alle medewerkers van deze afdeling hartelijk danken voor de kennis die ze met mij hebben gedeeld en de gezelligheid op en ook buiten het lab.

Ook wil ik graag de studenten die ik begeleid heb tijdens mijn promotie traject bedanken voor hun inzet, **Yvette**, **Ilze**, **Jesse** en **Ursula**. Mede dankzij jullie is er mooie data gegenereerd en heb ik mijn geduld-gen (een soort van) ontdekt. Ik wens jullie veel succes voor de toekomst!

Mijn huidige collega's van de afdeling Farmacologie, Universiteit Utrecht, wil ik bedanken voor hun warme onthaal in de groep en hun interesse in mijn promotieonderzoek alsmede in mijn huidige project. Ook de borrels op het dakterras zijn bijzonder gezellig en nu al legendarisch met de Roos-Johan plek ☺. Momenteel zijn de werkzaamheden binnen de subgroepen nog vrij uiteenlopend, maar ik heb er alle vertrouwen in dat er mooie bruggen te slaan zijn en we hopelijk vele successen samen mogen beleven. Manoe, Miloš, Pedro and Michèle, my former Nijmegen colleagues who are actually now my Utrecht colleagues. Thanks for the support during my PhD project, the scientific discussions during meetings, but also the nice social activities we had during the past years! Also many thanks for the nice introduction in the Utrecht group, I was comfortable within no time. **Manoe** I really admire your scientific attitude and your patience with students. I am sure you were born for a career in science! **Miloš**, the Italian from Servia or the other way around ☺. I think you are one of the most critical (in particular on your own data) and hard-working persons I know and always willing to help out colleagues. Thanks for your collaboration, it is a pleasure working with you. **Pedro**, If something was lost (e.g. my pipettes) I always knew where to find it (your lab bench). Also, thanks

to you, we now know that our cells can survive overnight at room temperature. Unfortunately, you are going to leave our lab as you almost graduate. It was always fun working with you but also from a scientific point of view it was great to collaborate with you. I wish you all the best in Germany, or the Antarctic as you call it, you will manage! **Michèle**, together we published two nice papers! Your enthusiastic, social character and your interest in science will be key in your graduation to doctor. Ga zo door ☺! **Paul**, als jongste telg binnen de 'Roos-groep' staat je nog heel wat te wachten, maar met jouw sympathieke, vrolijke karakter en goede aanpak van wetenschappelijke vraagstukken weet ik zeker dat we over een paar een Dr. Paul in ons midden hebben. **Katja** and **Amer**, as of September you will start your PhD fellowship in Roos' group. I am looking forward to our collaboration and the papers we will publish in the future! To all (semi-)young and senior researchers in the department of Pharmacology: I am looking forward to celebrate scientific victories or PhD graduate parties in the future ☺. **Aletta**, **Paula** and **Johan**, no matter what, I will never forget my first conference abroad within this department. Thanks Aletta for taking care of us!

Uiteraard zijn er ook buiten het werk om veel mensen die me altijd gesteund hebben. Allereerst wil ik graag de **familie Jansen** en **Gudde** bedanken voor hun hartverwarmende steun en interesse. De appjes, mailtjes, kaartjes en smsjes om mij succes te wensen voor een congres, te feliciteren als er een artikel geaccepteerd was of als ik een prijs had gewonnen waardeer ik enorm! Ook al wisten jullie niet precies wat ik dan gepubliceerd had of wat ik moest presenteren, jullie waren er niet minder trots om. Veel dank daarvoor! Eén van de hoogtepunten betreffende support was de ontvangst na mijn dynamische Turkije trip; **Vicky**, **Bianca**, **Stender**, tante **Rikie** en **ma** met n spandoek, champagne en bloemen op station Veenendaal-de Klomp. Dat was echt fantastisch en zal ik nooit vergeten! Brigitte, bedankt voor de feedback op mijn NL samenvatting, ik sluit de kans niet uit dat er in dit dankwoord hier en daar wat bijwoorden niet geheel correct zijn ☺. Daarnaast wil ik de familie Albers bedanken voor hun support, de gezellige feestjes zorgden er altijd weer voor dat ik het werk even kon loslaten. In het bijzonder wil ik schoonma bedanken; bij jou staat de deur altijd open voor een bakkie koffie en een gezellig praatje. Jouw energieke en positieve houding is bewonderingswaardig! Bedankt voor je steun in voor- en tegenspoed.

Zeker ook wil ik **Linda**, **Jan-Willem**, **Sven**, **Jeantine**, **Chris, Miriam** en **Tom** bedanken voor jullie interesse in mijn promotiewerk en de support tijdens deze periode. De gezelligheid tijdens feestjes, Normaal concerten, Zwarte Cross en

andere events zit altijd goed en het is dan ook erg fijn om mensen zoals jullie om me heen te hebben. **Linda**, we kennen elkaar al vanaf de HLO en zijn altijd nog goede vriendinnen. Het is bijzonder prettig om te weten dat er mensen zijn bij wie de deur altijd open staat! **Marleen** en fam. Albers, menig uur heb ik tijdens mijn promotieonderzoek bij jullie paardgereden en daardoor kon ik mijn hoofd even helemaal leeg maken. Fijn dat dit mogelijk was! **Roos** (Heck), als ik ging lessen bij jou dan stapte ik naderhand altijd met een positieve flow van mijn paard en kon ik met nieuwe energie weer aan het werk. Dank daarvoor!

En dan natuurlijk **Sebastiaan** en **Elmy**, bedankt voor jullie belangstelling naar mijn promotie onderzoek de afgelopen jaren. Het is fijn om familie om je heen te hebben waarvan je weet dat ze er voor je zijn; van het samen vieren van behaald succes tot het regelen van een nieuwe eettafel nadat deze een *Canis lupus* aanval niet overleefd had. Dank daarvoor!

Pa en **ma**, toen ik de kans kreeg om het PhD-traject in te gaan was er vanuit jullie kant geen minuut twijfel of ik het wel zou volbrengen. Echter, zonder jullie enorme toewijding, steun en vertrouwen was dit proefschrift niet geworden wat het nu is. Letterlijk niet, gezien pa voor de eerste fiber experimenten nog een op maat gemaakte ring heeft ontwikkeld zodat ik de functionele testen uit kon voeren. Als er een artikel werd afgewezen of experimenten mislukten, wisten jullie me wel weer te stimuleren zodat ik vol goede moed verder ging. Het is bijzonder fijn om een warme (ook letterlijk: lang leve de roodgloeiende houtkachel) en liefdevolle familie om je heen te hebben! Deze mijlpaal is nu bereikt, maar ik hoop nog vele (wetenschappelijke) hoogtepunten met jullie te mogen vieren. Dankjulliewel!

En dan natuurlijk, mijn rots in de branding: **Bennie**. Op jou kan ik vertrouwen en ik weet dat je er altijd voor me bent. Je laat me vrij in wat ik wil doen en staat altijd achter mijn keuzes, zonder enige twijfel. Bedankt voor je onvoorwaardelijke steun en liefde! Een goede thuisbasis is het fundament voor succes, zeker ook in de wetenschap. En dat zit bij ons wel goed! Ik hoop dat we in de toekomst nog veel successen samen mogen vieren, bedankt dat je er voor me bent!